UNIVERSITY OF LONDON THESIS

Degree phd Year 2007 Name of Author TABASSAM ISMAIL

UCL DEPARTMENT OF ELECTRONIC
& ELECTRICAL ENGINEERING

Feed-forward Linearisation of a Directly Modulated Semiconductor Laser and Broadband Millimetre-wave Wireless over Fibre Systems

Tabassam Ismail

A thesis submitted to the University of London for the degree of Doctor of Philosophy

Department of Electronic and Electrical Engineering
University College London

February 2007

ProQuest LLC
789 East Eisenhower Parkway
P.O. Box 1346
Ann Arbor, MI 48106-1346

Feed-forward Linearisation of a Directly Modulated Semiconductor Laser and Broadband Millimetre-wave Wireless over Fibre Systems

Abstract

This thesis is concerned with reduction of non-linear distortion in a directly modulated uncooled semiconductor laser using feed-forward compensation and investigating the performance of broadband millimetre-wave wireless over fibre systems.

One of the key elements that determine the performance in a fibre optic link is the linearity of the optical source. Direct modulation of an uncooled semiconductor laser diode is a simple and cost effective solution. However, the distortion and noise generated by the laser limit the achievable dynamic range and performance in a system. Feed-forward linearisation is demonstrated at 5 GHz, the highest operating frequency reported, with 26 dB third order intermodulation distortion suppression and simultaneous noise reduction leading to enhanced spurious free dynamic range of 107 dB (1Hz). The effectiveness of feed-forward in a multi-channel system is investigated. Laser non-linearity can cause spectral re-growth and interchannel distortion that can completely mask the adjacent channel. A significant 11 dB interchannel distortion suppression and 10.5 dB power advantage is obtained compared to the non-linearised case. These results suggest that feed-forward linearisation arrangement can make a practical multi-channel or multi-operator wireless over fibre system.

In the second part of this thesis the first experimental transmission of wireless data over fibre with remote millimetre-wave local oscillator delivery using a bi-directional semiconductor optical amplifier in a full duplex system with 2.2 km coarse wavelength division multiplexing fibre ring architecture is demonstrated. The use of bi-directional SOAs in place of unidirectional erbium doped fibre amplifier or unidirectional SOAs, together with the use of CWDM and optical distribution of the local oscillator signal allow substantial reduction in overall complexity and cost. Successful transmission of data over 12.8 km fibre is achieved with clear and well defined constellations and eye diagrams as well as 10.5% and 7.8 % error vector magnitude values for the downlink and uplink directions, respectively.

The thesis also presents an implementation and performance of a millimetre-wave gigabit wireless over fibre system. CWDM devices such as uncooled laser diodes and passive components are used for the first time in a gigabit system allowing cost savings compared to dense WDM. This makes such solutions more attractive for millimetre-wave access systems. Optically modulated gigabit wireless data signals to and from the base stations are distributed at 5 GHz and up-converted using a remotely delivered LO source. Eye diagrams and bit error rate are measured to assess the system performance.

Acknowledgements

First, I would like to extend my heartfelt gratitude to my supervisor Professor Alwyn J. Seeds for his guidance and suggestions throughout the course of this project. Much of this would not have been possible without his tremendous support and encouragement during the difficult times. I am also grateful to Dr John E. Mitchell for his invaluable advice and helpful discussions.

I would like to thank past and present colleagues in the Ultra-Fast Photonics group for their help and making the duration of the research very enjoyable: Cyril Renaud, Marianna Pantouvaki, Martyn Fice, Seung-Fei Kong, Jack Chuang, Ed Burr. Special thanks to Chin-Pang Liu for his assistance in the lab. I would also like to thank the workshop (Trevor Hamer and Jim Vansickle) for their assistance in designing laser mounts.

Finally, I would like to thank my parents for their patience and continuous support through these years.

Table of Contents

List of Figures

List of Tables

List of Acronyms

2G	Second Generation mobile standard
3G	Third Generation mobile standard
AP	Access Point
ASE	Amplified Spontaneous Emission
ASK	Amplitude Shift Keying
BER	Bit Error Rate
BPF	Band Pass Filter
BPSK	Binary Phase Shift Keying
BS	Base Station
BWA	Broadband Wireless Access
CATV	Cable TV
CDMA	Code Division Multiple Access
CNR	Carrier to Noise Ratio
CS	Central station
CSMA/CA	Carrier Sense Multiple Access / Collision Avoidance
CTB	Composite Triple Beat
CW	Continuous Wave
CWDM	Coarse Wavelength Division Multiplexing
DAS	Distributed Antenna System
dB	Decibel
dBc	Decibel relative to carrier
dBm	Decibel milliwatt
DBPSK	Differential Binary Phase Shift Keying
DEMUX	Demultiplexer
DFB	Distributed Feed-Back
DPSK	Differential Phase Shift Keying
DR	Dynamic Range
DRO	Dielectric Resonator Oscillator
DSBSC	Double Side-Band Suppressed Carrier
DSSS	Direct Sequence Spread Spectrum
DWDM	Dense Wavelength Division Multiplexing

EAM	Electro-Absorption Modulator
EAT	Electro-Absorption Transceiver
EDFA	Erbium Doped Fibre Amplifier
EIRP	Equivalent Isotropically Radiated Power
EOM	Electro-Optic Modulator
ETSI	European Telecommunications Standard Institute
EVM	Error Vector Magnitude
FBG	Fibre Bragg Grating
FDM	Frequency Division Multiplexing
FDMA	Frequency Division Multiple Access
FHSS	Frequency Hopping Spread Spectrum
FWA	Fixed Wireless Access
Gbit/s	Gigabit per second
GHz	GigaHertz
HIPERACESS	High Performance Radio ACCESS
IEEE	Institute of Electrical and Electronics Engineers
IF	Intermediate Frequency
IM	Intensity Modulation
IMDD	Intensity Modulation Direct Detection
ISM	Industrial, Scientific and Medical
ISO	Isolator
LAN	Local Area Network
LD	Laser Diode
LED	Light Emitting Diode
L-I	Light vs Current
LMDS	Local Multipoint Distribution Services
LNA	Low Noise Amplifier
LO	Local Oscillator
LPF	Low Pass Filter
MM-wave	Millimetre-wave
Mbit/s	Megabit per second
MMDS	Multichannel Multipoint Distribution System
MMIC	Microwave Monolithic Integrated Circuit
MMF	Multi Mode Fibre
MQW	Multiple Quantum Well
MUX	Multiplexer
MVDS	Multipoint Video Distribution Services

MZM	Mach-Zehnder Modulator
NF	Noise Figure
OADM	Optical Add Drop Multiplexer
OFDM	Orthogonal Frequency Division Multiplexing
OIL	Optical Injection Locking
OIPLL	Optical Injection Phase Lock Loop
OPLL	Optical Phase Lock Loop
PD	Photo-detector or Photodiode
PRBS	Pseudo Random Bit Sequence
PSK	Phase Shift Keying
QAM	Quadrature Amplitude Modulation
QPSK	Quadrature Phase Shift Keying
RF	Radio Frequency
RIN	Relative Intensity Noise
RN	Remote Node
SCM	SubCarrier Multiplexing
SFDR	Spurious Free Dynamic Range
SMF	Single Mode Fibre
SNR	Signal to Noise Ratio
SOA	Semiconductor Optical Amplifier
SSB	Single Side Band
TDM	Time Division Multiplexing
TDMA	Time Division Multiple Access
UTC	Uni-Travelling Carrier
UTC-PD	Uni-Travelling Carrier Photodiode
VCSEL	Vertical Cavity Surface Emitting Laser Diode
VSA	Vector Signal Analyser
VSG	Vector Signal Generator
WDM	Wavelength Division Multiplexing
WiMAX	Wireless Interoperability for Microwave Access
WLAN	Wireless Local Area Network
WoF	Wireless over Fibre

Chapter 1

Introduction

This chapter provide a background and an overview of the thesis. In the first Section 1.1 a brief overview of mobile phone and wireless systems is given. Millimetre-wave (mm-wave) characteristics and main applications are briefly considered. Section 1.2 provide a discussion on wireless local area network (WLAN) technologies and main standards such as IEEE802.11a/b/g. Wireless over Fibre (WoF) technology has been proposed as a cost effective approach for distribution of microwave and mm-wave broadband services and various signal transport schemes are considered in Section 1.3. The fibre has the potential to deliver a wide range of services with huge bandwidth and low loss. The relative merit of direct and external modulation is outlined and issues like noise and distortion properties in optical links are reviewed in Section 1.4. The objectives of this thesis and novel achievements are summarised in Section 1.5. Section 1.6 provides details of structure for the rest of the thesis. The last Section 1.7 summarises the conclusion.

1.1 Microwave and Millimetre wave Frequencies

Wireless systems have gained extensive acceptance for mobile and fixed communications such as cellular communications. For a number of years the extension of mobile systems to broader bandwidth and a variety of services has been explored in activities around the world [1]. Traditionally, only voice traffic had to be accommodated but now many more demands are being placed on the network. The predicted growth in mobile phone traffic and the move towards enhanced mobility will lead to a need for a wireless infrastructure that provides increasing bandwidth per user. In order to offer broadband services (voice, data, multimedia services), these systems will need to offer higher data transmission capacities well beyond the present day standards of wireless systems. Wireless LAN (IEEE802a/b/g) offering up to 54 Mbit/s operating at 2.4 GHz and 5 GHz, and 3G mobile networks (IMT2000/UMTS) offering up to 2 Mbit/s [2] operating around 2 GHz, are some of today's main wireless standards. IEEE802.16 or Worldwide Interoperability for Microwave Access (WiMAX) is another standard aiming to bridge the last mile through mobile and fixed wireless access to the end user at frequencies between 2-66 GHz. Future broadband wireless networks will operate at microwave frequencies to deliver high bit rate (> 150 Mbit/s) signals to mobile users. Mobile and fixed wireless access systems are planning to move towards higher transmission rates. For instance, the 4th generation of mobile phones should be able to support a maximum data rate of 100 Mbit/s, while future development of the

IEEE 802.11n standard for WLAN target 500 Mbit/s. The need for increased capacity leads to higher operating frequencies (above 6 GHz) and smaller radio cells. To reduce the system installation and maintenance cost of such systems it is imperative to make base stations (BS) as simple as possible. Fiber optic systems now play a key role in long haul communication traffic and with the progressive evolution of Ethernet standards; optical fibre is penetrating into broadband local access.

The demand for higher wireless transfer data rates and the limited spectrum resources in the microwave range drives research towards millimetre-wave[1] (mm-wave) frequencies (i.e. above 30 GHz). This will provide more radio spectrum resource and better frequency reuse due to reduced cell size [3]. Internet traffic is being dominated by the transport of high bandwidth multi-media content, such as video broadcasting and peer-2-peer traffic with expectations of continued growth. Remote medical diagnostics/surgery applications also require huge bandwidth. For instance, the distribution of high quality video requires a raw data throughput of 1 Gbit/s. Multiple input multiple output (MIMO) is an emerging technology that can be used for developing Gbit/s wireless transmission systems [4]. Within the European Community (EC) the frequency range 40.5 GHz to 42.5 GHz has been allocated for Multipoint Video Distribution Services (MVDS) and the EC RACE Mobile Broadband System (MBS) envisages the use of the frequency range from 62 GHz to 66 GHz for the provision of broadband services to pedestrians and vehicles. A wide variety of applications for mm-wave systems is discussed in [4]. The FCC allocated an un-precedent 7 GHz of spectrum for licence free operation between 57-64 GHz, this compares to about 500 MHz of spectrum allocated between 2-6 GHz for wi-fi and other license free applications. An overview of research and development trends in mm-wave application systems in Japan and other countries is discussed in [5]. High attenuation of mm-wave signals has the associated advantage of small cells when deploying microcell and picocell systems, particularly beneficial in wireless LAN where the cells are essentially confined to small size. In addition, only for fixed access, antennas can be designed to be highly directional. As a result, any multipath that may exist in the channel is significantly attenuated by the antenna side lobes.

One disadvantage of mm-wave frequencies is their short propagation distance, resulting in smaller radio coverage cell size due to higher propagation losses (i.e., high oxygen absorption at 60 GHz) which greatly limits the wireless coverage area and therefore requires a large number of BSs to cover a given area. This also has the implication that the bandwidth obtained at GHz frequencies enables relatively compact, highly efficient and narrow beam width antennas to be designed. With directional antenna more gain could be provided for the wireless link budget, which could therefore allow increased cell radius, thereby reducing the number of BSs required for full coverage.

Systems designed for widespread coverage are not suitable for high density regions. To cope with the increasing traffic volume and large coverage of the network, high capacity can be achieved by splitting cells [6]. Small cells are used to increase capacity and have the benefit that adjacent cell

[1] The millimetre wave band is strictly between 30-300GHz and microwave frequencies in the band of 3-30 GHz.

interference is minimum and can have a high degree of frequency reuse factor. The concept of frequency reuse involves a frequency channel which can be used multiple times in different cells provided the cells are sufficiently far apart. If the same frequency channel is reused every N cells, and cluster size is N then the reuse factor is 1/N. The total area to be covered is divided into a number of small cells, each being served by its own BS. This is achieved by breaking the "macrocells" into a number of "microcells" (200-1000m diameter), each of which will use the same spectrum. This effectively reduces the size of each cell thus reducing the traffic loading and hence congestion. The smaller cells also allow the antenna power to be reduced because of shorter transmission distances. Microcells are designed to provide coverage with limited interference to the outside world and high capacity for high traffic densities in urban and suburban areas to users both outdoors and within buildings. Progressive cell splitting leads to picocells to provide a more localised coverage than microcells, such as inside buildings where coverage is poor or when there are large numbers of users. Picocells offer greater frequency reuse, lower power transmitters, and higher throughput.

1.1.1 Radio frequency propagation characteristics

As the transmission frequency is increased to the mm-wave range, the propagation losses also increase. Systems designed to operate in the frequency range around 30 GHz (10-66 GHz in general) are typically limited to operate with an unobstructed line of sight (LOS) link, due to significant attenuation through trees experienced at these frequencies. The attenuation in the atmosphere increases significantly, and the effects of rain, fog, snow, oxygen and water vapour resonance's place limitations on the range of transmission. Figure 1.1 give curves of atmospheric attenuation versus frequency for propagation over the microwave and mm-wave range and shows the loss effects. The frequency band at 60 GHz is of particular interest for MBS offering high bit rates of about 155 Mbit/s. The 62-63 GHz band is allocated for the downlink while 65-66 GHz is allocated for the uplink transmission. The high attenuation approximately 14 dB/km at 60 GHz [7] allows small cells to be used with reduced power and high spectral efficiency due to high frequency reuse. Like all radio links that operate above 10 GHz, intense rainfall significantly limits the distance over which 60 GHz links can transmit data.

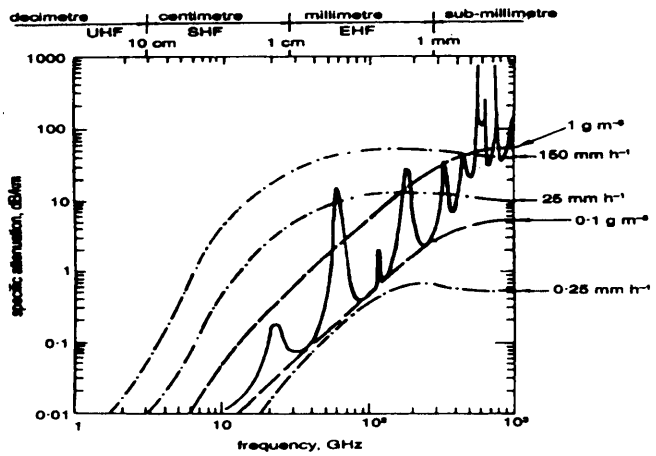

Figure 1.1 Attenuation versus frequency for microwave and mm-wave range [7]

Oxygen absorption-this is an unique property that does not affect lower frequencies. Oxygen attenuates 60 GHz signals by 12-16 dB per km, which is the main reason that 60 GHz links cannot cover the distances achieved by other mm-wave links. The impact of the small beam sizes coupled with oxygen absorption makes the links highly immune to interference from other 60 GHz radios, since another link in the immediate vicinity will not interfere if its path is even moderately different from the first link, and any radio operating beyond the immediate vicinity will have its signal severely attenuated by the oxygen attenuation. These two factors make the signal highly secure.

1.1.2 Wireless systems/technologies

Fixed wireless systems

With increased demand for broadband services new wireless systems will operate at mm-wave frequencies such as Local Multipoint Distribution Services (LMDS) at 28 GHz, Microwave Video Distribution Services (MVDS) at 40 GHz (0.5-1 km cell) and Mobile Broadband System (MBS) at 60 GHz.

Wimax (802.16)

The two driving forces of modern internet are broadband, and wireless. The WiMax (IEEE 802.16) standard combines the two and provides a high speed internet access over a wireless connection. Since it can be used over relatively long distances, it is an effective "last mile" solution for delivering broadband to the home, and for creating wireless "hot spots" in places like airports, college campuses, and small communities. WiMAX will provide high speed network connections and thereby serve as a backbone for IEEE802.11 WLAN hotspots.

The first version of the IEEE802.16 was introduced in Dec 2001 and defines WirelessMAN air interface standard for fixed broadband wireless access (BWA) metropolitan area networks (MANs) [8]. The standard covers a wide range of frequencies from 10 to 66 GHz and propagation mechanism in this region of spectrum restricts the use of this system to LOS [9]. An amendment of the 802.16a standard to support 2-11 GHz using an enhanced version of the same basic medium access control layer along with new physical layer specifications, is also developed [10]. IEEE802.16a in Jan 2003 was extension for 2-11 GHz, targeted for non line of sight, point to multi point applications like "last mile" broadband access.

The channels used in this physical environment are large. Typical channel bandwidth allocations are 20 or 25 MHz (US) or 28 MHz (Europe). With raw data rates in excess of 120 Mbit/s, this environment is well suited for point-to-multipoint access serving applications from small office/home office through medium to large office applications. The standard supports a wide variety of physical layer including various modulation schemes. On the uplink, support for QPSK is mandatory while 16 QAM and 64 QAM are optional. The downlink supports QPSK and 16 QAM while 64 QAM is optional. Support for such a variety of modulation schemes permits trade off efficiency for robustness

and vice versa. The standard is designed to accommodate either Time Division Duplexing (TDD) or Frequency Division Duplexing (FDD) deployments, allowing for both full and half duplex terminals in the FDD case. Table 1.1 lists the main parameters for the WiMAX.

	802.16	802.16a/REVd	802.16e
Completed	Dec 2001	802.16a: Jan 2003 802.16 REVd	2005
Spectrum	10-66 GHz	2-11 GHz	< 6 GHz
Channel Conditions	Line of sight only	Non line of sight	Non line of sight
Bit rate	32-134 Mbps (28 MHz channel)	Up to 75 Mbps (20 MHz channel)	Up to 15 Mbps
Modulation	QPSK, 16 QAM and 64QAM	256 sub-carrier OFDM using QPSK, 16, 64 256 QAM	Same as 802.16a
Mobility	Fixed	Fixed	Pedestrian Mobility
Channel Bandwidths	20, 25 and 28 MHz	Selectable channel bandwidth between 1.25 and 20 MHz	5 MHz (Planned)
Typical Cell Radius	1-3 Miles	3 to 5 miles; max range 30 miles based on tower height, antenna gain, transmit power	

Table 1.1 Main parameters for WiMAX IEEE802.16 [11]

Local Multi-point Distribution Services (LMDS)

LMDS is a fixed point to multipoint broadband wireless technology that operates in the 28 GHz band and offers coverage over distances up to 3-5 km and is an effective solution for last mile distribution. In the US, frequencies from 28 GHz through 31 GHz are used for LMDS. As a result of the propagation characteristics in this frequency range LOS is required. LMDS systems use a cellular like network architecture, though services are fixed, not mobile. Point-to-point systems are also capable of using the LMDS frequencies and can reach slightly further distances due to the increased antenna gain. Services using LMDS technology include high speed internet access, voice, data and video services. Throughput capacity and distance of the link depends on the modulation method used. Data transfer rates for LMDS can reach up to 1.5 Gbit/s but typically may average around 38 Mbit/s (downstream) and 200 Mbit/s for the upstream.

Multi-channel Multi-point Distribution Services (MMDS)

MMDS is a broadband wireless point-to-multipoint service used for general purpose broadband networking and is an alternative method of cable television. The MMDS band uses microwave frequencies from 2-3 (2.5-2.7 in the US) GHz with distances of up to 35 miles cell diameter non LOS.

Higher frequency bands are not chosen for MMDS due to higher free space or path attenuation. A typical data rate is 0.5-3 Mbit/s using OFDM modulation and transmission power used is generally in the 1 to 100 W range.

Mobile Broadband System

The MBS is a mm-wave system that will provide users a mean of radio access to broadband services supported on customer premises networks or offered directly by public fixed networks. This concept requires MBS to provide a mobile/moveable wireless extension to wired networks for information rates exceeding 100 Mbit/s operating in the 40 and 60 GHz band.

Other Technologies

UWB (UltraWide Bandwidth)

UWB is a promising technology for transmission at ultra high speed over short wireless links limited by the low power level signals transmitted by UWB devices and extremely short duration (on the order of picoseconds) impulses or bursts of RF energy. Data can be transmitted over a wide spectrum of frequencies for short to medium distances around 15 to 100 m. The UWB radio typically have short range in outdoor and indoor environments since the power level is regulated to –41 dBm/MHz across most of the 3.1 to 10.6 GHz spectrum. Current UWB devices can transmit data up to 100 Mbit/s, compared to the 1 Mbit/s of Bluetooth and 54 Mbit/s of 802.11a/g. It is anticipated that UWB can be used to send data over short distance personal area networks that link wireless devices such as notebooks, PCs, and PDAs in businesses and homes. UWB is also fast enough to accommodate multimedia traffic, including video, voice, and data. The modulation scheme is OFDM and the user access is TDMA.

Deploying UWB wireless networks for ultra-high speed transmissions may be difficult due to the large bandwidth requirements and short propagation distances of wireless UWB signals. The coverage of such networks can be extended by remoting the antenna units from the central station using optical links for both indoor and outdoor applications. The extremely wide occupied bandwidth (3.1 – 10.6 GHz) of UWB signals make optical fibre links suitable transmission means for delivering UWB signals from a centralised location to remote nodes (Access Points) and vice-versa. Wah *et al* demonstrated RF signal of UWB transmitted over multimode fibre using VCSELs [12]. Binary Phase Shift Keying (BPSK) UWB signals directly modulate an 850-nm optical carrier of a 7.5 GHz bandwidth VCSEL laser at data rates ranging from 100 to 400 Mbits/s. The spectrum of the BPSK UWB signal was measured from 1.96 to 10.34 GHz which exceeds the bandwidth of the VCSEL used. Measured results show dispersion in the link caused by modal dispersion arising from multimode fibre.

1.2 Wireless Local Area Network and Standards

Since wireless local area networks (wireless LANs) provide more flexibility and convenient connections than wired networks, there is an increasing demand recently. Two WLAN configurations are possible: Infrastructure mode or peer-to-peer mode. The simplest configuration is the peer-to-peer which is an ad hoc network formed by a group of devices (depending on the number of users in the network) in which the wireless units exchange information with other units directly. In a more complex WLAN infrastructure mode, shown in Figure 1.2 the wireless units transmit and receive information through an access point (AP). The AP receives the information signal and resends it to other mobile units. In this operation the AP is located to provide optimal coverage and multiple APs are used to provide coverage over a wide area. The AP can be connected to a LAN through a wired Ethernet connection. Each AP forms a microcell similar to a cellular system. Roaming is one of the main advantages, allowing users to move freely between different cells, while maintaining connectivity.

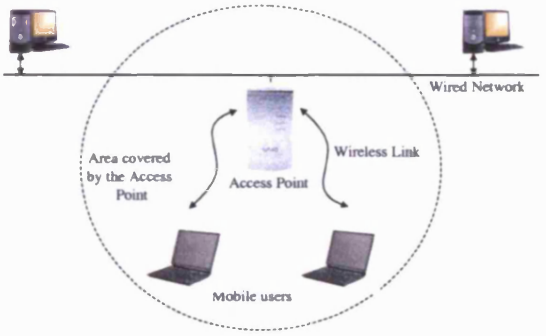

Figure 1.2 Network for WLAN

1.2.1 WLAN standards

Over the past few years, different WLAN technologies and standards have been developed. Two main WLAN standards are: The Institute of Electrical and Electronics Engineers (IEEE) IEEE802.11 and the European Telecommunications Standards Institute (ETSI) HiperLAN-HIgh PERformance Radio LAN [13]. These standards are designed to operate in the unlicensed frequency bands and have the advantage of not requiring a license which greatly reduces the cost of deploying wireless systems. WLAN Instrumentation (or Industrial), Scientific and Medical (ISM) frequency band is 83.5 MHz from 2.400 GHz to 2.4835 GHz and Unlicensed National Information Infrastructure (U-NII) band at 5 GHz is used.

The IEEE802.11 standard in 1997 is one of the first generations for WLAN networks and later IEEE802.11b was introduced in 1999. These two WLAN standards, IEEE802.11 and IEEE802.11b were designed to operate in the unlicensed 2.4 GHz ISM band and support a maximum data rate of 2 Mbit/s and 11 Mbit/s respectively [14]. The original IEEE802.11 standard employ DBPSK and DQPSK modulation scheme to achieve data rates of 1 and 2 Mbit/s. The IEEE802.11b standard adds

5.5 Mbit/s and 11 Mbit/s data rates and is compatible with the 802.11 standard [15]. The modulation scheme of 802.11b is direct sequence spread spectrum (DSSS) using complementary code keying (CCK) to provide higher data rates and the chipping rate is 11 MHz, which is the channel bandwidth. Changing both the spreading factor and/or the modulation format varies the bit rate. The IEEE802.11g standard is also for 2.4 GHz with a maximum data rate of 54 Mbit/s using both 64 QAM and CCK to provide higher bandwidth and compatibility with 802.11b devices [16]. The IEEE802.11b spectrum at 2.4 GHz has recently become crowded by various other wireless devices operating in the same band such as cordless telephones and mobile portable devices (Bluetooth). In addition, the 2.4 GHz band suffers from microwave oven interference. Wireless LAN technologies using the ISM band must be equipped to deal with interference of all kinds.

The next generation of WLAN in the 5 GHz band take advantage of the IEEE802.11a standard, which was motivated by the release of 300 MHz of spectrum for unlicensed operation in the 5 GHz U-NII band at the beginning of year 2000. In addition to a larger bandwidth available compared to the 2.4 GHz ISM band, which allows higher data rates, the 5 GHz band is also relatively free of interference from other devices. The IEEE802.11a standard can transmit a range of data rates from 6 to 54 Mbps employing OFDM technology at 5 GHz carrier frequency [17]. The 300 MHz bandwidth available for IEEE802.11a is nearly four times the spectrum available for IEEE802.11b, which is about 83 MHz. From 300 MHz bandwidth, there is a continuous 200 MHz portion extending from 5.15 to 5.35 GHz, and a separate 100 MHz from 5.725 to 5.825 GHz. The lower 100 MHz is restricted to maximum power of 50 mW, the next 100 MHz to 250 mW, and the final 100 MHz to a maximum of 1 W to support outdoor communication.

ETSI [19] has developed standards and specifications for HiperLAN 1 and HiperLAN 2 (for mobile broadband short range access network). HiperLAN 1 provides high speed radio LAN system operating in the 5.15-5.30 GHz band which is divided into 5 channels with a peak power of 1 W supporting maximum data rates of 23.5 Mbps (typical data rate is 20 Mbit/s). HiperLAN 1 uses two different modulation formats: a simple 2 level FSK formats for low data rate, and Gaussian minimum shift keying (GMSK) for high data rate. The 2 level FSK formats use a symbol rate of 1.470 Mbit/s; in this case this is also the bit rate. For high data rate, HiperLAN 1 uses a 23.5294 Mbit/s GMSK modulation. The HiperLAN 2 standard was published in April 2000 and is the second in a series of ETSI WLAN standards. (The HiperLAN 1 standard was never commercially launched). It also operates in the 5 GHz band using OFDM with 52 sub-carriers per channel providing a maximum data rate of about 54 Mbit/s. 48 sub-carriers carry data and 4 sub carriers are pilots which facilitate phase tracking for coherent demodulation. A channel spacing of 20 MHz is used, allowing 19 channels in the allocated European spectrum. BPSK, QPSK and 16 QAM are supported modulation schemes, 64 QAM is optional. In the lower frequency band 5.150 GHz to 5.350 GHz, the first nominal carrier frequency is 5.180 GHz and the last one is 5.320 GHz. The RF power permitted in this band is 200 mW mean EIRP for indoor use only. In the upper frequency band from 5.470 GHz to 5.725 GHz, the first nominal

carrier frequency is 5.500 GHz and the last one is 5.700 GHz with a power limit of 1W for indoor and outdoors.

To allow interoperability WLAN standards have been developed worldwide. Table 1.2 summarises the worldwide WLAN standards operating in the unlicensed 5 GHz frequency band. The high speed wireless access network type a (HiSWANa) standard was published by the Association of Radio Industries and Business (ARIB) [18]. This is a Japanese standard for WLAN in the 5 GHz band, and is very similar to the HiperLAN 2 standard in Europe.

	IEEE802.11a	Hiperlan/2	HiSWANa
Region	United States	Europe	Japan
Unlicensed frequency band of operation	5.15-5.35 GHz 5.725-5.825 GHz	5.15-5.35 GHz 5.47-5.725 GHz	5.15-5.25 GHz
Maximum data rate	54 Mbps		
Modulation technique	OFDM BPSK, QPSK, 16 QAM, 64 QAM		
Network topology	Peer-to-peer/infrastructure		

Table 1.2 Worldwide WLAN standards in the 5 GHz band

Future Wireless LANs

Conventional IEEE 802.11a/b/g WLAN's operating in the congested 2.4 and 5 GHz frequency bands are limited in terms of capacity and coverage. Multiple Input Multiple Output (MIMO) in combination with OFDM has been proposed to enhance their range and throughput. Wireless routers using MIMO technology in the 2.4 GHz band (802.11g) specified up to 108 Mbit/s have been introduced on the market. As the deployment of WLAN grows, there is a push to higher data rates. As a result moving to higher frequencies such as 40 and 60 GHz has been proposed, where LANs approaching 100 Mbit/s are the subject of research. Although these higher frequencies offer large amounts of spectrum, the radio system typically requires directional antennas for robust links. Therefore, they are more suited to fixed links, and the use of 2.4 GHz and 5 GHz bands will continue to have broader applicability.

ETSI [19] has developed standards and specifications for broadband radio access networks that cover a wide range of applications intended for different frequency bands. Major systems are HiperACCESS (for fixed wireless broadband access network) and HiperLINK (high speed radio links for static interconnections). HiperACCESS operates at 17 GHz (3-5 km cell), and provides outdoor, high speed (25 Mbit/s typical data rate) fixed radio access to customer premises and is capable of supporting multi-media applications. Technologies such as HiperLAN 2 might then be used for distribution within the premises. HiperLINK provides very high speed (up to 155 Mbit/s data rate) radio links for static interconnections intended for frequency of operation at 17 GHz and is capable of multi-media applications. A typical use is the interconnection of HiperACCESS networks and/or HiperLAN access points into a fully wireless network.

The requirements for high data rates will push carrier frequencies into mm-wave (60 GHz). For instance, the AWACS (ATM Wireless Access Communication System) is defined for 19 GHz with a data rate of 70 Mbit/s and a cell radius of 50-100m. The project will support limited, slow speed mobility as in line with expected use of high data rate services. The System for Advanced Mobile Broadband Applications (SAMBA) is a European union collaborative project and will operate at 40 GHz with 34 Mbit/s and the MEDIAN (wireless broadband CPN/LAN for professional and residential multimedia applications) will operate at 61.2 GHz at a data rate of 155 Mbit/s with a radio cell size of 10m [20]. The system is based on a multi-carrier modulation scheme (OFDM) and a TDD access technique which is adaptive to the actual user required data rates (up and downlink). The high frequencies result in smaller radio cells due to increased radio propagation losses and this means that numerous radio access points (or BSs) are required to cover a large area. The deployment and maintenance of such systems is economically infeasible, unless the cost and complexity of individual radio access points are significantly low. However, having smaller radio cells enhances efficient frequency spectrum utilisation.

	Wireless LAN standards					
	802.11	802.11b	802.11g	802.11a	Hiperlan 1	Hiperlan 2
Operating Frequency (GHz)	2.40-2.4835	2.40-2.4835	2.4 GHz	5.15-5.35 5.725-5.825	5 GHz	5.15-5.35 5.47-5.725
Channel separation (MHz)	22 (DSSS), 1 (FHSS)	25 MHz		20 MHz	23.5 MHz	20 MHz
Maximum data rate (Mbps)	1, 2 BPSK (1) QPSK (2)	11 (1, 2, 5.5, 11) DBPSK (1) DQPSK (2) CCK (5.5, 11)	54 BPSK (6, 9) QPSK (12, 18) 16 QAM (24, 36) 64QAM(54)	54 BPSK (6, 9) QPSK (12, 18) 16 QAM (24, 36) 64QAM(54)	23.5	54 BPSK (6, 9) QPSK (12, 18) 16QAM (24, 36) 64 QAM (54)
Radio Technology	FHSS or DSSS	DSSS	OFDM	OFDM	Single carrier	OFDM
Modulation scheme	GFSK (FHSS), DBPSK or DQPSK (DSSS)	BPSK, QPSK, CCK	BPSK, QPSK, 16 QAM, 64 QAM OFDM	BPSK, QPSK, 16 QAM 64 QAM OFDM	FSK or GMSK	BPSK, QPSK, 16 QAM, 64 QAM OFDM
Allocated bandwidth		83.5 MHz (26 MHz Japan)		300 MHz (100 MHz-Japan)		455 MHz
Occupied bandwidth		26 MHz (per channel)		16.6 MHz (per carrier)		16.6 MHz (per carrier)
Maximum channels		13 channels (Europe)	13 channels (Europe)	8 channels		
Carriers per channel	79	1 (DSSS)	48 data and 4 pilot	48 data and 4 pilot	1	48 data & 4 pilot

Transmit power mW	10 mW EIRP< 100 mW Maximum output power : USA:1000mW Europe:100mW Japan:10 mW/MHz	Up to 100 mW (20 dBm) 30 mW (15 dBm) common	Up to 100 mW (20 dBm) 30 mW(15 dBm) common	Up to 0.1 W 30mW common P_{max}=50mW (5.15-5.25) P_{max}=250mW (5.25–5.35) P_{max}=1W (5.725-5.825)		
Maximum o/p power	30 dBm	30 dBm	30 dBm	35 dBm (EIRP)	30 dBm (EIRP)	30 dBm (EIRP)

Table 1.3 Summary of main specifications for various Wireless LAN standards [14, 15, 16, 17]

Spread Spectrum Technology

Spread spectrum is the most commonly used WLAN technology and trades off bandwidth efficiency for reliability and security. It provides reliable and secure transmission in the ISM band by spreading the signal over a range of frequencies. The signal bandwidth is increased without increasing the data rate. Spread spectrum technology allow the chip rate to remain constant while the data rate changes. For example, a 1 Mbit/s rate has a spreading factor of 11, using BPSK modulation. QPSK replaces BPSK in order to double the bit rate to 2 Mbit/s at the same spreading rate of 11. Two kinds of spread spectrum technologies exist. These are Frequency Hopping Spread Spectrum (FHSS) and the Direct Sequence Spread Spectrum (DSSS) [21].

FHSS uses a narrowband carrier that changes frequency in a pattern known to both the transmitter and the receiver. When properly synchronised a single channel is maintained between the transmitter and the receiver. FHSS appears as short duration impulse noise to a different receiver. To ensure high security the bandwidth in FHSS technology is used inefficiently and therefore the system has lower throughput (1 and 2 Mbps). Since the frequency used for transmission is constantly changing FHSS systems are less prone to interference and are more secure compared to DSSS systems. Direct sequence spread spectrum spreads the signal energy over a large bandwidth and provides highly reliable transmission with relatively small SNR. DSSS generates a redundant bit pattern for each transmitted bit. The bit pattern, called a chip or chipping code, enables receivers to filter out signals that don't use the same bit pattern, including noise or interference. As a result more bandwidth is used to transmit the information.

Orthogonal Frequency Division Multiplexing (OFDM)

To support higher data rates, a multi-carrier modulation scheme OFDM is used. OFDM was originally used in consumer products in digital audio and digital video broadcasting and ADSL modems. OFDM is seen as the modulation technique for broadband wireless communications systems such as wireless LANs and point-to-multipoint distribution systems because it provides increased robustness against fading and multi paths. OFDM divides the signal into several individually modulated sub carriers, all of which are transmitted in parallel. The advantage of this is that the relative amount of time dispersion

per sub-carrier caused by multi path delay spread is decreased significantly. Furthermore, introducing a guard time in every OFDM symbol eliminates inter-symbol interference (ISI). In traditional frequency division multiplexing systems, the channel spacing is typically greater than the symbol rate. This is done in order to avoid overlapped spectrum. However, in OFDM, the sub-carriers are orthogonal to one another and the frequency spectrum of each sub-carrier overlaps the frequency spectrum of adjacent sub-carriers without interfering with one another. The channels can be placed closer together resulting in a more efficient use of allocated bandwidth. Orthogonality is achieved by spacing the carriers at durations equal to the reciprocal of the symbol duration. Two signals are orthogonal in a given interval if, when multiplied together and then integrated over that interval, the result is zero.

OFDM benefits from increased spectral efficiency due to the reduced sub-carrier spacing. The sub-carriers are modulated using phase shift keying (PSK) or quadrature amplitude modulation (QAM) and then translates to a high frequency signal at 5 GHz. This is similar to conventional frequency division multiplexing (FDM) or sub-carrier multiplexing, except for the stringent requirement of orthogonality between the sub-carriers. In comparison to single carrier modulation systems, OFDM has greater complexity since it is more sensitive to frequency offset and phase noise. Furthermore, orthogonal encoding leads to a relatively high peak to average power ratio, which reduces the power efficiency of the RF amplifier. Some of the OFDM parameters defined in the IEEE 802.11a standard include 52 sub-carriers, 312.5 kHz sub-carrier spacing, and 20 MHz channel spacing. 48 of the sub channels are used for the data, and the remaining four are for error correction. Other parameters in the OFDM standard are given in Table 1.4.

Data rate (Mbps)	6, 9, 12, 18, 24, 36, 48, 54
Modulation	BPSK, QPSK, 16QAM, 64QAM
Number of sub-carriers	52
Number of Pilots	4
OFDM symbol duration	4us
Guard interval	800 ns
Sub-carrier spacing	312.5 kHz
-3dB bandwidth	16.56 MHz
Channel spacing	20 MHz

Table 1.4 Main parameters of the OFDM standard [17]

1.2.2 WLAN transmission performance

The main parameters to consider are signal spectral mask, error vector magnitude (EVM) values, signal to noise ratio (SNR) and power levels. The receiver sensitivity is the minimum RF signal power level required at the input of the receiver for satisfactory system performance at a defined error rate. The receiver sensitivity is different depending on the standard being used and the data rate that is being

transmitted. For IEEE802.11 standard the receiver sensitivity is defined as -80 dBm for the 1 Mbit/s and -75 dBm for the 2 Mbit/s specifications. For the IEEE802.11b the minimum input level sensitivity is equal to -76 dBm. For IEEE802.11a standard the lower 100 MHz is restricted to a maximum power of 50 mW (17 dBm), the next 100 MHz to 250 mW (24 dBm), and the final 100 MHz to a maximum of 1 W (30 dBm) to support outdoor communication. The receiver sensitivity varies with the data rate and is given in Table 1.5. The 802.11a standard allowable error vector magnitude (EVM) values in % is also given. In 802.11a data rates of 6, 9, 12 and 24 Mbit/s are mandatory for compliance with the standard, and data rates above 24 Mbit/s are optional and an EVM of 15.8% is specified. The EVM specification for IEEE802.11b is 35% and maximum transmitter EVM is 5.62% for 802.11g.

One of specifications adopting OFDM, IEEE802.11a defines only sensitivities as a function of data rate. These sensitivities are based on the assumption that the noise figure of the receiver should be 15 dB. $(S/N)_{min}$ can be calculated using three parameters specified in IEEE802.11a; sensitivity, noise figure and occupied bandwidth. It is assumed that the occupied bandwidth is 16.6 MHz. For example at 12 Mbit/s $(S/N)_{min}$=(-79 dBm)-(-101.7 dBm $N_{thermal}$)-(15 dB NF_{sys})=7.7 dB

Data rate (Mbit/s)	6	9	12	18	24	36	48	54
Modulation	BPSK	BPSK	QPSK	QPSK	16 QAM	16 QAM	64 QAM	64 QAM
Sensitivity (dBm)	-82	-81	-79	-77	-74	-70	-66	-65
$(S/N)_{min}$ (dB)	4.7	5.7	7.7	9.7	12.7	16.7	20.7	21.7
EVM %	56.2	39.8	31.6	22.3	15.8	11.2	7.9	5.6

Table 1.5 Receiver sensitivity requirements for IEEE802.11a together with EVM [17]

1.3 Overview of Wireless over Fibre

Wireless LAN systems using the IEEE802.11a/b/g standards are growing rapidly in popularity. With increased demand for broadband services new wireless systems will operate at mm-wave frequencies such as LMDS at 30 GHz, MVDS at 40 GHz and MBS at 60 GHz. The large number of BSs required at these frequencies and the difficulty of engineering mm-wave systems favour wireless over fibre (WoF) technologies. The WoF approach seem to be the successful technology for cost effective solution because it simplifies the BS and allow sharing of expensive equipment to be located at the CS [22]. It also enables dynamic allocation of capacity based on traffic demands or control of services due to centralisation of the switching, modulation and other functions [23].

For a full duplex operation, signals at the BS and CS undergo electrical to optical conversion before transmission over fibre [24]. Microwave modulated optical signals are generated by modulating the light from an optical source and transmitting these signals via optical fibre. The high capacity bandwidth and low signal loss of optical fibre has led to it being the preferred transmission method for conveying data over large distances. The link loss is almost independent of the fibre length and frequency and this is particularly useful for mm-wave systems. The wide transmission bandwidth of the fibre is also attractive for UWB and other future wireless systems; hence it is a future proof technology. Since the fibre is smaller in diameter it is lightweight, less expensive and has excellent immunity against electromagnetic interference (EMI).

In WoF systems, directly modulated laser sources are preferred to provide a compact solution and minimise system cost. In these systems laser non-linearity is a key issue and the Spurious Free Dynamic Range (SFDR) is the most important parameter. Laser Relative Intensity Noise (RIN) and non-linearities introduced by direct modulation of laser diodes introduce distortion that limit the dynamic range and hence degrade the system performance. The maximum power level is limited by the system non-linearities, which cause distortion, and the noise floor limits the minimum power level. The optical link from BS to the CS (uplink) requires a very low noise and distortion characteristics since the radio signal power received at the BS fluctuates greatly, due to fading, shadowing or changes in distance between the BS and the mobile station [25]. On the other hand, the dynamic range requirements for the downlink is less demanding than for the uplink since each carrier has constant intensity [26]. However, the noise and distortion for the downlink must be small enough so that their undesired emission from the BS may not interfere with other channels. Dynamic range requirements for analog fibre optic links in fibre fed wireless microcells results in 100 $dB.Hz^{2/3}$ for optical transmitter [27] assuming an absolute spurious free condition for each channel [28]. To achieve this economical considerations suggest the use of compensated low cost lasers rather than extremely linear but expensive devices.

In the case of remote BS antennas the link span is usually in the range of some 100 m up to about 2 or 3 km. Jung *et al* [29] have examined the feasibility of using coaxial cable as opposed to fibre for

microcellular personal communication. In [30] it was shown that fibre links are appropriate and more cost effective than coaxial links for remote antenna feeding in a GSM network for link length of > 100 m. Future systems will use higher frequency bands (1.8 GHz for GSM, 2 GHz for UMTS, 2.4 GHz for IEEE802.11b and 5.2 GHz for IEEE802.11a) [31] to accommodate the data requirements. With increased carrier frequency loss due to the coaxial link is much greater and transmission is preferred via fibre. The advantage of WoF [32] is that being (RF) modulation format transparent allows signals from several operators using different modulation formats to share a common infrastructure. WoF can distribute broadband and multi-service signals such as cellular (2G, 3G) and wireless LAN (802.11a/b/g) [33, 34]. This allows easier re-configurability since standards and a service change require upgrades at the CS only, not at each BS and hence is more cost effective.

WoF has many applications due to its simple, low loss and effective structure in distributing high frequency signals. Some of the main applications [35] are mobile communication [36], wireless LAN, broadband wireless access, multimedia (such as HD-TV, video on demand and interactive multimedia services), satellite communications and intelligent transportation system. A WoF based road vehicle communication system is described in [37] where several radio BSs communicate with a CS over WoF connections. WoF technology has attracted much of attention in recent work for cellular radio and is extensively used to enhance coverage inside buildings [38, 39, 40] especially in office buildings, but also in locations such as airports, shopping malls. It is hard to provide adequate 3G coverage within buildings without the use of in-building distributed antenna systems (DAS). Penetration from outdoor coverage is unreliable and insufficient, so installation of indoor system is inevitable. A DAS enables an in building installation with a centralised wireless architecture. Both single mode and MMF can transmit RF signals over km distances using directly modulated low cost laser sources [41, 42, 43]. A MMF fibre feeder for CDMA based digital cellular and wireless LAN systems is proposed in [44]. A high performance single mode VCSEL developed for analogue applications has been evaluated for use in a WoF for WCDMA in-building distributed antenna system [45]. Various bi-directional single fibre link for antenna remoting have been demonstrated [46, 47]. A bi-directional fibre optic link permit duplex signal transmission within a single fibre and leads to cost reduction. A bi-directional WoF link employing optical frequency multiplication in the downlink and an optical uplink transmission employing intensity modulation direct detection is demonstrated experimentally [48]. Hybrid free space optical and RF wireless links have also been investigated for broadband wireless networks [49].

1.3.1 Signal transport schemes RF, IF, Baseband

Wireless over fibre systems are commonly classified into three main types of transport schemes: Radio Frequency (RF), Intermediate Frequency (IF) or baseband over fibre. The choice of architecture determines the hardware required at the BS and its complexity. A full duplex system may combine different schemes on the downlink and uplink [50].

RF over fibre

The simplest approach is to use RF over fibre where signals are transported directly at RF or mm-wave over the optical link as shown in Figure 1.3. This has the benefit that the link is transparent since the signals do not undergo any frequency translation. The BS architecture is also reduced in size and greatly simplified requiring only amplification and optical to electrical and electrical to optical conversion. In addition centralised control and processing of the signals allow easier upgradeability and re-configurability. However, at mm-wave frequencies direct transmission of RF signals is challenging because high frequency opto-electronic components are expensive. Large bandwidth photo-diodes with good conversion efficiencies are required both at the CS and BS. External modulation is carried out using a high speed modulator such as a Mach-Zehnder Modulator (MZM) or Electro-absorption modulator (EAM). However, these are expensive, have high insertion loss and good dynamic range performance is required. Full duplex transmission of 60 GHz mm-wave signal using an Electro-absorption Transceiver (EAT) has been demonstrated [51]. Furthermore, Single Sideband (SSB) modulation is needed to overcome chromatic dispersion which is more troublesome than at IF frequencies. The effect of dispersion at a wavelength of 1.55 μm for mm-wave modulated optical signals will limit the transmission distance and induce severe power degradation in the detected RF power of the mm-wave signal [52]. Dispersion effects can be significantly reduced using a single dual electrode MZM to generate optical SSB modulation as proposed by Smith *et al* [53, 54]. The generation, transportation and distribution of modulated optical signals in mm-wave WoF systems has been extensively studied [55, 56,].

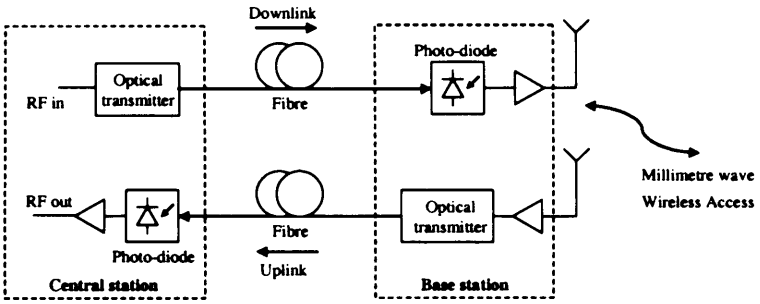

Figure 1.3 Illustration of RF (mm-wave) over fibre system configuration

Chromatic Dispersion

In conventional intensity modulation, the optical carrier is modulated to create two modulation sidebands which are spaced from the carrier by the modulating frequency. When using standard optical fibre (with a chromatic dispersion parameter, D, typically around 17 ps/nm/km at a wavelength of 1550 nm), the modulated optical signal will experience chromatic dispersion as it propagates over the fibre. The two sideband experience different amount of phase shifts because they travel at different velocities owing to fiber chromatic dispersion. Upon reaching the optical receiver, whenever the relative phase

difference between two sidebands becomes out of phase, the photo-detected signal powers are greatly suppressed [57]. The RF power varies in a periodic manner with complete power suppression occurring at certain distances along the fibre length when the phase difference between the two beat signals is equal to 180 degrees.

The dispersion induced penalty on the detected RF power is dependent on the modulation frequency, dispersion parameter and the fibre transmission length. Propagation through fibre results in repetitive length dependent nulls in the received power. The first null occurs at a fibre length L metres, given by [58]:

$$L = \frac{c}{2Df^2\lambda^2} \tag{1.1}$$

where D is the dispersion parameter in ps/nm/km, f (GHz) is the modulation frequency, λ is the wavelength and c is the velocity of light in a vacuum. Millimetre wave operation at 1550 nm is therefore restricted to length of < 3 km at 30 GHz and < 800 m at 60 GHz if large power penalties are to be avoided [59]. When the modulating frequency reduces to 12 GHz the -3 dB RF power loss occurs at a fibre distance of 12 km. With lower modulating frequency i.e. 5 GHz the effect of dispersion is greatly reduced and signals can be transmitted at RF by direct modulation of an optical source.

Since fibre induced dispersion penalties are severe in direct detection optically fed mm-wave systems, it is necessary to consider alternatives, which may mitigate this problem. Techniques to cope with the effect of fibre dispersion mainly focus on heterodyne techniques [60] and other schemes based on chirped fibre gratings [61]. The transmission of two phase correlated optical modes separated by the desired mm-wave frequency in heterodyne technique will not be affected by fibre chromatic dispersion since there is only a single beat RF component generated at the receiver. In conventional intensity modulation, it is obvious that the dispersion effects can be overcome by elimination of one of the optical sidebands to generate optical single sideband (SSB) modulation. A convenient technique to produce optical single sideband modulation is via optical filtering where one of the optical sidebands is rejected [62]. Although both the optical carrier and the sideband experience a phase shift due to dispersion, there is only a single beat signal generated at the photo-detector therefore the detected RF power is not affected by dispersion. The filtering of the sideband can be performed using a fibre Bragg grating as a narrowband notch filter where the reflective band coincides with the wanted optical sideband. While this technique is easy to implement, the limited flexibility makes the implementation difficult to accommodate for any changes in the mm-wave frequency.

IF over fibre

Another scheme to reduce fibre chromatic dispersion effect is to transmit the radio signals over fibre at IF rather than mm-wave frequencies with remote up-conversion performed at the BS as shown in Figure 1.4. The dispersion penalty on the detected signal is greatly reduced by lowering the modulating frequency. The MODAL (Microwave Optical Duplex Antenna Link) [63] project has demonstrated a

30 GHz system using a mm-wave carrier to down-convert signals to a lower IF (2GHz). Depending on the frequency of the IF carrier and the modulation bandwidth of the optical sources, either direct or external modulation can be considered. Direct modulation of a laser source at the BS provides a low cost architecture for the uplink. The intermodulation characteristic of the link is greatly improved and optical components with less stringent requirements can be used. Another advantage is that the link efficiency is higher at lower microwave frequencies and lower cost optoelectronic components can be used [64] with the potential for substantial cost savings. However, the complexity of the BS increases since a LO signal and a mixer is required for frequency conversions [65]. This may also be a limitation when considering the ability to upgrade the network. The requirement of a LO at each BS may not be a problem at low frequencies, where low cost, low phase noise MMIC based LO sources are likely to be available. But at mm-wave, it may be more desirable to deliver the LO remotely to the BS from the CS on a separate wavelength multiplexed with the IF signals. The LO can be shared between the uplink and downlink, using a mm-wave splitter and dispersion penalties can be made negligible using heterodyne generation techniques [66] such as Optical Injection Phase Lock Loop (OIPLL) [67].

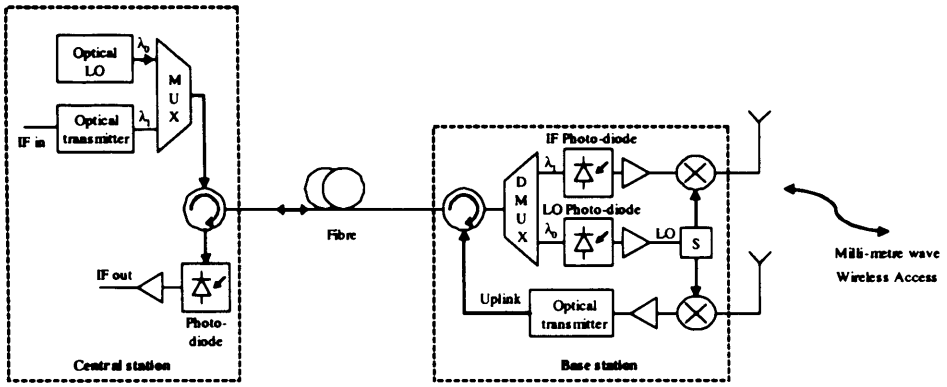

Figure 1.4 Illustration of IF over fibre system with optical LO delivery

Baseband over fibre

In a baseband over fibre transport scheme (also referred to as Digital over fibre), data is transmitted at baseband over the optical link. On the downlink the detected baseband signal at the BS need to be imposed on a mm-wave carrier prior to transmission through the air interface. Similarly, on the uplink from the receiving antenna, the data carrying mm-wave signal need to be down-converted to baseband data before being imposed onto an optical carrier and transmitted over fibre towards the CS. The main benefit of this scheme is the greatly reduced effects of chromatic dispersion and it is therefore attractive for architectures that require long transmission links. The scheme also enables the use of mature digital and microwave technology and low speed opto-electronic devices. However, the reduced effects of dispersion is at the expense of a more complicated BS as additional hardware and signal processing circuits are required at the BS (such as up/down conversion and demodulation) to

process the received and transmitted radio signal. This results in a complex BS architecture and hence it is harder to produce a cost effective approach.

Wireless over Fibre based WLAN

The demand for broadband wireless LAN is increasing meaning that higher carrier frequencies will be used to allow higher data rates. For instance WLAN for the 11 Mbps (IEEE802.11b) operate in the 2.4 GHz band, while the IEEE802.11a offering 54 Mbps operate in the 5 GHz band. To provide large area network coverage such as at an airport, delivery of the WLAN signals to remotely located BSs using optical fibre is preferred because of higher transmission loss associated with microwave coaxial cables. For these networks to go broadband, the capacity of the network must also be increased. Copper based wired LANs that feed wireless LAN will not be adequate due to higher loss and will have to be replaced by high capacity infrastructure using optical fibre. Also, current systems are not upgradeable when a new 802.11 standard is introduced since a new installation is needed which can be difficult to manage.

It is important to note that the physical layer performance (link gain, phase noise, dynamic range, etc) of a WoF system may not be the only limitation to their application for wireless signal distribution. In the point to multipoint system configurations, the nature of the Medium Access Control (MAC) protocol of the wireless systems may place limitations on the maximum fibre link distance. This is due to the fact that by centralising all signal processing functions at the CS, the mobile unit access to radio resources at the BS is also controlled remotely. As a result, extra signal propagation delay imposed by the fibre link might interfere with the MAC protocol timing boundaries [68], leading to either poor performance (data throughput) or failure of the MAC protocol [69].

The medium access control of the IEEE802.11 uses Carrier Sense Multiple Access with Collision Avoidance (CSMA/CA) as the fundamental access [70]. The IEEE802.11 MAC provides a fair access to the shared wireless medium. If the wireless terminal unit senses that the medium is busy, or has just successfully transmitted a frame, it executes a back off, waits a random time before attempting to access the medium again. The limits of this time wait, and other time out are built into the protocol, on the basis of the anticipated maximum cell sizes (air propagation delay) [71]. Thus the introduction of extra signal delays owing to the fibre link may cause some of the protocol timing limits to be exceeded, resulting in reduced performance or failure of the protocol altogether. Thus in distributed MAC protocols, only short fibre links may be accommodated. The maximum length of fibre that could be deployed in a IEEE802.11b standard is 1948 m (according to the minimum timeout value defined in the standard) [72]. In contrast, centrally scheduled MAC schemes, such as HiperLAN/2 and IEEE802.16, the effect of the additional propagation delay is less severe since the timing between different phases are allowed to be adjusted by the BS [68]. Therefore, centrally controlled MAC protocols are generally perceived to be more suitable for long wireless over fibre distribution links [69].

1.3.2 Sub-carrier multiplexing (SCM)

The advantage of analogue optical links is that RF or microwave signals can be directly modulated onto an optical carrier for transport without having to demodulate and remodulate. However, due to nature of analog signals or sub-carriers, the requirements on optical link, in terms of SNR and linearity, are much more stringent than digital optical links.

A single channel can be used by multiple users using some sort of multiple access technique to distinguish different radio channels by either utilising different frequency, time slots or code allocations. Frequency division multiple access (FDMA) discriminates different customer units in frequency whereby each customer is allocated a distinct frequency carrier. Similarly, time division multiple access (TDMA) allocates different time slots for different users while code division multiple access (CDMA) is based on spread spectrum techniques and different users transmit at the same time and in the same frequency band but are allocated a unique receiving or accessing code.

SCM technique can be employed in analogue optical links to achieve high data rate and is an effective way to exploit the vast bandwidth provided by SMF. Such a distribution scheme is common and attractive scheme for the optical distribution of multiple RF channels. An example of SCM based system is represented in Figure 1.5. In SCM, radio signals are frequency division multiplexed together and the radio signals either directly or externally modulate the optical carrier [73]. The total effective

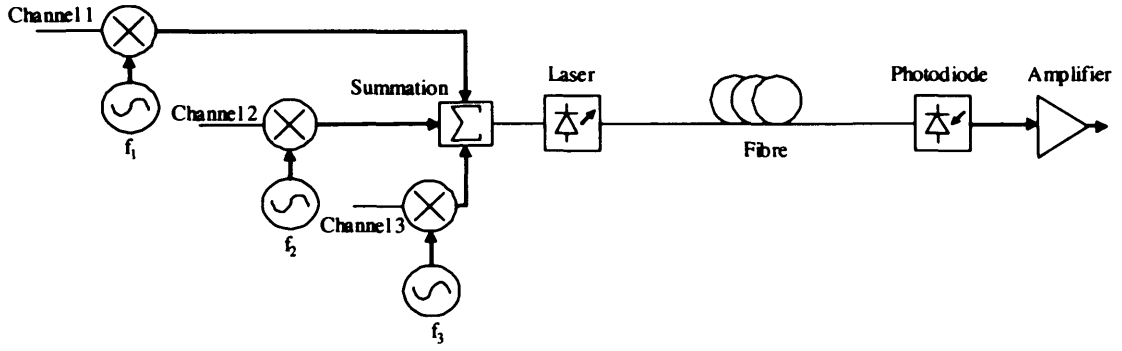

Figure 1.5 Sub-carrier multiplexed transmission

modulation index in a sub-carrier multiplexed system must be small enough so that clipping of the signal is not introduced. It occurs because when a number of random signals are added together it can be hard to determine what the maximum amplitude of the combined signals will be. At the receiver the desired channel is separated by an electrical filter after photo-detection. SCM is simple to implement and allows for fast deployment as it does not require any specialised complex circuitry for synchronisation. Furthermore the services carried by different sub-carriers are independent of each other. However, due to the non-linearity of the electrical to optical conversion, intermodulation distortion resulting from the interactions between the sub-carriers can cause degradation in the system performance. In a multi-channel system, transmitter distortion results in signal crosstalk. The net result is that the SNR is decreased and performance is degraded.

1.3.3 Direct and external modulation

Modulation techniques can be categorised as direct and indirect modulation [74]. In the simplest, intensity modulation direct detection (IMDD) the microwave signal is modulated on an optical carrier, using either a directly modulated laser source or a CW light source with an external modulator [75] shown in Figure 1.6. The resulting intensity modulated signal is transmitted through fibre to the photodiode where the modulation is returned to the electrical domain.

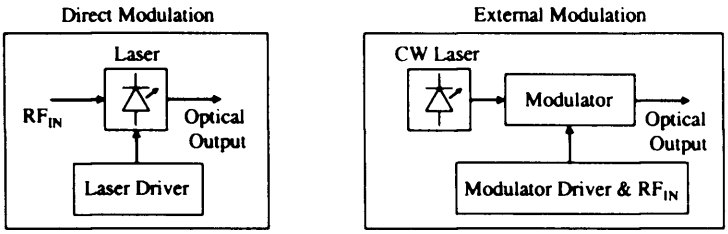

Figure 1.6 Direct and external modulation

The main advantage of direct modulation is its simplicity [76, 77], small size, low power consumption, simple drive electronics and low cost. The modulating signal is combined with the bias current which drives the laser and the output light intensity is proportional to the modulating signal. When the laser diode is directly modulated non-linear fluctuations of the electron and photon density in the active region cause non-linear distortion. These distortion products act as a limitation on the use of direct modulation system in the high frequency region. Direct modulation of the laser is also limited in frequency by the inherent bandwidth of the laser diode. Directly modulated lasers with a bandwidth as high as 40 GHz have been reported for unpackaged lasers [78] at a very high bias current. Modulation bandwidth exceeding 25 GHz has been achieved for a packaged 1550 nm DFB laser [79]. It has been shown that using external injection into the laser enhanced modulation response of the device can be obtained [80].

Directly modulated semiconductor lasers are of considerable interest for applications in microwave sub-carrier multiplexing and cable television (CATV). For high quality transmission these systems require modulated lasers to be highly linear with minimum distortion. However, undesired effects such as frequency chirp, non-linearity of the laser diode and intermodulation distortion (IMD) limit the system performance. If the non-linearity of the laser is sufficiently large then IMD can give rise to interchannel interference. In addition, intensity noise introduced by the laser may degrade the system signal-to-noise (SNR) ratio. High SNR can be achieved by increasing the modulation signal level in optical sources; however, harmonic distortion and IMD increase with increased optical modulation depth or input power. These are the major obstacles to the applications of direct modulation in a WoF system.

An alternative to a directly modulated laser is a CW light source (such as an unmodulated semiconductor laser) [81] with an external modulator (MZM or EAM) [82]. Since the functions of light generation and modulation are separated, this provides the flexibility to optimise both the laser

and the modulator. The MZM operates on the principle that the optical carrier is split into two waveguides of equal amplitude signals, the phase of one of these signals is shifted via the linear electro-optic effect, and the signals are recombined. When the optical carriers are set to a 0° phase difference, they sum to give a signal of maximum amplitude. When the carriers are set to a 180° phase difference they cancel. The main problem with external modulated transmitter is the relatively high insertion loss and they exhibit non-linear light vs voltage transfer functions. The second order harmonic distortion in external modulators is lower then directly modulated lasers depending on the bias. However, depending on the frequency of operation the third order intermodulation distortion can be higher in external modulators than semiconductor lasers. The typical insertion loss of the MZM is about 7 dB which includes 3 dB from the waveguide loss at the combiner and an additional 3 dB loss since the modulator has to be biased at a half power point. Ti:$LiNbO_3$ optical modulator have been demonstrated with a -3 dB modulation bandwidth of more than 75 GHz with a driving voltage of 5.0 V at a wavelength of 1.5 μm [83] and at 100 GHz [84]. An externally modulated source has low chirp and reduces the need for dispersion compensation. However, there are several disadvantages associated with the use of external modulators. They tend to be bulky, expensive and consume much RF power. Also since the modulator bias voltage point drifts a control circuit is required.

Electro-absorption modulators (EAMs) are attractive because of their small size, low drive requirements, DC drift free operation and the ability to be integrated with lasers and/or semiconductor optical amplifiers. This type of modulator offers lower power consumption than LiNbO3 MZ type modulators [85]. A feature of the electro-absorption wave guide structure is that they can be utilised both for modulation and photo-detection, thus enabling the assembly of an electro absorption transceiver (EAT) as a single device. The EAT can operate in a completely passive mode, making it possible to construct simple BSs with a low device count, however the limited dynamic range and output power from the passive EAT make them better suited for picocellular environments. Westbrook *et al* [86] proposed a bi-directional link eliminating the need for an optical source at the remote BS by incorporating an EAM that may be simultaneously used as a photo-detector and a modulator. They also proposed optimising the device so that the EAM detects and modulates without dc power, allowing the unit to be completely passive. However, to achieve this EAM is not operated at its optimum point for photo-detection or for modulation; hence the performance is degraded for uplink and downlink. Wake *et al* [87] incorporated an EAM in a fibre radio link to demonstrate a passive remote antenna BS. Wake *et al* also showed that further experimental improvements could allow radio cells with up to 100 m coverage at an operating frequency of 2 GHz to be achieved. The major drawback for applying this passive picocell concept to mm-wave fibre radio systems are the poor opto-electronic and electro-optic conversion efficiencies at higher frequencies. The passive picocell [88] concept distributes these signals through optical fibre as microwave modulated optical signals with a combined modulator/detector at each BS to provide a transceiver radio path.

It has also been shown that an electro-absorption modulator (EAM) can be used as a single component in a radio access point [88]. This concept was demonstrated using a commercial 2.4 GHz radio LAN providing wireless Ethernet at a data rate of 3 Mbit/s. The schematic of the experimental layout is shown in Figure 1.7. A Wireless LAN at 60 GHz has also been demonstrated using WoF approach [89]. In general, the WoF system must be able to distribute wireless LAN signals efficiently and according to specifications in the standard.

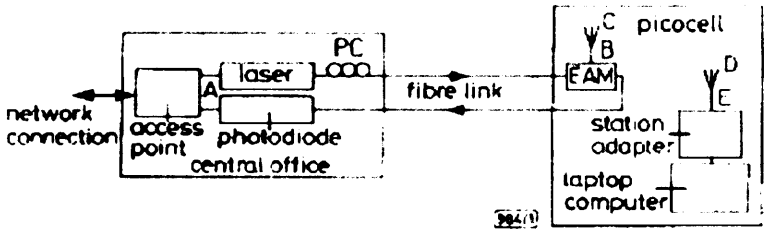

Figure 1.7. Experimental layout of a wireless over fibre based WLAN system [88]

A compact mm-wave transceiver has been developed for a WLAN system [90] and a 60 GHz EAT has been investigated by Kitayama *et al* [91] to realise a low cost BS. An experiment using an electro-absorption transceiver mixer (EATX) device has also been demonstrated. The EATX simultaneously acts as a mm-wave photo-detector, an IF band external modulator, and an IF to RF up-converter. However, further research is required to manufacture a cost effective EAT operating at mm-wave frequencies, while optimising the modulation characteristics and responsivity of the device and minimising crosstalk between the two channels.

Using an Asymmetric Fabry-Perot Modulator (AFPM) as a modulator and a detector significantly reduces the complexity of the BSs. The downlink signal is detected by the AFPM and radiated by the antenna. The radio uplink signal received by the antenna is fed to the AFPM, which in turn modulates the residual light left from the downlink direction [92]. This residual light, now carrying the uplink signal is reflected by the AFPM back to the CS. Simultaneous wireline (600 MHz) and wireless 5.5 GHz transmission of data over cable service interface specification (DOCSIS) [93] signals in a hybrid fibre radio access network is presented using a packaged AFPM [94]. The AFPM is employed at the BS and acts simultaneously as a photo-detector and an optical modulator. The non-linearity and SFDR have been studied theoretically [95].

1.4 Characteristics of Optical Links

This section introduces the main considerations involved in analog fiber optic links. In WoF systems the linearity performance and the required dynamic range is often more stringent for uplink than downlink. For the downlink, multiple channels with equal power levels are transmitted from the CS to the BS and further to mobile unit. However in the uplink path, where no user transmitter power control techniques are employed, propagation path loss, multi-path fading and the varying positions of users in a radio cell can result in large variations in received signal powers at the remote BSs. When a number

of high power signals are received at the BS, the mixing of the signals in a non-linear device cause third order intermodulation distortion (IMD) terms. This places a stringent requirement on the dynamic range of the uplink in a WoF system and the impact of optical non-linearities arising from the non-linear electrical to optical conversion is far more severe on the uplink than the downlink. The distortion can significantly degrade the quality of lower power received signals to the point that the signal quality is so poor that the channel is unusable. Hence it is important to characterise the dynamic range of the optical transmitter in the BS.

1.4.1 Optical transmitters

The goal of the analog link is to provide an RF output signal that is a good reproduction of the RF input. Typically, the fibre, optical amplifiers, photo-detector, and RF power amplifiers have a very good performance in terms of linearity. It is the optical transmitter that usually limits the performance of the link. For a semiconductor laser, the distortion physically originates from the non-linear characteristics of the laser, including non-linearity of the light-current (LI) curve, the carrier-photon interaction, or from spatial hole-burning [96]. Distortion at the transmitter can also occur due to the clipping of the signal. If the signal amplitude is too large, the signal will be clipped due to the laser threshold. The clipping distortion sets a limit on the maximum allowed modulation index. Transmitter distortion is extremely important for multi-channel systems and leads to a reduction in the dynamic range of the system. For applications where the device linearity is not high enough, techniques have been developed to linearise the transmitter.

1.4.2 Noise sources in fibre optic system

For optical links where a large dynamic range is desirable, a low system noise is necessary. The noise floor of the link determine the minimum detectable RF signal, while the non-linearities in the link limit the maximum RF signal power and channels that can be transmitted. One of the dominant sources of noise in a link is the laser noise termed Relative Intensity Noise (RIN). Laser intensity noise is caused by fluctuations due to spontaneous light emissions. Operating conditions, such as bias level and modulation frequency, also directly affect the noise level. The presence of external feedback or reflections into the laser also increase this noise and reduce signal to noise ratio (SNR) resulting in higher BER. RIN is the ratio of the mean square optical intensity noise to the square of the average optical power and is given by:

$$RIN = \frac{\langle \Delta P \rangle^2}{P^2} dB/Hz \tag{1.2}$$

where $<\Delta P^2>$ is the mean square optical intensity fluctuation (in a 1 Hz bandwidth) at a specified frequency, and P is the average optical power. The ratio of the optical powers squared is equivalent to the ratio of the detected electrical powers. Thus, RIN can be expressed in terms of detected electrical powers and equation (1.2) can be rewritten as:

$$RIN = \frac{N_{elec}}{P_{AVG(elec)}} dB/Hz \tag{1.3}$$

where N_{elec} is the power spectral density of the photo-current and $P_{AVG(elec)}$ is the average power of the photocurrent. The noise power in IMDD link typically consists of three effects; thermal noise, shot noise and laser intensity noise. The total system noise, N_T is the summation of the individual noise terms and is given by:

$$N_T = N_{th} + N_q + N_L (W/Hz) \tag{1.4}$$

where N_{th} is the contribution of thermal noise power per Hz, N_q is the shot noise power per Hz, N_L is the laser intensity noise power per Hz. The shot and intensity noise depend on detected optical power. The thermal noise limits the sensitivity of the receiver and expressed in dB relative to the room temperature is –174 dBm/Hz. For a system at a given temperature, thermal noise is constant, but shot noise varies with average power. Shot noise (N_q) is produced by the quantum nature of photons arriving at the detector. The noise produced is related directly to the amount of light incident on the photodiode. The mean squared noise current is

$$\langle i_n^2 \rangle = 2qI_{PD}B \tag{1.5}$$

where q is the charge on the electron, I_{PD} is the photodiode current due to the average optical power input, and B is the electrical noise bandwidth (typically normalised to 1 Hz). The familiar equation $P=I^2R_L$ where R_L is the load resistance of the amplifier input, is used to convert this noise current into units of power. Therefore, the shot noise power, Nq, in a one Hz bandwidth, becomes:

$$N_q = 2qI_{PD}R_L \tag{1.6}$$

The value of the laser intensity noise is found from Equation (1.4) by subtracting the values of shot and thermal noise from the total system noise.

$$N_L = N_T - N_q - N_{th} \tag{1.7}$$

When the noise of the laser exceeds the shot noise or thermal noise, the total system noise is essentially equal to the laser intensity noise. In such cases, RIN_{Laser} equals RIN_{System}.

1.4.3 Carrier-to-Noise ratio (CNR)

An important parameter used to characterise the quality of a link is the ratio between the received carrier signal and the unwanted total noise introduced through the link known as the carrier to noise ratio (CNR). Since noise is always added in a link, the input CNR is always higher than the output CNR. It is important to ensure that the received CNR of a channel is large enough to maintain acceptable signal quality. The CNR of a WoF system can be represented by [97]:

$$\frac{C}{N} = \frac{\frac{1}{2}m^2 I_{ph}^2}{\left(RIN.I_{ph}^2 + 2qI_{ph} + \langle I_{th}^2 \rangle\right)BW} \tag{1.8}$$

where m is the optical modulation depth (proportional to RF power), I_{ph} is the received dc photocurrent, I_{th} is the input noise current spectral density, BW is the signal bandwidth, and q is the charge on the electron. The first term in the denominator of equation (1.8) is the RIN of the laser, the second is the shot noise, and the third is the thermal noise. It can be observed from Equation (1.8) that in order to achieve a link with large CNR, it is necessary to employ lasers with low RIN and to reduce the receiver bandwidth as much as possible. A further limit is set by distortion. Second order products can be removed easily by filtering since they are far from the signal frequency band. However third order IMD products can be included with the CNR resulting in a ratio that represents the carrier to noise plus distortion ratio (CNDR) and this can be represented by [97]:

$$\frac{C}{(N+D)} = \frac{\frac{1}{2}m^2 I_{ph}^2}{\left(RIN.I_{ph}^2 + 2qI_{ph} + \left\langle I_{th}^2 \right\rangle\right)BW + IMD} \tag{1.9}$$

If the signal strength is too small compared to the strength of the noise and the IMD terms, it will not be possible for a link to operate correctly and for digital transmission this will result in a bit error. For a link that is transmitting QPSK signals, Harada *et al* [97] indicated that a minimum CNDR ($CNDR_{min}$) of 13.8 dB was required to achieve a BER of less than 10^{-6}.

Noise Factor and Noise Figure

The Noise Factor (F) is a degradation of the SNR as the signal passes through a device and is the ratio of the SNR power at the input to the SNR power at the output and the definition is

$$NoiseFactor(F) = \frac{SNR_{in}}{SNR_{out}} \tag{1.10}$$

where SNR_{in} and SNR_{out} are the signal to noise ratio at the input and output of the system respectively which are represented as:

$$\begin{aligned} SNR_{in} &= \frac{P_{in}}{N_{in}} \\ SNR_{out} &= \frac{P_{out}}{N_{out}} = \frac{GP_{in}}{N_{out}} \end{aligned} \tag{1.11}$$

where P_{in} is the input RF power, N_{in} is the noise at the input, G is the gain of the system and N_{out} is the noise at the output. The noise figure (NF) can be obtained from the noise factor (F) by $NF = 10\log(F)$ where the noise figure is in dB. The linear version of the noise figure, the noise factor, is a unit less quantity. Substituting Equation (1.11) into Equation (1.10) enables the noise figure to be expressed as:

$$NoiseFigure(NF) = N_{out} - N_{in} - G \tag{1.12}$$

The overall system NF depends on the noise figure and gain of each block in the system. The receiver noise figure determines the receiver sensitivity defined as the minimum signal level that the system can

detect with acceptable output SNR. The sensitivity of the receiver in units of dBm is given by:

$$Sensitivity[dBm] = -174dBm/Hz + NF_{system} + 10Log(B) + 10Log(S_o/N_o)_{\min} \quad (1.13)$$

where the first term on the right hand side of the above equation is the noise power at 290 degrees K, NF_{system} is the system noise figure, B is the bandwidth and the last term is the minimum acceptable output SNR in dB. In the case when digital modulation is used, the minimum acceptable output SNR is a function of the required BER and the modulation method used.

1.4.4 Dynamic range

One of the most important figures of merit in a wireless over fibre system is the spurious free dynamic range (SFDR) which defines the linearity of the optical link. The minimum RF input power where the output signal is equal to the noise floor is known as the minimum detectable signal (MDS). The maximum RF input power is the point corresponding to where the power of the non-linearity distortion terms are equal to that of the noise floor. This range of input powers between the minimum and maximum RF input powers where the signal is above the noise or distortion products is known as the SFDR. It is defined as the power difference between the signal and the system noise floor, at the point when the intermodulation distortion power equals the system noise floor. Dynamic range takes into account both the distortion and noise, hence is often used to describe the performance of a transmitter. The distortion can originate from several sources: 2nd and 3rd harmonics of the signals, intermodulation distortion, and laser threshold clipping. SFDR is a strong function of frequency, and for directly modulated lasers has its lowest value at frequencies near the relaxation oscillation frequency. Thus, lasers are typically modulated at frequencies well below this frequency. The SFDR also depends on the noise bandwidth because this affects the output noise level [98].

To characterise the link dynamic range the SFDR can be calculated [99]. To determine the SFDR the input power is virtually decreased until the distortion level equals the noise floor. The signal power, or fundamental tone, varies with a slope of 1. The third order IMD terms vary with a slope of 3. If higher order intermodulation terms are present they will also give a contribution and the SFDR is then not calculated correctly. The noise floor used can either be the laser RIN limited value, or the total link noise, including receiver thermal noise. If the system under investigation is assumed to be thermal noise limited, SFDR can be defined by:

$$SFDR = \frac{2}{3}\left(IP_3 - NF - G - N_{th} - 10\log_{10} B\right) \quad (1.14)$$

where IP3 is the third order intercept point where the fundamental signal power is equal to the generated third order intermodulation product, NF is the noise figure in dB, N_{th} is the thermal noise power which is calculated to be -174 dBm/Hz at room temperature and B is the system bandwidth. The SFDR must be high enough for the services to be accommodated and can also be estimated by substituting equation (1.12) into equation (1.14):

$$SFDR = \frac{2}{3}(IP_3 + N_{in} - N_{out} - N_{th} - 10\log_{10} B) \quad (1.15)$$

1.4.5 Modulation quality measurements

Digital bits are transferred onto an RF carrier by varying the carrier's magnitude and phase such that, at each clock transition, the carrier occupies any one of several specific locations on the I versus Q plane. Each location encodes a specific data symbol, which consists of one or more data bits. A constellation diagram shows the valid locations (for example, the magnitude and phase relative to the carrier) for all permitted symbols, of which there must be 2^n, given n data bits transmitted per symbol. Thus to demodulate the incoming data, the exact magnitude and phase of the received signal for each clock transition must be accurately determined. The layout of the constellation diagram and its ideal symbol locations is determined by the modulation format (QPSK, 16QAM).

There are a number of different ways to measure the quality of a digitally modulated signal. Error vector magnitude (EVM) expressed as a percentage is the most widely used modulation quality metric in most wireless standards and can provide a great deal of insight into the performance of digitally modulated signals. EVM can quantify the errors in digital modulation and is sensitive to any impairment of signals which affects magnitude and phase of the demodulated signal. The EVM is the vector difference between the ideal reference signal and the measured signal. Figure 1.8 shows a graphical representation of these differences. In reality a number of events (phase noise, non-linearity, modulation or data errors etc) can cause any of the symbols to shift from their ideal place.

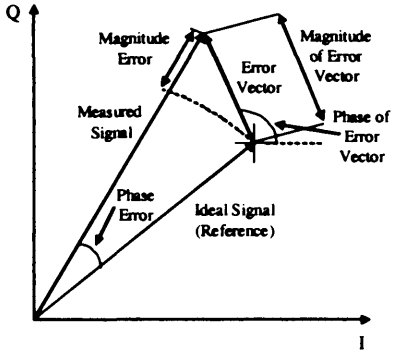

Figure 1.8. Error vector and related parameter [100]

The error vector is a complex quantity that contains a magnitude and a phase component which involves residual noise and distortion. It is possible to use EVM to calculate the BER via SNR. It is desirable to keep the error vector to a minimum for accurate transmission of data and to have the value of SNR as high as possible. The relation between SNR and EVM can be approximated by [101]:

$$SNR = -20\log(EVM/100\%) \quad (1.16)$$

Transmission performance can also be directly characterised using the BER and it is conventional to consider transmission as error free for BER $<10^{-9}$. The power penalty indicates the necessary adjustment of the receiver power as a result of transmission degradation to maintain BER of 10^{-9}.

1.5 Objectives and Novel Achievements of the Thesis

The objectives and novel achievements of this work are as follows. A complete list of publications originating from the achieved results is given in 1.5.2.

1.5.1 Objectives of the thesis

A number of objectives for this thesis can be identified and these are summarised below:

1. To investigate highly linear microwave modulated optical sources to achieve 3rd order SFDR exceeding 95 dB.Hz$^{2/3}$ enabling several operators using different modulation formats to use the same broadband wireless infrastructure.
2. To realise optical feed-forward technique at microwave frequency (5 GHz) with wide bandwidth for improving the SFDR of commercially available directly modulated uncooled DFB lasers.
3. To consider automatic adjustment of feed-forward parameters to overcome environmental changes for optimum distortion cancellation and system performance.
4. Investigate low cost architectures for broadband wireless systems which make efficient use of optical fibre plant, since fibre may have to be leased for outdoor applications.
5. To study the use of a bi-directional Semiconductor Optical Amplifier (SOA) in a fibre supported wireless systems to reduce system complexity and cost. This will allow both up and down link paths to use the same amplifier and permit full duplex signal transmission within a single fibre leading to 50% reduction in the amount of fibre required.
6. To demonstrate the feasibility and performance advantages of proposed architectures through the construction of a system demonstrator for a mm-wave Gbit/s wireless over fibre system.
7. Finally to examine the use of non-temperature controlled components to deliver greatly reduced system cost.

The main challenges in the design and implementation of mm-wave systems is low cost network architecture for the transmission of broadband signals to a number of BSs using a bi-directional fibre link. A satisfactory solution of this problem will provide a very important advance in the development of low cost technologies for mm-wave over fibre systems.

1.5.2 Novel achievements of the thesis

The novel achievements of this thesis are as follows:

1. The first application of optical feed-forward linearisation to achieve large dynamic range in WoF systems.
2. The first implementation of feed-forward technique at 5.2 GHz for linearisation of an uncooled, low cost, commercially available 1550 nm DFB laser. This operating frequency is required for the IEEE802.11a standard and is the highest reported for a feed-forward linearised laser.

3. Development of a wide bandwidth feed-forward system showing a record 500 MHz bandwidth at 5. 2 GHz with at least 24 dB distortion suppression.
4. First transmission experiment using feed-forward in a multi-channel data transmission for a WoF system at 2.4 GHz and 5.8 GHz.
5. New architecture using low cost Coarse Wavelength Division Multiplexing (WDM) components and the first investigation of uncooled optical sources in a WDM optically fed mm-wave wireless systems, through the use of wavelength routeing and up/down conversion using optical LO distribution with a potential for major cost reduction.
6. The first investigation of a bi-directional SOA for complexity and cost reduction in fibre fed wireless systems.
7. The highest demonstrated data rate (1 Gbit/s) in a mm-wave over fibre transmission system without optical amplification using CWDM passive components and uncooled laser sources.

This research has led to the publication of the following papers:

T. Ismail and A. J. Seeds, "Nonlinear distortion reduction in directly modulated semiconductor laser using feed-forward linearisation", *Proc. London Communications Symposium*, pp. 325-328, 2003.

T. Ismail, C. P. Liu and A. J. Seeds, "Uncooled directly modulated high dynamic range source for IEEE802.11a wireless over fibre LAN applications", *Optical Fibre Communications (OFC),* FE3, 2004.

T. Ismail and A. J. Seeds, "Feed-forward linearisation of directly modulated laser for radio over fibre wireless LAN", *Second NEFERTITI Winter School in Microwave Photonics*, 2004.

T. Ismail and A. J. Seeds, "Laser diode nonlinearity compensation using feed-forward linearisation in a fibre radio system", *Postgraduate Research Conference in Electronics, Photonics, Communications & Networks, and Computing Science (PREP),* 2004.

T. Ismail, C. P. Liu, J. E. Mitchell and A. J. Seeds, "Multi-Channel broadband wireless transmission over fibre using feed-forward linearised uncooled DFB laser", *European Conference on Optical Communication (ECOC),* Tu3.5.2, 2004.

T. Ismail, C. P. Liu, J. E. Mitchell and A. J. Seeds, "Interchannel distortion suppression for broadband wireless over fibre transmission using feed-forward linearised DFB laser", *IEEE International Topical Meeting on Microwave Photonics (MWP),* TE-2, pp. 229-232, 2004.

T. Ismail and A. J. Seeds, "Improved laser dynamic range using feed-forward linearisation in a radio over fibre system for WLAN", *Proc. London Communications Symposium*, pp. 249-252, 2004.

T. Ismail, C. P. Liu, J. E. Mitchell, A. J. Seeds, X. Qian, A. Wonfor, R. V. Penty and I. H. White, "Bidirectional transmission of broadband wireless signals using a millimetre wave over fibre CWDM ring architecture", *NEFERTITI Workshop on Millimetre Wave Photonic Devices and Technologies for Wireless and Imaging Application (MPWI)*, 2005.

T. Ismail, C. P. Liu, J. E. Mitchell, A. J. Seeds, X. Qian, A. Wonfor, R. V. Penty and I. H. White, "Full-duplex wireless-over-fibre transmission incorporating a CWDM ring architecture with remote millimetre-wave LO delivery using a Bi-directional SOA", *Optical Fibre Communications (OFC)*, OThG7, 2005.

T. Ismail and A. J. Seeds, "Compensation of laser diode intermodulation distortion in a radio over fibre system", *Postgraduate Research Conference in Electronics, Photonics, Communications & Networks, and Computing Science (PREP)*, 2005, UK.

T. Ismail, J. E. Mitchell and A. J. Seeds, "5.8 GHz OFDM signal transmission in a Radio over Fibre system", *NEFERTITI Workshop on Photonics in Wireless Communications (PWCom): Cost effective solutions and future technologies*, 2005.

T. Ismail, J. E. Mitchell and A. J. Seeds, "Linearity enhancement of a directly modulated uncooled DFB laser in a multi-channel wireless-over-fibre system", *IEEE MTT-S International Microwave Symposium (IMS)*, TU1A-2, 2005.

T. Ismail, C. P. Liu, J. E. Mitchell, A. J. Seeds, X. Qian, A. Wonfor, R. V. Penty and I. H. White, "QPSK wireless data over 12.8 km fibre transmission with remote millimetre-wave LO delivery using a Bi-directional SOA in a full-duplex system incorporating a 2.2 km CWDM fibre ring architecture", *IEEE Photon. Technology Lett.*, vol. 17, no. 9, pp. 1989-1991, 2005.

T. Ismail, C. P. Liu, J. E. Mitchell and A. J. Seeds, "Feed-forward linearised uncooled DFB laser in a multi-channel broadband wireless over fibre transmission at 5.8 GHz", *IEEE International Topical Meeting on Microwave Photonics (MWP)*, 2005.

T. Ismail, J. E. Mitchell and A. J. Seeds, "Transmission of WiMAX OFDM data in a wireless over fibre system using a directly modulated DFB laser with remote LO delivery", *The 2nd Institution of Engineering and Technology International Conference on Access Technologies*, pp. 77-80, 2006.

C. P. Liu, T. Ismail and A. J. Seeds, "Broadband access using wireless over fibre", *BT Technology Journal*, vol. 24, no. 3, 2006 (Invited paper).

1.6 Thesis Organisation

The structure for the rest of this thesis is as follows:

Chapter 1 is the introductory chapter and presents the background material for the thesis and provide an overview of WoF technology with literature references on different architectures. Millimetre-wave frequencies and radio propagation characteristics are briefly discussed and concepts for microcells and picocells are introduced. Direct and external modulation schemes are compared and important parameters for analogue optical links are discussed. The chapter concludes with statement of the objectives, a summary of novel achievements and outline for reminder of the thesis.

Chapter 2 introduce the problem imposed by laser non-linear distortion, its effects on dynamic range and overall system performance. Non-linear effects in laser diodes are presented. Various linearisation techniques are outlined that have been proposed in the literature. Electrical (Pre-distortion), optical (Dual parallel, Optical injection locking) and electro-optical linearisation techniques (Optoelectronic feedback, Quasi-feedforward and Optical feed-forward) are discussed which can enhance the performance of optical sources. Furthermore, a comparative study of these techniques discusses the advantages and disadvantages of each method.

Chapter 3 describe the theoretical and experimental work and discuss feed-forward in a greater depth. This includes theoretical analysis of the linearisation system and experimental work performed for the first demonstration of a 5 GHz feed-forward system using uncooled DFB lasers. Each aspect of amplitude, phase and path matching is explained in detail. Ageing and temperature effects require feed-forward to be readjusted; therefore possible adaptive techniques are discussed. The result of two tone measurements and SFDR are presented on a feed-forward linearised laser diode. Multi-channel data transmissions at 2.4 GHz and 5.8 GHz is also described in a WoF system

Chapter 4 discusses wireless over fibre networks together with a review of mm-wave over fibre literature. Heterodyne techniques such as optical injection locking are described for the generation of a 40 GHz LO signal to allow frequency up/down conversion at the BS for mm-wave applications. Network architectures such as star, star tree, bus and ring are discussed and compared. The ring architecture is described in greater details and important factors such as flexibility and protection against faults are identified. A link budget calculation is done for the proposed low cost Gigabit/s system and simulation results are presented. Finally, the use of a SOA in a WoF system is described with important considerations for SOA non-linearity.

Chapter 5 presents experimental results for full duplex Bi-directional RF and mm-wave over fibre systems. A 2.4 GHz feed-forward linearised laser is used in a WoF system to improve the performance of the BS in a 2.2 km fibre ring. The first experimental demonstration of a full duplex mm-wave system is performed using a bi-directional SOA system with a remote LO delivery. Finally, a low cost Gbit/s solution proposed in Chapter 4 is experimentally demonstrated with 1 Gbit/s differential phase shift keying (DPSK) data.

Chapter 6 concludes this thesis with a summary of the main results and discussion concerning novel achievements. Recommendations for future work in this field are also highlighted.

1.7 Conclusion

This chapter has given the background to this work and introduced fixed wireless mm-wave systems and wireless LAN technologies. An introduction to WoF and various signal transport schemes has been given which highlight the advantages of centrally controlled hardware leading to simple and low cost remote BSs. In contrast to mm-wave over fibre, the effect of fibre chromatic dispersion on the distribution of IF frequency signals is much less severe and these signals can be transported over longer fibre distance. In addition, the IF over fibre technique has the benefit that low bandwidth devices can be used for IF signals leading to potential cost savings. The drawback of requiring an LO source at the BS can be overcome by remote delivery of the LO from the CS thereby simplifying the BS. The relative merit of direct and external modulation has been outlined and issues such as noise and distortion properties in optical links are discussed. Direct modulation provides a low cost solution but suffers from limited modulation bandwidth, high chirp, non-linearity and noise. External modulation has the best performance (high optical power, low chirp, low noise), with a trade-off of high cost and power consumption. The chapter concludes with a statement of the objectives of this thesis, a summary of the novel research results achieved and an outline of the structure for the remaining chapters.

References

[1] W. Honcharenko, J. P. Kruys, D. Y. Lee and N. J. Shah, "Broadband wireless access", *IEEE Commun. Mag.*, pp. 20-26, 1997.

[2] R. E. Schuh, C. Schuler and M. Mateescu, "An architecture for radio-independent wireless access networks", *Proceedings 49th Annual Int. Vehc. Tech. Conf. (VTC)*, vol. 2, pp. 1227-1231, 1999.

[3] S. Komaki and E. Ogawa, "Trends of fibre optic microcellular radio communication networks", *IEICE Trans. Electron.*, vol. E79-C, no. 11, pp. 98-104, 1996.

[4] A. J. Paulraj, D. A. Gore, R. U. Nabar, H. Bölcskei, "An Overview of MIMO Communications-A Key to Gigabit Wireless", *Proceedings of the IEEE*, vol. 92, no. 2, pp. 198-218, 2004.

[5] T. Ihara and K. Fujimura, "Research and development trends of millimetre wave short range application systems", *IEICE Trans. Commun.*, vol. E79-B, no. 12, pp. 1741-1753, 1996.

[6] R. C. V. Macario, "Cellular radio principles and design", second edition, *Macmillan press Ltd.*

[7] J. Lavergnat, M Sylvain, "Radio wave propagation Principles and techniques", *John Wiley & Sons Ltd.*

[8] IEEE Std. 802.16-2001, IEEE standard for local and metropolitan area networks, Air Interface for Fixed Broadband Wireless Access Systems.

[9] C. Eklund, R. B. Marks, K. L. Stanwood and S. Wang, "IEEE standard 802.16: A technical overview of the WirelessMAN air interface for broadband wireless access", *IEEE Commun. Mag.*, pp. 98- 107, 2002.

[10] IEEE Std. 802.16-2004, IEEE standard for local and metropolitan area networks, Part 16: Air Interface for Fixed Broadband Wireless Access Systems.

[11] WiMAX Forum 2004

[12] M. Y. Wah, Y. Chia, and L. Y. Ming, "Wireless ultra wideband communications using radio over fiber", *IEEE Conference on Ultra Wideband Systems and Technologies*, pp. 265-269, 2003.

[13] I. R. Johnson and S. K. Barton, "Standards for wireless LANs", *IEE Colloquium on Wireless Technology Digest.* pp. 5/1-5/5, 1996.

[14] http://standards.ieee.org/getieee802/802.11.html IEEE Std 802.11, 1999 edition, Wireless LAN Medium Access Control (MAC) and Physical Layer (PHY) Specifications.

[15] http://standards.ieee.org/getieee802/download/802.11b-1999.pdf IEEE Std 802.11b, 1999, Wireless LAN Medium Access Control (MAC) and Physical Layer (PHY) Specifications: Higher-Speed Physical Layer Extensions in the 2.4 GHz Band.

[16] http://standards.ieee.org/getieee802/download/802.11g-2003.pdf IEEE Std 802.11g, 2003, Wireless LAN Medium Access Control (MAC) and Physical Layer (PHY) Specifications: Further Higher Data Rate Extensions in the 2.4 GHz Band.

[17] http://standards.ieee.org/getieee802/download/802.11a-1999.pdf IEEE Std 802.11a, 1999, Wireless LAN Medium Access Control (MAC) and Physical Layer (PHY) Specifications, High-speed Physical Layer in the 5GHz Band.

[18] A. Doufexi, A. Armour, M. Butler, A. Nix, D. Bull and J. McGeehan, "A comparison of the HiperLAN/2 and IEEE802.11a wireless LAN standards", *IEEE Commun. Mag.*, vol. 40, pp. 172-180, 2000.

[19] http://portal.etsi.org/bran/kta/Hiperlan/hiperlan2.asp

[20] J. Mikkonen, C. Corrado, C. Erci and M. Progler, "Emerging wireless broadband networks", *IEEE Commun. Mag.*, pp. 112-117, 1998.

[21] A. M. Street, P. N. Stavrinou, D. C. O'Brien and D. J. Edwards, "Indoor optical wireless systems-A review", *IEEE J. Optical and Quantum Electron.*, vol. 29, pp. 349-378, 1997.

[22] D. Wake, "Radio over fibre systems for mobile applications", in Radio over Fibre Technologies For Mobile Communications Networks, H.Al-Raweshidy & S. Komaki, ed. Artech House, Inc, USA, 2002.

[23] D. Wake and K. Beachman, "A novel switched fibre distributed antenna system", *European Conference on Optical Communications (ECOC)*, vol. 5, pp. 132-135, 2004.

[24] H. Ogawa, D. Polifko and S. Banba, "Millimeter-wave fibre optics systems for personal radio communications", *IEEE Trans. Microwave Theory & Tech.*, vol. 40, pp. 2285-2293, 1992.

[25] R. E. Schuh, D. Wake, B. Verri and M. Mateescu, "Hybrid fibre radio access: A network operators approach and requirements", *Proceedings 10th Microcoll Conference*, pp. 211-214, 1999.

[26] J. C. Fan, C. L. Lu and L. G. Kazovsky, "Dynamic range requirements for microcellular personal communication systems using analog fiber-optic links", *IEEE Trans. Microwave Theory & Tech*, vol. 45, no. 8, pp. 1390-1397, 1997.

[27] R. C. Williamson, "Dynamic range requirements for analog fibre optic links in fibre fed wireless microcells", *Optical Fibre Communication (OFC)*, ThF, 1995.

[28] D. M. Cutrer, J. B. Gorges, T. H. Le and K. Y. Lau, "Dynamic range requirements for optical transmitters in fibre fed microcellular networks", *IEEE Photon. Technol. Lett.*, vol. 7, no. 5, pp. 564-566, 1995.

[29] H. Jung and O. K. Tonguz, "Comparison of fibre and coaxial link for access network in microcellular PCS", *Electron. Lett.*, vol. 32, no. 5, pp. 425-426, 1996.

[30] S. Hunziker and W. Baechtold, "Cellular remote antenna feeding: optical fibre or coaxial cable", *Electron. Lett.*, vol. 34, no. 11, pp. 1038-1040, 1998.

[31] A. J. Seeds, "Wireless access over optical fibre: from cellular radio to broadband: from UHF to millimetre waves", *IEEE Laser & Electro-Optics Society (LEOS)*, vol. 2, pp. 471-472, 2002.

[32] H. Yamamoto, K. Utsumi, M. Miyashita, M. Kurono, Y. Serizawa, Y. Shoji and H. Ogawa, "Fibre optic sectorised remote antenna systems for millimetre wave broadband wireless access networks", *IEICE Trans. Electron.*, vol. E86-C, no. 7, pp. 1191- 1196, 2003.

[33] Y. Fuke, Y. Ito and Y. Ebine, "Radio on fiber system for personal digital cellular and IMT-2000", *IEEE Int. Topical Meeting Microwave Photonics (MWP)*, Tu2.2, pp. 53-56, 2002.

[34] P. Hartmann, X. Qian, R. V. Penty and I. H. White, "Broadband multimode fibre (MMF) based IEEE802.11a/b/g WLAN distribution system", *IEEE Int. Topical Meeting Microwave Photonics (MWP)*, TA-5 pp. 173-176, 2002.

[35] K. Morita, H. Ohtsukai, "The new generation of wireless communications based on fibre radio technologies", *IEICE Trans. Commun.*, vol. E76-B, no. 9, pp. 1061-1068, 1993.

[36] Y. Ebine, "Development of fiber radio systems for cellular mobile communications", *IEEE Int. Topical Meeting Microwave Photonics (MWP)*, F-10.1, pp. 249-252, 1999.

[37] H. Harada, K. Sato and M. Fujise, "A radio on fibre based millimetre wave road vehicle communication system by a code division multiplexing radio transmission scheme", *IEEE Trans. Intelligent Transportation Systems*, vol. 2, no. 4, pp. 165-179, 2001.

[38] A. J. Seeds, "Broadband access using wireless over fibre systems", *CLEO*, CMH3, pp. 131-133, 2005.

[39] H. Al-Raweshidy, K. M. Glaubitt and P. Faccin, "In-Building coverage for UMTS using radio over fibre technology", *IEEE Wireless Personal Multimedia Commun.*, vol. 2, pp. 581-585, 2002.

[40] H. Sasai and S. Morikura, "Demonstration of radio on fibre transmission using wide dynamic range scheme for IMT-2000 cellular systems", *IEICE Trans. Electron.*, vol. E86-C, pp. 1153- 1158, 2003.

[41] D. Wake, S. Dupont, J. P. Vilcot and A. J. Seeds, "32 QAM radio transmission over multimode fibre beyond the fibre bandwidth", *IEEE Int. Topical Meeting Microwave Photonics (MWP)*, 2001.

[42] D. Wake, S. Dupont, C. Lethein, J. P. Vilcot and D. Decoster, "RF transmission over multimode fibre for distributed antenna system applications", *Electron. Lett.*, vol. 37, pp. 1087-1089, 2001.

[43] P. Hartmann, M. Webster, A. Wonfor, J. D. Ingham, R. V. Penty, I. H. White, D. Wake and A. J. Seeds, "low cost MMF based wireless LAN distribution systems using uncooled directly modulated DFB laser diodes", *European Conference on Optical Communication (ECOC)*, vol. 3, pp. 804-805, 2003.

[44] Y. Matsunaga and M. Shibutani, "A short span optical feeder for wireless personal communication systems using multimode fibers", *IEICE Trans. Electron.*, vol. E79-C, no. 1, pp. 118-123, 1996.

[45] K. A. Persson, C. Carlsson, A. Alping, A. Haglund, J. S. Gustavsson, P. Modh and A. Larsson, "WCDMA radio over fibre transmission experiment using singlemode VCSEL and multimode fibre", *Electron. Lett.*, vol. 42, no. 6, 2006.

[46] J. T. Gallo and K. D. Breuer, "Bi-directional photonic links for RF applications", *IEEE Laser & Electro-Optics Society (LEOS)*, ThE3, pp. 42-43, 1998.

[47] G. Steiner, W. Baechtold and S. Hunziker, "Bidirectional single fibre links for base station remote antenna feeding", *European Conference on Networks & Optical Communications (NOC)*, 2000.

[48] M. G. Larrode, A. M. J. Koonen, J. J. V. Olmos and A. Ng'Oma, "Bidirectional radio over fibre link employing optical frequency multiplication", *IEEE Photon. Technol. Lett.*, vol. 18, pp. 241-243, 2006.

[49] H. Izadpanah, T. Elbatt, V. Kukshya, F. Dolezal and B. K. Ryu, "High availability free space optical and RF hybrid wireless networks", *IEEE Wireless commun.*, pp. 45- 53, 2003.

[50] H. Ogawa, "Microwave and millimetre wave fibre optic technologies for subcarrier transmission systems", *IEICE Trans. Commun.*, vol. E76-B, no. 9, pp. 1078-1090, 1993.

[51] K. Ikeda, T. Kuri, Y. Takahashi and K. Kitayama, "Full duplex transmission using 2 RF port electroabsorption transceiver with photonic up and down conversions for millimetre wave radio on fibre system", *IEICE Trans. Electron.*, vol. E86-C, no. 7, pp. 1138-1145, 2003.

[52] D. Novak, G. H. Smith, A. J. Lowery, H. F. Liu and R. B. Waterhouse, "Millimetre wave fibre wireless transmission systems with reduced effects of fibre chromatic dispersion", *IEEE J. Optical and Quantum Electron.*, vol. 30, pp. 1021-1031, 1998.

[53] G. H. Smith and D. Novak, "Full duplex wireless system using electrical and optical SSB modulation for efficient broadband millimetre wave transport", *IEEE Int. Topical Meeting Microwave Photonics (MWP)*, FR2-2, pp. 223-227, 1997.

[54] G. H. Smith, D. Novak and Z. Ahmed, "Overcoming chromatic dispersion effects in fibre wireless systems incorporating external modulators", *IEEE Trans. Microwave Theory & Tech.*, vol. 45, no. 8, pp. 1410-1415, 1997.

[55] C. Lim, A. Nirmalathas, D. Novak, R. Waterhouse and G. Yoffe, "Millimetre-wave broad-band fibre-wireless system incorporating baseband data transmission over fibre and remote LO delivery", *IEEE J. Lightwave Technol.*, vol. 18, pp. 1355-1363, 2000.

[56] C. Lim, A. Nirmalathas, D. Novak, R. Waterhouse, and K. Ghorbani, "Full-duplex broadband fibre-wireless system incorporating baseband data transmission and a novel dispersion tolerant modulation scheme", *IEEE MTT-S Int. Microwave Symposium (IMS)*, vol. 3, pp. 1201-1204, 1999.

[57] H. Schmuck, "Comparison of optical millimetre-wave system concepts with regard to chromatic dispersion", *Electron. Lett.*, vol. 31, pp. 1848-1849, 1995.

[58] U. Gliese, S. Norskov and T. N. Nielsen, "Chromatic dispersion in fibre optic microwave and millimetre wave links", *IEEE Trans. Microwave Theory & Tech.*, vol. 46, no. 10, pp. 1716-1724, 1998.

[59] R. Hofstetter, H. Schmuck and R. Heidemann, "Dispersion effects in optical millimetre-wave systems using self-heterodyne method for transport and generation", *IEEE Trans. Microwave Theory & Tech.*, vol. 43, pp. 2263-2276, 1995.

[60] R. A. Griffin, P. M. Lane and J. J. O'Reilly, "Dispersion tolerant subcarrier data modulation of optical millimetre wave signals", *Electron. Lett.*, vol. 32, no. 24, pp. 2258-2260, 1996.

[61] J. Marti, J. M. Fuster and R. I. Laming, "Experimental reduction of chromatic dispersion effects in lightwave microwave transmissions using tapered linearly chirped fibre grating", *Electron. Lett.*, vol. 33, no. 13, 1997.

[62] J. Park, W. V. Sorin and K. Y. Lau, "Elimination of the fibre chromatic dispersion penalty on 1550 nm millimetre wave optical transmission", *Electron. Lett.*, vol. 33, no. 6, pp 512-513, 1997.

[63] J. J. O'Reilly, P. M. Lane, M. H. Capstick, H. M. Salagado, R. Heidemann, R. Hofstetter and H. Schmuck, "RACE R2005: Microwave optical duplex antenna link", *IEE Proceedings-J.* vol. 140, no. 6, pp. 385-391, 1993.

[64] D. Novak, A. Nirmalathas, C. Lim C. Marra and R. B. Waterhouse, "Fibre radio challenges and possible solutions", *IEEE Int. Topical Meeting Microwave Photonics (MWP)*, 2003.

[65] P. Shen, N. J. Gomes. P. A. Davies, W. P. Shillue, P. G. Huggard and B. N. Ellison, "High purity millimetre wave photonic local oscillator generation and delivery", *IEEE Int. Topical Meeting Microwave Photonics (MWP)*, pp. 189-192, 2003.

[66] U. Gliese, T. N. Nielsen, S. Norskov and K. E. Stubkjaer, "Multifunction fibre optic microwave links based on remote heterodyne detection", *IEEE Trans. Microwave Theory & Tech.*, vol. 46, no. 5, 1998.

[67] L. A. Johansson and A. J. Seeds, "Generation and transmission of millimetre wave data modulated optical signals using an optical injection phase lock loop," *IEEE J. Lightwave Technol.*, vol. 21, no. 2, pp. 511-520, 2003.

[68] B. L. Dang and I. Niemegeers, "Analysis of IEEE802.11 in radio over fibre home networks", *Proc. of IEEE Conf. on Local Computer Networks (LCN)*, pp. 744-747, 2005.

[69] M. Garcia Larrode, A. M. J. Koonen, P. F. M. Smulders, "Impact of radio over fibre links on the wireless protocols", *proc. Nefertiti Workshop*, 2005.

[70] T-S. Ho and K-C. Chen, "Performance analysis of IEEE802.11 CSMA/CA medium access control protocol", *Personal, indoor and mobile radio communication (PIMRC)*, pp. 407-411, 1996.

[71] J. Pavon and S. Choi, "Link adaptation strategy for IEEE802.11 WLAN via received signal strength measurement", *International Conference on Commun. (ICC)*, pp. 1108-1113, 2003.

[72] B. Kalantarisabet and J. E. Mitchell, "MAC constraints on the distribution of 802.11 using optical fibre", *Eurpoean microwave conference (EuMW)*, 2006.

[73] P. A. Davies and N. J. Gomes, "Subcarrier multiplexing in optical communication network", *in Analogue Optical Fibre Communications*, Editors; B. Wilson, Z. Ghassemlooy and I Darwazeh, The Institution of Electrical Engineers, London, pp. 1-32, 1995.

[74] W. E. Stephens and T. R. Joseph, "System characteristics of direct modulated and externally modulated RF fibre optic links", *IEEE J. Lightwave Technol.*, vol. 5, no. 3, pp. 380-387, 1987.

[75] C. Cox III, E. Ackerman, R. Helkey and G. E. Betts, "Techniques and performance of intensity-modulation direct-detection analog optical links", *IEEE Trans. Microwave Theory & Tech.*, vol. 45, no. 8, pp. 1375-1383, 1997.

[76] A. J. Seeds, "Microwave photonics", *IEEE Trans. Microwave Theory & Tech.*, vol. 50, no. 3, pp. 877-887, 2002.

[77] R. S. Tucker, "Wideband semiconductor lasers and optical modulators for communications", *IEEE Trans. Microwave Theory & Tech.*, pp. 831-832, 1988.

[78] S. Weisser, E. C. Larkins, K. Czotscher, W. Benz, J. Daleiden, I. Esquivias, J. Fleissner, J. D. Ralston, B. Romero, R. E. Sah, A. Schonfelder and J. Rozenweig, "Damping limited modulation bandwidths up to 40 GHz in undoped short cavity $In_{0.35}Ga_{0.65}As$-GaAs multiple quantum well lasers", *IEEE Photon. Technol. Lett.*, vol. 8, no. 5, pp. 608-610, 1996.

[79] P. A. Morton, T. Tanbun-Ek, R. A. Logan, N. Chand, K. W. Wecht, A. M. Sergent and P. F. Sciortino, "Packaged 1.55 μm DFB laser with 25 GHz modulation bandwidth", *Electron. Lett.* vol. 30, no. 24, pp. 2044-2047, 1994.

[80] A. Kaszubowska, P. Anandrajah and L. P. Barry, "Improved Performance of a hybrid radio/fibre system using a directly modulated laser transmitter with external injection," *IEEE Photon. Technol. Lett.*, vol. 14, pp. 233-235, 2002.

[81] C. H. Cox, G. E. Betts and L. M. Johnson, "An analytic and experimental comparison of direct and external modulation in analog fibre optic links", *IEEE Trans. Microwave Theory & Tech.*,vol. 38, no. 5, pp. 501-509, 1990.

[82] A. Stohr, R. Heinzelmann and D. Jager, "Millimetre wave bandwidth electroabsoroption modulators and transceivers", *IEEE Int. Topical Meeting Microwave Photonics (MWP)*, pp. 128-128, 2000.

[83] K. Noguchi, H. Miyazawa and O. Mitomi, "75 GHz broadband Ti:$LiNbO_3$ optical modulator with ridge structure", *Electron. Letts.*, vol. 30, no. 12, pp. 949- 951, 1994.

[84] K. Noguchi, H. Miyazawa and O. Mitomi, "Millimetre wave Ti:$LiNbO_3$ optical modulators", *IEEE J. Lightwave Technol.*,vol. 16, pp. 615-619, 1998.

[85] T. Iwai, k. Sato and Koi-ichi. Suto, "Reduction of dispersion induced distortion in SCM transmission systems by using predistortion linearized MQW-EA modulators", *IEEE J. Lightwave Technol.*, vol. 15, no. 2, pp.169-178, 1997.

[86] L. D. Westbrrok, L. Neol and D. G. Moodie, "Full duplex 25 km analogue fibre transmission at 120 Mbit/s with simultaneous modulation and detection in an electroabsorptioon modulator", *Electron. Lett.*, vol. 33, pp. 694-695, 1997.

[87] D. Wake and G. D. Moodie, "Passive picocell – prospect for increasing the radio range", *IEEE Int. Topical Meeting Microwave Photonics (MWP)*, pp. 269-271, 1997.

[88] D. Wake, D. Johansson and D. G. Moodie, "Passive picocell: a new concept in wireless network infrastructure", *Electron. Lett.*, vol. 33, no. 5, pp. 404-406, 1997.

[89] K. Kojucharow, H. Kaluzni, M. Sauer and W. Nowak, "A WLAN at 60 GHz–Novel system design and transmission experiments", *IEEE MTT-S Int. Microwave Symposium (IMS)*, vol. 3, pp. 1513-1516, 1998.

[90] K. Takahashi, S. Fujita, H. Yabuki, M. Inoue and G. Wu, "Millimetre wave wireless LAN system employing compact and cost effective 156 Mbps transceiver MCMs", *IEICE Trans. Electron.*, vol. E86-C, no. 8, pp. 1512-1519, 2003.

[91] K. I. Kitayama, T. Kuri, R. Heinzelmann, A. Stohr. D. Jager and Y. Takahashi, "A Good prospect for broadband millimetre wave fibre radio access system-an approach to single optical component at antenna base station", *IEEE MTT-S Int. Microwave Symposium (IMS)*, vol. 3, pp. 1745-1748, 2000.

[92] C. P. Liu , A. J. Seeds, J. Chadha, P. Stavrinou, G. Parry, M. Whitehead, A. Krysa and J. Roberts, "Bi-directional transmission of broadband 5.2 GHZ wireless signals over fibre using a multiple quantum well asymmetric fabry perot modulator/photodetector", *Optical Fiber Communications (OFC)*, FM8, pp. 738-740, 2003.

[93] A. Martinez, V. Polo and J. Marti, "Simultaneous baseband and RF optical modulation scheme for feeding wireless and wire line heterogeneous access networks", *IEEE Trans. Microwave Theory & Tech.*, vol. 49, pp. 2018-2024, 2001.

[94] H. Pfrommer, M. A. Piqueras, J. Herrera, V. Polo, A. Martinez, S. Karlsson, O. Kjebon, R. Schatz, Y. Yu, T, Tsegaye, C. P. Liu, C. H. Chuang, A. Enard, F. V. Dijk, A. J. Seeds and J. Marti, "Full duplex DOCSIS/Wireless DOCSIS fibre radio network employing packaged AFPM based base stations", *IEEE Photon. Technol. Lett.*, vol. 18, no. 2, pp. 406-408, 2006.

[95] Y. Yu, S. Karlsson, C. P. Liu, R. Schatz, U. Westergren, O. Kjebon, C. H. Chuang, Sailing He, L. Thylen, A. B. Krysa, J. S. Roberts and A. J. Seeds, "Enhanced linear dynamic range of asymmetric fabry perot modulator detector", *IEEE Photon. Technol. Lett.*, vol. 18, no. 9, pp. 1040-1042, 2006.

[96] J. C. Froidure, C. Leburn, P. Megret, E. Jaunart, P. Georg, T. Tasia, M. Lamquin and M. Blondel, "Theoretical and experimental study of second order distortions in CATV DFB laser diodes", *IEEE Photon. Technol. Lett.*, vol. 7, no. 3, pp. 266-268, 1995.

[97] H. Harada, Hee-Jin. Lee, S. Komaki and N. Moringa, "Performance analysis of fibre optic millimetre wave band radio subscriber loop", *IEICE Trans. Commun.*, vol. E76-B, no. 9, pp. 1128-1135, 1993.

[98] C. H. Cox, E. I. Ackerman, G. E. Betts and J. L. Prince, "Limits on the performance of RF over fibre links and their impact on device design", *IEEE Trans. Microwave Theory & Tech.*, vol. 54, no. 2, pp. 906-920, 2006.

[99] W. I. Way, "Optical fibre based microcellular systems: An overview", *IEICE Trans. Commun.*, vol. E76-B, no. 9, pp. 1091-1102, 1993.

[100] Agilent Technologies Wireless Test Solutions Application Note 1313.

[101] M. Garcia. Larrode, A. M. J. Koonen, J. J. Vegas. Olmos, L. T. Monroy and T. C. W. Schenk, "RF bandwidth capacity and SCM in a radio over fibre link employing optical frequency multiplication", *Eurpean Conference on optical Communication (ECOC)*, vol. 3, pp. 681-682, 2005.

Chapter 2

Laser Non-linearity and Distortion Compensation Techniques

This chapter is concerned with investigation of non-linear distortion in a directly modulated DFB laser and a review of linearisation techniques proposed in the literature to compensate this distortion. After a brief Introduction 2.1, linearity and distortion characteristics are discussed to identify the need for linearisation in Section 2.2. Mechanisms responsible for generating distortion in a directly modulated DFB laser are analysed in Section 2.3 with static and dynamic characteristics. A literature review on distortion compensation techniques for directly modulated lasers and external modulators is presented in Section 2.4. In the last Section, 2.5, Conclusion, important results are summarised from this chapter.

2.1 Introduction

In communication systems transmitter linearity is an important factor. Any non-linear distortion generated by the transmitter such as third order intermodulation distortion (IMD) can give rise to adjacent channel interference, since these IMD products cannot be easily filtered. In analogue optical transmission non-linear distortion limits the achievable dynamic range of the optical link and hence severely degrades the system performance. The main source of non-linear distortion is non-linearity in the electro-optic conversion process, achieved through direct modulation of the optical transmitter or through external modulation with a Mach-Zehnder (MZ) modulator. Distortion in a directly modulated laser also increases as the modulation frequency approaches the laser relaxation oscillation. High dynamic range can be achieved by reducing the noise level of the optical source and IMD products. Several distortion reduction techniques have been proposed or demonstrated in the literature that uses microwave and opto-electronic devices to improve source linearity. Optical compensation technique in which linearisation is achieved using a combination of optical devices, for example connecting modulators in parallel or in cascade are also in use. An important property of all linearisation techniques is the frequency at which they operate and the amount of distortion reduction that can be achieved over a certain bandwidth.

2.2 Linearity and Distortion

It is highly desirable to have linear systems that generate minimum distortion. In these systems the output can be expressed as a linear combination of the input and only the frequency components that are present at the input are observed at the output and no extra frequency terms are generated. However, linear systems can impose magnitude and phase change on input signals and large input signals can drive linear systems into saturation causing non-linear operation. Systems which produce extra frequency components (i.e. additional sideband frequencies) that are not present at the input are defined to be non-linear. These additional terms produced at the output are harmonics and IMD products of the input frequencies.

For a single sinusoidal input to a non-linear system the additional frequency components generated are known as harmonics. These harmonics can be of 2^{nd}, 3^{rd} order or higher depending on the non-linearity of the system and sub-harmonics are also possible. The harmonics can be eliminated by filtering since they are outside the signal bandwidth of interest and do not pose a problem except for systems of an octave or greater bandwidth. In non-linear systems with multiple inputs the additional sum and difference terms are known as IMD. IMD results when two or more signals combine in a device with a non-linear transfer characteristic and produce unwanted signals. The additional components cause interference between adjacent channels and degrade the system performance.

There are two main techniques used in the modelling of non-linear devices, known as the power series and the Volterra series. The basic power series analysis is commonly used as a generalised formula for characterising non-linear devices. However, in its simple form the power series analysis does not take into account the phase components of the output terms. The Volterra series analysis is a complete model and hence takes into account the phase components. Thus, a Volterra series analysis is a more powerful analysis tool in aiding the determination of distortion than the basic power series analysis. However, the power series can be enhanced to take into account the phase effects. In the analysis to follow, the power series representation is used to demonstrate the creation of distortion products in a non-linear system.

The output $V_o(t)$ can be expressed as a power series of input signal $V_i(t)$ and the coefficients a, b, c, d etc, specify the nature of the non-linearity.

$$V_o(t) = a + b[V_i(t)] + c[V_i(t)]^2 + d[V_i(t)]^3 + \text{.....(higher order terms)} \tag{2.1}$$

Considering a single input with sinusoidal signal $\cos(\omega t)$, from (2.1), the output is

$$V_o(t) = a + b[\cos(\omega t)] + c[\cos(\omega t)]^2 + d[\cos(\omega t)]^3 + \text{.....(higher order terms)} \tag{2.2}$$

For systems with mild non-linearity only the first few terms need to be taken into account. Therefore,

$$V_o(t) = a + b[\cos(\omega t)] + \frac{c}{2}[1 + \cos(2\omega t)] + \frac{d}{4}[3\cos(\omega t) + \cos(3\omega t)] \tag{2.3}$$

The output contains the dc signal, components at the fundamental frequency ω, and distortion products at 2ω (second harmonic) and 3ω (third harmonic). The generation of harmonic products can fall within the operating bandwidth and create distortion at the output.

For a non-linear system with two input signals $V_i(t) = \cos(\omega_1 t) + \cos(\omega_2 t)$ of equal amplitude but at different frequencies ω_1 and ω_2 IMD products are generated. The output is:

$$V_o(t) = a + b[\cos(\omega_1 t) + \cos(\omega_2 t)] + c[\cos(\omega_1 t) + \cos(\omega_2 t)]^2 + d[\cos(\omega_1 t) + \cos(\omega_2 t)]^3 + ... \quad (2.4)$$

Expanding the second order term from (2.4) gives:

$$\begin{aligned} c[\cos(\omega_1 t) + \cos(\omega_2 t)]^2 &= c[\cos^2(\omega_1 t) + 2\cos(\omega_1 t)\cos(\omega_2 t) + \cos^2(\omega_2 t)] \\ &= c\left[\frac{1}{2}[1 + \cos(2\omega_1 t)] + \cos[(\omega_1 - \omega_2)t] + \cos[(\omega_1 + \omega_2)t] + \frac{1}{2}[1 + \cos(2\omega_2 t)]\right] \end{aligned} \quad (2.5)$$

Expanding the third order term from (2.4) gives:

$$d[\cos(\omega_1 t) + \cos(\omega_2 t)]^3 = d\begin{bmatrix} \frac{1}{4}[3\cos(\omega_1 t) + \cos(3\omega_1 t)] + \frac{1}{4}[3\cos(\omega_2 t) + \cos(3\omega_2 t)] + \\ \frac{3}{2}\cos(\omega_1 t)[1 + \cos(2\omega_2 t)] + \frac{3}{2}\cos(\omega_2 t)[1 + \cos(2\omega_1 t)] \end{bmatrix} \quad (2.6)$$

$$= d\begin{bmatrix} \frac{9}{4}(\cos\ \omega_1 t + \cos\ \omega_2 t) + \\ \frac{1}{4}(\cos\ 3\omega_1 t + \cos\ 3\omega_2 t) + \\ \frac{3}{4}[\cos(\ 2\omega_1 + \omega_2)t + \cos(\ 2\omega_2 + \omega_1)t] + \\ \frac{3}{4}[\cos(\ 2\omega_1 - \omega_2)t + \cos(\ 2\omega_2 - \omega_1)t] \end{bmatrix} \quad (2.7)$$

In addition to harmonic components IMD is also generated. The third order terms $(2\omega_1 - \omega_2)$ and $(2\omega_2 - \omega_1)$ or $(2f_1\text{-}f_2)$ and $(2f_2\text{-}f_1)$ are known as the IMD3 and are of particular interest in characterising a systems performance as they are very close to the original input frequencies ω_1 and ω_2 as shown in Figure 2.1 and cannot be easily filtered. In a communication network, these unwanted distortion components would appear in adjacent frequency channels and interfere with other signals. The

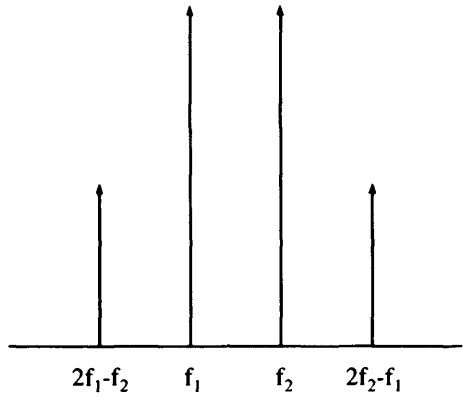

Figure 2.1 Third order intermodulation distortion

distortion products will appear on top of the signals and will reduce the signal-to-noise (SNR) of the wanted signals. Hence it is important to ensure that allowable distortion is kept within defined limits. Higher order terms such as fifth order intermodulation at $(3\omega_1 - 2\omega_2)$ and $(3\omega_2 - 2\omega_1)$ are also significant since they also fall within the operating bandwidth and can be troublesome. The second order distortion products at $(\omega_1 \pm \omega_2)$ frequencies generally pose no problem since they are outside the system bandwidth. However, this can be an issue in a multi octave bandwidth such as for the 900 MHz and 1800 MHz GSM system.

2.2.1 Two tone third order intercept point

The third order intercept point (IP3) is a figure of merit used to characterise the level of IMD3 at different power levels. It is defined as the point at which the power in the third order products $(2f_1-f_2)$ and the power of the fundamental tone (f_1) intersect. It is the theoretical value since the fundamental signal power and 3rd order distortion products compress before the intercept point can be reached. A commonly used method of defining IMD3 of a system is the two tone test, where two signals of equal amplitude are applied to the input. The IMD3 follow a line with a slope 3:1 and rise rapidly as the input signal levels are increased. Figure 2.2 illustrates this point. Second order distortion products will have a line with a slope of 2. At low signal levels the higher order contributions are insignificant.

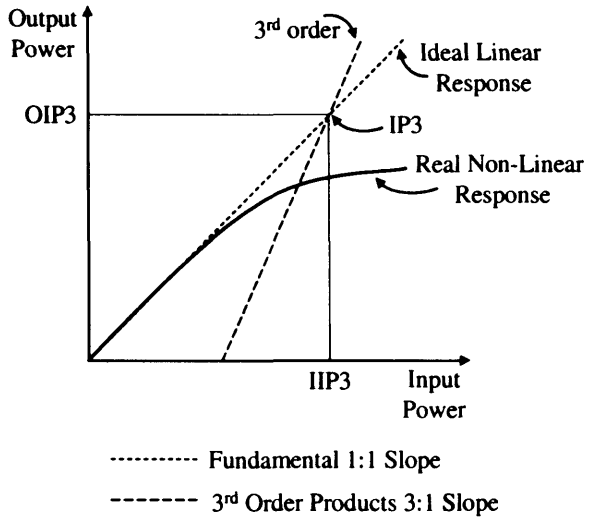

Figure 2.2 Illustration of the third order intercept point

However, at higher input power levels IMD3 curve can deviate from the 3:1 line. This is due to the contribution from higher order terms such as 5th order. The IP3 can be specified by either the input intercept power (IIP3) or the output intercept power (OIP3) at which the 3rd order products equal the desired signal. The IIP3 is related to the OIP3 by the gain as IIP3(dBm)=OIP3(dBm)-G(dB) where G is the gain in dB and IIP3 and OIP3 are the units of dBm. For a cascade of RF signal blocks, the system IIP3 depends on the IIP3 and the gain of each block.

2.2.2 The need for linearisation

The non-linearities produced by discrete signals such as unmodulated carriers are known as intermodulation products and appear at discrete frequencies. For a digitally modulated signal the effect of the non-linearity appear over a continuous band of frequencies and are often referred to as spectral re-growth. The resulting spectrum is of a stepped appearance with each step corresponding to a higher order of distortion. For mobile and radio applications, the spectral emissions from transmitters are very tightly controlled and as distortion increases the bandwidth of the output signal with respect to the input, spurious signals can fall within other transmission bands and cause interference. In a multi-channel data transmission the results of the generated spectral re-growth may overlap with adjacent channels and therefore cause interference. Also increased demand for wireless communications and linear modulation techniques such as 16 QAM, 64 QAM place demanding restrictions on spectral growth and hence require highly linear systems. The spectral re-growth must be maintained since the spectral efficiency is important due to limited available bandwidth within the spectral emission target. For modulation schemes such as these, one figure of merit that can be used to determine the linearity is the adjacent channel power ratio (ACPR) where the difference between the carrier and the distortion is defined in dBc (decibels with respect to carrier). The spectral mask for the IEEE802.11a standard is shown in Figure 2.3. Non-linear distortion especially IMD3 also reduces the dynamic range of a system leading to errors in transmission. Although the level of distortion falls rapidly as the power level is reduced the modulation depth will be reduced leading to reduced SNR and poor system performance. This will also result in a lower number of channels to be used reducing the system transmission capacity. System constraints, such as IMD3, spectrum spreading, and BER performance can be difficult to achieve with cheap commercial components. Also to prevent unnecessary power back off without compromising distortion requirements, linearisation techniques can be used. Linearisation techniques reduce output distortion, to allow the transmitter to be operated at a higher output power for a given level of distortion.

Linearisation techniques are also widely employed at microwave frequencies for power amplifiers [2] to reduce amplifier distortion and improve efficiency. A significant increase in 3rd order IP can be

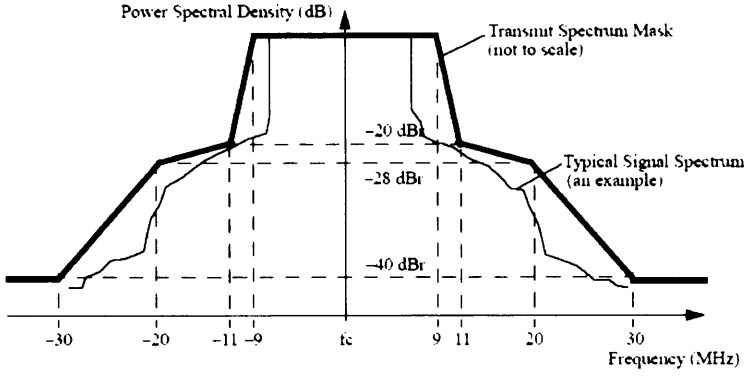

Figure 2.3 Transmit spectrum mask for IEEE802.11a WLAN standard [1]

achieved with linearisation for the same system specifications. Using an amplifier with very high output power rating and operating it in the linear region, well below saturation is not a cost effective solution. In a multi-carrier system, such as a cellular base station it is more cost effective to transmit several carriers through a common amplifier [3, 4]. However, the non-linear behaviour of the power amplifier gives rise to IMD3 between the carriers within the bandwidth of the desired signals. For multi-carrier systems, the requirement for IMD3 distortion is that it must be at least 60 dB lower than the carrier output power level. Linearisation is an effective technique to reduce IMD3 and results in significantly higher output power operation of the amplifier.

2.3 Laser Diode Characteristics

A semiconductor laser is a preferred optical source for high speed optical communication as it can provide adequate power and can be directly modulated at microwave frequencies. The laser diode is a current driven device and converts the injected current to optical power output. This relationship can be seen in Figure 2.4. The optical output power consists of spontaneous and stimulated emission. At low bias currents i.e. below threshold the optical power of the laser is very small and due to spontaneous emission [5]. When the bias current is increased beyond the threshold current of the laser, stimulated emission becomes dominant over spontaneous emission and the optical power increases with injection

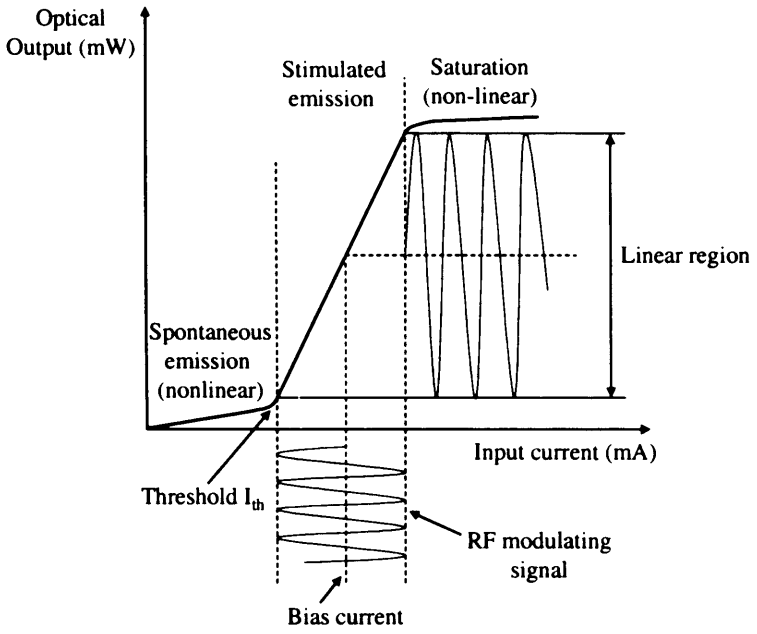

Figure 2.4 Typical laser diode transfer characteristics (LI curve)

current. At high bias current the Light vs Current (LI) slope changes because of saturated output power. The LI characteristics show several important parameters often considered when specifying lasers:

- Threshold current – The current level at which lasing begins.
- Modulation sensitivity – The slope of the LI characteristic, often refereed to as dL/dI, in mW/mA.
- Linearity – A perfectly linear device follows a straight line over the region of operation.
- Maximum Output – Most lasers exhibit a noticeable rollover effect as shown in Figure 2.4 where the non-linear LI relationship becomes noticeable.

Although, the slope of the laser optical output L versus the driving current I curve above threshold is near linear it may not be sufficiently so to meet the dynamic range requirements for analogue fibre optic links.

2.3.1 Modulation response of the laser

Direct modulation of the laser diode is a simple, low cost approach for transmitting microwave signals and is achieved by superimposing the modulating signal onto the bias current of the laser. The output of the laser is then a microwave modulated optical signal. Most systems require that the laser light intensity be a linear function of the bias current under large signal modulation. However, any non-linear distortion introduced by the directly modulated laser diode gives rise to distortion products, which can limit the dynamic range and hence the performance of the system [6]. Non-linear distortion generated by the semiconductor laser such as intermodulation distortion can give rise to interchannel interference which degrades the quality of the received signal and limits the number of channels. In general there are two factors causing non-linear distortion; static non-linearity and dynamic non-linearity.

In the low frequency range such as is used for cable TV systems (< 1 GHz), static distortion is caused by the non-linear light versus current characteristic of the laser diode. In order to achieve better linearity the bias current for the laser should be set above the threshold value since the frequency response of the laser is dependent on biasing conditions. For lasers with very linear LI curves, very low distortion has been observed at low frequency. In contrast, for high frequency (> 1 GHz) systems, distortion increase significantly, and originates from the non-linear rate equations. Dynamic distortion due to non-linear interaction between electrons and photons in the laser cavity is dominant. Generally, the intensity modulation response of a laser diode is linear at lower frequencies and the non-linear distortion become more severe as modulating frequency increases and approaches the relaxation oscillation frequency. The modulation bandwidth of a laser diode is limited by the relaxation oscillation frequency. Improving the modulation bandwidth increases the linear region of the laser response, hence increasing the available bandwidth and reducing non-linear distortion. Recent work has shown that the modulation bandwidth of a laser can be improved by injecting external light into the laser cavity [7].

Non-linear distortion also depends on the modulation depth and can occur due to threshold clipping (over modulation distortion). Distortion due to LI curve non-linearity and over modulation is independent of modulation frequency. Leakage currents, thermal effects, and electron photon interactions can generate detrimental second and third harmonic distortions and intermodulation distortion (IMD). Other non-linearties may be caused by optical reflections or feedback into the laser. Optical feedback can considerably enhance IMD and harmonic distortion of a laser diode [8]. This may be greatly reduced by optical isolators. Several laser diode models have emerged and are generally based on the single mode rate equations. A study into semiconductor laser modelling is presented in [9, 10, 11]. The laser rate equations describe the non-linear interactions between injected carriers and photons in the laser active area. For single mode laser the rate equations are given below and described in [5].

$$\frac{dN}{dt} = \frac{I}{ev} - \frac{N}{\tau_{sp}} - g(N - N_o)(1 - \varepsilon S)S \tag{2.8}$$

$$\frac{dS}{dt} = \Gamma g(N - N_o)(1 - \varepsilon S)S - \frac{S}{\tau_{ph}} + \Gamma\beta\frac{N}{\tau_{sp}} \tag{2.9}$$

where

- N is the electron density in the conduction band
- S is the photon density in the lasing mode
- I is the current injected to the active region
- e electron charge
- v volume of active region
- g the optical gain factor
- Γ optical confinement factor
- τ_{ph} photon life time
- τ_{sp} spontaneous electron lifetime
- N_o transparent (threshold) carrier density
- ε power gain compression parameter
- β probability of spontaneous emission of a photon in phase with the lasing mode

Equation (2.8) states that the rate of increase in carrier density in the laser active region is proportional to the rate of current injection, less the rate of reduction in carriers due to spontaneous emission less the rate of reduction in carriers due to stimulated emission. Equation (2.9) states that the rate of increase in photon density in the laser active region is proportional to the fraction of optical confinement factor of stimulated emitted photons which are confined into the laser active region, the rate of loss of photons and the fraction β of spontaneous emitted photons which are coupled into the lasing mode. Gain compression enters the laser rate equations by the factor (1-εS) and has important implications for the linearity characteristics of a laser diode [9].

Since the laser dynamics described by the rate equations are intrinsically non-linear, harmonic and IMD occurs during this process which limit system performance. The harmonic distortion of the laser is an important consideration in CATV applications where the band of interest is on the order of a decade in width. Theoretical and experimental studies of second order distortions in CATV DFB laser diodes are presented in [12]. A detailed study of laser non-linearities and the implications for multi-channel subcarrier multiplexed fibre optic systems is presented by Salgado *et al* [13]. Lau, *et al* [14] have used a small signal analysis of the rate equations to calculate harmonic and intermodulation distortion of 1310 nm and 1550 nm lasers under microwave signal modulation. Non-linear theoretical models including, large signal [15] and Volterra series [16] have been presented for the study of laser diodes. Linearity and third order intermodulation distortion in DFB semiconductor lasers is investigated in [17] with the influence of several non-linearities, such as spatial hole burning, gain

compression, leakage current and relaxation oscillation [18]. It has been shown that spatial hole burning in DFB lasers play an important role in determining the non-linear distortion at low frequencies [19]. Spatial hole burning is caused by the coupling between the DFB grating and the active region creating a non-uniform distribution of the light intensity along the laser axis, which is power dependent. This effect has been shown to be responsible not only for an additional non-linearity of the laser curve but also for the gain and loss (threshold gain) above threshold becoming power dependent. An analytical expression for the 2nd order harmonic distortion caused by spatial hole burning in DFB lasers is investigated in [20]. An enhanced semiconductor laser model for analogue optical links is developed [21]. Important laser characteristics such as relaxation oscillation peak frequency and modulation bandwidth are evaluated under different conditions.

As the dc bias of the laser is increased, the bandwidth will generally increase. This is typically due to the relaxation oscillation characteristics that vary with bias. The response tends to peak before rolling off and this is the region of relaxation oscillation. The origin of the laser resonance derives from the interaction between the optical power density and the excess carrier density in the cavity. An increasing current leads to an increase in the carrier concentrations and this in turn leads to an increase in the recombination radiation density, which after a further delay, stimulates recombination and causes the carrier concentrations to fall. Because of the time delay, the fall overshoots the equilibrium value and an oscillation occurs [23]. The natural frequency of the system, f_o, is a function of the optical decay time constant, τ_{ph}, and the carrier recombination time constant, τ_{sp}. However, the interactions are

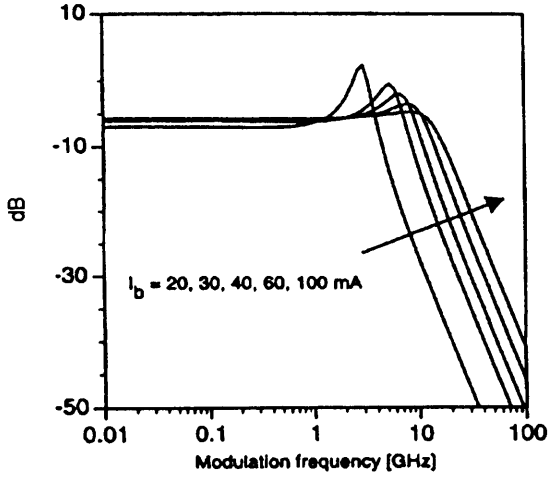

Figure 2.5 Modulation response of a DFB laser at various bias levels [22]

non-linear, so the analysis is complicated and the resonance frequency depends on the amount by which the laser bias level exceeds the threshold current, I_{th}. The variation of resonant frequency of a laser and its bias current is shown in Figure 2.5. Care must be taken when modulating the laser in this region, because this is where noise and distortion properties are often at their worst. The frequency, at which the peak of the modulation response occurs, known as the resonance frequency (f_r) can be approximated by equation (2.10) [23].

$$f_r^{\,2} = \frac{I_o - I_{th}}{4\pi^2 \tau_{sp} \tau_{ph} I_{th}}$$

$$f_r = \frac{1}{2\pi\sqrt{\tau_{sp}\tau_{ph}}}\left[\frac{I_o - I_{th}}{I_{th}}\right]^{\frac{1}{2}} \tag{2.10}$$

where f_r is the resonant frequency of the laser

I_o is the applied bias current and I_{th} is the threshold current of the laser

τ_{ph} is the photon lifetime (typical values are in the order of ps)

τ_{sp} is the carrier recombination time constant

The photon lifetime τ_{ph} represents the amount of time a photon spends in the laser cavity before either being emitted or absorbed and sets the upper limit to the modulation capability of a laser diode. From Figure 2.5 it can be observed that as the bias is increased, the resonance frequency and therefore the bandwidth of the laser is increased. Damping of the oscillation frequency increases with the bias current and can be approximated by [23].

$$\beta = \frac{I_o}{2\pi\tau_{sp} I_{th}} \tag{2.11}$$

In practice, several more complex effects such as spectral hole burning contribute to an increase in the damping term β, and so reduces the resonance peak and hence modify the laser modulation response. The response is also affected by parasitic effects, especially by the capacitance and by the stray inductance and capacitance associated with the packaging. Figure 2.6 shows the modulation response of a practical laser and this differs significantly from that of the ideal case as shown in Figure 2.5. It can be seen that at high bias currents, the resonance frequency of the laser increases with the increasing bias, but the modulation bandwidth of the laser decreases.

Linearising the laser transmitter used in fibre optic links is a more feasible approach allowing compensated low cost lasers rather than highly linear but expensive devices. To reduce non-linear distortions in semiconductor lasers, several linearisation techniques have been proposed and these will be discussed in the next section.

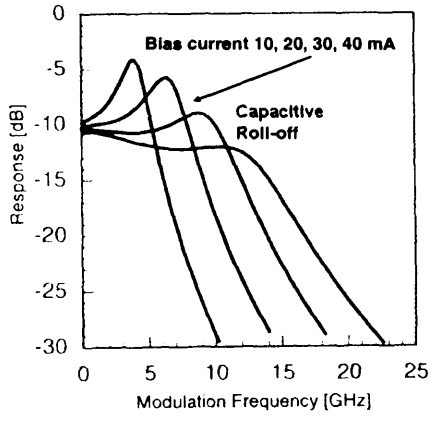

Figure 2.6 Practical modulation response of a laser diode [22]

2.4 Distortion Compensation Techniques

In this section distortion compensation techniques for optical transmitters are discussed together with limitations for each linearisation scheme.

2.4.1 Predistortion

Predistortion also known as complementary distortion [24] is considered to be the simplest and perhaps the most straightforward of the linearisation techniques [25]. It is preferred since it needs only one laser diode compared to the two required for feed-forward and the quasi-feed-forward. Predistortion is the predominant technique for linearising directly modulated optical transmitters and external modulators [26, 27, 28] and has also been widely used in linearisation of RF amplifiers utilised in wireless communications [29].

In this technique compensation is achieved when the RF input signal is intentionally predistorted before passing through the non-linear device. The non-linear devices in the predistortion circuit generate distortion products that are equal in amplitude but opposite in phase with the distortion produced by an optical transmitter (semiconductor laser or external modulator) such that the overall response is linear and distortion free. This requires modelling the non-linear analysis of the laser diode [27] to be compensated in order to be able to design the predistortion circuit to cancel the distortion signal. A basic explanation of the predistortion linearisation technique is shown in Figure 2.7.

A detailed functional block diagram of predistortion compensation with RF spectrum is shown in Figure 2.8 [30]. The circuit consists of two parts: a linear and a non-linear part. The linear section simply consists of a coaxial cable providing delay to ensure that the signals at the final coupler are delay matched. The RF signal is split into two paths using a splitter. Majority of the distortion free signal is passed through the microwave delay line and then into the final combiner, while a portion is coupled into a path with predistortion circuit consisting of non-linear devices. The non-linear part is further subdivided into second and third order paths. The RF input signal is fed into both the quadratic and cubic law devices to generate non-linear signals having the same amplitude with 180 degree phase difference to that produced by a laser diode. Ideally, the non-linear elements in the predistortion circuit represent second, third and higher orders of distortion. But in practice, a simultaneous control of both second and third order predistortion is very difficult to achieve. The quadratic and cubic law devices

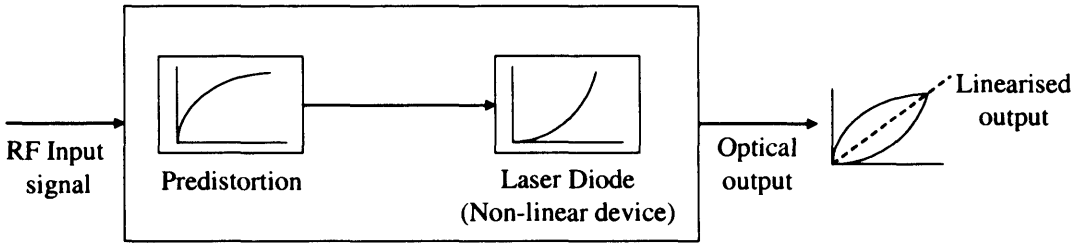

Figure 2.7 Basic principle of predistortion compensation.

can be diodes, which do not require high bias voltage, or field effect transistors biased near pinch off [31]. Schottky diodes are also very popular active devices as distortion generators because of their fast response and low power consumption. Usually two diodes are used in the distortion path in an anti-parallel arrangement connected in shunt [32, 33] and operating as gain compressors or expanders by increasing the signal that they reflect. For small signal levels the gain of the linear and the distorted paths are constant and no predistortion signal is generated.

Amplifiers are included to provide gain in the loop to overcome input and output splitter and combiner loss. A variable amplitude and phase control is included for fine adjustment of the signal so that it is equal to that produced by the laser. Frequency tilt shaping networks have been implemented to let the correcting signals match the laser HD2 and HD3 curves in the whole operational band [34]. The amount of second and third order distortion recombined with the signal at the output can be adjusted relative to the amplitude of the undistorted signal in the delay branch.

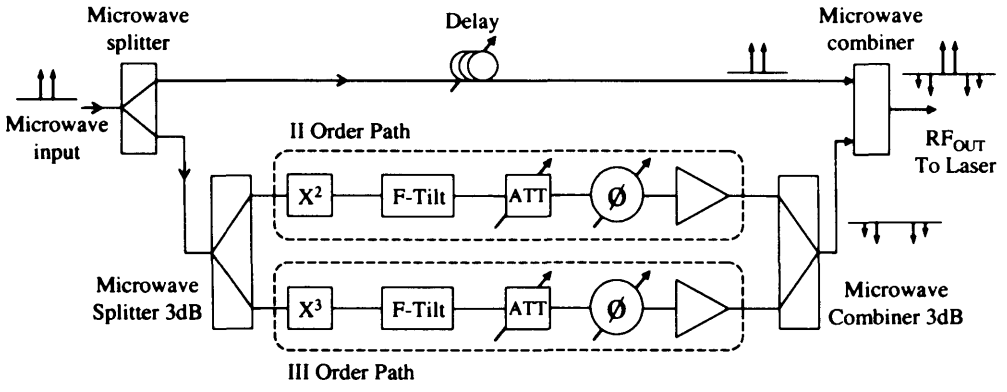

Figure 2.8 Diagram of Predistortion compensation

Predistortion has been investigated in analogue applications such as AM-VSB modulated lightwave CATV transmission systems. The non-linear distortion properties of optical devices can severely limit the system performance and give rise to serious harmonic and intermodulation distortion. Typical specifications for a CATV trunk system [35] requires Carrier to Noise Ratio (CNR) > 55 dB, Composite Second Order (CSO)[1] < -65 dBc and Composite Triple Beat (CTB)[2] < -60 dBc for good picture quality [36]. MZ interferometers (MZI's) are common external modulators for optical transmitters and have been widely used in CATV systems. Second order distortion products primarily limit the DFB lasers, while third order distortion products limit MZ modulators. Biasing the modulator at the inflection point eliminates the CSO [33]. In principle second order IMD can be filtered out if the bandwidth is less than one octave. However CATV transmission systems operate with bandwidths of many octaves.

[1] CSO refers to superposition of all terms within a stated bandwidth of a particular frequency, which are due to second order distortion.

[2] CTB refers to superposition of all terms within a stated bandwidth of a particular frequency, which are created by the mixing of three frequencies.

Several authors have tested and reported predistortion linearisation on both semiconductor lasers and modulators. However, recently the focus has moved to the linearisation of modulators only. This is because semiconductor lasers have both second and third order distortion and these distortion products are frequency dependent. Predistortion circuits for compensating more than one order of distortion are very difficult to design. Normally, only one particular order of distortion can be reduced. For modulators, distortion is well defined. If biased at the quadrature point, second order distortion can become negligible and only third order distortion needs to be reduced. Predistortion linearisation is therefore more suitable for linearising modulators.

A second order predistorter was reported by Darcie *et al* [37] to reduce CSO without increasing CTB in a multi-channel system. A comparison of non-linear distortion in CATV for semiconductor lasers versus external modulators is carried out in [36, 38]. To meet these stringent demands Childs *et al* [31] described predistortion technique which reduce the dominant distortion of a DFB laser and external modulators by 12 and 14 dB, respectively, allowing a large increase in modulation index. The scheme has been used in optical transmitters to compensate laser non-linearity for CATV signals with frequencies between 50 MHz and 550 MHz [39].

Compensation of non-linear distortion in modulators has been demonstrated using the predistortion circuit [32, 40, 41,] for CATV systems. Chiu *et* al [42] developed a CMOS lineariser for external modulators with an arcsine transfer function that is the inverse of the raised cosine transfer function of the modulator. A feedback loop is also implemented to stabilise the transmitter against long term drifts of the modulator bias point or circuit component values, caused by thermal drift or device degradation. The field effect transistor based arcsine circuit generates odd order harmonics that cancel those of the modulator biased at the quadrature point. A 14 dB improvement in SFDR from 85 $dB.Hz^{2/3}$ to 99 $dB.Hz^{2/3}$ has been achieved with IMD suppression of 17 dB at 1.3 GHz. A monolithic predistortion linearisation circuit with application to externally modulated analogue links has been designed with 17 dB suppression of 3^{rd} order IMD from DC to 1.3 GHz [43]. Experimental results on a fully digital bias compensation loop have been reported to eliminate the bias drift in MZ modulators. To detect the drift in the bias point of the modulator a low frequency pilot tone with small amplitude is added to the RF signal. Bias drift in the modulator gives rise to even order harmonics of the pilot tone which are detected and demodulated to generate a correction signal to be applied to the modulator bias. The entire process of filtering, down conversion and integration of the pilot tone distortion is preformed in the digital domain resulting in a high performance and low cost solution. With fully digital bias compensation loop 25 dB suppression of 2^{nd} order distortion is achieved. More recently predistortion has been investigated for improving linearity of MZ modulators in wireless over fibre systems and IMD3 products were reduced by more than 15 dB [44].

A predistortion circuit fabricated in MMIC technology has been developed that operates up to 10 GHz [45]. The circuit improved dynamic range by 3 dB from 108 $dB.Hz^{2/3}$ to 111 $dB.Hz^{2/3}$. A MMIC pre/postdistortion circuit for an analogue fibre optic link based on a MZ modulator is also designed

[46]. This circuit improved the link SFDR by 3 dB to 110 dB.$Hz^{2/3}$. Two balanced branches of diodes (configuration shown in [46]) provide a symmetrical non-linear transfer function, which can compensate that of the modulator. The dc bias current source charges the capacitors and sets the diode operating points which control the level of introduced non-linear distortion. The pre/postdistortion circuit is fabricated using a GaAs HBT process. The resulting dynamic range can be further improved with the proposed predistortion circuit when using a low voltage MZ modulator.

In 1999 Steiner *et al* [47] designed an adaptive predistortion circuit in microstrip technology using a microcontroller to adjust the control voltages to reduce laser 3rd order IMD by 20 dB over a frequency range of 1750 MHz to 1870 MHz. The cubic law device consists of two anti parallel diodes. For adaptive predistortion the control voltages for the phase shifter and the attenuator have to be readjusted due to laser ageing effects. Down converting and low pass filtering of the IMD3 generates a mixing signal proportional to the IMD3 in the transmission band. After analogue to digital conversion, a microcontroller tracks the phase and amplitude for maximum IMD3 cancellation. The adaptive technique has reduced IMD3 by 20 dB over 120 MHz bandwidth and the SFDR improved from 72 dB to 78.7 dB.

Roselli *et al* [48] designed and demonstrated a predistortion circuit for wireless over fibre systems in the frequency range of 500 MHz to 2 GHz, for multiservice GSM, DCS and GPRS cellular services. A reduction of about 10 to 15 dB for the second and third order harmonic distortion has been achieved over the bandwidth of 1710-1890 MHz covering the cellular bands. Further improvements to the circuit have been reported in [30].

Fernando *et al* [49] demonstrated laser non-linearity compensation using higher order adaptive filters. Pre-compensation is done for the downlink while post-distortion is done for the uplink. With this approach accurate measurement of link parameters is not required because the filters are adapted from the distortion of the input/output baseband signal.

A CMOS adaptive predistortion lineariser designed to extend the dynamic range of direct and externally modulated links by suppressing both 2nd and 3rd order distortion is demonstrated in [50]. The circuit is designed in 180 nm CMOS technology and second and third order non-linear distortion is generated using the I-V characteristics of non-linear semiconductor device. A feedback control loop using a PC running Labview is implemented for adaptive technique. The distortion products are filtered and fed to the PC equipped with a data acquisition card. The algorithm monitors power of the distortion products while sweeping the amplitude and phase control for minimum intermodulation distortion power. The circuit reduced IMD3 by 19 dB across a bandwidth of 90 MHz centred at 295 MHz and improved SFDR by 6 dB for direct and externally modulated links.

A predistortion lineariser combined with fabry perot LD for wideband code division multiple access (W-CDMA) wireless over fibre system is reported [51]. A 20 dB improvement in the IMD3 component is obtained over the bandwidth of 60 MHz.

Limitations

Predistortion compensation has been shown to be a very effective technique for reducing distortion in optical transmitters (both directly modulated lasers and external modulators) for applications in CATV and cellular communication. Predistortion is more suitable for linearising modulators because if the modulator is biased at a quadrature point, then second order distortion can become negligible and only third order distortion needs to be reduced.

The main advantages of this scheme are simplicity of circuit design, small physical size, low power consumption and the fact that it uses only one optical transmitter. However, the disadvantages of predistortion for directly modulated lasers lie in the way distortion correction is generated, which is independent of the non-linear characteristics of the laser diode and must be matched to individual laser. Only one particular order of distortion can be reduced since the complexity of the electrical circuit increases due to difficulty of controlling the harmonics and IMD at the same time. For perfect cancellation of distortion products an exact inverse transfer characteristic of the laser diode is required and this is extremely difficult to achieve over a wide operational bandwidth [27]. Also the performance of predistortion circuits at high frequency can become difficult to predict due to parasitic capacitance and inductance associated with the junction diodes or other non-linear elements used [25], hence realisation is difficult at microwave frequencies. Since most practical predistortion linearisers are analysed and designed as cubic distortion generators to compensate 3^{rd} order IMD products, significant 5^{th} and 7^{th} order products at high input power levels are not generally compensated. Also unlike feedback and feed-forward compensation, predistortion does not reduce laser relative intensity noise.

Although, complete distortion cancellation cannot be achieved over a wide range of modulation frequency due to difficulties in matching, 10 dB improvements for CATV and cellular communication applications are more common. The highest frequency for laser linearisation using predistortion has been reported at 2 GHz [48] for cellular bands in a wireless over fibre system.

2.4.2 Dual parallel modulation

A dual parallel modulation technique is constructed using two optical transmitters in parallel and employs phase shift modulation to improve linearity of optical sources. A diagram of the dual parallel modulation technique is shown in Figure 2.9. Experimental results have been reported [52] using this technique for LED linearisation to reduce harmonic distortion. A 25 dB improvement in second harmonic distortion at a modulation frequency of 3.1 MHz for multi-channel signal transmission is demonstrated. In this method the incoming signal is equally divided into two parts. Two signals with phase difference provided by a phase shifter modulate separate optical transmitters. The modulated optical signals are combined using an optical coupler then transmitted over fibre and finally detected by a photodiode at the receiver. If the two transmitters have matched light current characteristics, second order or higher order terms are related to the phase difference. Therefore, by selecting the phase difference appropriately, a selective order distortion is cancelled. This technique can be applied to

compensate harmonic distortion of any order. For second harmonic reduction a 90° phase shift is required while a 60° phase shift cancels the third harmonics [24]. In general, the n^{th} order distortion is cancelled when the phase angle between the two modulating signals is equal to π/n. The advantage of this technique is the simplicity and high degree of distortion cancellation can be achieved. However since different phase shifts are required to cancel different harmonics, all harmonics cannot be reduced simultaneously [53]. Another disadvantage is that since there is phase difference between the two modulation signals, there is a partial cancellation of the fundamental signal and hence a signal power penalty.

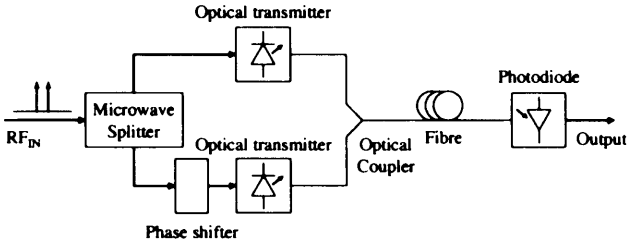

Figure 2.9: Dual parallel modulation scheme

In 1990 Korotky *et al* [54], first examined the use of dual parallel modulation scheme for low distortion analogue optical transmission using intensity modulators for CATV systems. Since the requirement on linearity is particularly stringent and can be limitation for CATV applications where the numbers of frequency multiplexed channels are large, typically 40 or more linearisation techniques are employed. The dual parallel technique consists of two intensity modulators and the distortion created by a secondary modulator cancels the distortion produced by the primary modulator. The optical input power is split into two parts to feed the primary and the secondary modulator, with the primary modulator receiving more optical power. The RF drive power is split so that the secondary modulator is modulated by an RF signal stronger than that of the primary modulator and has a higher modulation depth and greater distortion. Because the secondary modulator receives less optical input power, its output will have a weaker signal than the primary output. The distortion in the secondary modulator output is however equal to that of the primary modulator because the modulation is stronger. The secondary modulator is biased at a quadrature point 180° from the point chosen for the primary modulator. A phase shifter is employed to maintain the phase difference between the primary and secondary modulator outputs so that when combined and photo-detected the distortion will cancel with a small cancellation of the fundamental signal. The overall output is thus weaker, but free from distortion. Since both modulators are biased at quadrature points, second order distortion products are eliminated. More then 20 dB of third order distortion cancellation has been demonstrated by Brooks *et al* [55] for two lithium niobate Mach-Zehnder interferometers in a multi-tone video spectrum.

The dual parallel modulation scheme can be implemented using two approaches. In the first approach using a single optical source, where the optical power is split and launched into two modulators and the outputs of which are then coherently recombined. However, a phase modulator is

required in one of the two MZ outputs paths in order to maintain quadrature between the primary and secondary signals to prevent the recreation of distortion products in the optical output signal. In the second approach, using a separate optical source for each of the modulators the effects of coherent recombination can be eliminated. Although this does not require the additional phase modulator, it does require two optical sources that must be accurately maintained at a constant power ratio. Practical implementations will require adjustment of the electrical drive signals or provision for trimming the optical splitters and combiners [54]. A modified approach by Ackerman *et al* [56] has been reported for broadband linearisation using a single MZ modulator. The feasibility of a dual parallel technique for the reduction of IMD in broadband systems using a single modulator is reported by Loyassa *et al* [57]. This implementation offers less complexity than the standard dual parallel technique and can operate in the millimetre wave frequency range.

Dynamic range enhancement of the electro-absorption modulator (EAM) for wireless over fibre system is demonstrated in [58, 59] using the dual parallel scheme. A reduction of 23 dB in IMD3 and increase in dynamic range by 19.6 dB to 110 $dB.Hz^{2/3}$ at 8 GHz is achieved. The EAM offers advantages of low driving voltage, a small size, and monolithic integration capability with other optical components. Two modulators are connected in parallel to compensate non-linearity of the main modulator using a phase reversed non-linearity of the other modulator Linearisation is obtained by controlling the DC bias voltages of each modulator separately, so that the distortions have a 180 degrees phase difference. Integrated dual electro-absorption modulator is also proposed in [60]. This device can suppress two non-linear components simultaneously by controlling two bias points rather than one bias point to suppress one non-linear component, but can lead to increased system complexity. Also the operating bandwidth is restricted to narrowband [58].

Jung *et al*, experimentally demonstrated the dual parallel modulation technique to reduce IMD3 in DFB laser diodes and achieved 16 dB [61, 62] and 20 dB [63] reduction at 2.2 GHz. Since only two laser diodes and one optical coupler is required it is considered to be very simple and easy to implement. The scheme exploits the fact that when the laser diode is directly modulated by RF signals, frequency chirping influences the amplitude and phase of the RF signal. However, frequency chirping is dependent on dc bias current. Therefore, by controlling only the bias current of the second laser, the amplitude and phase difference of IMD3 can be made out of phase and hence suppression is achieved when the signals are combined at the photodiode. Although reduction is achieved for IMD3 at a certain bias level, the IMD5 products are not fully compensated as the signals are differently affected by frequency chirping [63]. The condition to satisfy the IMD3 signals may not completely satisfy the out of phase condition of IMD5. Frequency chirping is also affected by input RF power. Therefore, to tune the suppressed RF power at a different level, a new bias value is set. Also the technique is only suitable for narrow band applications and is sensitive to the variation of optical wavelength, since the phase variations of each frequency component of modulated signal by frequency chirping is slightly different. This would require cooled type sources and a wavelength locking mechanism. Further work is required

for this technique to be used in a practical system since the two lasers are of different wavelengths and the suppression condition will not be maintained after transmission over fibre with same bias conditions due to chromatic dispersion effects.

2.4.3 Linearisation of external modulator

Linearisations of external modulators have been reported in the electrical and optical domain [64]. Some of these less common linearisation techniques are described here.

Polarisation mixing modulator

The dual polarisation technique for reducing IMD in optical modulators has been demonstrated by Johnson *et al* [65]. The modulator must support TE and TM polarisation modes. The two modes see different transfer functions and the modulator bias must be adjusted such that both polarisation modes are biased at the half power point with slopes of opposite signs. This involves adjusting the polariser to allow a suitable TE to TM power ratios into the modulator, the cubic response of the TE mode can exactly cancel that of the TM mode, resulting in improved linearity. Reductions in IMD as high as 21 dB have been reported in the kHz range. In [66] the author reports IMD reduction by 14 dB over the frequency range of 3.6 to 5.6 GHz. However the main limitations are that the scheme requires a large dc bias and an accurate TE-TM power ratio [67].

Cascade coupling modulators

Cascaded compensation is a suitable linearisation technique for lightwave system. A reduction of 30 dB in second order distortion has been experimentally observed [53]. Linearised cascaded modulators have been reported [68] for CATV systems with SFDR of 115 $dB.Hz^{2/3}$ and 34 dB reduction in IMD3. In this scheme two modulators are cascaded, with couplers having fixed coupling ratios.

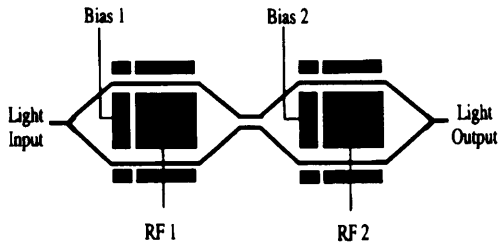

Figure 2.10: Schematic representation of the cascaded linearised modulator [68]

It is the second modulator that compensates for the non-linearities introduced by the first modulator. Suppression of non-linear distortion is achieved by adjusting the bias voltages (not necessarily set at quadrature point) of the two modulators and the relative amplitude and phases of the RF input signal to each modulator. This technique has the advantage that it is completely passive. The linearisation takes place entirely on the optical chip; thus, the modulator's frequency response is not

limited by the bandwidth of electronic components as in the case of electronic linearisation. For the cascaded modulators, crosstalk problems are less severe than the parallel scheme and a lower bias voltage is usually required compared with other modified directional coupler schemes. The main disadvantage of this approach is that precise and critical adjustments of the bias voltages and the amplitudes and phase of the RF signals at the input ports are required. Another problem is its temperature sensitivity. When the temperature changes, the bias points of the two modulators drift in opposite directions; thus, the third order distortion increases sharply. Therefore, extra circuitry is needed to control the bias voltages and stabilise the temperature. Betts *et al* [69] investigated series connection of an MZ with a second MZ of reduced extinction (i.e. an optical power imbalance between arms so that the transmission is never zero) produces a linearised modulator to improve dynamic range. This technique has the advantage that it avoids the optical power splitting/combining difficulties of the parallel MZ. However these reduced extinction series MZ designs require two critical control adjustments and incur a noise figure penalty of approximately 6 dB compared to a single MZ, mainly due to the constraint of simultaneously minimising both second and third order distortion.

LiNbO3 MZ modulators are widely employed. Such modulators, however, suffer from the DC drift effect and require control circuits. Compared with LiNbO3 modulators, MQW-EA modulators are superior because they are DC drift free and offer lower power consumption [70]. An electro-absorption modulator (EAM) is an attractive device for low chirp, small size, and low driving voltage. Especially, the EAM monolithically integrated with a DFB laser (EAM-DFB) is the most practical device utilising the EAM, because the high coupling efficiency, between the EAM and laser in the integrated structure leads to high output power of the modulated light, providing its advantage over other modulators such as $LiNbO_3$ MZ and contributes to reduce system size and cost [71]. Linearisation of MQW electroabsorption modulator using an all optical frequency insensitive technique has been investigated [72]. A comparison of analogue RF photonic links using a variety of linearised electro-optic modulators is discussed in [73].

Meng *et al* [74] investigated electro-optical predistortion to eliminate the need for broadband non-linear electrical devices. The non-linear element in this scheme is an additional MZ modulator (i.e. distorter) and has a higher modulation index and therefore larger distortion. The distortion components produced by the distorter are combined with the fundamental signal at the output of the predistorter to drive the primary modulator to reduce IMD3. Both the primary and distorter modulators are biased at the quadrature point. The RF input signal is divided into the linear and distortion path. The linear path is a time delay line to keep a 180 degrees phase difference between the two paths.

Mathai *et al* [75], reported a balanced electro-absorption modulator for analogue optical links, to allow simultaneous suppression of all even order distortions, third order IMD and laser RIN independent of the bias point. By biasing the balanced electro-absorption modulator at the third order null and operating the link in balanced mode, 7.5 dB suppression of second order distortion and 2 dB suppression of laser RIN was experimentally demonstrated. Employing the new balanced modulator

shows great improvement in the overall link performance compared to conventional links using a single electroabsorption modulator. Optical delay lines and variable optical attenuators on the upper and lower output arms are required to compensate for RF phase and amplitude mismatch, respectively. At higher frequencies, fibre path length matching becomes more stringent.

2.4.4 Injection locking techniques

The transmission capacity of a system employing direct laser modulation is generally limited by the bandwidth of semiconductor lasers. The non-linear distortion becomes more severe as modulating frequency approaches the relaxation oscillation frequency, due to the non-linear coupling between electrons and photons. Therefore, if the relaxation frequency of the laser is increased, then the intrinsic non-linear distortion can be reduced in the GHz range. Several, research groups have shown theoretically that the use of external optical injection locking technique can enhance the modulation bandwidth of a laser diode, and hence improve the system performance at high frequencies [76, 77, 78, 79,].

In this scheme, light from the master laser is injected into a directly modulated DFB slave laser. The optical circulator allows injection through the front facet of the slave, and provides an additional stage of isolation for unwanted light coupling from the slave to master laser. The slave laser is locked to the master laser and the laser non-linearities are reduced. A Polarisation controller is required to adjust the polarisation of the injected light. The locking behaviour of slave laser strongly depends on two parameters: the injection ratio and detuning frequency. The injection ratio is defined as the power ratio of the injected signal into the slave laser cavity from the master laser. The detuning frequency is the frequency shift of the injected signal with respect to the free running frequency of the slave laser.

Meng *et al* [80] experimentally investigated the effects of optical injection locking on the non-linear distortion of a directly modulated semiconductor laser. The authors reported that under strong injection locking with –8 dB injection ratio and –15 GHz frequency detuning, the second and third harmonic distortions were suppressed from 2-4 GHz, with 15 dB reduction in IMD3 from 1.4-3 GHz. The SFDR increased from 95 $dB.Hz^{2/3}$ to 100 $dB.Hz^{2/3}$. The improved performance results from the dramatic increase of relaxation frequency of the DFB laser from 4.1 GHz in the free running case to 13.6 GHz under injection locking. In [79] BPSK data transmission on a sub-carrier was investigated. With optical injection locking open eye diagrams and BER $<10^{-9}$ has been achieved at sub-carrier frequency of 1.8 times the bandwidth of the free running laser.

The injection locking scheme is considered to be simple and can significantly enhance the modulation bandwidth. However, wavelength difference between the master and the slave laser is important for satisfying the locking condition and this is controlled by temperature tuning the master laser. For an optimised operation, the injection wavelength has to be carefully chosen to be slightly longer than that of the slave laser [81]. Since the locking range is not very wide this may limit the

practicality of this method. Several authors have reported the use of optical injection locking to enhance the modulation bandwidth of laser diodes [82, 83].

Chrostowski *et al* [84, 85] investigated optical injection locking in VCSELs and demonstrated simultaneous reduction of RIN and improvement of dynamic range. The author reports a record SFDR of 111 $dB.Hz^{2/3}$ for a directly modulated VCSEL. When the laser is injection locked, fewer carriers are needed to achieve lasing threshold. The spontaneous emission of the laser, and therefore its noise, is reduced. In addition, the resonance frequency enhancement for some injection conditions further reduces the noise value. The combination of these two factors results in RIN reduction of an injection locked laser. Modulation bandwidth in excess of 35 GHz has been demonstrated experimentally with this technique [86]. A record resonance frequency of > 40 GHz have also been reported for VCSEL [87].

Non-linear distortion suppression by sidemode optical injection locking has been demonstrated by Seo *et al* [88] with more than 10 dB reduction in IMD3 at 2.8 GHz. In this scheme, light from an external laser (master laser) is injected into the sidemode of the transmitting laser (slave laser) and not the fundamental mode. When the light of the master laser is injected into the slave laser sidemode, then its fundamental mode is significantly suppressed and the sidemode becomes dominant. With increasing injection power from the master laser, the slave laser fundamental mode is suppressed. The distortion suppression range can be widened by a factor of about two compared with external optical injection locking. This overcomes the narrow stable locking range problem associated with optical injection locking demonstrated by Meng *et al* [80], as locking occurs within the relatively large lasing frequency detuning range between the master and slave, and is typically tens of GHz.

2.4.5 Opto-electronic feedback

Opto-electronic (electro-optical) feedback has been used to improve linearity in analogue optical transmitters such as light emitting diodes (LEDs) for cable TV (CATV) systems [24, 89]. This method operates in the same way as electronic feedback invented by Harold S Black in 1927 [90] and a reduction of both noise and distortion in the optical output signal can be achieved by the feedback loop.

In opto-electronic feedback a sample of the modulated output signal is detected using a photodiode to monitor the optical feedback signal, amplified, phase inverted and then compared with the electrical input signal to produce an error signal which drives the source so that the modulated

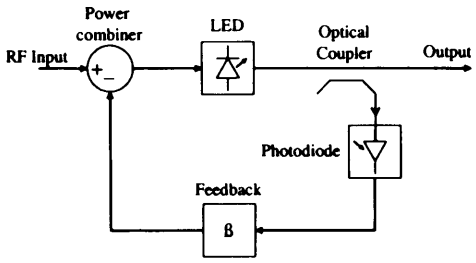

Figure 2.11: Basic schematic of Opto-electronic feedback

output closely resembles the electrical input [53]. The amount of distortion compensation depends on feedback loop gain [91]. Figure 2.11 illustrates the basic schematic of Opto-electronic feedback compensation demonstrated by Grijp *et al* [92] for LED linearisation with 2nd and 3rd order harmonics reduced by 10 dB and the noise level reduced by 12 dB. In [53] second and third order distortions were compensated by 12 and 4 dB respectively and intensity noise suppression using this technique has been demonstrated [93]. Further improvement in linearity and noise performance can be obtained by reducing the loop delay [94].

The advantage of feedback lies in the fact that the correction signal is generated from the distorted output signal and is therefore, at any instant, adapted to the output of the system. Thus this method is not restricted to 2nd order cancellation only. Although the application of negative feedback is relatively simple, it is however, the loop stability that imposes limitations on the performance and hence the bandwidth of the signals that can be handled. Since the loop gain and the loop delay must be decreased towards higher frequencies to maintain stability, reduction of non-linear distortion decreases.

Limitations

The limitation of opto-electronic feedback is that large bandwidth requirements can create problems at high frequencies since the finite time delay around the feedback loop reduces the bandwidth over which stable linearisation can be achieved. In practice, it is difficult to make the feedback system respond to signal changes greater than several MHz because of the delay with the associated components. Since the rate of change of phase with respect to time is equal to the angular frequency, then the delay of the network is given by:

$$\tau = \frac{\Delta\phi}{\Delta\omega} \tag{2.12}$$

The frequency $\omega=\omega_{180}$ can be calculated by setting the phase term equal to 180° and evaluating for a given delay τ, that is:

$$\Delta\omega_{180} = \frac{\pi}{\tau} \text{ or } \Delta f_{180} = \frac{1}{2\tau} \tag{2.13}$$

As the delay τ increases, the bandwidth over which the system is stable ($f < f_{180}$) becomes progressively smaller. Hence the unity gain bandwidth is limited by the loop propagation delay [37] to $f < 1/(2\tau)$ where τ is the total open loop propagation delay. Considering a system using discrete components it would be difficult to make $\tau < 0.5$ nS, giving a delay limited unity gain bandwidth of 1 GHz. In a practical system this could further be reduced to 500 MHz due to delay in feedback path. This means opto-electronic feedback can only be employed for applications such as CATV and so cannot be used for high capacity access networks. Progress on monolithic integration circuit may lead to feedback circuits that can operate in the GHz region [25].

Another issue resulting from feedback is that the output power of the optical transmitter is reduced. A modified opto-electronic feedback configuration is proposed by Liu [95], which combines

the opto-electronic feedback and feed-forward technique. In this scheme, the error signal tapped from the optical output is combined with the direct reference delayed path and then applied to the optical source. Since only negative feedback of the error signal is applied, the output signal power will not be greatly reduced by the feedback loop. Although this leads to a slight increase in circuit complexity, it has the advantage of higher output power compared to conventional feedback with only one optical source. Other drawbacks include increased complexity of the circuit that has to be built around the specific optical transmitter and the deterioration of loop performance due to temperature and ageing effects on the characteristics of the feedback components. Since the time delay associated with the feedback loop may result in an unstable operation of the circuit, it is only suitable for frequencies in the order of few hundred MHz, and therefore is not widely adopted.

2.4.6 Quasi-Feed-forward

Quasi-feed-forward compensation is a technique that combines predistortion and feed-forward to provide linearisation [24]. This scheme uses two optical sources (LEDs or semiconductor lasers) and the distortion produced by one non-linear device is cancelled with the opposite distortion component produced by another device [25]. Figure 2.12 shows the circuit diagram for Quasi-feed-forward compensation.

The principle of operation is that the incoming input signal is split into three paths. In one of the paths, the signal modulates Laser 1 which generates optical signal plus distortion. The signal plus distortion is detected by the photodiode, amplified and then inverted. At the hybrid coupler the inverted signal plus distortion from Laser 1 is subtracted from the reference path. The output of the hybrid coupler is the distortion products inverted in phase. The error signal is then amplified by the error

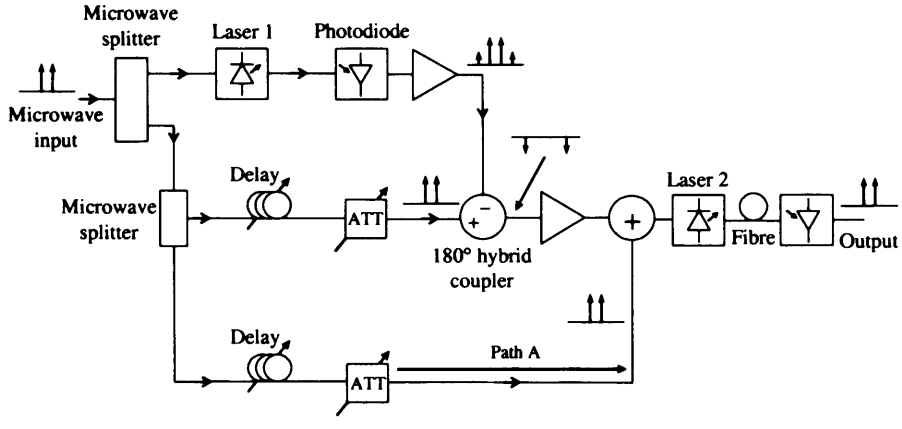

Figure 2.12 Principle of Quasi-feed-forward compensation

amplifier and combined in a coupler with another reference signal coming from the third path. The output of this coupler then modulates the secondary Laser 2. If Laser 2 has the same distortion characteristics as Laser 1, then it will generate distortion which is equal in amplitude but opposite in

phase. For effective cancellation of the distortion products this requires the two sources to be of similar characteristics which can be very difficult.

Adjustment in amplitude and phase is made so that the distortion products create a compensating signal equal in amplitude and opposite in phase to the distortion generated by Laser 2. In this technique the first laser provides the compensating signal and it is the second laser that is linearised by predistorting the input modulation signal. From the system diagram it can be seen that the error-detecting part of this compensation scheme is exactly the same as that used in optical feed-forward compensation (discussed later). The main difference between the two techniques is the method used to achieve distortion compensation [89].

To demonstrate the feasibility, the scheme was applied to an optical transmitter such as a LED for multi-channel signal transmission. An improvement of more than 33 dB in second order and 17 dB in third order distortion has been achieved [96], and more than 35 dB in second order and 20 dB in third order distortion in a system transmitting three TV channels simultaneously was shown by Patterson *et al* [97]. The linearised system is capable of video signal transmission over a distance of at least 2 km without repeaters. In [89] it is shown that using quasi-feed-forward technique, analogue transmitters can be designed with less then -80 dB harmonic distortions for multi-channel video transmission.

Limitations

Although Quasi-feed-forward has been shown to be an effective cancellation technique using LED's, it is expected that the same technique could also be applied for the linearisation of lasers. However, the difficulty in implementing this scheme is due to large variation in device characteristics over time. For effective cancellation this requires the two optical sources to be identical or of similar characteristics. With non-identical devices, the compensation will generally be not effective and a variety of design compromises can be affected.

2.4.7 Feed-forward

The feed-forward technique was first developed in 1924 by Harold S Black [98] as a means to compensate noise and distortion in repeaters for long distance carrier telephony However, its use was overshadowed by the simplicity of feedback, which was also invented by Black three years later. Feed-forward was largely ignored until the late 1960s when was applied in RF applications by Seidel *et al* at Bell Laboratories in an attempt to reduce IMD in travelling wave tube amplifiers [90]. Since the 1970s interest in feed-forward grew mainly due to broad bandwidth cancellation and good stability. The technique has been widely used for IMD reduction in both optical transmitters [24] and RF amplifiers utilised in wireless communications.

The feed-forward compensation is very similar to the quasi-feed-forward technique, but does not require two transmitters with similar characteristics. The circuit for this scheme is shown in Figure 2.13 with the relevant electrical spectra. The basic operation of feed-forward circuit is that the input

signal is split into two paths; one path modulates the primary laser while the other path is used as a reference signal. Detecting the signal from Laser 1 and comparing it with the time delayed reference

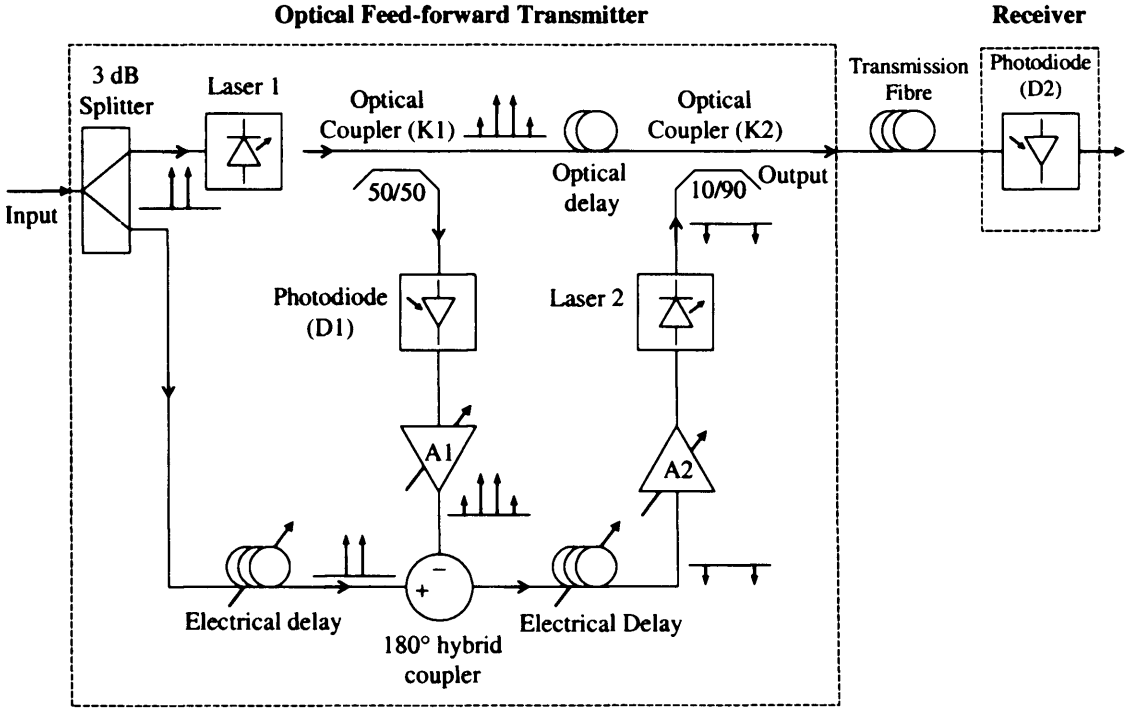

Figure 2.13: Schematic diagram of the Optical Feed-forward Transmitter

path provides an error signal at the output of the 180 degree hybrid coupler which is then amplified and modulates the secondary laser. The modulated optical signal from Laser 2 is combined with the optical signal of Laser 1 to cancel the distortion products when detected by the PIN photodiode. For maximum cancellation of the distortion products amplitude and phase matching is required both for the carrier suppression loop and the distortion cancellation loop. This is facilitated with the use of variable gain amplifiers and microwave phase shifters.

In the late 1970s, with the growing demand for cable television (CATV) systems many authors investigated the possibility of employing feed-forward compensation to linearise LEDs [24, 89] and directly modulated semiconductor lasers in order to meet the stringent specifications for CATV. In 1991 Fock *et al* [99, 100] experimentally investigated feed-forward for 1.3 μm directly modulated semiconductor lasers and achieved more then 14 dB reduction of second order and 3rd order IMD reduction of 10 dB over the frequency range of 100 MHz to 1.5 GHz. A few months later, the same author reported the first demonstration of reduced intensity noise in a semiconductor laser using feed-forward compensation [99]. Previously noise reduction of 12 dB has been reported [92] using opto-electronic feedback for narrowband systems. In [101] it was shown that RIN decreased by nearly 8 dB by increasing the cavity length and further reduction in RIN is achieved by reducing the p-doping concentration of the active layer. With feed-forward the intensity noise had been reduced by more then 10 dB over the frequency range 1.7-3.0 GHz together with simultaneous improvement in second

harmonic distortion of 25 dB at 2.4 GHz and third order IMD reduction by more than 10 dB from 2.1 – 3.0 GHz. The maximum improvement in intensity noise observed was 14 dB limited by the instrument. In 1992 [102], the same author carried out further experimental work on noise reduction and presented theoretical estimation of noise limitations of feed-forward compensation. This simultaneous reduction of noise and distortion was attributed to the fact that distortion products can be viewed as a form of noise in a feed-forward system. One of the conclusions made in this work was that "the condition for maximum improvement in intensity noise is also the condition for maximum suppression of distortion".

In 1993 Hassin *et al* [103, 104] reported theoretical simulation and experimental results to achieve distortion cancellation of 20 dB over a bandwidth of 850 MHz. Ideal case simulated feed-forward results showed a distortion reduction of about 92 dB to a level of -138 dBc. However simulations of practical system with optical phase and amplitude match of less than 2 degrees and 0.5 dB respectively, showed non-linear distortion reduction of approximately 30 dB. It was emphasised that the system performance is dominated by amplitude and phase match between the two optical signals and obtaining such accuracy is very difficult over a wide bandwidth. A more achievable match of 5 degrees and 1 dB resulted in distortion reduction of 20 dB.

Vahldieck [105] reported experimental results in 1994 achieving a 10 dB noise reduction over a bandwidth of 400 MHz for CATV networks and an average of 18 dB non-linear distortion improvement using optical feed-forward. In the same year Buxton *et al* [106] also demonstrated an average of 10 dB noise reductions over the frequency range up to 400 MHz together with distortion products lower than -60 dBc in order to meet the specifications for the distribution of CATV system.

Feed-forward compensation has also been investigated in linearisation of external modulators by Ridder *et al* [107] to reduce distortion. Experimental results demonstrated signal suppression of > 15 dB over the frequency range of 50-300 MHz and > 25 dB from 300-500 MHz. A reduction of 35 dB in IMD is demonstrated in [108]. Iwai *et* al [109] discussed the use of feed-forward to compensate signal distortion due to non-linearity of the modulator's L-V characteristics for CATV transmission systems. MQW-EA modulators are considered to be beneficial since they are drift free (dc drift effect) and can be monolithically integrated with DFB lasers. Since the L-V characteristic depends on device temperature, a control circuit is necessary to drive the modulator in a stable condition. Signal distortion is suppressed by 12-15 dB. The author also states that the degradation of signal distortion cancellation due to group delay difference can be well suppressed even after 10 km transmission by minimising the wavelength difference between the two sources to <0.36 nm as long as the influence of beat noise is ignored.

An optical free space feed-forward system was demonstrated by Sweet *et al* [110] in 2002 together with simulation results showing theoretical reduction in IMD3 of around 50 dB. However, practically reduction of 20 to 25 dB is possible.

In 2004 Phillips *et al* [111] analysed the performance of a feed-forward transmitter in terms of clipping distortion for CATV systems (from 55 MHz to 529 MHz) and demonstrated that with electrical filtering, a modulation depth of 28% can be achieved in comparison to 22% without linearisation. Increasing the optical modulation depth improves the signal-to-noise ratio.

More recently in 2005 feed-forward has been investigated in wireless over fibre systems between 1.8-2.3 GHz to overcome chromatic dispersion limitations using vector control theory [112]. Experimental results demonstrate 38 dB IMD3 reductions even after 20 km of fibre transmission. This approach overcomes the limitations of transmission distance for optical feed-forward transmitter.

Much of the previous work on linearisation of optical transmitters using feed-forward technique has been for CATV distribution and wireless over fibre system for cellular communications up to frequencies of order 2 GHz.

Limitations

Interest in feed-forward technique is mainly due to the significant reduction of distortion products that can be achieved over a wide bandwidth while simultaneously reducing the laser noise [106, 113]. Feed-forward has the ability to suppress distortion of any order and is not limited to 3rd IMD reduction. The feed-forward scheme is theoretically tested and results show that this linearisation techniques performs equally well for a large number of channels [104] making it practical in a SCM system.

The need for an auxiliary laser diode, the consequent cost and circuit complexity, has always been considered the main disadvantages of this technique, and often discourages its use. Also, strict requirements for phase and amplitude matching of the signals being cancelled in each loop of feed-forward affect the overall performance of the system. Since wavelength separation between the two lasers is required to prevent signal beats, this results in dispersion penalty that needs to be considered causing phase mismatch between the compensating signal from Laser 2 and the corrective signal from Laser 1. To overcome, the system can be optimised for maximum performance at a given transmission length of fibre.

2.5 Conclusion

A review of different linearisation techniques schemes has been given in this chapter. The choice of distortion compensation technique depends on a number of factors such as the frequency range, the distortion performance required and the acceptable complexity of the linearisation circuitry. However, the most promising technique for distortion reduction at microwave frequencies [99] is feed-forward compensation.

Opto-electronic feedback and quasi-feed-forward compensation have been used to linearise LEDs in narrowband systems. There are two issues, which limit the feedback method for practical applications. The time delay associated with the feedback loop may result in an unstable operation of

the circuit at high frequencies; hence the loop delay must be small. The other problem is that the output power of the optical source is reduced. The main disadvantage of the quasi-feed-forward compensation is that two lasers with identical distortion characteristics are required which can be difficult. Pre-distortion has been used to improve laser linearity but requires non-linear elements whose distortion is exactly same as the laser distortion over a broad bandwidth. Although feed-forward is a relatively complicated scheme it offers a significant reduction of distortion products of all order with simultaneous reduction of intensity noise and can be implemented for broadband linearisation. A major advantage of this approach as opposed to quasi-feed-forward is that the two laser sources do not need to be identical and the distortion characteristics of the devices do not need to be known [25]. Hence it is possible to achieve cost reduction using a less linear and therefore less expensive secondary laser. Unlike opto-electronic feedback, this method overcomes the delay limitations and is stable. Since there is a continuous forward signal flow there is no feedback path then this means that feed-forward is unconditionally stable and allows operation over wide bandwidth. The fact that the error correction signal is directly extracted from the distorted signal and does not need to be independently generated as in pre-distortion compensation means that individual matching to a laser is not required. Therefore, it can achieve better distortion cancellation over wide bandwidths than other techniques together with reduction of higher order (such as 5^{th} and 7^{th}) distortion products.

The focus of this thesis aims to advance and contribute to the work already done by providing broadband linearisation for frequencies up to 6 GHz using feed-forward linearisation. This has the potential to use directly modulated lasers with enhanced dynamic range in wireless over fibre systems for applications in WLAN using the IEEE802.11a standard and the WiMAX (IEEE802.16). Feed-forward linearisation has not previously been demonstrated at modulation frequencies above 3 GHz or with low cost uncooled lasers at 1550 nm, as required for IEEE802.11a wireless systems operating at 5.2 GHz. Previous work on feed-forward linearisation has relied on accurate adjustment of microwave devices for maximum distortion cancellation. The aim is to investigate and discuss automatic control of this parameter. Adaptive techniques are required to compensate for changes such as component aging or temperature drift. The penalty, however, is extra complexity.

In the following chapter, discussion includes design optimisation and practical implementation of the feed-forward system for simultaneous reduction of laser RIN and distortion to improve the dynamic range of a directly modulated DFB laser. Theoretical analysis together with experimental results are presented in greater detail.

References

[1] http://standards.ieee.org/getieee802/download/802.11a-1999.pdf IEEE Std 802.11a, 1999, Wireless LAN Medium Access Control (MAC) and Physical Layer (PHY) Specifications, High-speed Physical Layer in the 5GHz Band.

[2] J. Cha, J. Yi. J. Kim and B. Kim, "Optimum design of a predistortion RF power amplifier for multicarrier WCDMA applications", *IEEE Trans. Microwave Theory Tech.*, vol. 52, pp. 655-663, 2004.

[3] Y. K. Gary Hau, V. Postoyalko and J. R. Richardson, "Design and characterisation of a microwave feed-forward amplifier with improved wide band distortion cancellation", *IEEE Trans. Microwave Theory Tech.*, vol. 49, no. 1, pp. 200-203, 2001.

[4] T. Yin Yum, Q. Xue and C. H. Chan, "Amplifier linearisation using compact microstrip resonant cell", *IEEE Trans. Microwave Theory Tech.*, vol. 52, pp. 927-934, 2004.

[5] N. Tayebi and M. Kavehrad, "Laser nonlinearity compensation for radio subcarrier multiplexed fiber optic transmission systems", *IEICE Trans. Commun.*, vol. E76-B, no. 9, pp. 1103-1114, 1993.

[6] T. E. Darcie and R. S. Tucker, "Intermodulation and harmonic distortion in InGaAsP lasers", *Electron. Lett.*, vol. 21, pp. 665-666, 1985.

[7] A. Kaszubowska, P. Anandrajah and L. P. Barry, "Enhanced performance of an optically fed microwave communication system using a directly modulated laser transmitter with external injection", *IEEE Laser & Electro-Optics Society (LEOS)*, vol. 1, TuW4, pp. 314-315, 2001.

[8] J. Helms, "Intermodulation and harmonic distortions of laser diodes with optical feedback", *IEEE J. Lightwave Technol.*, vol. 9, no. 11, pp. 1567-1575, 1991.

[9] R. S. Tucker, "High speed modulation of semiconductor lasers", *IEEE J. Lightwave Technol.*, vol. 3, no. 6, pp. pp. 1180-1192, 1985.

[10] K. C. Sum and N. J. Gomes, "Integrated microwave optoelectronic simulation of semiconductor laser transmitter", *Microwave and Optical Technology Lett.* vol. 14, no. 6, pp. 313-315, 1997.

[11] K. C. Sum and N. J. Gomes, "Microwave optoelectronic modelling approaches for semiconductor lasers", *IEEE Proc. Optoelectron*, vol. 145, no. 3, pp. 141-146, 1998.

[12] J. C. Froidure, C. Leburn, P. Megret, E. Jaunart, P. Georg, T. Tasia, M. Lamquin and M. Blondel, "Theoretical and experimental study of second order distortions in CATV DFB laser diodes", *IEEE Photon. Technol. Lett.*, vol. 7, no. 3, pp. 266-268, 1995.

[13] H. M. Salgado and j. O'Reilly, "Accurate performance modelling of subcarrier multiplexed fibre/radio systems: Implications of laser nonlinear distortion and wide dynamic range", *IEEE Trans. Commun.*, vol. 44, no. 8, pp. 988-996 1996.

[14] K. Y. Lau and A. Yariv, "Intermodulation distortion in a directly modulated semiconductor injection laser", *Appl. Phys. Lett.*, vol. 45, pp. 1034-1036, 1984.

[15] W. I. Way, "Large signal nonlinear distortion prediction for a single mode laser diode under microwave intensity modulation", *IEEE J. Lightwave Technol.*, vol. 5, pp. 305-315, 1987.

[16] T. K. Biswas and W. F. McGee, "Volterra series analysis of semiconductor laser diode", *IEEE Photon. Technol. Lett.*, vol. 3, no. 8, pp. 706-708, 1991.

[17] J. Chen, R. J. Ram and R. Helkey, "Linearity and third order intermodulation distortion in DFB semiconductor lasers", *IEEE J. Quantum Electronics*, vol. 35, no. 8, pp. 1231-1237, 1999.

[18] G. Morthier, "Influence of the carrier density dependence of the absorption on the harmonic distortion in semiconductor lasers", *IEEE. J. Lightwave Technol.*, vol. 11, no. 1, pp. 16-20, 1993.

[19] G. Morthier, K. David and P. Vankwikelberge, "A new DFB laser diode with reduced spatial hole burning", *IEEE Photon. Technol. Lett.*, vol. 2, no. 6, pp. 388-340, 1990.

[20] G. Morthier and R. Baets, "Analytical formulation of the spatial hole burning induced distortion in DFB lasers and some implications for CATV laser design", *Int. Semiconductor Laser*, Th2.4, pp. 173-174, 1996.

[21] S. Ghoniemy, L. MacEachern and S. Mahmoud, "Extended robust semiconductor laser modelling for analog optical link simulations", *IEEE J. Selected Topics in Quantum Electronics*, vol. 9, no. 3, pp. 872-878, 2003.

[22] G. Morthier and P. Vankwikelberge, "Handbook of distributed feedback laser diodes", Artech House.

[23] J. Gowar, "Optical communication systems", *Second edition, Prentice Hall* International Series in Optoelectronics 2000.

[24] J. Straus and O. I. Szentesi, "Linearised transmitters for optical communications", *IEEE Int. Symp. Circuits Systems Proceedings*, pp. 288-292, 1977.

[25] R. S. Tucker, "Linearisation techniques for wideband analog transmitters", *Summer Topical Meeting Digest (LEOS)*, ThC1, pp. 54 – 55, 1992.

[26] M. Nazarathy, J. Berger, A.J. Ley, I. M. Levi and Y. Kagan, "Progress in externally modulated AM CATV transmission systems", *IEEE J. Lightwave Technol.*, vol. 11, pp. 82-104, 1993.

[27] Hung-Tser Lin and Yao-Huang Kao, "Nonlinear distortions and compensations of DFB laser diode in AM-VSB lightwave CATV applications", *IEEE J. Lightwave Technol.*, vol. 14, pp. 2567-2574, 1996.

[28] G. C. Wilson, T. H. Wood, M. Gans, J. l. Zyskind, J. W. Sulhoff, J. E. Johnson, T. Tanbun-Ek and P. A. Morton, "Predistortion of electroabsorption modulators for analog CATV systems at 1.55 μm", *IEEE J. Lightwave Technol.*, vol. 15, pp.1654-1662, 1997.

[29] Hyun-Min Park, Dong-Hyun Baek, Kye-Ik Jeon and S. Hong, "A predistortion lineariser using envelope feedback technique with simplified carrier cancellation scheme for class A and class AB power amplifiers", *IEEE Trans. Microwave Theory Tech.*, vol. 48, pp. 898-904, 2000.

[30] L. Roselli, V. Borgioni, F Zepparelli, F. Ambrosi, M. Comez, P. Faccin and A. Casini, "Analog laser predistortion for multiservice radio over fibre systems", *IEEE J. Lightwave Technol.*, vol. 21, pp. 1211-1223, 2003.

[31] R. B. Childs, V. A. O'Byrne, "Predistortion linearisation of directly modulated DFB lasers and external modulators for AM video transmission", *Optical Fiber Communication (OFC)*, WH6, 1990.

[32] G. C. Wilson, T. H. Wood, M. Gans, J. L. Zyskind, J. W. Sulhoff, J. E. Johnson, T. Tanbun-Ek and P. A. Morton, "Predistortion of electroabsortion modulators for analog CATV systems at 1.55 um", *IEEE J. Lightwave Technol.*, vol. 15, pp. 1654-1662, 1997.

[33] G. Wilson, "Predistortion techniques for linearisation of external modulators", *Summer Topical Meeting Digest (LEOS)*, FB2.1, pp. 39-41, 1999.

[34] F. Zepparelli, L. Roselli, F. Ambrosi, R. Sorrentino, P. Faccin and A. Casini, "Modelling and design of broadband predistortion circuit for Radio-over-Fibre systems", *IEICE Trans. Electron.*, vol. E85-C, pp. 519-526, 2002.

[35] D. Piehler, X. Zou, C-Y. Kuo, A. Nilsson, J. Kleefled, G. Garcia, J. D. Ralston and A. Mathur, "55 dB CNR over 50 km of fibre in an 80 channel externally modulated AM-CATV system without optical amplification", *Electron. Lett.*, vol. 33, pp.226-227, 1997.

[36] G. E. Bodeep and T. E. Darcie, "Semiconductor lasers versus external modulators: A comparison of nonlinear distortion for lightwave subcarrier CATV applications", *IEEE Photon. Technol. Lett.*, vol. 1, pp. 401-403, 1989.

[37] T. E. Darcie and G. E. Bodeep, "Lightwave subcarrier CATV transmission systems", *IEEE Trans. Microwave Theory Tech.*, vol. 38, pp. 524-533, 1990.

[38] A. H. Gnauck, T. E. Darcie and G. E. Bodeep, "Comparison of direct and external modulation for CATV lightwave transmission at 1.5 um wavelength", *Electron. Lett.*, vol. 28, pp. 1875-1876, 1992.

[39] K. Shuke, t. Yoshida, T. Ishihara, A. Kanazawa and M. Shibutani, "Development of 1GHz almighty fibre optic transmitter using 550 MHz LD for CATV system", *European Conference on Optical Communication (ECOC)*, Tu.P.03, pp. 385-388, 1995.

[40] M. R. Phillips, A. H. Gnauck, T. E. Darcie, N. J. Frigo, G. E. Bodeep and E. A. Pitman, "112 Channel split-band WDM lightwave CATV systems", *IEEE Photon. Technol. Lett.*, vol. 4, pp. 790-792, 1992.

[41] T. Iwai, K. Sato, Ko-ichi. Suto, "Reduction of dispersion induced distortion in SCM transmission systems by using predistortion-linearised MQW-EA modulators", *IEEE J. Lightwave Technol.*, vol. 15, pp. 169-178, 1997.

[42] Y. Chiu, B. Jalali, S. Garner and W. Steiner "Broadband electronic lineariser for externally modulated analogue fiber optic links", *IEEE Photon. Technol. Lett.*, vol. 11, pp. 48-50, 1999.

[43] V. Magoon and B. Jalali, "Electronic linearisation and bias control for externally modulated fiber optic link", *IEEE Int. Topical Meeting Microwave Photonics (MWP)*, WE1.6, pp. 145-147, 2000.

[44] A. Katz, W. Jemison, M. Kubak and J Dragone, "Improved radio over fibre performance using predistortion linearisation", *IEEE MTT-S Int. Microwave Symposium Digest*, vol. 2, pp. 1403-1406, 2003.

[45] L. Zhang, P. Myslinski, J. Chrostowski, H. Hua, O. Beroio, J. Lee and F. Harlow, "Ten GHz MMIC predistortion circuit for improved dynamic range of broadband analog fiber optic link", *Microwave and Optical Technol. Lett.*, vol. 11, pp. 293-295, 1996.

[46] P. Myslinski, C. Szubert, A. P. Freundorfer, P. Shearing, J. Sitch, M. Davies and J. Lee, "Over 20 GHz MMIC pre/postdistortion circuit for improved dynamic range broadband analog fiber optic link", *Microwave and Optical Technol. Lett.*, vol. 20, pp. 85-88, 1999.

[47] G. Steiner, S. Hunziker and W. Baechtold, "Reduction of 3rd order intermodulation of a semiconductor laser by an adaptive low cost predistortion circuit at 1.8 GHz", *Summer Topical Meeting Digest (LEOS)*, FB2.3, pp. 43-44, 1999.

[48] L. Roselli, V. Borgioni, F. Zapparelli, M. Comez, P. Faccin and A. Casini, "Predistortion circuit design for II and III order simultaneous linearisation in multiservice telecommunications apparatuses", *IEEE MTT-S Int. Microwave Symposium Digest*, vol. 3, pp. 1711-1714, 2002.

[49] X. N. Fernando, A. B. Sesay, "Adaptive asymmetric linearisation of radio over fibre links for wireless access", *IEEE Trans. Veh. Technol.*, vol. 51, pp. 1576-1586, 2002.

[50] R. Sadhwani, J. Basak and B. Jalali, "Adaptive electronic linearisation of fibre optic links", *Optical Fiber Communication (OFC)*, vol. 2, pp. 477-479, 2003.

[51] S. Tanaka, N. Taguchi, T. Kimura and Y. Atsumi, "A predistortion type equi-path lineariser designed for radio on fibre system", *IEEE Trans. Microwave Theory Tech.*, vol. 54, pp. 938-944, 2006.

[52] J. Straus, A. J. Springthorpe, O. I. Szentesi, "Phase shift modulation technique for the linearisation of analogue optical transmitters", *Electron. Lett.*, vol. 13, pp. 149-151, 1977.

[53] J. Straus, "Linearised transmitters for analog fibre links", *Laser Focus*, vol. 14, pp. 54-61, 1978.

[54] S. K. Korotky and R. M. Ridder, "Dual parallel modulation schemes for low distortion analog optical transmission", *IEEE J. Select. Areas Commun.*, vol. 8, pp. 1377-1381, 1990.

[55] J. L. Brooks, G. S. Maurer and R. A. Becker, "Implementation and evaluation of a dual parallel linearisation system for AM-SCM video transmission", *IEEE J. Lightwave Technol.*, vol. 11, pp.34-41, 1993.

[56] E. I. Ackerman, "Broad-Band linearisation of a Mach-Zehnder electro-optic modulator", *IEEE Trans. Microwave Theory Tech.*, vol. 47, pp. 2271-2279, 1999.

[57] A. Loyassa. M. Alonso, D. Benito and M. J. Garde, "Linearisation of electro-optic modulators at millimetre-wave frequencies", *Lasers & Electro-optical Society (LEOS)*, TuR4, pp. 275-276, 1999.

[58] Sang-Kook. Han, Duk-Ho. Jeon and Hyun-Do. Jung, "Dynamic range enhancement of electroabsorption modulated laser (EML) by phase change of intermodulation distortion component", *The International Society for Optical Engineering (SPIE)*, vol. 4581, pp. 58-67, 2001.

[59] Sang-Kook. Han, Duk-Ho. Jeon and Hyun-Do. Jung, "Linear electroabsorption modulation for radio on fiber systems", *IEICE Trans. Electron.*, vol. E85-C, pp. 527-533, 2002.

[60] Gyu-Woong. Lee and Sang-Kook. Han, "Linearisation of a narrowband analog optical link using integrated dual electroabsorption modulator", *Int. Topical Meeting Microwave Photonics (MWP)*, W-2.4, pp. 21-24, 1999.

[61] Hyun-Do. Jung and Sang-Kook. Han, "Dynamic nonlinearity reduction of DFB-LD by dual parallel modulation", *Lasers and Electro-Optics Society (LEOS)*, MH2, vol. 1, pp. 74-75, 2000.

[62] Hyun-Do. Jung and Sang-Kook. Han, "Nonlinear distortion suppression in dual parallel analog modulation of DFB-LD", *IEEE Int. Topical Meeting Microwave Photonics*, WE2.11, pp. 190-193, 2000.

[63] Hyun-Do. Jung and Sang-Kook. Han, "Nonlinear distortion suppression in directly modulated DFB-LD by Dual-Parallel modulation", *IEEE Photon. Technol. Lett.*, vol. 14, pp. 980 – 982, 2002.

[64] Y. Wang-Boulic, "A linearised optical modulator for redcing third order intermodulation distortion", *IEEE J. Lightwave Technol.*, vol. 10, pp. 1066-1070, 1992.

[65] L. M. Johnson and H. V. Roussell, "Reduction of intermodulation distortion in interferometric optical modulators", *Optics Lett.*, vol. 13, pp. 928-930, 1988.

[66] L. M. Johnson and H. V. Roussell, "Linearisation of an interferometric modulator at microwave frequencies by polarization mixing", *IEEE Photon. Technol. Lett.*, vol. 2, pp. 810-811, 1990.

[67] Pao-Lo. Liu, B. J. Li and Y. S. Trisno, "In search of a linear eletrooptic amplitude modulator", *IEEE Photon. Technol. Lett.*, vol. 3, pp. 144-146, 1991.

[68] D. J. M. Sabido, M. Tabara, T. K. Fong, Chung-Li. Lu and L. G. Kazovsky, "Improving the dynamic range of a coherent AM analog optical link using a cascaded linearised modulator", *IEEE Photon. Technol. Lett.*, vol. 7, pp. 813-815, 1995.

[69] G. E. Betts and F. J. O'Donnell, "Microwave analog optical links using suboctave linearised modulators", *IEEE Photon. Technol. Lett.*, vol. 8, pp. 1273-1275, 1996.

[70] T. Iwai and K. Sato, "Dispersion induced distortion in AM-SCM transmission systems employing linearised MQW-EA modulator", *Electron. Lett.*, vol. 31, pp. 1272-1273, 1995.

[71] H. Kawanishi, Y. Yamauchi, N. Mineo, Y. Shibuya, H. Murai, K. Yamada and H. Wada, "Over 40 GHz modulation bandwidth of EAM integrated DFB laser modules", *Optical Fiber Communication (OFC)* vol.1, MJ3-1, 2001.

[72] K. K. Loi, J. H. Hodiak, X. B. Mei, C. W. Tu and W. S. C. Chang, "Linearisatioon of 1.3 um MQW electroabsorption modulators using an all optical frequency insensitive technique", *IEEE Photon. Technol. Lett.*, vol. 10, pp. 964-966, 1998.

[73] W. H. Bridges and J. H. Schaffner, "Comparison of analog RF photonic links using a variety of linearised electro-optic modulators", *Summer Topical Meeting Digest (LEOS)*, WC1, pp. 3-4, 1995.

[74] X. J. Meng, A. Yacoubian and J. H. Bechtel, "Electro-optical predistortion technique for linearisation of Mach-Zehnder modulators", *Electron. Lett.*, vol. 37, pp. 5145-1547, 2001.

[75] S. Mathai, F. Cappelluti, T. Jung, D. Novak, R. B. Waterhouse, D. Sivco, A. Y. Cho, G. Ghione and M. C. Wu, "Experimental demonstration of a balanced electroabsorption modulated microwave photonic link", *IEEE Trans. Microwave Theory Tech.*, vol. 49, pp. 1956-1961, 2001.

[76] J. Wang, M. K. Haldar, L. Li and F. V. C. Mendis, "Enhancement of modulation bandwidth of laser diodes by injection locking", *IEEE Photon. Technol. Lett.*, vol. 8, pp. 34-36, 1996.

[77] J. M. Liu, H. F. Chen, X. J. Meng and T. B. Simpson, "Modulation bandwidth noise and stability of a semiconductor laser subject to strong injection locking", *IEEE Photon. Technol. Lett.*, vol. 9, pp. 1325-1327, 1997.

[78] M. H. Pua, M. K. Haldar, F. V. C. Mendis and H. K. Garg, "Reduction of nonlinear distortion in semiconductor lasers with external light injection", *Information, Communications and Signal Processing (ICICS)*, pp. 1153-1157, 1997.

[79] Xue-Jun. Meng, D. T. K. Tong, T. Chau and M. C. Wu, "Demonstration of an analog fiber-optic link employing a directly modulated semiconductor laser with external light injection", *IEEE Photon. Technol. Lett.*, vol. 10, pp. 1620-1622, 1998.

[80] X. J. Meng, T. Chau and M. C. Wu, "Improved intrinsic dynamic distortion in directly modulated semiconductor lasers by optical injection locking", *IEEE Trans. Microwave Theory Tech.*, vol. 47, pp. 1172-1176, 1999.

[81] N. H. Chan, C. Shu and K. L. Lee, "Performance improvements in high frequency modulation of a laser diode under enhanced optical feedback", *IEEE Photon. Technol. Lett.*, vol. 14, pp. 1650-1652, 2002.

[82] A. Kaszubowska, P. Anandrajah and L. P. Barry, "Enhanced performance of an optically fed microwave communication system using a directly modulated laser transmitter with external injection", *IEEE Laser & Electro-Optics Society (LEOS)*, vol. 1, TuW4, pp. 314-315, 2001.

[83] A. Kaszubowska, P. Anandrajah and L. P. Barry, "Improved Performance of a hybrid radio/fibre system using a directly modulated laser transmitter with external injection", *IEEE Photon. Technol. Lett.*, vol. 14, pp. 233 – 235, 2002.

[84] L. Chrostowski, Chin-Hao. Chang and C. J. Chang-Hasnain, "Reduction of relative intensity noise and improvement of spur-free dynamic range of an injection locked VCSEL", *IEEE Laser & Electro-Optics Society (LEOS)*, WBB2, pp. 706-707, 2003.

[85] Chih-Hao. Chang, L. Chrostowski and C. J. Chang-Hasnain, "Injection locking of VCSELs", *IEEE J. Select. Topics Quantum Electron.*, vol. 9, pp. 1386-1393, 2003.

[86] S. K. Hwang, J. M. Liu and J. K. White, "35 GHz modulation bandwidth in injection locked semiconductor lasers", *IEEE Laser & Electro-Optics Society (LEOS)*, WBB4, pp. 710-711, 2003.

[87] L. Chrostowski, X. Zhao, C. J. Chang-Hasnain, R. Shau, M. Ortsiefer and M. C. Amann "Very high resonance frequency (> 40 GHz) optical injection locked 1.55 μm VCSELs", *International Topical Meeting on Microwave Photonic (MWP)*, WA-4, 2004.

[88] J-H. Seo, Y-K. Seo and W-Y. Choi, "Nonlinear distortion suppression in directly modulated DFB lasers by sidemode optical injection", *IEEE MTT-S Int. Microwave Symposium*, vol. 1, pp. 555-558, 2001.

[89] J. Straus, "Linearised transmitters for analog fibre optical systems", *OSA/IEEE Conference on Laser & Electro-optical Systems*, TUGG2, pp. 18-19, 1978.

[90] C. McNeilage, E. N. Ivanov, P. R. Stockwell and J. H. Searls, "Review of feedback and feed-forward noise reduction techniques", *IEEE Frequency Control Symposium*, pp. 146-155, 1998.

[91] K. Asatani and T. Kimura, "Linearisation of LED nonlinearity by predistortions", *IEEE J. Solid State Circuits*, vol. sc-13, pp. 133-138, 1978.

[92] A. Van de Grijp, J. C. Koopman, L. J. Meuleman, A. J. A. Nicia, E. Roza and J. H. C. Van Heuven, "Novel electro-optical feedback technique for noise and distortion reduction in high-quality analogue optical transmission video signal", *Electron. Lett.*, vol. 17, pp. 361-362, 1981.

[93] G. De geronimo, S. Taccheo and P. Laporta, "Optoelectronic feedback control for intensity noise suppression in a codoped erbium-ytterbium glass laser", *Electron. Lett.*, vol. 33, pp. 1336-1337, 1997.

[94] M. Nakamura, K. Nitta, T. Komatsubara, M. Okajima and T. Ozeeki, "LED linearisation for video bandwidth transmission employing a monolithically integrated PIN-PD", *Electron. Lett.*, vol. 20, pp. 651-653, 1984.

[95] Q. Z. Liu, "Linearised optical transmitter with modified feedback technique", *The International Society for Optical Engineering (SPIE)*, vol. 3006, pp. 250-255, 1997.

[96] J. Straus and O. I. Szentesi, "Linearisation of optical transmitters by a quasi-feedforward compensation technique", *Electron. Lett.*, vol. 13, pp. 158-159, 1977.

[97] R. E. Patterson, J. Straus, G. Blenman and T. Witkowicz, "Linearisation of multichannel analog optical transmitters by quasi-feedforward compensation technique", *IEEE Trans. Commun.*, vol. 27, pp. 582-588, 1979.

[98] H. S. Black (1929), U.S. Patent 1,686,792, issued Oct. 9, 1929.

[99] L. S. Fock and R.S. Tucker, "Simultaneous reduction of intensity noise and distortion in semiconductor lasers by feedforward compensation", *Electron. Lett.*, vol. 27, pp. 1297-1299, 1991.

[100] L. S. Fock and R.S. Tucker, "Reduction of distortion in analogue modulated semiconductor lasers by feedforward compensation", *Electron. Lett.*, vol. 27, pp. 669-671, 1991.

[101] P. Hill, R. Olshansky, J. Schlafer and W. Powazinik, "Reduction of relative intensity noise in 1.3 μm InGaAsP semiconductor lasers", *Applied Physics Lett.*, vol. 50, pp. 1400-1402, 1987.

[102] L.S. Fock, A. Kwan and R.S. Tucker, "Reduction of semiconductor laser intensity noise by feedforward compensation: Experiment and Theory", *IEEE J. Lightwave Technol.*, vol. 10, pp. 1919-1925, 1992.

[103] D. Hassin and R. Vahldieck, "Feed-forward linearisation of analogue modulated laser diodes–theoretical analysis and experimental verification", *IEEE Trans. Microwave Theory Tech.*, vol. 41, pp. 2376-2382, 1993.

[104] D. Hassin and R. Vahldieck, "Improved feed-forward linearisation of laser diodes-simulation and experimental results", *IEEE MTT-S Int. Microwave Symposium Digest,* pp. 727-730, 1990.

[105] R. Vahldieck, "Using optical feedforward linearisation to reduce noise and intermodulation distortion of Fabry-Perot lasers for cable television distribution networks", *European Microwave Conference,* vol. 2, pp. 1685-1690, 1994.

[106] B. Buxton and R. Vahldieck, "Noise and intermodulation distortion reduction in an optical feedforward transmitter", *IEEE MTT-S Int. Microwave Symposium Digest,* pp.1105-1108, 1994.

[107] R. M. Ridder and K. Korotky, "Feed-forward compensation of integrated optic modulator distortion", *Optical Fiber Communication (OFC),* WH5, pp. 78-80, 1990.

[108] J. D. Farina, B. R. Higgins and J. P. Farina, "New linearisation technique for analog fibre-optic links", *Optical Fiber Communication (OFC),* ThR6, pp. 283-285, 1996.

[109] T. Iwai, K. Sato and Ko-ichi. Sato, "Signal distortion and noise in AM-SCM transmission systems employing the feedforward linearised MQW-EA external modulator", *IEEE J. Lightwave Technol.,* vol. 13, pp. 1606-1612, 1995.

[110] C. S. Sweet and R. J. Green, "Feed-forward non-linear correction for an optical free space system for mobile RF", *IEE Photonics Professional Network, Photonics Access Technologies,* 2002.

[111] M. R. Phillips and J. Zhang, "Analysis of clipping distortion in an SCM lightwave transmitter with feed-forward correction", *Optical Fiber Communication (OFC),* MF86, 2004.

[112] Sang-Hyun. Park and Young-Wan. Choi, "Significant suppression of the third order intermodulation distortion in transmission system with optical feed-forward linearised tranmitter", *IEEE Photon. Technol. Lett.,* vol. 17, pp. 1280-1282, 2005.

[113] R. S. Tucker, "High speed optoelectronic components for microwave and millimetre wave applications", *Asia Pacific Microwave Conference,* vol. 1, pp. 307-308, 1992.

Chapter 3

Feed-forward Linearisation: Theory and Experimental Results

In Chapter 2 distortion compensation techniques were discussed. Among all the techniques feed-forward shows great potential for simultaneous reduction of distortion and noise in a directly modulated semiconductor laser at microwave frequencies. This chapter concentrates on explaining the operation of the feed-forward scheme in considerable detail and experimentally assesses the circuit performance. After an Introduction 3.1, to feed-forward, theoretical analysis is presented in Section 3.2 to determine the distortion and noise reduction that can be achieved. System evaluation is carried out in Section 3.3 to investigate component specifications and how they affect the overall feed-forward performance. Section 3.4 considers adaptive techniques to overcome component ageing effects, and temperature drift. The experimental arrangement for feed-forward linearisation is demonstrated in Section 3.5, with results in Section 3.6 for reduction of intermodulation distortion and noise to improve dynamic range in a directly modulated laser. Distortion measurements are carried out for spectral re-growth using broadband data to assess system performance with feed-forward enabled and disabled for the 2.4 GHz and 5 GHz bands intended for IEEE802.11b/g and IEEE802.11a systems respectively. In the last, Section, 3.7, Conclusion important results are summarised from this chapter.

3.1 Introduction

Figure 3.1 shows the implementation of the optical feed-forward linearised transmitter used to compensate distortion and noise generated in a directly modulated laser L_1. The circuit requires two semiconductor lasers, a monitoring photodiode, microwave devices such as amplifiers, variable attenuators and an adjustable delay line. The system is made up of two loops:

i) The inner loop- (error determination loop or signal cancellation loop) and

ii) The outer loop- (error injection loop or distortion cancellation loop)

The operation of feed-forward can be clearly seen by referring to two tone test spectra shown at various points throughout the system. Considering the inner loop first, the RF input signal is split into two paths at the input splitter C_1, one of which modulates the primary laser L_1 while the other is the error free reference path. Due to non-linearity of laser L_1, the optical modulated output signal contains

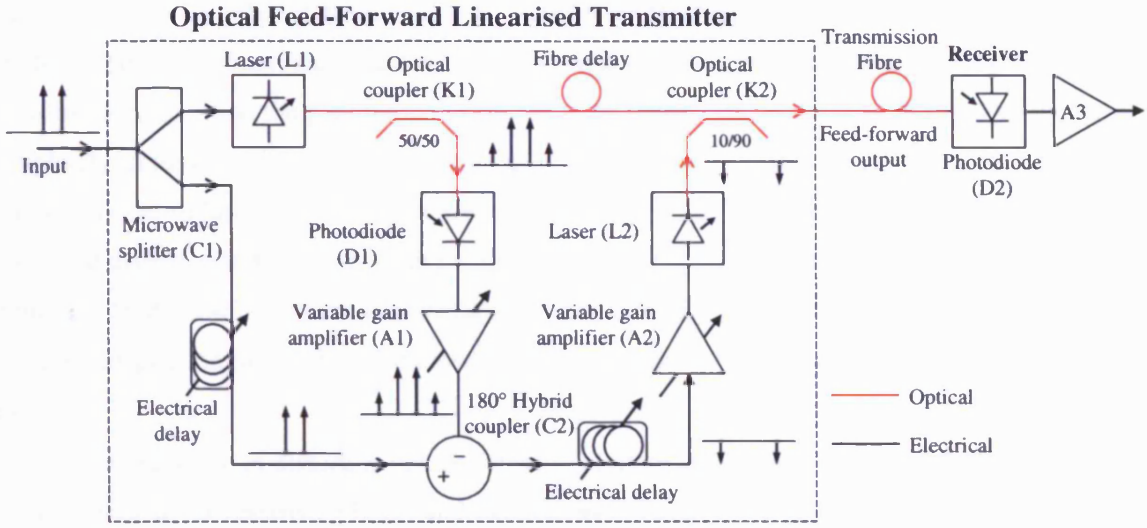

Figure 3.1 Diagram of the feed-forward system

distortion products resulting in additional frequency terms known as intermodulation distortion (IMD). The output is split through a 50:50 optical coupler K_1 and is then detected using a photodiode D_1, followed by a variable gain amplifier A_1.

The output of the amplifier A_1 containing the signal and the distortion products together with the intensity noise generated in laser L_1 is subtracted from the error free reference path at the 180° hybrid electrical coupler C_2. The resulting output signal ideally should consist of the error signal only (i.e. the non-linear distortion products and the detected noise of the primary laser L_1). This part of feed-forward is called the signal cancellation loop.

The error signal at the output of the electrical coupler C_2 is 180 degrees phase shifted and is injected into the distortion cancellation loop. The signal is amplified using an amplifier A_2 before modulating the secondary laser L_2. The modulated optical output signal from laser L_2 is an optical representation of the error signal (i.e. distortion products) at the output of the primary laser L_1, but inverted in sign [1, 2]. Since laser L_2, is directly modulated with the phase inverted distortion products, it can be assumed to operate linearly and not generate significant distortion of its own [3]. The output of laser L_2 is combined with the optical signal from laser L_1 in the 90:10 optical coupler K_2. The combined optical signals from the output of coupler K_2 are then transported over fibre and the cancellation of distortion and intensity noise takes place at the receiver. The photodiode functions as a broadband in phase microwave combiner, coherently adding the detected RF signals. The unwanted distortion signals add in anti-phase resulting in an output with suppressed distortion products. Enabling and then disabling the output of the secondary laser L_2 determines the performance of the system with and without feed-forward.

Both the signal cancellation loop and the distortion cancellation loop require correct amplitude and phase for cancellation of the carrier signal at the electrical coupler C_2 and distortion products at the

receiver photodiode D_2. This is facilitated with variable attenuators and variable gain amplifiers for amplitude matching and microwave cables fine tuned with electrical phase shifters for phase matching. For broadband cancellation the path length also need to be delay matched. Theoretically distortion can be completely removed [4]. However, amplitude and phase mismatch caused by the non-ideal frequency response of lasers and other microwave components such as amplifiers and photodiode limit the amount of distortion reduction that can be obtained in a practical feed-forward system.

Although feed-forward is a more complicated scheme than predistortion, it provides a promising solution for linearisation of directly modulated optical transmitters. The advantages of feed-forward are as follows:

- Significant reduction of distortion can be achieved at more than 1 GHz and the technique therefore is more suitable for linearising lasers and modulators for microwave applications.
- Simultaneous reduction in distortion and laser relative intensity noise (RIN) is possible over a wide bandwidth [5].
- Reduction in higher order distortion products
- Small optical power penalty
- Unlike predistortion second and third order distortion can be eliminated and thus this method can be applied to both lasers and modulators.

The advantages mentioned above for feed-forward come at the expense of a requirement for a high degree of matching in both amplitude and phase for virtually all of the system components. The performance of the system is very much dependent on the degree of amplitude and phase matching of the signals within the loop for distortion cancellation. Accurate path matching is required for broadband cancellation. The lack of feedback path in a feed-forward system means that it cannot monitor its own performance and hence correct for gain or phase changes due to temperature or ageing effects. Although perfect cancellation can be achieved by manual setup this may drift over time and can degrade the performance.

3.2 Theory

3.2.1 Analysis of feed-forward

The overall transfer function related to the input and output of feed-forward in Figure 3.1 can be derived. The optimum component values of the system are deduced from the transfer function. The electrical coupler C_2 must provide a 180 degree phase shift for carrier and distortion cancellation to be achieved. The assumptions made in these derivations are,

-Laser diodes L_1 and L_2, amplifiers and other electronic components have linear phase and flat magnitude response

-The effects of electrical reflection between the connections of various components are negligible

-The distortion introduced by the amplifiers A_1 and A_2 is negligible

-The input to the secondary laser is small and the distortion generated in it is therefore negligible

-There is no attenuation in the time delay reference path.

-The input splitter C_1 is an ideal 3 dB coupler

Assuming no distortion is generated by laser L_1 and the amplitude and propagation delay in the system is matched then the transfer function can be written as in equation (3.1):

$$\frac{V_{out}}{V_{in}} = \frac{1}{2}\left[q_{e1}(1-K_1)(1-K_2) + \left(1 - q_{e1}K_1\Re_1 R_L G_1\right)G_2 q_{e2} K_2\right] \tag{3.1}$$

V_{out} is the modulated output of the linearised source (V)

V_{in} is the modulating input signal (V)

q_{e1} and q_{e2} are the quantum efficiency of laser L_1 and laser L_2 (W/V)

$\Re_1$ is the responsivity of the photodiode D_1

C_1 is the input splitter and C_2 is the 180 degrees hybrid coupler

K_1 and K_2 are the coupling coefficients of the optical couplers

G_1 and G_2 are the gain for amplifiers A_1 and A_2

R_L is the input resistance of amplifier A_1

The input signal V_{in} is split into two paths using a microwave splitter C_1. The optical modulated output signal from laser L_1 is:

$$\frac{V_{in} q_{e1}}{2} \tag{3.2}$$

The output of laser L_1 is split using an optical coupler K_1. The top path directly arrives at the output coupler K_2. A sample of the output signal is coupled by K_1, detected by the photodiode D_1 and is

amplified by A_1. The input to the electrical coupler C_2 must give 180 degrees phase shift for cancellation to occur. So

$$C_{2(Input1)} = \frac{-V_{in} q_{e1} K_1 \Re_1 R_L G_1}{2} \tag{3.3}$$

The second input signal to the coupler C_2 is from the direct path that is the delayed version of the input signal. The two signals are combined in C_2 to give an error signal which is amplified by A_2 and modulates the secondary laser L_2. The optical output error signal of laser L_2 is

$$L_{2(out)} = \frac{V_{in}(1 - q_{e1} K_1 \Re_1 R_L G_1) G_2 q_{e2}}{2} \tag{3.4}$$

The output of laser L_2 is combined with the optical signal from laser L_1 in the output coupler K_2. This gives the optical output signal V_{out}

$$V_{out} = \frac{1}{2}[V_{in} q_{e1}(1 - K_1)(1 - K_2) + V_{in}(1 - q_{e1} K_1 \Re_1 R_L G_1) G_2 q_{e2} K_2] \tag{3.5}$$

Rearranging (3.5) gives the transfer function of the system

$$\frac{V_{out}}{V_{in}} = \frac{1}{2}[q_{e1}(1 - K_1)(1 - K_2) + (1 - q_{e1} K_1 \Re_1 R_L G_1) G_2 q_{e2} K_2] \tag{3.6}$$

Further analysis can be derived taking into account the delay effects and the distortion generated from laser L_1 [6]. The output of the primary laser L_1, $V_{L1}(t)$, for an input signal, $V_{in}(t)$, is:

$$V_{L1}(t) = \frac{q_{e1}}{2}[V_{in}(t) e^{-j\omega\tau_{L1}} + V_{d1}(t)] \tag{3.7}$$

where τ_{L1} is the delay introduced by the primary laser at an angular frequency ω and $V_{d1}(t)$ is the distortion generated by laser L_1. The proportion of the signal fed to the photodiode D_1 is determined by the coupling ratio of K_1 and after amplification by amplifier A_1, the input signal to the electrical coupler C_2 is

$$V_{C2(1)}(t) = \frac{q_{e1} K_1 \Re_1 R_L G_1}{2} V_{in}(t) e^{-j\omega\tau_{P1}} + q_{e1} K_1 \Re_1 R_L G_1 V_{d1}(t) \tag{3.8}$$

τ_{P1} is the total delay in the laser L_1 path. The other input to the electrical coupler C_2 is from the direct reference path, assuming paths are matched and the delay element is lossless, then:

$$V_{C2(2)}(t) = \frac{V_{in}(t)}{2} e^{-j\omega\tau_{T1}} \tag{3.9}$$

where τ_{T1} is the delay in the direct path for phase matching. The electrical coupler C_2 provides a phase shift of 180° to the signal from the laser path. The two signals are combined and the error output is

$$\begin{aligned} V_{err}(t) &= -V_{C2(1)}(t) + V_{C2(2)}(t) \\ V_{err}(t) &= -\frac{q_{e1} K_1 \Re_1 R_L G_1}{2} V_{in}(t) e^{-j\omega\tau_{P1}} - q_{e1} K_1 \Re_1 R_L G_1 V_{d1}(t) + \frac{V_{in}(t)}{2} e^{-j\omega\tau_{T1}} \end{aligned} \tag{3.10}$$

For the carrier signal to be completely removed from the error signal, the following conditions must hold $\tau_{P1} = \tau_{T1}$ and

$$G_1 = \frac{1}{q_{e1} K_1 \Re_1} \tag{3.11}$$

The resulting error signal is then

$$V_{err}(t) = -q_{e1} K_1 \Re_1 R_L G_1 V_{d1}(t) \tag{3.12}$$

The output from the primary laser L_1, having passed through the top path is

$$V_{T2}(t) = \frac{q_{e1}(1-K_1)}{2} V_{in}(t) e^{-j\omega(\tau_{L1}+\tau_{T2})} + q_{e1} V_{d1}(t)(1-K_1) e^{-j\omega\tau_{T2}} \tag{3.13}$$

where τ_{T2} is the fibre delay in the top path. This is the main signal path for K_2. The second input to K_2 is derived from the error signal $V_{err}(t)$, after amplified by A_2 modulates laser L_2:

$$V_{L2}(t) = -q_{e1} K_1 \Re_1 R_L G_1 G_2 q_{e2} V_{d1}(t) e^{-j\omega\tau_{L2}} \tag{3.14}$$

$V_{L2}(t)$ is the modulated output from laser L_2 and τ_{L2} is the delay introduced by laser L_2 and the associated components in the path. The two signals are combined at the final coupler K_2 to give output:

$$V_{out}(t) = V_{T2}(t)(1-K_2) + K_2 V_{L2}(t)$$

$$V_{out}(t) = \frac{q_{e1}(1-K_1)(1-K_2)}{2} V_{in}(t) e^{-j\omega(\tau_{L1}+\tau_{T2})} + q_{e1}(1-K_1)(1-K_2) V_{d1}(t) e^{-j\omega\tau_{T2}} \tag{3.15}$$
$$- q_{e1} K_1 \Re_1 R_L G_1 G_2 q_{e2} K_2 V_{d1}(t) e^{-j\omega\tau_{L2}}$$

In order for the distortion products, $V_{d1}(t)$, to cancel perfectly, the following condition must hold: $\tau_{T2} = \tau_{L2}$ and

$$G_1 G_2 = \frac{(1-K_1)(1-K_2)}{K_1 K_2 \Re_1 q_{e2}} \tag{3.16}$$

The final output is then:

$$V_{out}(t) = \frac{1}{2} q_{e1}(1-K_1)(1-K_2) V_{in}(t) e^{-j\omega(\tau_{L1}+\tau_{T2})} \tag{3.17}$$

Thus, the output signal is a time delayed replica of the modulated input signal with the distortion removed from laser L_1. The derivation presented assumed that the second laser L_2 is linear and the gain and phase balance of feed-forward system was perfect. Neither of these criteria will exist in a practical system. If distortion from the secondary laser L_2 is considered then equation (3.14) becomes:

$$V_{L2}(t) = -q_{e1} K_1 \Re_1 R_L G_1 G_2 q_{e2} V_{d1}(t) e^{-j\omega\tau_{L2}} + V_{d2}(t) \tag{3.18}$$

where $V_{d2}(t)$ is the distortion generated by the secondary laser L_2. The final output then becomes

$$V_{out}(t) = \frac{1}{2} q_{e1}(1-K_1)(1-K_2) V_{in}(t) e^{-j\omega(\tau_{L1}+\tau_{T2})} + K_2 V_{d2}(t) \tag{3.19}$$

3.2.2 Reduction of distortion

To further understand the factors affecting the amount of distortion reduction achievable by the feed-forward system, the output signal of the feed-forward transmitter is determined.

If an input electrical signal of 2Acos(ωt) is assumed then the output of the feed-forward transmitter can be determined. Since the signal is split into two by the -3 dB power splitter the signal modulating laser L_1 is Acos(ωt). Due to non-linearity of laser L_1 its output will contain the fundamental signal q_{e1}Acos(ωt), but also distortion products such as second and third harmonics. In this derivation, only second harmonic distortion is considered for simplicity. However, the treatment for third harmonic and other types of noise signals is very similar.

Considering first the output power of the electrical coupler C_2 i.e. the output of the signal cancellation loop, this signal is made up of signals from two paths. One of the input signal S_L to C_2 originates from laser L_1, passes through the coupler K_1, is detected by the photodiode D_1 and then amplified by A1. Thus this signal is given by:

$$S_L = q_{e1}K_1\Re_1R_LG_1A[\cos(\omega t)+D_{HD}\cos(2\omega t)] \tag{3.20}$$

Where D_{HD} is the ratio of magnitude of the fundamental signal to that of the second harmonic and represents the amount of distortion in the primary laser L_1. The second input signal S_R to C_2 is the reference signal without attenuation from the time delay path. Hence

$$S_R = A\cos(\omega t+\theta_1) \tag{3.21}$$

θ_1 represents the phase difference that still exists between the two paths after adjusting the phase shifter in the variable delay line. Therefore, the total signal S_{error} at coupler C_2 is

$$S_{error} = A\cos(\omega t+\theta_1)-q_{e1}K_1\Re_1R_LG_1A\cos(\omega t)-q_{e1}K_1\Re_1R_LG_1AD_{HD}\cos(2\omega t) \tag{3.22}$$

The output error signal from C_2 is amplified by A_2 to modulate the secondary laser L_2 and is given by

$$S_{L2} = S_{error}G_2q_{e2} \tag{3.23}$$

Substituting equation (3.22) into equation (3.23)

$$S_{L2} = [A\cos(\omega t+\theta_1)-q_{e1}K_1\Re_1R_LG_1A\cos(\omega t)-q_{e1}K_1\Re_1R_LG_1AD_{HD}\cos(2\omega t)]G_2q_{e2} \tag{3.24}$$

This forms one part of the feed-forward output. The other part comes from laser L_1, delayed by the fibre delay. This signal S_{L1} at the input of the optical coupler K_2 is

$$S_{L1} = q_{e1}(1-K_1)A[\cos(\omega t+\theta_2)+D_{HD}\cos(2\omega t+\theta_2)] \tag{3.25}$$

Again θ_2 is the phase difference between paths caused by the fibre delay. Hence the output of feed-forward transmitter S_{out} is

$$S_{out} = S_{L1}(1-K_2)+S_{L2}K_2 \tag{3.26}$$

Substituting equations (3.24) and (3.25) into equation (3.26) the expression is

$$S_{out} = [q_{e1}(1-K_1)A[\cos(\omega t+\theta_2)+D_{HD}\cos(2\omega t+\theta_2)]](1-K_2)+$$

$$\{[A\cos(\omega t+\theta_1)-q_{e1}K_1\Re_1R_LG_1[A\cos(\omega t)]-q_{e1}K_1\Re_1R_LG_1AD_{HD}\cos(2\omega t)]G_2q_{e2}\}K_2 \quad (3.27)$$

Collecting the terms

$$S_{out} = (1-K_1)(1-K_2)q_{e1}A\cos(\omega t+\theta_2)+$$

$$G_2q_{e2}K_2A[\cos(\omega t+\theta_1)-q_{e1}K_1\Re_1R_LG_1\cos(\omega t)]+ \quad (3.28)$$

$$AD_{HD}[q_{e1}(1-K_1)(1-K_2)\cos(2\omega t+\theta_2)-q_{e1}K_1K_2\Re_1R_LG_1G_2q_{e2}\cos(2\omega t)]$$

In the ideal case, the phase shifters in the variable delay line and the gain of amplifiers are adjusted. The condition for carrier cancellation in the signal cancellation loop is

$$\cos(\omega t+\theta_1) = q_{e1}K_1\Re_1G_1\cos(\omega t) \quad (3.29)$$

$$\text{when } \theta_1 = 0 \quad (3.30)$$

$$G_1 = \frac{1}{q_{e1}K_1\Re_1} \quad (3.31)$$

Where G_1 is the optimum value for amplifier A_1. Similarly the condition for zero distortion is

$$q_{e1}(1-K_1)(1-K_2)\cos(2\omega t+\theta_2) = q_{e1}K_1K_2\Re_1G_1G_2q_{e2}\cos(2\omega t) \quad (3.32)$$

$$\text{when } \theta_2 = 0 \quad (3.33)$$

$$G_1G_2 = G_{Total} = \frac{(1-K_1)(1-K_2)}{K_1K_2\Re_1q_{e2}} \quad (3.34)$$

G_{Total} is the optimum value for gain product G_1G_2 for total cancellation of distortion to occur. If equation (3.30) and equation (3.31) are satisfied, then the carrier cancellation loop is correctly adjusted and there is no amplitude and phase mismatches. If all four conditions in equations (3.30), (3.31), (3.33), and (3.34) are met, the output of the transmitter will contain only the linearised signal.

3.2.3 Theoretical prediction of distortion cancellation

The feed-forward system consists of two cancellation loops, the inner loop for the carrier cancellation and the outer loop for distortion cancellation and the operation can be theoretically explained with the use of vectors. The vector representation of the cancellation process is shown in Figure 3.2 where a reference signal has a amplitude of 1 and phase of 0 degrees and a mismatched cancelling signal with amplitude 1+δA and a phase of 180+ϕ degrees [7]. The resultant vector (r) is related to the phase error

and amplitude imbalance. For perfect cancellation the resultant vector i.e. the suppressed signal has a very small magnitude almost equal to 0. However, practically ideal cancellation is not possible and it is useful to estimate the amount of mismatch that can be tolerated for a certain amount of required suppression. Using the cosine rule, the magnitude of the resultant vector r, can be calculated from equation (3.35)

$$r^2 = (1+\delta A)^2 + 1 - 2(1+\delta A)\cos\phi \tag{3.35}$$

This is the general equation for calculating the magnitude of the sum of two vectors. In the ideal case of feed-forward, assuming that the two vectors are equal in magnitude i.e. δA=0 and 180° out of phase then the two signals cancel each other and distortion is completely removed. The amount of cancelled signal is thus a function of two variables, the amplitude mismatch δA and the phase mismatch ϕ. Rewriting equation (3.35) the cancellation in dB can be calculated.

$$R(dB) = 10Log\left(\left|10^{\frac{\Delta A(dB)}{10}} + 1 - 2\times 10^{\frac{\Delta A(dB)}{20}}\cos\phi\right|\right) \tag{3.36}$$

where ΔA is the amplitude mismatch and ϕ is the phase mismatch. The relationship between the cancellation and the phase/amplitude error can be plotted using equation (3.36) and represented in several ways:

- The amplitude mismatch for a fixed phase
- The phase mismatch for fixed amplitude
- The range of amplitude and phase mismatch

Theoretical curves are produced to predict the level of distortion cancellation in feed-forward loop as a function of amplitude and phase mismatch and this is shown in Figure 3.3. To achieve a given degree of cancellation specific tolerances must be met. For example, 40 dB cancellation requires a phase balance of 0.5° and an amplitude match better than 0.05 dB. This illustrates the difficulty in constructing circuitry that will provide large distortion cancellation. It is evident that the higher the

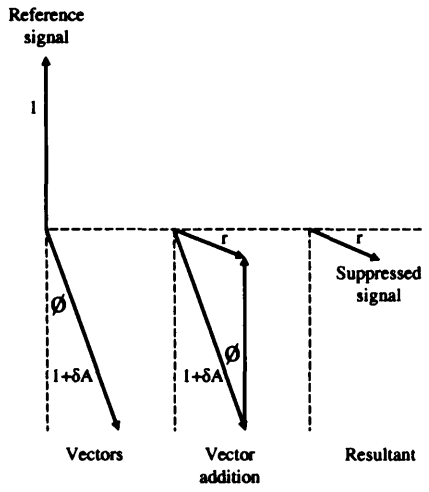

Figure 3.2 Vector signal cancellation

desired cancellation and wider the bandwidth the more difficult it is to meet the strict phase and amplitude requirements. As a result, there is a trade off between the operating bandwidth, which is effectively the frequency range over which the required balance can be obtained and the distortion cancellation. For optimum performance both lasers (L_1 and L_2) should have a flat response and phase over the band of operation. Alternative solutions may be required to match the response of the two cancelling paths such as the use of gain and phase equalisers to achieve the required amplitude and phase balance. However, this is a complex and a difficult approach.

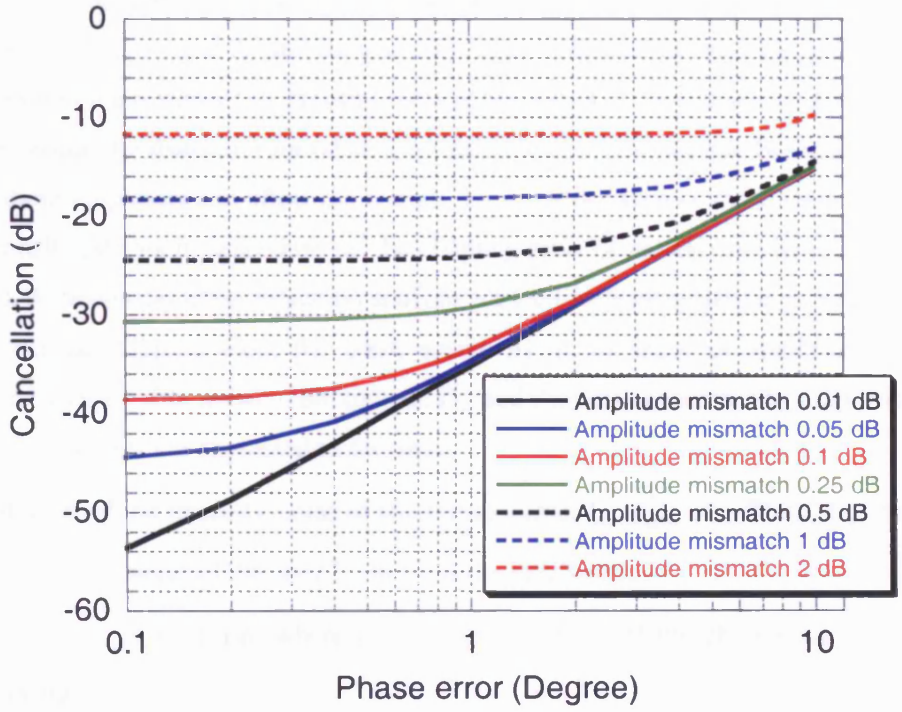

Figure 3.3 Theoretical distortion cancellation in feed-forward dependent on amplitude and phase mismatch

3.2.4 Laser noise reduction

An additional advantage of feed-forward scheme (as previously mentioned) is its potential to reduce RIN of a laser. The noise introduced in the primary laser L_1 can be considered as an additional signal not present in the reference path and hence will appear as part of the error signal at the output of the electrical coupler C_2. The error signal at the output of the electrical coupler C_2 contains distortion products and noise is obtained by comparing the reference signal with the output signal of laser L_1. Therefore, when combining the correcting signal from laser L_2 with the main signal from laser L_1 cancellation of distortion and noise can be achieved assuming gain and phase balance of the overall system is matched. Therefore, feed-forward not only eliminates distortion but also noise and indeed any other spurious signals present at the output of laser L_1 which are not present in the reference path. This is a useful benefit of the feed-forward system, as it allows relatively low noise lasers to be

constructed with high third order intercept point, resulting in a improved dynamic range. Fock *et al* [5] have experimentally demonstrated simultaneous reduction of distortion and noise using feed-forward.

The amount of linearisation and improvement in intensity noise is limited by distortion and noise added to the system by laser L_2. While the distortion from laser L_2 is typically small, because the error signal modulating this laser is small, the RIN added to the system may be relatively large. The proportion of noise coupled to the output from laser L_2 depends on the choice of coupling ratio for K_2 and this can be minimised using a coupler that has a ratio of 10 dB or more but then it is necessary to increase drive to L_2. The presence of shot noise associated with the photocurrent in the photodiode D_1 and the amplifier noise in A_1 and A_2 and the intensity noise generated by laser L_2, ultimately limit the maximum achievable improvement in intensity noise at the output of the transmitter and the achievable dynamic range. While the distortion introduced by amplifiers A_1 and A_2 can be neglected, the noise introduced by these amplifiers can affect the overall noise performance of the system. The noise gain must be kept small and this is dependent on the coupling ratio of optical couplers K_1 and K_2 (to be discussed later). A theoretical noise limitation analysis for feed-forward system is presented in [8].

In the carrier cancellation loop, the noise source n1 at the input of amplifier A_1 comprises intensity noise of laser L_1, shot noise of photodiode D_1, and the noise generated by amplifier A_1. These mean square noise currents are expressed as follows:

- The contribution of the intensity noise of the primary laser L_1, $\overline{i_{RIN_1}^2}$, is $RIN_1 i_1^2 B$ where RIN_1 is the relative intensity noise of the laser L_1 and B is the bandwidth.
- The shot noise, $\overline{i_{shot}^2}$, is $2i_1 eB$ where i_1 is the photocurrent of the photodiode D_1 and e is the electronic charge
- The noise generated by amplifier A1, $\overline{i_{amp_1}^2}$, can be written as $\frac{4kTF_1B}{R_1}$, where k is the Boltzmann constant, T is the temperature in Kelvin, F_1 is the noise factor and R_1 is the input resistance of A_1.

Since the noise contributions are not correlated, the noise source n1 is the sum of their mean squared noise current, and is expressed as follows:

$$n1 = \overline{i_{RIN_1}^2} + \overline{i_{shot}^2} + \overline{i_{amp_1}^2} \quad \text{A}^2/\text{Hz} \tag{3.37}$$

Substituting the expressions of noise contributions into equation (3.37) gives

$$n1 = RIN_1 i_1^2 B + 2i_1 eB + \frac{4kTF_1B}{R_1} \tag{3.38}$$

The noise source n2 after the carrier cancellation loop and at the input of the amplifier A_2 is the sum of the noise source n1 and the noise generated by amplifier A_2. Thus, this amplifier noise is written as

$$\frac{4kTF_2B}{R_2} \tag{3.39}$$

Where F_2 is the noise factor of amplifier A_2, and R_2 is the load resistance. The noise source n2 is written as:

$$n2 = \left(RIN_1 i_1^2 B + 2i_1 eB + \frac{4kTF_1 B}{R_1} \right) G_1 + \frac{4kTF_2 B}{R_2} \tag{3.40}$$

G_1 is the gain of amplifier A_1. The total noise, that modulates laser L_2, is denoted by propagation noise n_p. If the amplifier A_2 has a gain of G_2, this propagation noise is expressed as:

$$n_p = \left\{ \left(RIN_1 i_1^2 B + 2i_1 eB + \frac{4kTF_1 B}{R_1} \right) G_1 + \frac{4kTF_2 B}{R_2} \right\} G_2 \tag{3.41}$$

Expanding the term in equation (3.41) gives,

$$n_p = RIN_1 i_1^2 BG_1 G_2 + 2i_1 eBG_1 G_2 + \frac{4kTF_1 B}{R_1} G_1 G_2 + \frac{4kTF_2 B}{R_2} G_2 \tag{3.42}$$

In addition to the propagation noise n_p, the intensity noise of the secondary laser L_2 also contributes to the output signal of the feed-forward system. If a photodiode D_2 followed by an amplifier A_3 is used to detect the output optical signal from the feed-forward system, the noise source n3 at the input of the amplifier A_3 consists of several noise contributions. These are:

- The propagation noise n_p
- The intensity noise of the secondary laser L_2 is $\eta RIN_2 i_2^2 B$,
- The intensity noise of the primary laser L_1 in the top path of feed-forward is $(1-\eta) RIN_1 i_2^2 B$
- The shot noise of the photocurrent in photodiode D_2, $2i_2 eB$, and the noise generated by amplifier A_3, $\frac{4kTF_3 B}{R_3}$

where RIN_2 is the relative intensity noise of the secondary laser L_2, i_2 is the photocurrent of the photodiode D_2 and η is the optical combination ratio defined as the fraction of the total average optical power at the output of the feed-forward system that comes from laser L_2. The noise source n3 is expressed as:

$$\begin{aligned} n_3 = &\left[(1-\eta) RIN_1 i_2^2 B - \eta RIN_1 i_1^2 G_1 G_2 B \right]^2 + 2i_2 eB + \frac{4kTF_3 B}{R_3} + \\ &\eta RIN_2 i_2^2 B + \eta \left(2i_1 eBG_1 G_2 + \frac{4kTF_1 B}{R_1} G_1 G_2 + \frac{4kTF_2 B}{R_2} G_2 \right) \end{aligned} \tag{3.43}$$

Since the intensity noise of the laser L_1 is coming from the main path and the noise contribution coming from the laser L_2 path are correlated and opposite in sign (refer to equation (3.43), in principle they cancel when

$$(1-\eta) RIN_1 i_2^2 B = \eta RIN_1 i_1^2 G_1 G_2 B \tag{3.44}$$

or

$$(1-\eta)i_2^2 = \eta i_1^2 G_1 G_2 \tag{3.45}$$

The other noise contributions are uncorrelated to the noise cancellation. Therefore, the sum of the other noise contributions n_m, cannot be cancelled by the feed-forward compensation and limit the system noise performance. The minimum noise achievable with feed-forward compensation (the noise limit) is therefore:

$$n_m = \eta RIN_2 i_2^2 B + \eta\left(2i_1 eG_1G_2B + \frac{4kTF_1G_1G_2B}{R_1} + \frac{4kTF_2G_2B}{R_2}\right) + 2i_2eB + \frac{4kTF_3B}{R_3} \tag{3.46}$$

Note that the shot noise due to photocurrent in the photodiode D_2 and the noise generated by the pre-amplifier A_3 are not involved in the noise limitations of a feed-forward system. The feed-forward can only reduce RIN generated by laser L_1. The other noise contributions, which include RIN from laser L_2, shot noise from photodiode D_1 and thermal noise from amplifiers, are intrinsic to the feed-forward system and thus limit its noise performance. For improved noise performance the first stage amplifier A_1 should have a low noise figure.

3.3 System Evaluation

3.3.1 Effect of loop imbalance

The performance of feed-forward compensation depend on the degree of amplitude and phase matching that can be achieved in each of the loop. Any imbalance in the first loop (signal cancellation loop) will affect the reduction of the carrier signal at the output of the electrical coupler C_2. Depending on the level of the suppressed carriers in the first loop and the linearity of the secondary laser L_2 this can lead to further distortion and intermodulation products being generated. Ideally, maximum carrier suppression will be achieved when the two combining signals at the hybrid coupler C_2 are equal in amplitude with a 180 degrees phase difference.

The amount of distortion signal that the feed-forward system can tolerate from laser L_2 also depends on the coupling ratio of the optical coupler K_2. If this ratio is small, say 0.1, only one tenth of the distortion from the secondary laser L_2 will be coupled to the output of the transmitter. This means that in the case of a small coupling ratio of K_2, the carrier signal only needs to be kept small so that laser L_2 does not introduce an excessive amount of distortion. Hence, complete removal of carrier signal is not essential. Once the carriers are suppressed to the IMD3 level then there is no need to further reduce the carriers. This means that the carrier cancellation loop does not need to be tuned to a high degree of accuracy. In practice, a 30 dB of carrier suppression is sufficient so that the laser L_2 is driven in the linear region.

The situation is completely different for the second loop (distortion cancellation loop). Any imbalance of amplitude and phase mismatch in this loop will directly affect the amount of distortion reduction that can be achieved at the output of the feed-forward system. The performance of the system

for distortion cancellation can be improved with increased coupling ratio of K_2, but at the same time noise reduction deteriorates and therefore a compromise has to be made between both effects. The selection of the coupling ratio for K_2 is an important design parameter and is discussed further in section 3.3.4.

3.3.2 Loop cancellation bandwidth

In the signal cancellation loop of the feed-forward, cancellation of carriers takes place. The cancellation bandwidth of the first loop is thus equal to the maximum bandwidth of the input signal or carrier spacing. In the second loop, distortion products are cancelled which appear at frequencies outside the band and therefore the cancellation bandwidth is larger than the first loop. The cancellation bandwidth of the second loop can be defined, as the bandwidth over which significant distortion appears and is dependent on the non-linearity of the primary laser L_1.

3.3.3 Broadband cancellation

In each of the feed-forward loop, there are two signal paths, one of which is the reference path used to compensate for the delay in the laser path. For cancellation at a single frequency equal amplitude and 180 degrees phase difference is sufficient. However, for broadband cancellation the delays introduced in the two paths should also be equal. The delay elements simply consist of microwave delay line and are adjusted using a variable phase shifter until a delay match is achieved, that is until the slopes of the phase response are equal through the two paths. While coaxial cables are broadband components, delay filters have become an increasingly popular method of incorporating delay with operating frequencies near 2 GHz. Although delay filters offer low insertion loss and relatively small size compared to coaxial cables they are custom specified and hence the manufacturing cost is high. Semi rigid cable can also be used for delay matching but its size can be quite large considering minimum bend radius and diameter of these cables.

When the two paths are matched then the cancellation is independent of the electrical wavelength of the signal and therefore the frequency of the modulating signal. If the delay through the reference path is not matched and is too short or too long then the cancellation becomes narrowband. Even with a delay mismatch present, it is still possible to achieve high levels of suppression but over a narrow bandwidth. A network analyser is used to determine if the delay mismatch is too long or too short. In an ideal broadband system, paths with equal amplitude, opposite phase and equal delay would completely cancel distortion over an unlimited bandwidth. However, in practice difficulties of accurately matching amplitude and phase impose limit on the amount of cancellation possible over a finite bandwidth.

Amplitude flatness

Amplitude flatness is very important for accurate cancellation and can be measured as a deviation from

the constant gain and can be affected by amplitude ripples across the bandwidth of interest. Standing waves arising from impedance mismatch and/or imperfect device behaviour cause amplitude ripple. In any feed-forward loop, the desired loop suppression determines the required amplitude flatness. A compensation network can be used to improve the amplitude flatness so that the overall amplitude slope of the feed-forward path is within the specified limit by introducing a slope with the opposite gradient. The wider the bandwidth, the harder it is in practice to reduce amplitude and phase ripple to within a fraction of a dB necessary to achieve high values of loop suppression. Delay mismatch and frequency dependent effects such as amplitude and phase ripple prevent signals from being precisely matched over a wide bandwidth and ultimately set the practical limit on the otherwise theoretically unrestricted bandwidth of feed-forward operation.

3.3.4 Component selections

The desirable characteristics for each of the major system components, how they might be achieved and what figures are obtainable in practice are discussed. The amount of distortion reduction achieved rests mainly on the accuracy of the amplitude and phase matching of the signals. It is important that the amplitude characteristic of the primary laser L_1 deviate as little as possible from an ideal flat response with respect to frequency. This is essential in order to maximise cancellation of the carrier signal in the error signal. The amount of delay introduced by laser L_1 should be minimum as this will determine the value of the matching time delay element in the reference path. The larger the value of time delay required in the reference path, the physically larger the delay element must be and, more importantly, the greater the loss this element will introduce.

The distortion introduced into the system by the secondary laser L_2, though this will be small compared to that produced by laser L_1 can be a limiting factor. This distortion is not compensated for and determines the overall circuit performance. This can be minimised by ensuring laser L_2 is driven by smaller signal levels. Therefore, it is necessary to keep the carrier power input to the secondary laser L_2 low to reduce the IMD generated. The frequency and phase response of the electrical coupler C_2 need to be good in order to ensure a high degree of suppression of the main signal energy in the error signal.

Imperfect matches between the paths can be caused by electrical and optical reflections. Electrical reflections are often caused by impedance mismatch between components in the feed-forward system. For example, reflections at the input of the lasers L_1 and L_2 because the input impedance of the lasers is not equal to the transmission line characteristic impedance of 50 ohms. To assist in impedance matching electrical isolators can be used at the input of these devices.

Optical reflections can influence the laser linearity and increase the non-linear distortion in the laser. The reflections may be caused by spliced fibre or by optical connectors. To minimise these reflections optical isolators can be used between the laser L_1 output and the photodiode D_1 and between the laser and the fibre ends.

Consideration in choosing the optical coupling ratio

Discussions in the previous sections concentrated on analysing the conditions for the reduction of noise and distortion in the feed-forward system. Various design tradeoffs are required in the design and one of the major design considerations is the choice for the optical couplers K_1 and K_2.

The first and most important criterion for choosing K_1 and K_2 is that enough power must be provided at the output of the feed-forward transmitter for power budget. As expected the signal to noise ratio (SNR) is improved for the system by coupling more light from laser L_1 to the output, since the signal is modulated almost entirely by this laser L_1. However, if too much power is directed to the output then this mean that the coupling coefficients of coupler K_1 and K_2 are small and this will increase the noise gain of the feed-forward and the gain required in each loop will increase for distortion reduction. As a result, more than two wideband amplifiers may be required to provide high gain, thus adding to the cost of the system. It is also important to note that the noise gain of the system strongly depends on the coupling of K_1 and this will degrade the noise performance of the feed-forward. Consequently, a large K_1 i.e. more power into the signal cancellation loop can in fact reduce noise but a significant amount of power will be lost in the coupler as well. The coupling ratio of K_2 has a strong influence in determining the final performance of the system and must be small. Otherwise excessive amount of RIN from laser L_2 will be coupled to the output. However, for the carrier cancellation loop a high coupling ratio (50%) is required for the optical coupler K_1 to avoid large amplification for the RF amplifier after the photodiode D_1. In order to have noise reduction K_1 should be around 50% so that noise gain can be kept small while enough power is directed to the output of the transmitter.

A small coupling ratio for the optical coupler K_2 (i.e. 10%) is desired to maximise RIN reduction by a feed-forward scheme. On the other hand, in order to maximise the linearisation a large (i.e. 50%) coupling ratio for L_2 is preferred. In terms of power budget, it is advantageous to choose K_1 to be small but then the value of K_2 must be large, otherwise the optimum gain will increase. Thus, there exist a compromise between the potential of the scheme to reduce non-linear distortion and intensity noise.

3.3.5 Dispersion penalty

Dispersion penalty applies to feed-forward system performance as a result of wavelength separation between the two lasers followed by fibre chromatic dispersion and should be taken into account. When the optical output of both lasers are combined at the final optical coupler K_2 and then transported over fibre, the two laser wavelengths being different travel independently. This leads to optical phase mismatch between the main signal from the primary laser L_1 and the correcting signal from the secondary laser L_2 at the receiver resulting in penalty in the available linearisation or distortion reduction. Even if the system is optimised for maximum performance at a given transmission length, optical phase error will result when the actual length is different. A dispersion induced timing error (Δt) between the two optical signals can be calculated as in equation (3.47).

$$\Delta t = D(\lambda) \times \Delta\lambda \times L \tag{3.47}$$

where D(λ) is the fibre chromatic dispersion coefficient (evaluated at wavelength that is an average between the two lasers wavelengths), Δλ is the wavelength separation between the two lasers and L is the difference in length between the actual transmission length and the length for which the system was optimised (normally 0 km). This timing error is then converted to a corresponding phase error using equation (3.48).

$$\Delta\phi = 2\pi f \Delta t \tag{3.48}$$

The impact of optical phase error on the reduction of non-linear distortion is then evaluated using equation (3.36). For example, a 40 dB cancellation requires a phase balance of 0.5° and an amplitude match well than 0.05 dB. It can be assumed that the amplitude is matched at 0.05 dB and it is the phase that is changed caused by fibre dispersion. Figure 3.4 shows the linearisation at different fibre length, of a system optimised for transmission through 0 km (practically a few meters) of fibre. In this analysis it is assumed that the wavelength separation is 3.2 nm between the two lasers and that the fibre chromatic dispersion coefficient is 17 ps/nm.km. These values are taken from the experimental system, described later in this chapter. It can be seen that dispersion penalty is more severe for high frequency signals such as 5.2 GHz as opposed to 2.4 GHz. This is due to the fact that a given dispersion induced timing error, translates to larger phase mismatch at higher frequency signals. Figure 3.4 also show the available linearisation as a function of wavelength separation reduced to 0.5 nm between the two lasers. A large improvement in distortion reduction performance can be achieved using narrow wavelength separation between the two lasers.

It is important to mention that dispersion penalty can be completely avoided if the system is designed for one given transmission length. Also, to minimise dispersion penalties, sources with

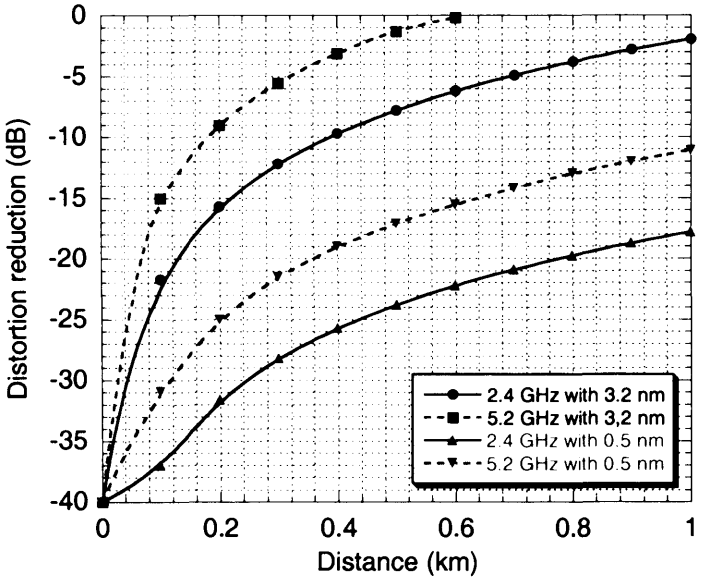

Figure 3.4 Feed-forward distortion reduction with dispersion penalty

similar wavelengths should be used by slightly changing the delay in one of the signal path in feed-forward. It should be noted that the two lasers should not be identical and are required to have slightly different wavelengths, so that they do not interfere to avoid optical beating. Wavelength separation of the two lasers > 0.5 nm assures no optical beating distortion will affect the system with a bandwidth of few GHz and this also takes into account the allowance for accuracy of wavelength tracking with temperature.

A feed-forward circuit is proposed in [9] which overcomes the dispersion limitations using adaptive phase tuning. However, the proposed feed-forward linearised transmitter needs to well know the accurate transmission distance and fibre dispersion after setting up the transmission link. The vector modulator compensates distortion using phase adjustment by voltage and is controlled by a microcontroller. The realisation of this system seems to be difficult for practical applications. Also it is required that the vector modulator has a large phase range [10].

3.4 Adaptive Feed-forward Linearisation

Although feed-forward allows operation over a theoretically unrestricted bandwidth the amplitude and phase matching characteristics are critical to the system performance and it is necessary to ensure these requirements can be maintained over broad bandwidth with time. Even if the signal and the distortion cancellation loop are optimised, they are likely to drift due to temperature variation or change in laser characteristics leading to mismatch. To overcome these issues adaptive techniques are considered so that the amplitude and phase is continuously adjusted to achieve the best cancellation [11]. To allow the system to monitor its own performance and then perform the necessary correction requires some form of feedback system around the feed-forward loops. Since feed-forward has two loops, therefore two separate feedback loops are required: one to correct for the amplitude/phase mismatch in the first loop (carrier cancellation loop) to minimise the carrier signal, and the second to correct for the amplitude/phase mismatch in the distortion cancellation loop to minimise the amount of distortion present in the final output. The intention here is to give a brief overview of some of the techniques.

Figure 3.5 shows the general principle of loop control whereby information on a loop balance is acquired and fed back to control the gain and phase of the loop. The control of the amplitude and phase can be achieved with variable phase shifters and attenuators or with vector modulators. It is first necessary to obtain information on how well a particular loop is balanced and then feed back the information in order to adjust the gain and phase until the required loop suppression is achieved. Thus with automatic control, the loops are continuously monitored and the required output linearity is maintained. Both digital and/or analogue techniques can be used for loop control. Due to differences in the nature of the cancellation signal, however (in one case carriers and in the other distortion), different control techniques are required in the first and the second loop. For example, acquiring accurate information on loop balance can be difficult in the distortion cancellation loop since the reduction of distortion products takes place at the receiver. The phase of the signals is affected by fibre dispersion

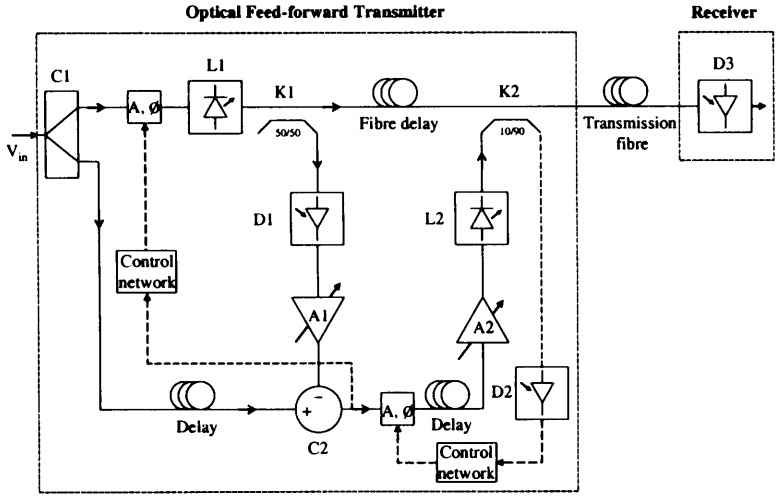

Figure 3.5 Adaptive feed-forward

as a function of wavelength difference and this can further complicate the loop design. However, this limitation can be overcome using vector control theory proposed in [9] or using two lasers with narrow wavelength spacing to minimise dispersion effects. A vector control circuit is employed which compensates the distortion regardless of dispersion or distance. After transmission of signals over fibre, amplitude mismatch can be ignored because of same attenuation coefficient on the fibre, hence only the phase is of concern.

The compensation circuit for gain and phase adjustment shown in Figure 3.5 could appear in a number of different locations around the two loops of feed-forward system. One point to consider is the linearity of these components, since any distortion generated will appear at the output. For example, in the signal cancellation loop the adjustment components could be placed in the reference path or either before or after the primary laser L_1. If they are placed in the time delay path then their distortion will appear in the error signal and amplified by the error amplifier. If however, they are placed before the primary laser L_1, then their distortion will appear as part of the laser, and it will be corrected as such at the final output. For this reason a position prior to the primary laser is usually considered to be optimum for these components. In the case of the distortion cancellation loop, if the adjustment components are placed before the amplifier then the distortion from these components will be amplified by the error amplifier and appear directly in the output signal. However, this is mainly dependent on the amount of distortion generated by the amplitude/phase compensation circuit. It is also important to note that if the adjustment circuit is placed after the error amplifier A_2 then the input signal to these devices is of large magnitude and they may generate excessive distortion.

3.4.1 Adaptive nulling

The automatic correction systems rely upon adaptive nulling of the unwanted signals at the various stages through the system. In the carrier cancellation loop, the error signal at the output of the electrical coupler consists of intermodulation products from the primary laser and the suppressed carriers. Unless the loop suppression exceeds the intermodulation performance, residual carrier power is the dominant contribution to the error signal. Thus, if the level of residual power could be detected, then it could be used as a control parameter for the first loop, that is, the amplitude and phase are varied until the error becomes minimum. The function of the distortion cancellation loop is to cancel the distortion products at the receiver and hence it is the distortion components of the final output signal, which must be monitored and minimised in this case. Figure 3.6 shows a possible implementation of this type of control scheme [6].

Energy minimisation

A simple method of assessing the level of the tones within the error signal is simply to detect the overall energy of the signal. In general, the level of the distortion products is small relative to the wanted signals, and thus the wanted signal energy will dominate. Thus a system can be designed in

which the overall energy of the error signal is minimised by automatic adjustment of the gain and phase components using voltage control. The use of energy minimisation in both parts of a feed-forward correction loop is illustrated in Figure 3.6. The detector could be any form of broadband energy detector, a simple example being an envelope detector used to generate a dc output signal that is proportional to the level of RF input power. This approach may well be all that is required for the error signal in some systems, as large amounts of rejection of the remaining input signal energy below the level of the intermodulation products is not usually required.

Digital techniques can also be used [12] where the output of the analog-to-digital converter (ADC)

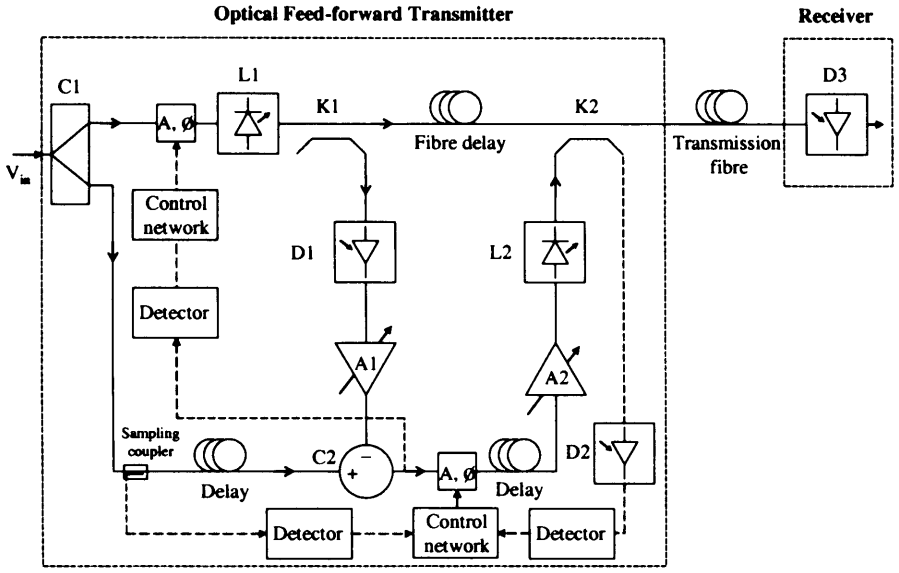

Figure 3.6 Adaptive feed-forward using energy minimisation technique

is used together with some form of algorithm to control the amplitude and phase (e.g. PIN diodes P-type, intrinsic, N-type) until the detected power becomes a minimum. In its simplest form, the algorithm simply compares the current and previous values of detected power and then changes the amplitude or phase to see if the detected power increases or decreases. If the power decreases, then the direction of change in amplitude and phase is maintained, alternatively, if the power increases, the direction of change in amplitude and phase is reversed [7]. The algorithm then continues, ensuring that loop balance is maintained over changes in primary laser output and temperature. In order to increase the speed with which the algorithm converges to the gain and phase settings for minimum power, more complex search algorithms can be used. There are however a number of practical issues which need to be considered when using such control schemes. For example, the dynamic range of the power detector, the resolution of the digital-to-analog converter (DAC), the speed of convergence are important factors in determining the overall performance. A digital signal processing (DSP) controlled adaptive feed-forward amplifier is demonstrated in [13].

In the case of the distortion cancellation loop, two detectors are required. An output detector is required to ascertain the level of the signal plus distortion present at the output and an input detector is

necessary to provide an accurate indication of the input power level, and more importantly, any changes in that level (e.g. due to power control variations). Whilst it would be possible to utilise an output detector alone, the extremely long time constant required in the detector (due to extremely small changes in output level resulting from distortion level changes) mean that it could easily be fooled by even small changes in input (and hence output) level. Utilising this technique for the distortion cancellation loop is usually unsatisfactory for these reasons. The wanted signal energy present at the output will be very large with respect to the remaining distortion and any changes in this distortion level will thus have an almost negligible effect on the output signal energy. As a result the problem of detecting these small changes in energy becomes almost impossible and an alternative solution is required.

Adaptive techniques have been used for the design of a microwave feed-forward amplifier. Song *et al* [14], proposed an adaptive method with analogue controller for CDMA signals whereby a sample of the reference signal (containing only carriers) is correlated with the error signal (containing distortion plus carriers). This approach requires automatic level controller, magnitude comparator and phase comparators together with adjustable amplitude and phase shifters.

Coherent detection

A solution to the problem inherent in broadband energy detection systems is to employ some form of coherent detection or correlation process instead [6]. Figure 3.7 shows an example of this control scheme. In the case of the carrier cancellation loop a sample of the original input reference signal (containing only carriers) is correlated with the error signal (containing distortion plus carriers) to generate a suitable feedback signal. This information is fed back to the gain and phase control components, and loop balance is obtained when the reference signal is uncorrelated with the error

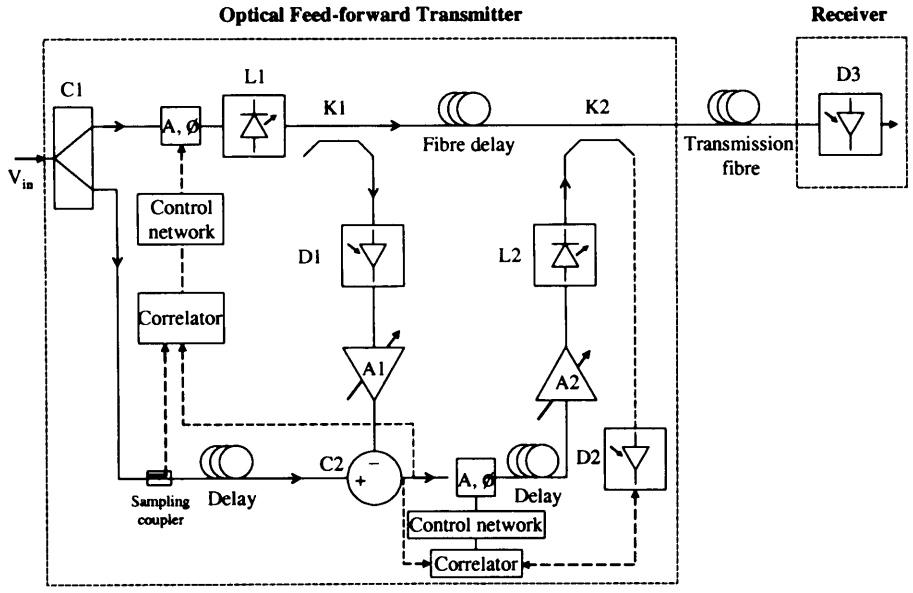

Figure 3.7 Adaptive feed-forward using correlation technique

signal (now containing only distortion). The distortion cancellation loop correlation process utilises the final output signal and the error signal and this process assumes that the rejection of the carrier signal components from the error signal is very good. It is necessary to ensure good rejection of the carrier signal components in order to subsequently ensure that the result of the correlation process is influenced only by the distortion components and not by the wanted signal. The advantage of this type of control scheme is that it can compensate for rapid changes.

3.4.2 Pilot signal (Carrier injection)

In feed-forward the distortion cancellation loop which cancels distortion is different to the carrier cancellation loop which cancels carriers. The information on how well the loop is balanced is in the distortion rather than the carriers. Since the relative levels of carrier power and distortion power is typically large it is more difficult to detect the distortion. One solution to the problem of detecting low level output distortion is to use a special pilot signal, which is suppressed in the same way as distortion in the distortion cancellation loop. If the pilot signal is suppressed, then the distortion generated from the main laser is also suppressed.

One possible implementation of this is shown in Figure 3.8. The pilot signal (additional carrier) is injected into the feed-forward circuit prior to the primary laser L_1 to simulate the distortion generated and then detected at the output using the original pilot as a reference. The injected carrier output from laser L_1 will pass to the output coupler K_2 via the optical delay in the usual manner. A sample of the carrier will also be present in the error signal and will be amplified by the error amplifier A_2 before modulating laser L_2 and then being fed to the output coupler K_2 in antiphase. The amplitude of the pilot signal is sampled at the final coupler K_2. If the distortion compensation loop is adjusted correctly, then the injected signal will be cancelled at the final output, and hence the compensation circuitry must aim

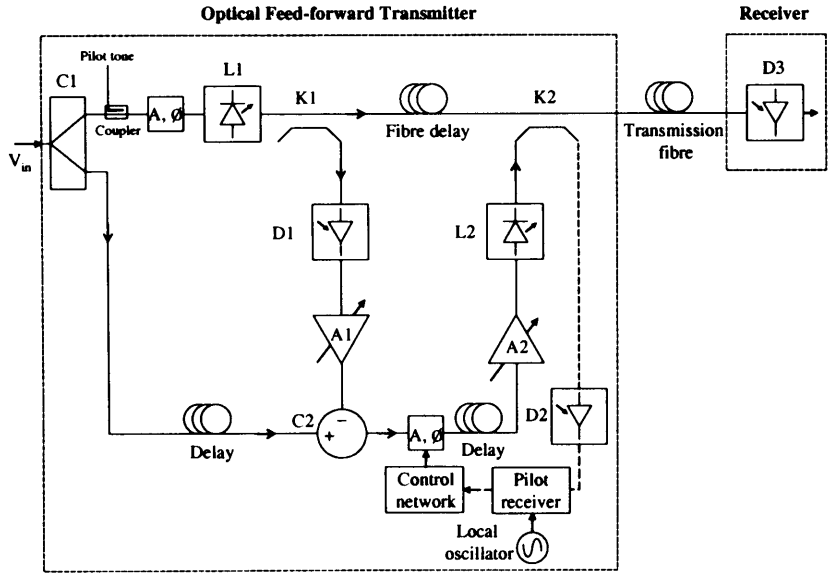

Figure 3.8 Pilot signal technique for adaptive feed-forward

to minimise this level in the output signal [15]. This can be achieved by the use of a narrowband receiver tuned to the injected carrier frequency and hence receiving the residual carrier level. Some form of intelligent controller can then monitor the output of the narrow band receiver and adjust the gain and phase components to minimise the residual carrier level and hence the output distortion is minimised. Myer [6] has patented an example of this type of pilot scheme. The intelligent controller in this case is provided by decreasing step size algorithm; although a microprocessor or digital signal processor could be used to provide a similar function.

There are a number of disadvantages with this technique. The injected carrier will be within the system bandwidth and can intermodulate with the wanted signals in the primary laser L_1 and create additional intermodulation products. Although, these should be eliminated from the final output of feed-forward, they are amplified by the error amplifier, modulate laser L_2 and may cause further distortion. Therefore, the level of the pilot signal is usually significantly less, typically 10 dB or 20 dB, than the level of the main input signal. Also this approach does not help in any way with the elimination of the carrier signals form the carrier cancellation loop and a different form of control must be used for this loop. This technique has been used in linearisation of RF amplifiers [15].

3.4.3 Feed-forward loop control using look up tables

An alternative technique, which does not require any direct knowledge of the loop balance, is the look up table [7]. If the response of a laser is well characterised such that the value of amplitude and phase give good loop suppression then these values can be tabulated as a function of certain control parameters and a control loop can be implemented (For example, the temperature can be used as a control parameter). Detectors can be used to determine the current condition and the corresponding amplitude and phase data are then read from a look up table and applied to gain and phase control networks. The data collected from production calibrations is stored in a micro-controller and the detectors check at regular intervals to see if new control signals for the amplitude and phase networks are required. A look up table method for temperature correction has been utilised for a feed-forward power amplifier to reduce IMD [7]. Look up tables have the advantage that no knowledge of the loop balance is required. The disadvantage of this approach is the time it takes to fully characterise a device is very time consuming and therefore expensive. Look up tables do, however, provide a relatively simple and potentially very effective method of loop control, which can be applied to both carrier and distortion cancellation loops.

3.4.4 Variable gain and phase compensation

The control of amplitude and phase to allow continuous fine tuning to constantly re-optimise performance is important in a feed-forward system. Both gain and phase control components (or combined circuits) have a number of desirable characteristics for use in feed-forward system, in addition to their individual requirements. The most important being the distortion generated by these

components must be minimum. This is particularly necessary if either or both components are employed in the reference path, but is still necessary to some extent wherever they are placed.

PIN diodes are commonly used in the design of attenuators. It is a semiconductor diode in which a high resistivity intrinsic I region is between the P type and N type regions. When the diode is forward biased, the charges are injected in the I region. The attenuation is controlled through the forward bias current, as the PIN diode is a current controlled device and its RF resistance value is set by the forward bias current. Since PIN diodes are non-linear devices they generate harmonic and intermodulation products to some degree. An alternative option for a simple and cost effective solution is to utilise a variable gain amplifier thus saving one element of the system to compensate for amplitude mismatch. Changing the dc voltage on the amplifier control pin allow the gain to be adjusted. However, the phase of the amplifier can change significantly as the gain is varied and this must be taken into account. A variable phase shift element can be employed utilising a varactor (or varicap) diode [16]. The diodes employed should be of the same type and appropriate for the frequency of operation of the phase shifter.

The use of PIN or varactor diodes introduce non-linear elements into the system and care must be taken to ensure that their use does not degrade the overall linearity performance. The components can suffer from a significant insertion loss, particularly when used at higher frequencies, and the cascade of the two elements (to provide both gain and phase control) can increase the gain requirement. Flat gain and linear phase response with frequency is important so that these components do not degrade the cancellation performance due to amplitude ripple or poor phase. Achieving a linear phase response is often more difficult particularly over a wide bandwidth. It is also important that the interaction between the gain and phase controllers is kept to a minimum.

3.4.5 Vector modulator

Using separate gain and phase control elements can introduce problems when they are employed directly one after another in cascade. The matching provided by one element will have an effect on the other and may cause its characteristics to change. For example, a variable attenuator will introduce a small phase change across its attenuation range. Likewise, a variable phase shift will introduce a small (typically < 1 dB) gain variation across its phase shift range. Although the changes will typically be small it can degrade the overall cancellation of the feed-forward system. An alternative is a vector modulator which has the ability to control both the amplitude and phase of the signal simultaneously.

Vector modulators are often used instead of discrete variable attenuators/phase shifter combinations. Although both approaches are used to vary the phase and amplitude of signals in the cancellation loop of a feed-forward, the vector modulator method is inherently faster, providing direct, access to the full 360 degree phase change. However, the loss in a vector modulator is likely to be greater than that possible with separate variable gain and phase components.

The RF input to the vector modulator is first split into two equal outputs with a 90 degrees phase difference between them. The in phase or 0 degrees channel is designated the I channel and the quadrature or 90 degrees channel is designated the Q channel. These two signals are applied to two power splitters that have PIN diodes and varactor diodes connected to them and form attenuator and phase shifter. The output from the phase shifter/attenuator are then combined in phase by another power combiner. The term IQ represent that the user can control both the in phase and quadrature phase components of the output signal. By controlling the relative amount of I and Q signal components that are summed continuous magnitude and phase control of the input signal is possible. A feed-forward amplifier has been developed for 5.725 to 5.850 GHz band for base station applications using a vector modulator for phase and attenuation control [17]. The AD8341 (Analog Devices) vector modulator can operate over a frequency range from 1.5 GHz to 2.4 GHz with gain and phase flatness less than 0.2 dB and 0.5 degree respectively [18]. The amplitude can be controlled from a maximum of 0 dB to less then -30 dB and the phase can be shifted continuously over the entire 360 degree range. This approach can provide significant cost and space savings over discrete, diode based amplitude and phase shifters. Simultaneous control of both gain and phase products simplify system implementation compared to discrete solutions.

3.5 Experimental Arrangement of Feed-forward

This section presents the experimental arrangement of feed-forward linearisation for a directly modulated semiconductor laser and describes the tuning and testing of the system. Characteristic response of the two lasers used in feed-forward is first discussed and then the loop setup at 5 GHz to monitor the system performance.

3.5.1 Characteristic response of the lasers

The two lasers used in feed-forward are commercially available fibre pigtailed DFB laser diodes with multiple quantum well structure and high temperature operation without active cooling. These lasers are first characterised by investigating the effect of bias current on the output power of the laser and the modulation response. A method for measuring the modulation response to estimate the bandwidth and the relaxation oscillation of a directly modulated laser is first discussed. As the dc bias of the laser is increased, the bandwidth is also increased, due to the relaxation oscillation characteristics that vary with bias. The response tends to peak before rolling off and this is the region of relaxation oscillation. Figure 3.9 shows the experimental arrangement for characterising the modulation response of the two lasers used in the feed-forward scheme. The bias current (I_{bias}) was applied to the laser using a bias T and is initially set to 20 mA. A network analyser (Hewlett Packard 8753D) was used to provide RF

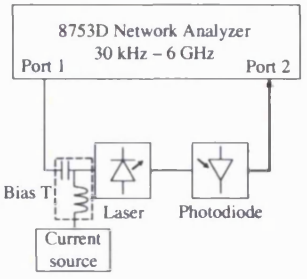

Figure 3.9 Circuit setup for characterising the laser modulation response

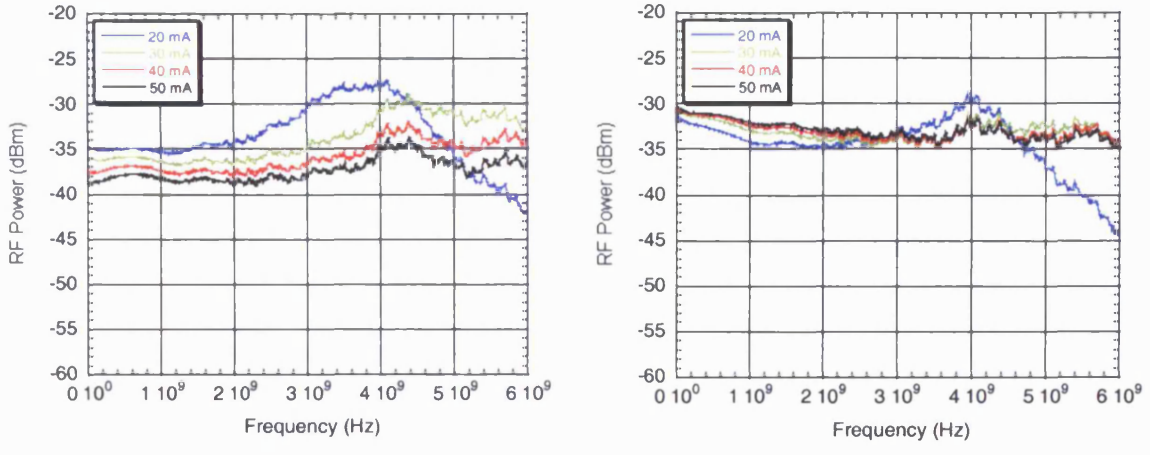

(a) (b)

Figure 3.10 Modulation response of the two lasers with varying bias current (a) Laser 1 and (b) Laser 2

modulating signal to the laser via port 1 for frequency range 0-6 GHz with 0 dBm power. The S_{21} of the network analyser was first calibrated by connecting port 1 directly to port 2 taking into account any cable loss. The laser is then connected and modulated by signal from port 1 of the network analyser and sweeps through 100 MHz to 6 GHz. The optical output power of the laser was directly detected using a discovery semiconductor DSC30S 18 GHz photo-detector and connected to port 2. This setup measures the frequency response of the laser and the photo-detector but from the manufacturer's data, the photo-detector has a -3dB bandwidth of 18 GHz, and the frequency response is flat within 0-9 GHz. Hence the measurement is a good representation of the laser modulation response. The frequency response obtained for both lasers used in feed-forward system with varying bias current is shown in Figure 3.10. The resonance frequency is about 4 GHz for both lasers at 20 mA bias current.

The resonant peak at 4 GHz is about 7 dB above the low frequency response for Laser 1 at a low bias current (20 mA). When the bias current is increased the bandwidth is improved and the amplitude of the resonant peak is reduced. Further increase in bias current produce a flat frequency response with higher bandwidth. It can also be observed that the modulation response of Laser 2 is reasonably flat up to approximately 6 GHz and is better then Laser 1 due to improved connection between the laser input and the RF SMA connector. Laser 1 is the primary laser used in the feed-forward that is to be linearised. Since the network analyser is limited to 6 GHz, the modulation frequency response beyond 6 GHz was measured using a Rhode and Schwarz SMP04 signal source and a HP 74000 lightwave spectrum analyser (LSA) shown in Figure 3.11 with bias current set to 40 mA. It can be clearly seen that beyond 6 GHz the response starts to fall for both lasers.

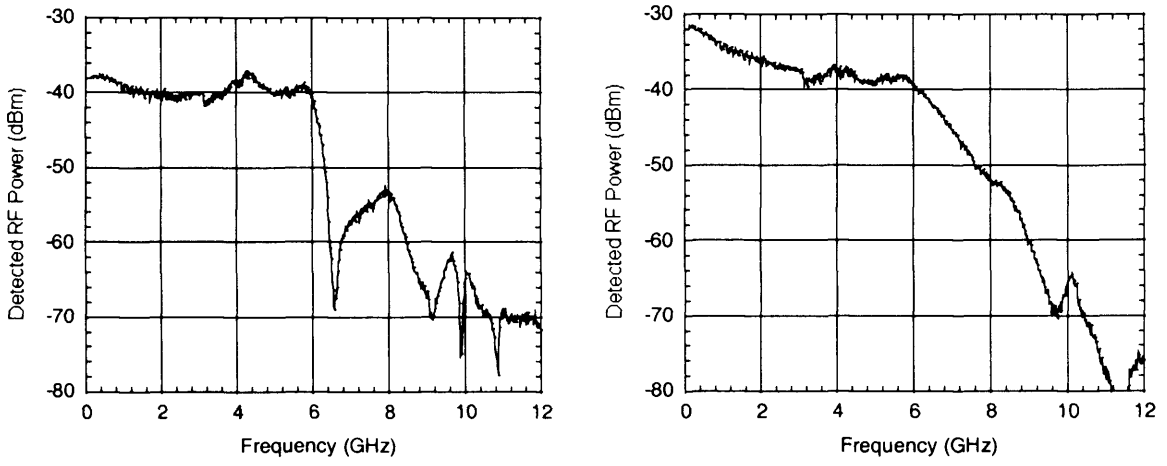

Figure 3.11 Modulation response of the two lasers up to 12 GHz (L1 left and L2 right)

Improved laser modulation response

The input resistance of the laser was measured to be around 5 Ω much less than the matching impedance (50 Ω) and contributes to impedance mismatch. Since laser impedance is low, when connected to a conventional 50 Ω source most of the incident RF power will be reflected back towards

the generators. The reflected power is referred to as the return loss (S_{11}). A 43 Ω surface mount resistor was added in series with the laser RF connector to improve impedance matching. It is possible to match the laser to a 50 Ω source in narrow band applications at low frequencies. In broadband applications matching becomes difficult especially at high frequency and hence the amplitude flatness of the modulation response is affected due to the standing waves arising (the sum of incident and reflected voltages) from laser impedance mismatch causing frequency dependent amplitude ripple. Since feed-forward technique is dependent on cancelling two signals of equal amplitudes with 180 degrees phase difference, variations in amplitude flatness due to reflections can cause imperfect cancellation of distortion and the level of suppression is affected. Any amplitude ripple is clearly undesirable when cancellation requires signal amplitude be matched to within a fraction of a dB. The S_{11} parameters of the two lasers were measured and are shown in Figure 3.12.

Although resistors have been used to match the laser input to a 50 Ω system, matching only occurs

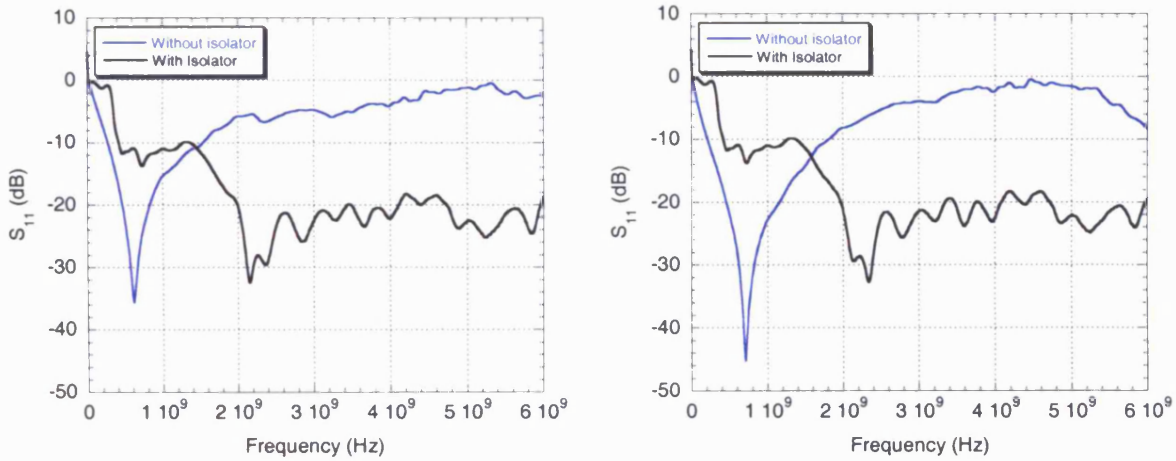

Figure 3.12 S_{11} measurement for the two lasers used in feed-forward system (L1 left and L2 right)

for low frequencies. At high frequencies in the GHz range impedance mismatch becomes worse and reactive components such as inductors and capacitors should be used since the characteristics of these devices vary with frequency. However, these elements can reduce the modulation bandwidth of the laser due to reactive losses. To further improve matching microwave isolators (2-8 GHz) were used with at least 20 dB isolation and the S_{11} are shown in Figure 3.12. This implies that RF signals reflected from the laser are attenuated by at least 20 dB and result in improved modulation response due to reduced reflections shown in Figure 3.13. Amplitude ripples can be observed for the modulation response in Figure 3.10 due to RF reflections but not in Figure 3.13. The ripples are removed because the reflection caused by unmatched impedance is reduced using RF isolators.

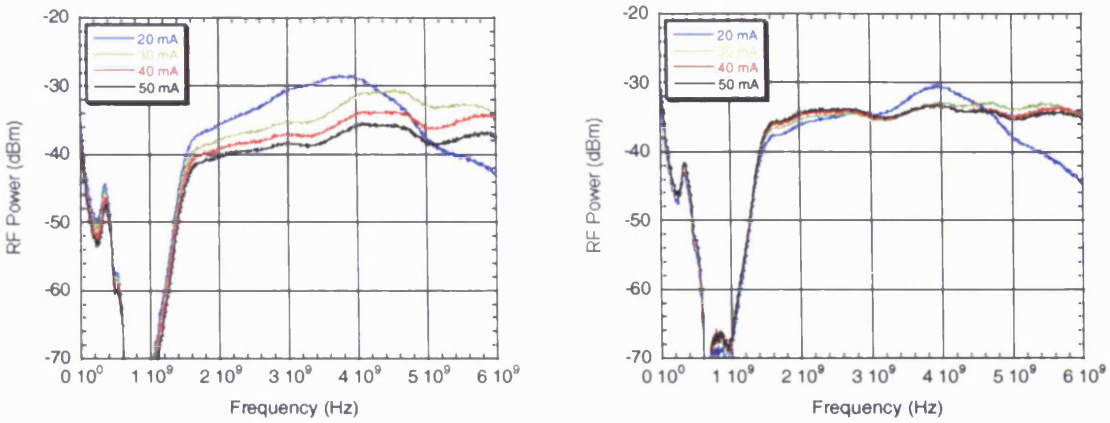

Figure 3.13 Improved modulation response using 2-8 GHz microwave isolators to minimise RF reflections (L1 left and L2 right)

Feed-forward laser wavelengths

The feed-forward system uses two optical sources. The light from the primary source and the secondary laser have slightly different wavelengths and beat noise may be induced due to mixing of the two wavelengths. Therefore care must be taken to separate the wavelengths. However, if wavelength separation between the two lasers is large then dispersion would have a greater effect on the overall distortion cancellation. As mentioned earlier in section 3.3.5 the two wavelengths should be relatively close to minimise dispersion penalty but sufficiently separated to avoid beating. The wavelengths for the two lasers were measured with varying bias current and the results are shown in Figure 3.14. The sidemode suppression ratio (SMSR) is > 45 dB for both lasers and the wavelength separation between the two lasers is 3.2 nm at a bias current of 40 mA.

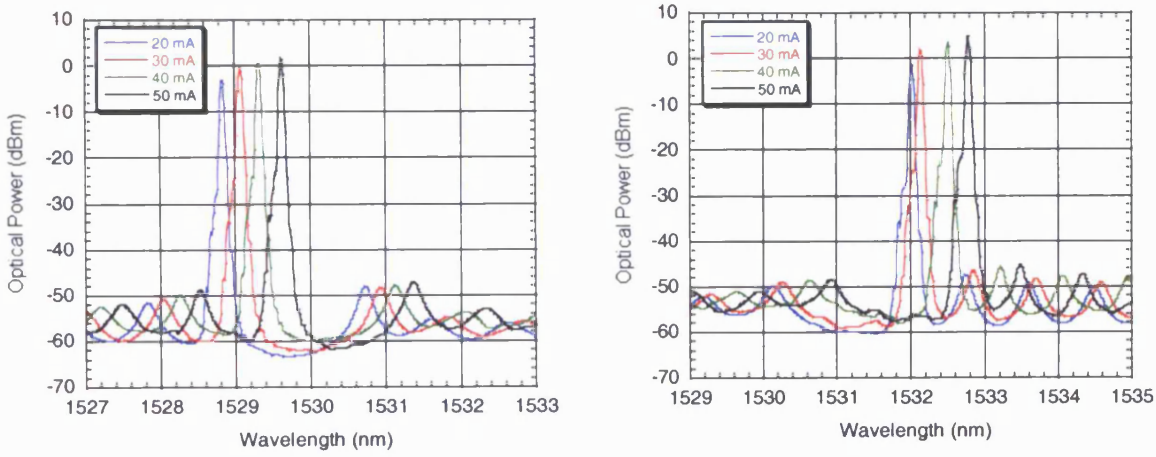

Figure 3.14 Wavelengths of the two lasers used in feed-forward. Left plot is for Laser 1 and the right plot for Laser 2

3.5.2 Experimental arrangements

The experimental setup of feed-forward system is shown in Figure 3.15. The threshold currents are 11 and 12 mA for laser L_1 and laser L_2 respectively. At a bias current of 40 mA the 3 dB bandwidth of both lasers is sufficient for experiment at 5 GHz. Laser L_1 wavelength is at 1529.6 nm, with a mean optical output power of 2 mW (3 dBm) at 40 mA bias current operating under uncooled conditions. Laser L_2 is of the same type as Laser 1 but operating at 1532.8 nm. Considerable impedance mismatch occurs at the connections of the power splitter C_1 and the primary laser L_1, and also between amplifier A_2 and the secondary laser L_2. In addition to the basic components, RF isolators are included to reduce electrical reflections. These reflections must be kept to a minimum to achieve optimum performance of the feed-forward system. Although the addition of fixed attenuators is effective in reducing reflections, these also cause some loss of signal and hence require additional amplifiers for extra gain.

The photo-detector D_1 used in the setup was a DSC30S 18 GHz low distortion InGaAs PIN photodiode. The amplifiers A_1 and A_2 are a pair of Miteq 8 GHz RF variable gain amplifiers with a noise figure of 1.8 dB. All components are selected to have a flat magnitude response and a linear phase response within their operating bandwidths to achieve large reduction of distortion.

The experimental system is designed to demonstrate simultaneous reduction of distortion and noise. The criteria for simultaneous reduction of noise and distortion is described in Section 3.2 and based on these criteria, the optical coupler K_1 is chosen to have a large coupling ratio (50% in this case) so that the noise is reduced and loss in the main signal to be kept to a minimum. A coupling ratio of 10% was selected for coupler K_2 so that only a small amount of intensity noise from laser L_2 is coupled to the output of feed-forward system. The optical and electrical components used in the implementation of the feed-forward system are listed in Table 3.1. The feed-forward could be enabled or disabled by simply connecting or disconnecting Laser 2 output from the optical coupler K_2.

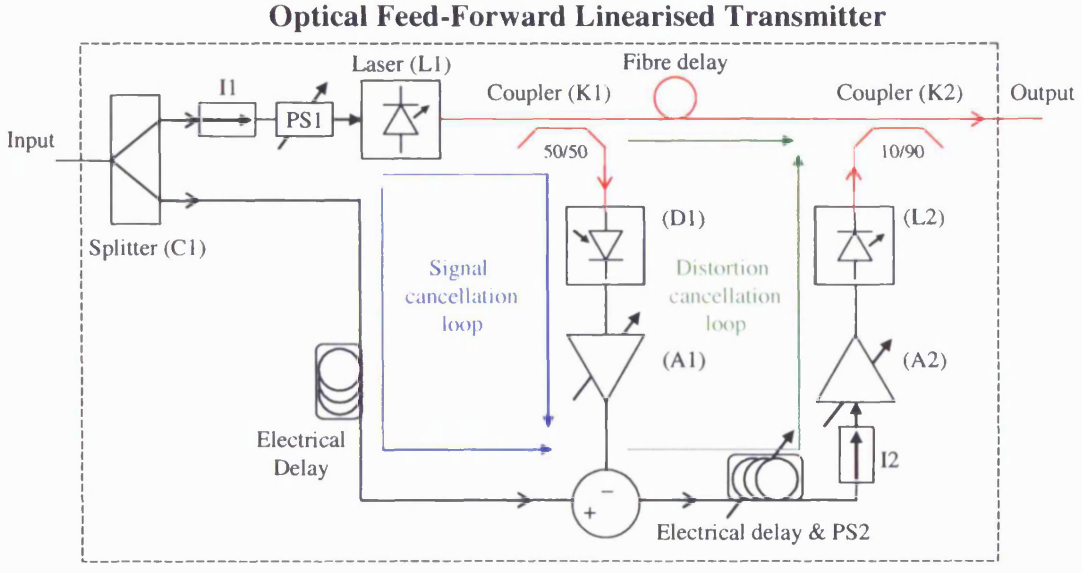

Figure 3.15 Overall feed-forward experimental arrangement

Component	Label	Model number	Description
Laser	L_1	Luminent OIC	CWDM uncooled 2 mW laser
Laser	L_2	Luminent OIC	CWDM uncooled 2 mW laser
Photo-detector	D_1	Discovery semiconductors DSC30S	18 GHz PIN photodiode,
Optical coupler	K_1	General Photonics NTC-15-50-FC/APC	1550nm, Coupling ratio 50:50, FC/APC 2x2 ports
Optical coupler	K_2	General Photonics NTC-15-10-FC/APC	1550nm, Coupling ratio 90:10, FC/APC 2x2 ports
Power splitter	C_1	Mini-Circuits ZFSC-2-10G	2-10 GHz power splitter
Power combiner	C_2	Krytar 4020124	1-12.4 GHz 180 degrees hybrid coupler
Amplifiers	A_1, A_2	Miteq AVG4-00100800-18	0.1-8 GHz, Gain 32 dB, Noise Figure 1.8 dB
Microwave isolators	I_1, I_2	Sonoma Scientific E2XB2	2-8 GHz Isolator, 20 dB isolation
Phase shifters	PS_1, PS_2	ARRA 9428A	Variable phase shifter 0-18 GHz

Table 3.1 List of components used in feed-forward experimental setup

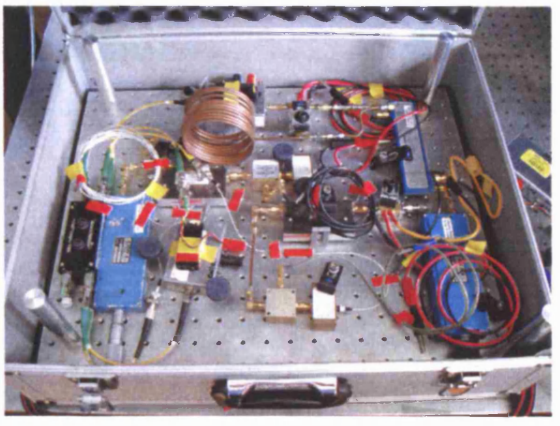

Figure 3.16 Overall feed-forward experimental arrangement in a case

3.5.3 Loop setup

To determine performance of the optical feed-forward system, it is convenient to employ single and two tone measurements. The level of second harmonic distortion can be significant due to non-linearity of a directly modulated semiconductor laser and third order IMD is important in multi-channel systems. Although distortion measurements can be done the performance over a wide bandwidth cannot be observed in real time. Also as mentioned previously the performance of the feed-forward system is dependent on tuning of the two phase shifters PS_1 and PS_2, and the gain of amplifiers A_1 and A_2. Adjusting the amplifier gain allow amplitude matching and phase matching is achieved by tuning the microwave phase shifters. Because the effects of these tuning parameters are inter-related, in order to fine tune the whole system, it is necessary to first tune the signal cancellation loop and then the distortion cancellation loop to form a complete system. Therefore, measurement performance of these loops were carried out using a network analyser to estimate the degree of balance maintained in the loops over a desired bandwidth and optimised for maximum cancellation. To ensure operation over a wide bandwidth, the length of the paths are exactly matched using delay lines. This ensures that the phase of the signals arriving at the cancellation points are exactly matched and independent of the frequency of modulation.

Carrier cancellation loop performance

Electrical amplitude matching requires the amplitude of the reference and sampled (measured after photo-detector 1) signals to be equal. Electrical phase match requires the group delay of the reference and sampled signals to be equal. To achieve phase matching it is essential that all components have good phase linearity over the required bandwidth. If the two paths in the inner loop have the same frequency response then a complete cancellation of the fundamental signal should be obtained at the output of the hybrid coupler C_2. Figure 3.17 shows the experimental setup for carrier cancellation loop measurement. Frequency response of the loop was measured using a Hewlett Packard 8753D network analyser with the reference path connected and disconnected. The sampled signal shows a relatively

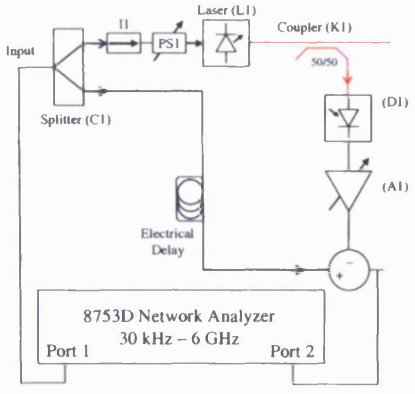

Figure 3.17 Experimental setup for carrier cancellation loop performance

flat amplitude response over the bandwidth of 2-6 GHz. The reference signal is passed through a length of semi-rigid RG402 cable to compensate for the signal delay in the optical sampling loop.

With accurate adjustment of the time delay and amplifier gain, maximum cancellation of the fundamental signal over the bandwidth can be obtained. It was assumed that the laser is non-linear but the photodiode and the associated amplifiers are perfectly linear. An electro-optical component of this branch must have a flat frequency response and a linear phase versus frequency response over the band in which feed-forward linearisation is to be used; otherwise, the optical branch cannot be duplicated by an equivalent parallel electrical branch with frequency independent delay and attenuation. The direct path provides the reference signal in the correct magnitude and phase so that when combined with the output of the laser path the signal parts of the two paths are cancelled. The signals arrive at the power combiner C_2 with equal amplitude and phase. The output of the power combiner consists, in principle, only the inverted phase distortion products associated with the non-linearity of the laser. In practice there will also be residuals from a less than perfect cancellation of the fundamental signals. The cancellation will be broadband to the extent that the frequency dependent gains and phase shifts of the two parallel branches are identical. The two branches can be checked for similarity of phase/magnitude characteristics by substituting a network analyser at the output of the first combiner.

To match the gains of the two paths, the magnitude response of the individual paths are first measured using the network analyser. The difference in the gain of the paths is noted and appropriate attenuators are added. Fine tuning of amplitude to achieve maximum matching was obtained by adjusting the gain of amplifier A_1. This was done by slightly changing the control voltage of the amplifier. Matching the time delay on the other hand, requires more attention. The lengths of the paths were measured using the electrical delay facility on the network analyser. The principle is to use the time delay of the electrical cable, in the direct path to match the total time delay caused by optical fibres and the electrical cables in the laser path. Since high frequency signals are attenuated more than low frequency signals in the electrical cable, this leads to a phenomenon known as rolloff mainly affected by the length of RF cables resulting in amplitude mismatch between the sampled and the reference signal.

One problem is that the delay caused by the laser, the photo-detector and their fibre pigtails is about 23 ns. To match such a long time delay, about 5 meters of electrical cable is needed. Normal coaxial cable of this length has about 4 dB attenuation at 5 GHz and such attenuation is unacceptable in the feed-forward system. To reduce this problem, it was necessary to minimise electrical path length in the reference signal path. This however, requires shortening of the optical fibre in the sampled signals. As a result the fibre lengths of the pigtailed component were cut short as possible. This could not be fully achieved in the experimental setup since, lasers and photodiodes are equipped with a single mode fibre and the approximate length of this arrangement was about 2 m. 15 cm patch cords were used at the input and output of the optical coupler to allow convenient mechanical splicing. Due to these reasons the length of electrical delay in the reference path could not be reduced to less then 2.3 metres.

A 12 ns low loss semi rigid cable (RG402) delay line is used to reduce the delay difference between the two paths. With this semi rigid cable delay, the electrical time difference of the paths is reduced. However as mentioned before, these path lengths still need to be absolutely matched to achieve maximum performance. This was achieved by putting in appropriate length of coaxial cable in the shorter of the two paths. A variable phase shifter PS1 with a fine tuning range is then used to exactly match the time delay difference.

If the time delays of the two paths are not matched then the carrier rejection ratio dips sharply at various frequencies as a result of the time delay mismatch. The time difference of the laser and direct path is equal to the inverse of the frequency difference between two consecutive dips. From this information the time delay difference can be calculated. If the dips are at 920 MHz apart, this means the time difference is about 1.09 ns. With the time difference of the two paths known, a piece of coaxial cable of appropriate time delay is put in the shorter path to reduce the mismatch. Phase shifters and gain of amplifiers are fine tuned so that magnitude mismatch and phase mismatch of the paths are minimised.

Another issue of great importance was found to be matching between different components in the setup. Reflections between unmatched components cause a significant amplitude ripple and severely affect the performance of the feed-forward system. To demonstrate the effects of electrical reflections, responses were measured with and without microwave isolators. The gain and time delay of the carrier cancellation loop is adjusted to account for the removal of the isolator. The carrier rejection ratio fluctuates and is severely degraded. Hence to achieve good carrier cancellation, electrical reflections must be kept low. To improve matching electrical isolators between unmatched components can be inserted. In this way the magnitude of the reflected wave is reduced and a smoother amplitude response is obtained.

After optimising the parameters the loop is again tested and the results for carrier cancellation are shown in Figure 3.18 together with frequency response for the direct and laser path over the frequency

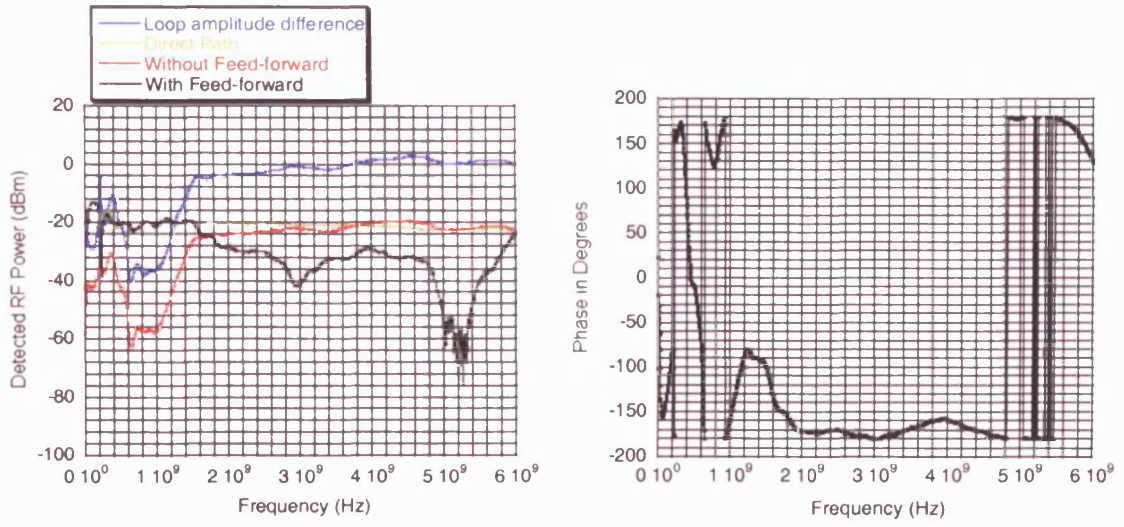

Figure 3.18 Carrier cancellation loop at 5.2 GHz, (left plot) amplitude matching and (right plot) phase matching

range from 0-6 GHz. It can be observed the amplitude is best matched in the 5 GHz frequency range. A carrier suppression of about 30 dB has been obtained over 400 MHz bandwidth centred at 5.2 GHz. This result was obtained when the phase and gain in the loop were adjusted for the best performance. A wider bandwidth can be obtained but with reduced amount of cancellation and a compromise has to be made between the amount of suppression and the desired bandwidth. The phase matching achieved was optimised in the 5 GHz region and is also shown in Figure 3.18. Linear phase in the amplifier and laser is important for maximum carrier suppression. The carrier cancellation is limited by the frequency response of laser L_1 and by the flatness of the gain response of the amplifier A_1. An increasing phase error at low frequency range (< 2 GHz) can be seen. This is due to the power splitter C_1 and RF isolator which have a lower end frequency of 2 GHz. The performance of the carrier cancellation loop is thus presented by the amount of the original input electrical signal being cancelled. The amount of cancellation is measured by comparing the frequency response of the loop using a network analyser with the reference path connected and disconnected. With accurate adjustment of time delay and amplifier gain, maximum rejection of the fundamental signal over a bandwidth can be obtained.

Distortion cancellation loop performance

To evaluate the performance of the distortion cancellation loop, measurements were also carried out using the network analyser. The setup for testing the error cancellation loop is shown in Figure 3.19. Optical amplitude match requires the amplitudes of the main and correcting signal to be equal. While the main signal is optical and shows a flat response over frequency, the correcting signal path contains electrical and RF components, which may lead to a large amplitude roll-off. Optical phase match requires the group delay of the main and correcting signals to be equal.

In the distortion cancellation loop the network analyser cannot be used directly to eliminate delay in the branches because the two branches carry different signal. However, if the electrical reference

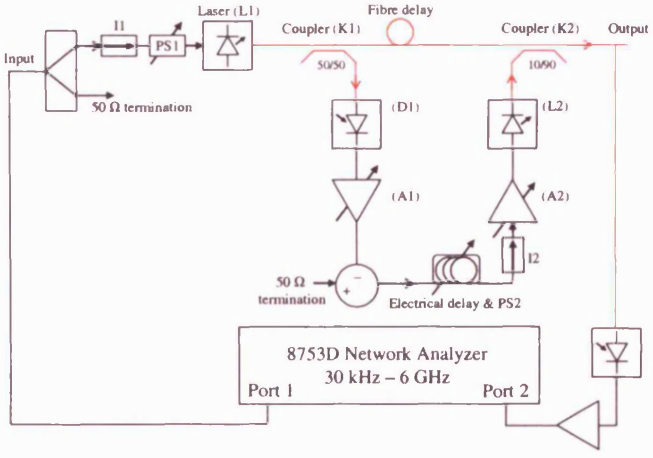

Figure 3.19 Experimental setup for distortion cancellation loop performance

signal to the second combiner C_2 is temporarily removed then the cancellation in the distortion loop can be observed on a network analyser. A 50 ohm termination is connected to the output of the splitter C_1 and input of the combiner C_2 to ensure proper matching. In this way entire modulation signal of the primary laser L_1 propagates through the laser path, which then modulates the secondary laser L_2. The modulation signal is then interpreted as an error signal. The optical output of laser L_2 is thus the inverted form of the signal from laser L_1. If the cancellation loop is correctly tuned, the distortion of the two lasers will cancel at the photo-detector. Frequency responses of the loop are measured with laser L_2 path connected and disconnected. The difference between these frequency responses is the suppression ratio and this indicates the performance of the error cancellation loop.

The tuning of gain and phase in the distortion cancellation loop is very similar to that in the carrier cancellation loop. To match the amplitude of paths the gain of the individual paths are measured. The differences in gain of the two paths are noted and appropriate attenuation is used to balance the gain mismatch. Fine tuning is achieved by changing the control voltage of the amplifier A_2. To match the time delay, the difference is calculated and an appropriate length of RF cable is used to compensate for the time mismatch and a phase shifter is used to achieve fine tuning. However, there is no need to use semi rigid delay lines as in the case of the carrier cancellation loop because both paths of the loops have optical fibres, which can provide long delay with negligible attenuation.

At the receiver photodiode D_2, cancellation of distortion is affected by unmatched phase between the signal plus distortion generated from the primary laser and the distortion generated from the secondary laser. This phase error is caused by time delay difference between two paths. By reducing the time delay in the optical fibre path periodic ripples are observed, which is the suppression ratio as a function of the frequency. This result was measured when the time delay was shortened by about 2 ns and the ripples have a period of about 500 MHz. The ripples indicated that reduction of distortion can be obtained over a small frequency range. It is therefore concluded that the time delay error causes reduction of distortion over a bandwidth. This phenomenon also indicates that the reciprocal of the period of ripples approximately represents the time delay error. Amplitude imbalance can decrease the amount of the reduction of distortion over the bandwidth in the feed-forward system. Both phase and amplitude balances show great importance in the reduction of distortion. Referring to the measured suppression ratios, effects of amplitude and phase errors can be estimated, and therefore the feed-forward system can be efficiently adjusted and optimised.

Again to demonstrate the effect of electrical reflections the RF isolator at the input of laser L_2 is disconnected. After adjusting the loop, the suppression is then measured and it was observed that electrical reflection could severely degrade the performance in the feed-forward system.

It should be remembered that the role of the carrier cancellation loop is to provide a negative signal for distortion compensation. The actual cancellation of the distortion is performed by the distortion cancellation loop. Therefore its performance provides a good indication of the amount of distortion reduction that can be achieved by the overall system. This means that while the feed-forward

system can tolerate some degradation to the performance of the carrier cancellation loop, the distortion cancellation loop must be finely adjusted. As mentioned before, optical phase matching is by far more critical and any degradation in performance of this loop will be reflected in the overall reduction of distortion by the feed-forward linearisation scheme.

The distortion cancellation loop is optimised and tested. Frequency responses were measured with and without blocking the light emitted by the secondary laser L_2. By taking the difference between these frequency responses, a suppression ratio which determines the loop performance is evaluated. The best adjustment in the outer loop can be achieved when the suppression of the error signal is at its maximum (the suppression ratio is at its maximum). Figure 3.20 show the distortion cancellation ratio as a function of the frequency over 0-6 GHz together with response for the direct and the laser path.

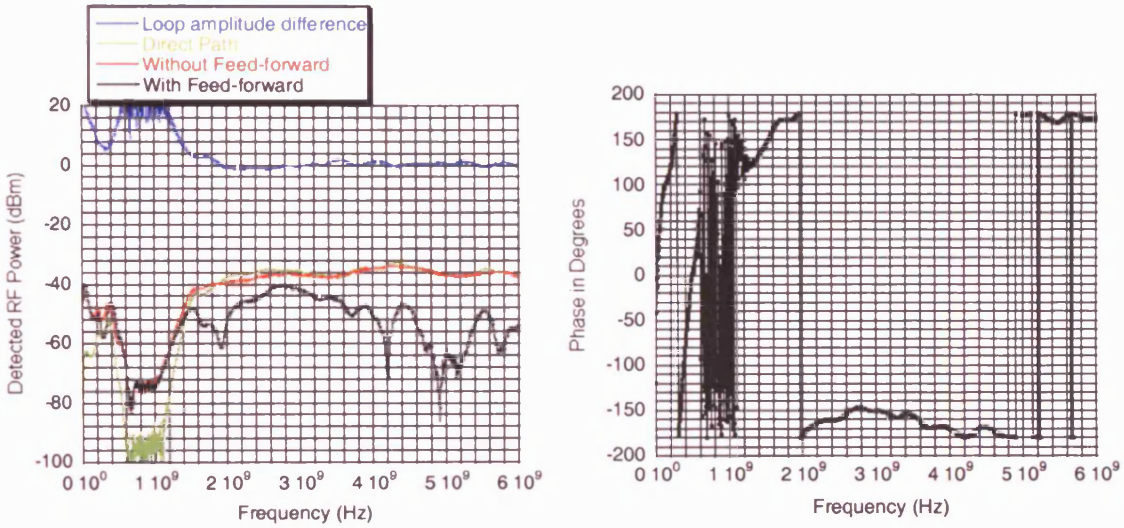

Figure 3.20 Distortion cancellation loop at 5.2 GHz amplitude matching (left plot) and phase matching (right plot)

More then 24 dB of the signal in the loop is suppressed over the frequency range from 4.8 GHz to 5.3 GHz. This result was obtained when the phase and gain in the loop were adjusted for best performance. The operational bandwidth of the feed-forward is limited to 500 MHz due to the frequency response of the lasers and the flatness of the gain amplifiers. Employing optical components with shorter fibre pigtails allows reduction of length of the microwave cables required for path length matching reducing the effect of the microwave frequency dependent loss, thus extending the bandwidth. Since the feed-forward performance is dependant on the quality of cancellation process, gain and phase controllers should ideally be automatically controlled to compensate for temperature drifts, component ageing and changes in response of the lasers.

3.5.4 Non-ideal device considerations

The performance of the feed-forward system is mainly determined by two factors, amplitude mismatch and phase mismatch between each path in the loop. Therefore the reduction of distortion depends

heavily on amplitude and phase balance. Careful and accurate adjustments in phase shifters and amplifiers are essentially required to achieve a good performance in the feed-forward system. In this section some of the main problems encountered in the practical implementation of the circuit which were not discussed before are briefly discussed. In addition, the effects of the non-ideal devices on the feed-forward system are also presented in this section.

Semiconductor lasers

A flat amplitude response and a linear phase response of the laser is required over the bandwidth because they can affect the reduction of distortion. Although the secondary laser is a non-linear device, the effect of its non-linearity is similar to the effect of the amplifier A_2.

Photodiode

The photodiode D_1 has a similar effect on the feed-forward system as the amplifier A_1. Non-linear distortion in the photodiode D_1 is not significant in the feed-forward system since photodiodes with high linearity are available. Moreover, a flat frequency response and a linear phase are found in the photodiode. Generally, the photodiode does not cause any severe effect but shot noise in the photodiode may affect the noise performance of the feed-forward system.

Optical connectors and splices

The quality of optical connectors and splices in the fibre used is another point of major importance. Optical reflections from imperfect optical connectors and splices can generate a noisy signal and also create distinct resonance like peaks, causing large amplitude and phase errors at certain frequencies. Due to the importance of minimising optical reflections in a feed-forward circuit optical isolators may be used. Also reflections at fibre joints can be minimised by the use of index matching gel, which can be a simple and very effective way of reducing optical reflections. The optical connectors deteriorate after being reused for many times and it is vital that the connectors are suitably cleaned every time they are connected. The use of FC/APC connectors can also help to eliminate reflections significantly.

Optical coupler

The optical coupler K_2 in which distortion is combined determines the combination ratio of the signal plus distortion generated by the primary laser to the error signal generated by the secondary laser. As mentioned previously this combination ratio must be carefully considered in the feed-forward system. To obtain minimum optical power penalty of the primary laser and to minimise noise generated into the system by the secondary laser, the optical combination ratio should be as low as possible, typically 0.1 or less. However, a larger modulation error signal of the secondary laser is required to compensate for the loss of the optical signal coupling at the optical coupler because of the small combination ratio and the secondary laser may be modulated by a very large signal.

Amplifier non-linear distortion

Non-linear distortion generated by RF amplifiers is another limiting factor, determining the degree of linearisation possible by this feed-forward scheme. The circuit is designed to reduce distortion generated by the primary laser, but non-linear distortion introduced to the system by other components is not compensated. Even if the circuit is capable of reducing laser distortion to less than –70 dBc, amplifiers non-linearity may cause the final level of distortion (in the output signal) to be as high as –60 to –50 dBc.

In general, the linearity of amplifiers depend on their input level. For amplifier 1 (following detector 1) in the circuit, this level is typically –40 dBm. Under these conditions amplifier distortion is small and imposes no problems. For amplifier 2 (driving laser 2) the input level is significantly higher and thus amplifier distortion may become a limiting factor. Also gain responses of amplifiers are key element in the feed-forward system performance. It is important that the amplifiers exhibit a flat gain and a linear phase over the bandwidth. These errors in the phase and gain can limit the cancellation of the fundamental signal and the reduction of distortion over the bandwidth.

3.6 Experimental Results

The overall experimental arrangement for distortion measurements including two tone and wireless over fibre transmission experiments is shown in Figure 3.21. The configuration of the feed-forward linearisation is employed to linearise the optical intensity output of Laser L_1, which is directly modulated. The detailed working principle of the feed-forward linearisation has been discussed earlier. The key point about the feed-forward linearisation is that Laser 2 is directly modulated with the small and phase inverted version of the distortion products generated by Laser 1, and can therefore be assumed to operate linearly and not generate distortion of its own [19]. The optical output of laser L_2 replicates the distortion products generated by laser L_1 with 180 degree phase shift and without the main modulated signal. The same principle applies when laser L_1 is directly modulated with two high power QPSK channels (discussed later). Therefore when the output from Lasers 1 and 2 are detected at the receiver, the distortion products are cancelled, leaving only the linearised signal from Laser 1. The carrier cancellation loop and the distortion cancellation loop were optimised first as discussed in Section 3.5.3 and then put together to form the complete feed-forward system. The amount of distortion reduction achieved by the system is measured for laser L_1 and a number of measurements were conducted. The performance of the circuit with and without feed-forward is determined simply by enabling and then disabling the output of the secondary laser L_2.

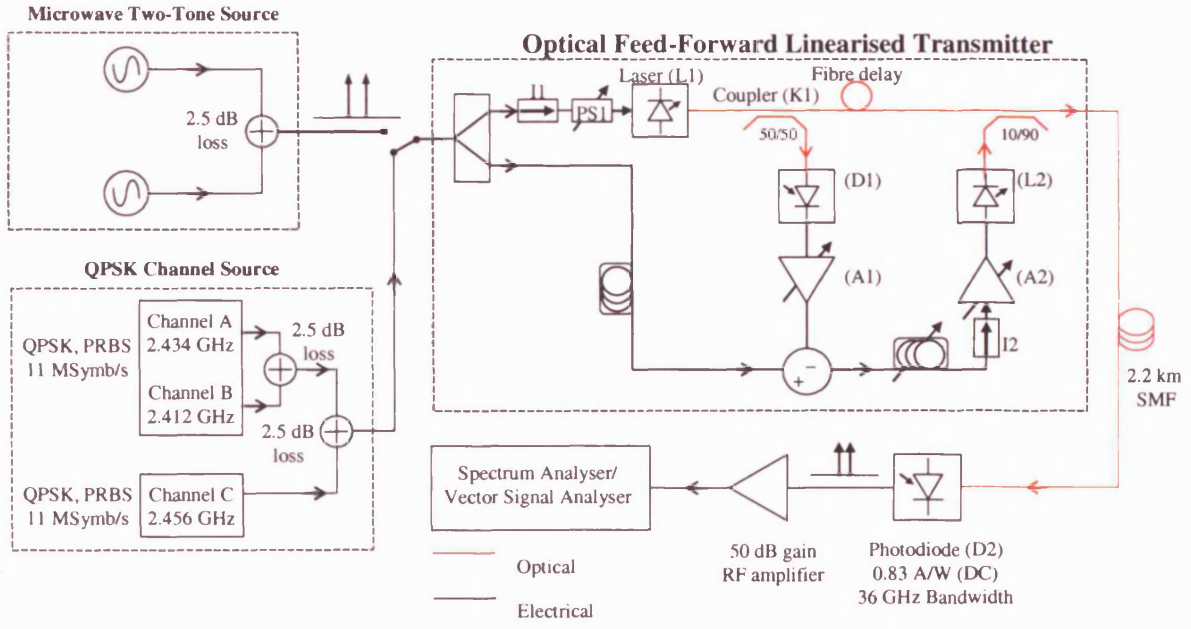

Figure 3.21 Overall feed-forward experimental arrangement

3.6.1 Two tone intermodulation distortion

Two tone measurements were carried out to evaluate reduction of third order intermodulation distortion of laser L_1 by feed-forward compensation. Two closely spaced microwave carriers were

supplied by combining the output of two Rhode & Schwarz SMP04 signal generators using a Mini-circuits ZFSC2-10G power combiner. Two tones test provide a more realistic way of examining the system performance than one tone test, since the reduction of distortion products falling close to the original tones (carriers) is measured. Figure 3.21 shows the experimental setup used for the two tone tests. The RF sources were set to 5.2 GHz separated by 10 kHz to measure third order intermodulation distortion (IMD) products at 2f1-f2 and 2f2-f1. Due to non-linearity of the laser third and higher order IMD products are generated. The function of the feed-forward is to remove the distortion products and ideally leaving only two carriers at the output.

The power of each RF signal was adjusted so that the laser was modulated at a modulation depth of 0.63 for each tone. Increasing the input power of each carrier at constant bias current can increase the optical modulation depth (OMD) per carrier. Dual junction microwave isolators with at least 40 dB isolation were used at the output of each RF source to provide sufficient isolation between the generators. Without isolators, the two signals may interfere with each other and produce IMD since the power combiner had only 11dB isolation. The IMD introduced by the signal generators was first characterised by connecting the output of the electrical coupler to the RF input of the lightwave spectrum analyser. It was found that this distortion was negligible due to isolators at the output of the signal generators. Third order IMD products from the feed-forward output is detected using the LSA. The internal electrical attenuation of the spectrum analyser was set to approximately 10 dB in order to reduce distortion introduced by the test equipment.

The linearisation process consisted of two stages. The first stage was the production of the error signal and the amount of carrier suppression achievable. The second stage focussed on the degree of linearisation obtainable through cancellation of the third order IMD products at the output of the feed-forward system. The error signal should ideally consist of only the IMD products from the laser. The distortion introduced into system in the laser path by the photo-detector D_1 and the amplifier A_1 was characterised to ensure that any distortion detected at the output of electrical coupler was from the laser only. This was done by first disabling the direct path and observing the signal at the RF input to the spectrum analyser. An attenuation of 3 dB was introduced before and then after the amplifier and the photo-detector, and any change in distortion products were investigated. Since there was not any substantial change in the distortion products, it was concluded that the distortion from the photo-detector and the amplifiers was negligible. This signal is subtracted with the undistorted signal in the reference path to introduce the electrical error signal at the output of electrical coupler. The carrier power level was reduced to –75 dBm which implies a carrier suppression of 40 dB. This is more than acceptable level of carrier suppression. The lower the power level of the carrier in the error signal, the lower the level of non-linear distortion products introduced by the secondary laser L_2.

The error signal obtained is amplified and modulates laser L_2 to provide the optical error signal. This error signal is coupled to the primary laser L_1, which consists of the carrier signal and IMD products. Figure 3.22(a) shows the detected electrical spectrum of the optical output without feed-

forward linearisation and it can be seen that significant levels of third and higher order intermodulation distortion products are present with IMD3 at 45 dB below the carriers. With feed-forward activated, the detected spectrum in Figure 3.22(b) shows a reduction in the levels of the distortion products, with IMD3 reduced by 26 dB to 71 dB below the carriers. It can be observed that the carrier power level remains the same under both conditions. From 5.1-5.3 GHz, suppression was at least 20 dB for IMD3 and 12 dB for higher order distortion products. In these measurements, the input modulation power to the microwave splitter was 6 dBm per carrier tone and the output spectra were detected using a Lightwave Signal Analyser (LSA) with 0.81 A/W responsivity at its optical input. In practice, the input to the feed-forward may have a finite level of distortion and the feed-forward cannot reduce this level but only maintain it. The output of the feed-forward is therefore only completely distortion free when the input signal contains no distortion.

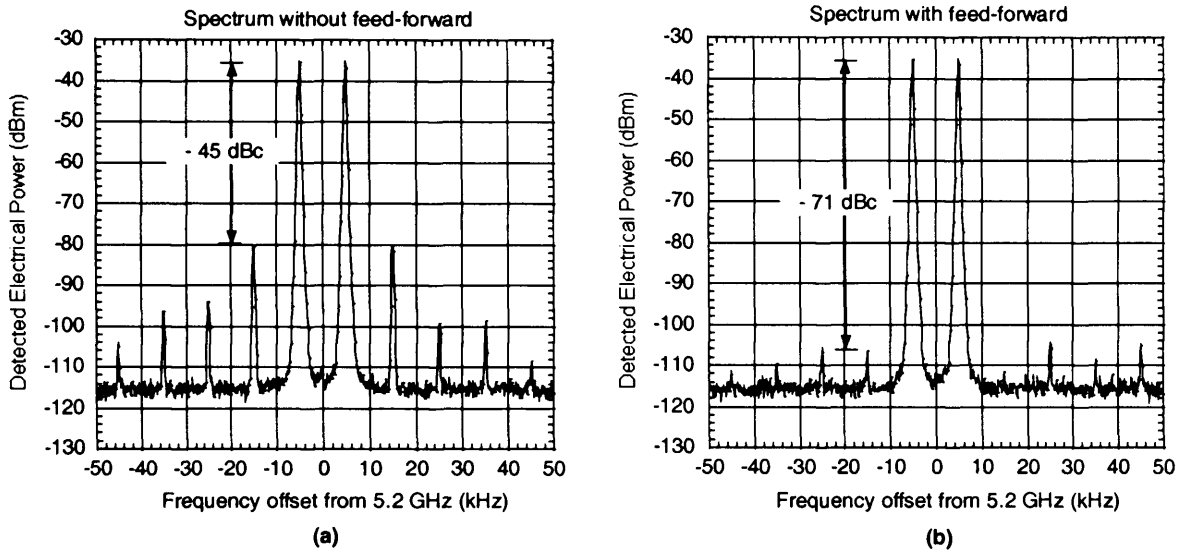

Figure 3.22 Detected electrical spectra of overall system under direct two-tone modulation (a) without feed-forward linearisation and (b) with feed-forward linearisation. The mean optical output powers of the overall system were 0.9 dBm in (a) and 1.7 dBm in (b). The microwave input power per tone @ 5.2 GHz ± 5 kHz is 5 dBm at the power splitter input.

3.6.2 Laser RIN reduction and dynamic range

The noise added by the primary laser L_1 can be thought of as an additional signal, which is not present on the reference path, and hence will appear as part of the error signal at the output of the electrical coupler C_2. It will therefore be corrected as part of the natural operation of the feed-forward process and assuming a perfect gain or phase balance for the overall system, will be eliminated at the output. Therefore, feed-forward not only eliminates distortion but also noise and indeed any other spurious signals present at the output of laser L_1 which are not present in the reference path. This is a useful benefit of the feed-forward system, as it allows relatively low noise lasers to be constructed with high third order intercept points, hence resulting in a large dynamic range.

To measure the spurious free dynamic range (SFDR) the RF input power levels of the two carriers to the microwave splitter were varied in steps of 1 dB and the corresponding output power levels of the two fundamental carriers and the IMD3 were measured. The results with and without feed-forward are shown in Figure 3.23. Since the combining splitter and RF cable had about 4 dB loss and the generators have the maximum power of 10 dBm, it was not possible to take results beyond 6 dBm. The RF power shown in the horizontal axis is at the terminal of the input splitter to the feed-forward system. Not only has the feed-forward reduced IMD3, the RIN has also been lowered. Measurement of the relative intensity noise (RIN) was performed with the optical output of the laser L1 directly connected to a LSA. Using the built in RIN measurement capability of the test equipment the RIN spectrum of the laser L1 in the frequency range of 5 GHz is recorded. The RIN was −141 dB (1 Hz) without feed-forward, and −150 dB (1 Hz) with feed-forward. The laser L1 must be of high power so that the intensity noise of the laser will be dominant over the noise in the measuring equipment. The noise floors in Figure 3.23 were limited by the laser RIN and equal to the equivalent electrical noise power spectral densities that would be delivered to a 50 Ω load by the photodiode of the LSA having 0.81 A/W responsivity. Using these RIN values and noting that the mean optical output power was 0.9 dBm without feed-forward and 1.7 dBm with feed-forward, the two noise floor limits were calculated to be −154 dBm (1 Hz) and −161 dBm (1 Hz), respectively. The respective SFDRs are therefore found to be 92 dB (1 Hz) and 107 dB (1 Hz), an enhancement of 15 dB using feed-forward linearisation.

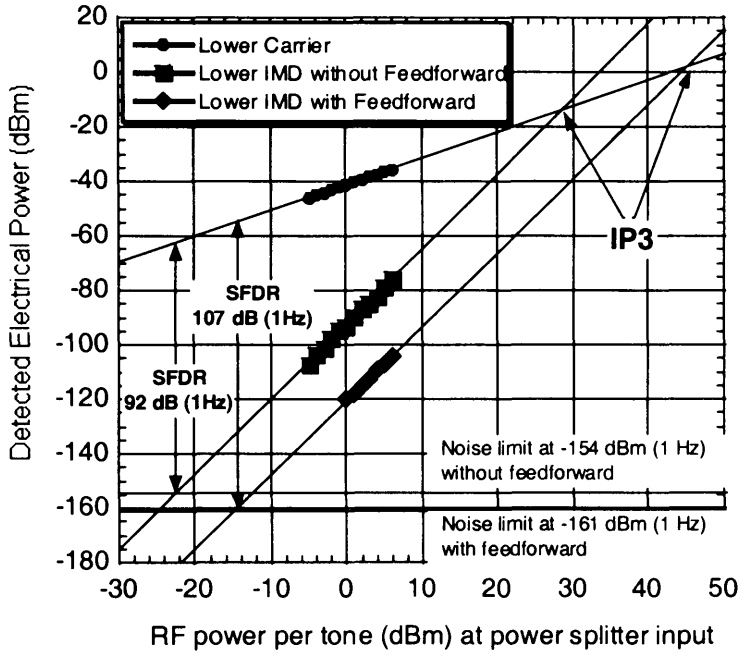

Figure 3.23 Dynamic range measurement of overall system with and without feed-forward linearisation @ 5.2 GHz ± 5 kHz

3.6.3 Spectral re-growth and interchannel distortion

The feed-forward system described in the previous section has also been used for broadband wireless Quadrature Phase Shift Keying (QPSK) data transmission experiment. The use of feed-forward linearisation at 2.4 GHz to compensate laser non-linear distortion in a multi-channel wireless-over-fibre system intended for WLAN applications is investigated. An access point (AP) can simultaneously receive high and low power signals, depending on how far the users are from the AP. Any non-linear components in the fibre-optic link such as a directly modulated laser can cause spectral re-growth (or broadening) of an input signal.

The effectiveness of feed-forward linearisation in suppression of the spectral re-growth caused by the non-linearity of Laser 1 is examined. A Vector Signal Generator (VSG) was used to provide two 11 Msymb/s QPSK channels, A and B, at 2.434 GHz and 2.412 GHz, respectively. Both Channels A and B were internally filtered with a root raised cosine function having a roll-off factor of 0.5 for reducing the occupied bandwidth. Channels A and B were combined in the microwave combiner before being applied to the input of the feed-forward transmitter for direct modulation. Channel A input power was fixed at +13 dBm and Channel B input power was varied. The frequencies of Channel A and Channel B correspond to two adjacent non-overlapping channels specified by the 802.11b (North America). The symbol rate is the same as that of 802.11b. The aim of the experiment was to consider the situation where the received power from a nearby user to the BS would generate a strong signal and to investigate how the spectral re-growth caused by the high power Channel A would interfere with the weak neighbouring Channel B which was far from the BS whose power was varied from -25 dBm to +13 dBm. The output from the optical feed-forward transmitter was transported over a 2.2 km length of SMF (dispersion 17ps/nm/km). The feed-forward could easily be enabled or disabled by simply connecting or disconnecting Laser 2 output from the optical coupler. The linearised modulated signal at the output of the photodiode was amplified and detected using a Rhode & Schwarz FSQ26 Vector Signal Analyser (VSA). The RF spectra of the two transmitted channels were measured with the feed-forward disabled and enabled as shown in Figure 3.24.

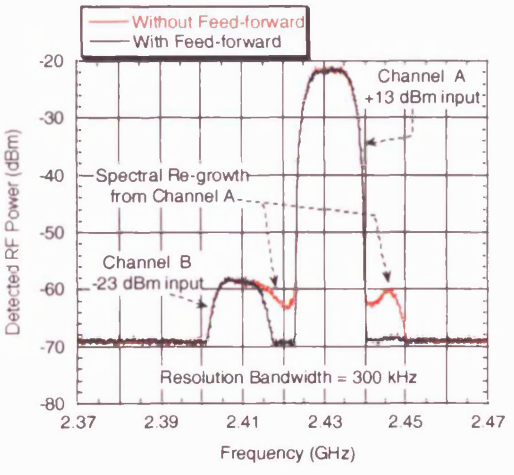

Figure 3.24 Detected RF spectra with and without feed-forward

When the feed-forward was disabled, the non-linearity generated from Laser 1 caused significant spectral re-growth from Channel A to interfere with the frequency band of the neighbouring Channel B. With the feed-forward enabled, the spectral re-growth was suppressed by at least 9 dB. Also with the spectral re-growth suppressed, the spectrum of Channel B can be seen more clearly.

The error vector magnitude (EVM) and the signal-to-noise ratio (SNR) for Channel B were measured in the presence of Channel A whose input power was fixed at +13 dBm throughout and the results are shown in Figure 3.25. EVM is the difference between the measured symbol and the ideal reference symbol. The EVM decreased and SNR increased with increasing Channel B input power. At -20 dBm, feed-forward reduced the EVM by 5 % and increased the SNR by 2 dB. The IEEE802.11b standard requires that the EVM not exceed 35% and it can be seen in Figure 3.25 that without feed-forward, Channel B would not be able to comply with this requirement for input levels below -23 dBm, whereas with feed-forward the specification is met for channel B levels as low as -26 dBm.

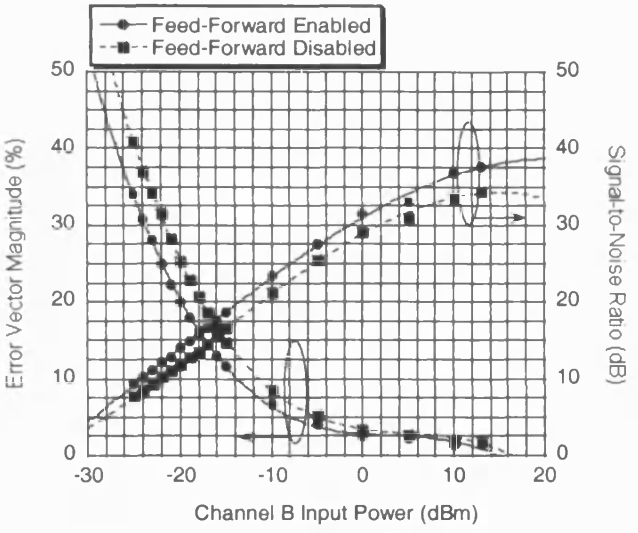

Figure 3.25 EVM and SNR vs. Channel B input power with Channel A at +13 dBm. Channel filter bandwidth: 20 MHz.

The quality of the measured eye-diagrams of the weaker Channel B were also affected by Channel A spectral re-growth. The eye-diagrams shown in Figure 3.26 were measured with the VSA set to the

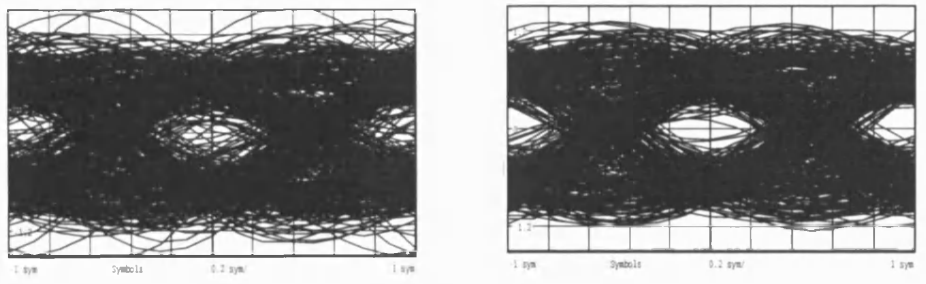

Figure 3.26 Detected -23 dBm Channel B in-phase eye-diagrams with Channel A at +13 dBm with feed-forward disabled (left) and enabled (right). Channel filter bandwidth: 20 MHz.

centre frequency of Channel B at 2.412 GHz and selecting a 20 MHz wide channel filter. With feed-forward enabled, the eye-diagram had a wider opening compared to when the feed-forward was disabled.

To see the effect of two strong channels the input powers of both Channels A and B were set equal at +13 dBm and the measured RF spectra in Figure 3.27 show that with the feed-forward disabled, there was strong intermodulation distortion caused by the two high input power signals directly modulating Laser 1. Any low power signals in the next neighbouring channel frequency bands would have been severely degraded. With feed-forward enabled, the intermodulation distortion was suppressed by more than 10 dB.

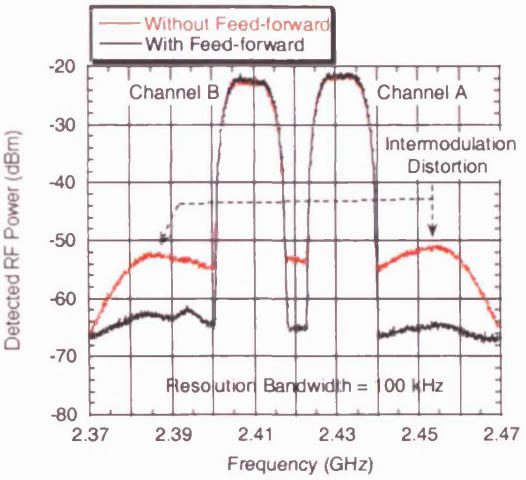

Figure 3.27 Detected RF spectra with feed-forward disabled (left) and enabled (right), both Channels A and B set at +13 dBm.

The impact of intermodulation distortion on a weaker adjacent channel is investigated using three QPSK channels [20]. A Rohde & Schwarz VSG was used to provide two 11 Msymb/s QPSK modulated signals at 2.434 GHz (Channel A) and at 2.412 GHz (Channel B). Both Channels A and B had a fixed power level at +13 dBm throughout and were internally filtered with a root raised cosine function having a roll-off factor of 0.5 for reducing the occupied bandwidth. An Agilent VSG provided Channel C with 11 Msymb/s QPSK modulated signal at 2.456 GHz. Channel C was internally filtered with a root Nyquist function having a roll-off factor of 0.5. A number of measurements were conducted with different Channel C power levels. All three QPSK channels were first combined using microwave combiners as illustrated in Figure 3.21 before being fed to the optical feed-forward linearised transmitter. With Channel C set at –23 dBm, the transmitted RF spectra with the feed-forward disabled and enabled were measured with a spectrum analyser. Under such a high power input, particularly from Channels A and B, Laser 1 generated a significant level of interchannel distortion as identified in Figure 3.28 in the non-linearised case. The weaker Channel C was effectively buried under and could not be readily distinguished from such distortion products in the RF spectrum. With the feed-forward enabled, the interchannel distortion was reduced by at least 11 dB and the spectrum of Channel C could then be clearly seen as in Figure 3.28.

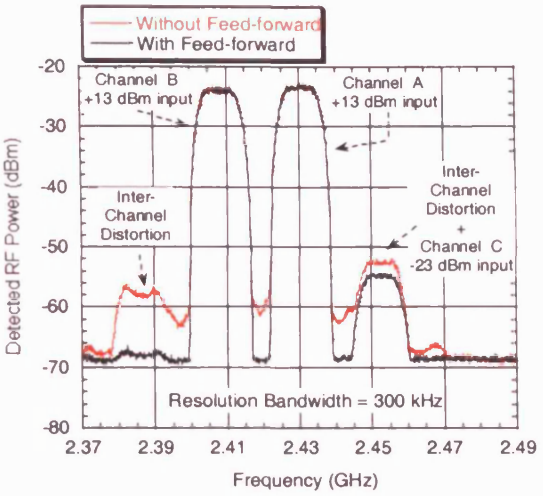

Figure 3.28 Detected RF spectrum of the three QPSK channels with and without feed-forward linearisation

To assess further the impact of the interchannel distortion on the weaker Channel C in the time domain and the effectiveness of the feed-forward linearisation, a VSA was used to measure the eye-diagram, the EVM and the SNR for Channel C. With the VSA tuned to the centre frequency of Channel C at 2.456 GHz and set to a 20 MHz channel filter bandwidth, the eye-diagrams and constellation points with feed-forward disabled and enabled were measured and are shown in Figure 3.29.

When the feed-forward was disabled, no eye-diagram could be detected which suggests that the interchannel distortion products from Channels A and B completely overwhelmed the weaker Channel C. When the feed-forward was enabled, a clear, open eye-diagram was obtained for Channel C. Such a dramatic difference in the quality of the received eye-diagrams illustrates how effective the feed-forward linearisation is in suppressing interchannel distortion. In Figure 3.29 only the in-phase eye-diagrams are shown since the corresponding quadrature phase ones were very similar.

The EVM and SNR for Channel C were measured as a function of channel input power and the results are plotted in Figure 3.30. The EVM decreased and SNR increased with increasing Channel C

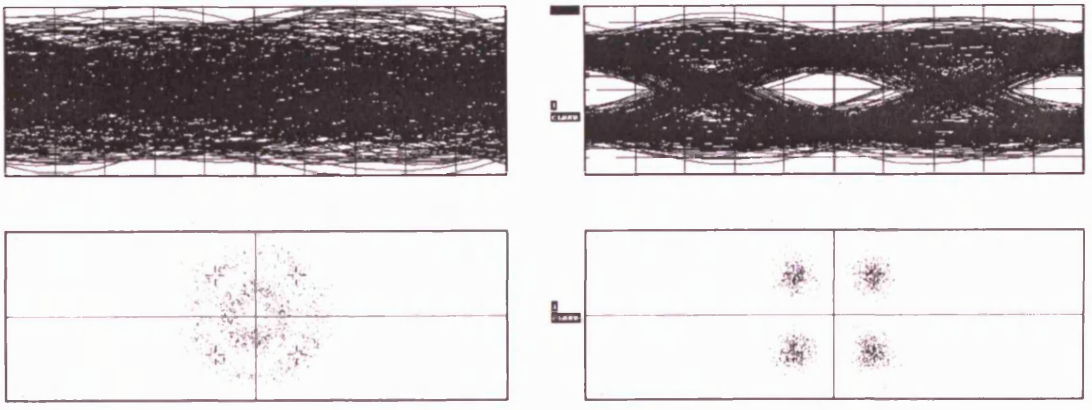

Figure 3.29 Detected -23 dBm Channel C in-phase eye-diagram and constellation points with feed-forward disabled (left) and enabled (right). Channel filter bandwidth: 20 MHz.

input power. At −14 dBm input power, the feed-forward linearisation reduced the EVM from 31 % to 10 % and increased the SNR from 10 dB to 20 dB. The IEEE802.11b standard requires that the EVM not exceed 35 % and it can be seen that without feed-forward, Channel C would not be able to comply with this requirement for input levels below −15.5 dBm, whereas with feed-forward the specification is met for Channel C levels as low as −26 dBm, a power advantage of 10.5 dB. It can be seen that the performance increase is greater for 3 channels than for 2 channels since the effect of intermodulation distortion is more severe then spectral re-growth.

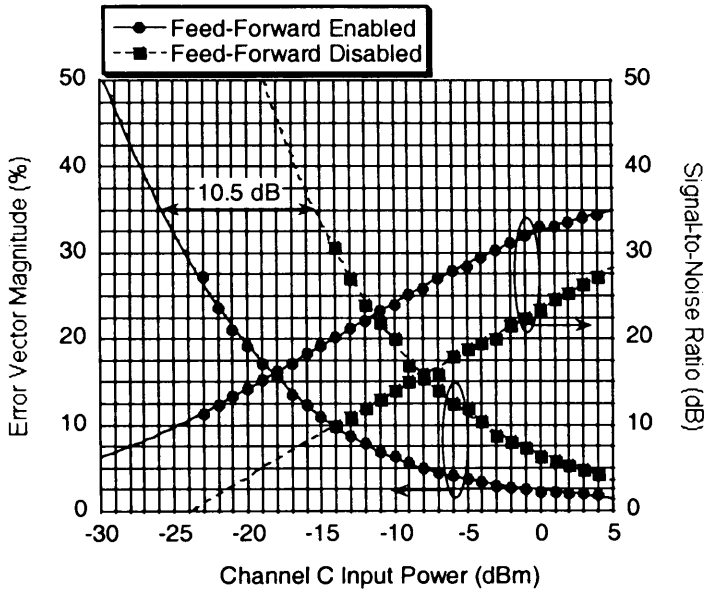

Figure 3.30 EVM and SNR vs. Channel C input power. Channel filter bandwidth: 20 MHz.

Spectral re-growth at 5.8 GHz

Data transmission was also carried out at 5.8 GHz for IEEE802.11a WLAN standard and IEEE802.16 Wimax standard. Two Rhode & Schwarz SMU200A VSGs were used to provide two channels, A and B, at 5.765 GHz and 5.785 GHz respectively and internally filtered with a root raised cosine function having a roll off factor of 0.5. The frequencies of the two Channels A and B follow the IEEE 802.11a standard channel allocation. The output power from the VSG for channel A was fixed at +12 dBm and Channel B input power was set to -23 dBm [21].

Before the measurements were taken feed-forward was optimised around 5.8 GHz operating frequency. The carrier cancellation loop and the distortion cancelling loop were optimised for maximum distortion cancellation according to the procedure described earlier. Figure 3.31 and Figure

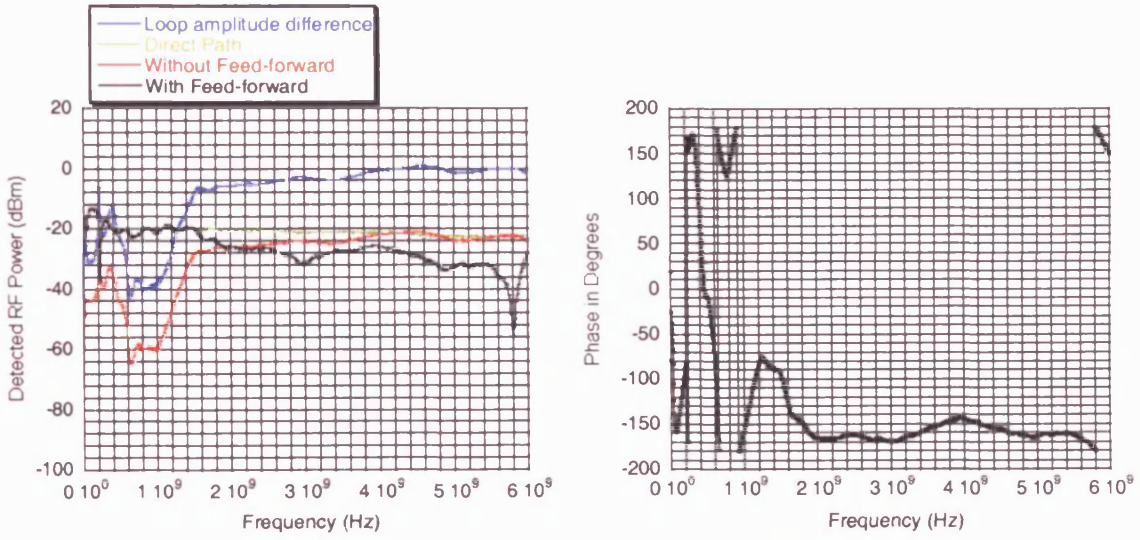

Figure 3.31 Carrier suppression loop at 5.8 GHz amplitude matching (left plot) and phase matching (right plot)

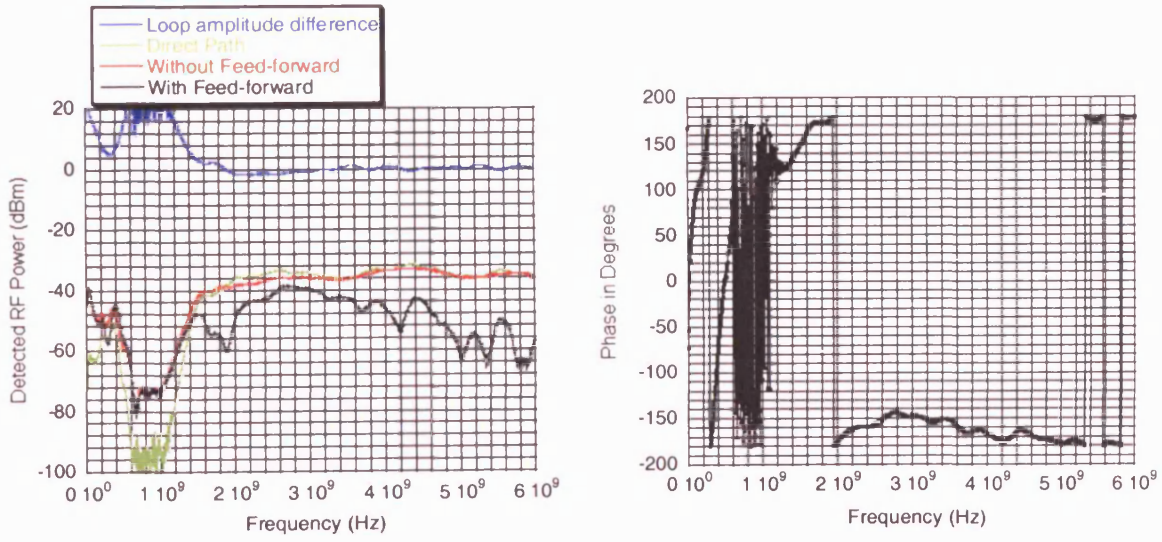

Figure 3.32 Distortion cancellation loop at 5.8 GHz amplitude matching (left plot) and phase matching (right plot)

3.32 show the response with a network analyser for the amplitude and phase matching response for the carrier cancellation loop at the output of the hybrid coupler and the distortion cancellation loop respectively. The RF spectra of the two 11 MSymb/s, 16 QAM channels were measured with the feed-forward disabled and enabled and are shown in Figure 3.33. With feed-forward enabled the spectral re-growth was suppressed by 20 dB allowing the spectrum of Channel B to be easily recovered.

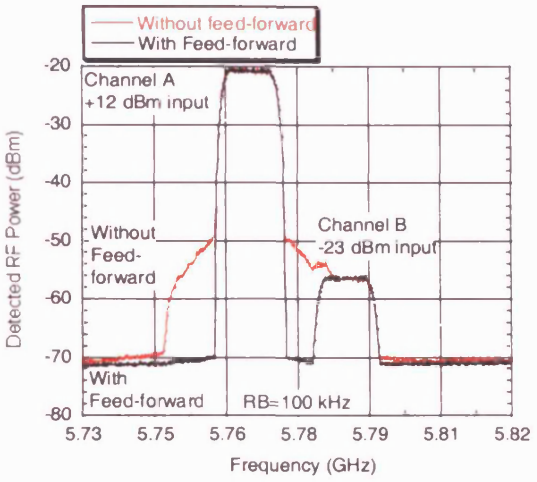

Figure 3.33 Detected RF spectrum with and without feed-forward at 5.8 GHz

A number of measurements were conducted using 16 QAM and 64 QAM. Eye-diagrams, constellation and EVM were measured using the VSA set to Channel B at a centre frequency of 5.785 GHz with a 20 MHz channel filter bandwidth and are shown in Figure 3.34 and Figure 3.35 with feed-forward enabled and disabled. Without feed-forward the quality of the measured eye-diagrams, constellation diagrams and EVM of the weaker channel B were severely affected by Channel A spectral re-growth. With feed-forward enabled, the eye-diagrams had wider opening and well defined constellations were observed. The EVM for Channel B was measured in the presence of Channel A, with input power fixed at +12 dBm. With feed-forward enabled the EVM improved from 24.9% to 9.3% for the 16 QAM and 19.8% to 5.2% for the 64 QAM signals. The modulated symbol rate from

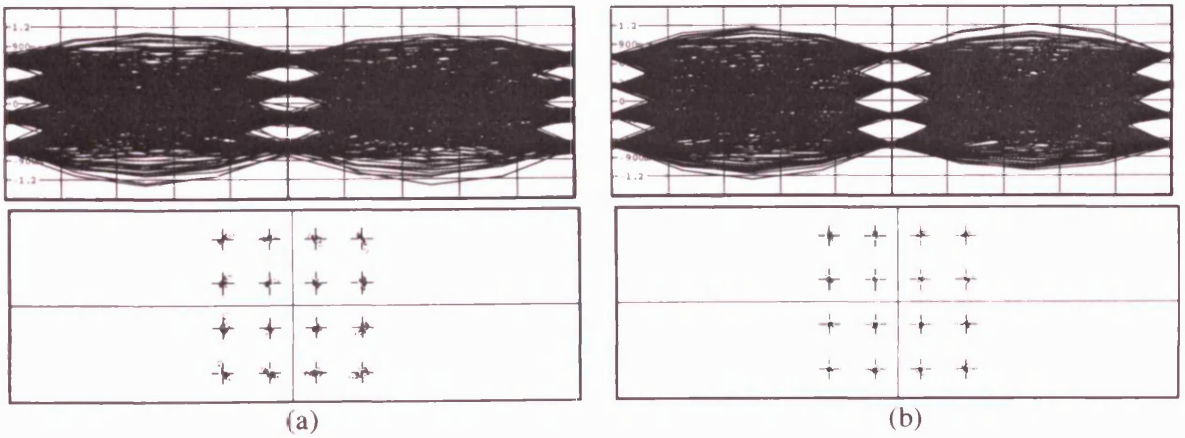

Figure 3.34 Detected Channel B eye and constellation diagrams for 16 QAM (a) without feed-forward (b) with feed-forward. EVM is 24.9% without feed-forward. EVM is 9.3% with feed-forward

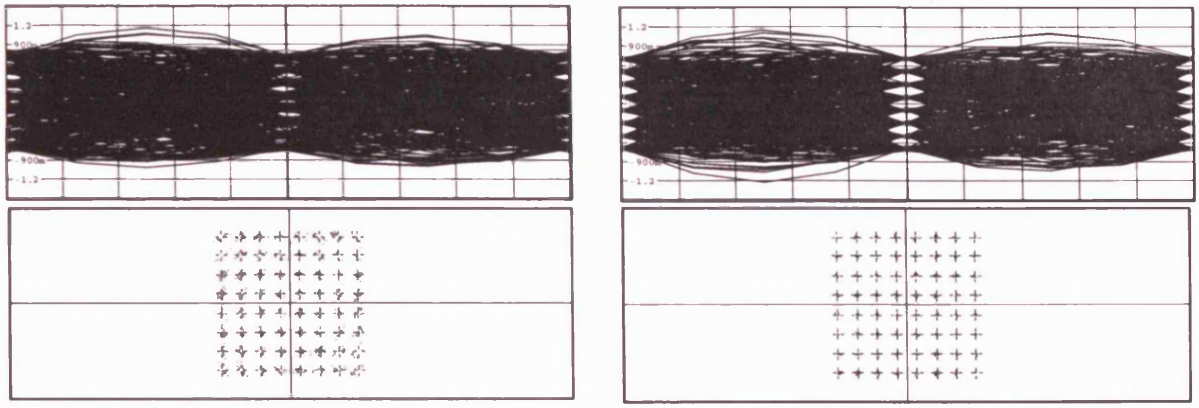

(a) (b)

Figure 3.35 Detected Channel B eye and constellation diagrams for 64 QAM (a) without feed-forward (b) with feed-forward. EVM is 19.8% without feed-forward. EVM is 9.3% with feed-forward.

the VSG was 11 MSymb/s. Since each 16 QAM symbol carries the information of 4 bits, the transmitted data rate is 44 Mb/s and with 64 QAM (6 bits) a data rate of 66 Mb/s is transmitted.

Finally the input powers of both Channel A and Channel B with 16 QAM signals were set equal to +10 dBm and the measured RF spectra are shown in Figure 3.36. With feed-forward enabled, the IMD was suppressed by 13 dB. Although feed-forward is able to provide a greater suppression for the IMD, this was limited by the available power from the signal source as can be seen in Figure 3.36. The output of the generator for Channel B had some residual distortion and this cannot be compensated with feed-forward. In such case feed-forward is unable to reduce these distortion products which are already at the input. From Figure 3.36 it can be observed that the feed-forward provides at least 10 dB suppression of third order IMD from 5.735 GHz to 5.810 GHz.

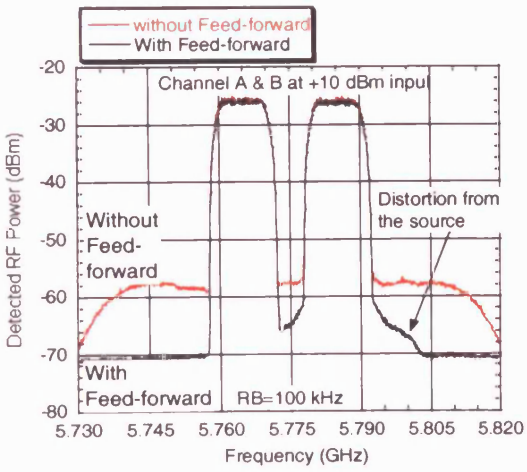

Figure 3.36 Detected RF spectra with feed-forward disabled (upper) and enabled (lower), both Channels A and B set at +10dBm.

3.7 Conclusion

In this chapter the operation of feed-forward system has been described in detail. Analysis of distortion reduction in feed-forward was presented. In particular, effects of amplitude and phase mismatch on distortion reduction are investigated. For accurate cancellation amplitude and phase must be closely matched. For example, a 40 dB cancellation requires a phase balance of 0.5° and an amplitude match better than 0.05 dB. It is clear that the higher the desired cancellation and wider the bandwidth the more difficult it is to meet the strict phase and amplitude requirements. It is found that the system performance is strongly affected by the cross coupling ratio of the optical couplers K_1 and K_2 and this involves a number of design tradeoffs.

An experimental setup of optical feed-forward system was built and the system evaluation is carried out to identify the criteria for optimum performance and component specifications. The operational bandwidth of feed-forward linearisation is limited to 500 MHz due to frequency dependent loss in the microwave cables. Further improvements involve employing optical components with minimum fibre pigtails, allowing a reduction in the length of microwave cables required for path matching. The tuning, testing and the experimental results are presented at 5.2 GHz to compensate noise and distortion in a low cost directly modulated 1550 nm uncooled DFB laser. This operating frequency is required for the IEEE802.11a standard and is also the highest reported to date for a feed-forward laser diode linearisation. The laser RIN has been reduced by 7 dB with simultaneous 26 dB suppression in the third order IMD. Reduction in both RIN and IMD has enhanced the SFDR by 15 dB to 107 dB (1Hz).

The linearisation scheme is demonstrated for the transmission of multi-channel broadband 11 Msymb/s QPSK modulated wireless channels centred around 2.4 GHz over 2.2 km SMF using an uncooled DFB laser. The spectral re-growth of the +13 dBm Channel A has been reduced by 9 dB resulting in a 5% reduction in the EVM of the neighbouring -23 dBm Channel B. Intermodulation distortion has also been suppressed by 10 dB when both channels A and B were set equal at +13 dBm.

For the first time feed-forward linearisation is used in the transmission of two high power and one low power 11 Msymb/s QPSK modulated signals centred around 2.4 GHz. The interchannel distortion from two high power channels has been suppressed by 11 dB, resulting in an EVM reduction from 31 % to 10 % and a SNR enhancement from 10 dB to 20 dB for a −14 dBm neighbouring Channel. An eye diagram could only be obtained with feed-forward enabled which demonstrates how effective this linearisation is in suppressing the interchannel distortion generated by a directly modulated DFB laser.

Laser non-linearity becomes worse with higher modulating frequency and demonstration centred around 5.8 GHz is carried out for the transmission of multi-channel broadband 11 MSymb/s, 16 QAM and 64 QAM wireless channels. These results suggest that feed-forward linearisation applied to directly modulated laser is an effective technique in obtaining the required system dynamic range and can make practical multi-channel wireless over fibre systems for wireless LAN applications.

References

[1] D. Hassin and R. Vahldieck, "Feed-forward linearisation of analogue modulated laser diodes–theoretical analysis and experimental verification", *IEEE Trans. Microwave Theory Tech.*, vol. 41, pp. 2376-2382, 1993.

[2] D. Hassin and R. Vahldieck, "Improved feed-forward linearisation of laser diodes-simulation and experimental results", *IEEE MTT-S Int. Microwave Symposium (IMS)*, pp. 727-730, 1990.

[3] L. S. Fock & R.S. Tucker, "Reduction of distortion in analogue modulated semiconductor lasers by feedforward compensation", *Electron. Lett.*, vol. 27, pp. 669-671, 1991.

[4] B. Buxton and R. Vahldieck, "Noise and intermodulation distortion reduction in an optical feed-forward transmitter", *IEEE MTT-S Int. Microwave Symposium (IMS)*, pp.1105-1108, 1994.

[5] L. S. Fock & R.S. Tucker, "Simultaneous reduction of intensity noise and distortion in semiconductor lasers by feed-forward compensation", *Electron. Lett.*, vol. 27, pp. 1297-1299, 1991.

[6] Peter Kenington, "High linearity RF amplifier design", Artech House INC, Norwood, MA, 2000.

[7] Nick Pothecary, "Feedforward linear power amplifiers", Artech House INC, Norwood, MA, 1999.

[8] L.S. Fock, A. Kwan and R.S. Tucker, "Reduction of semiconductor laser intensity noise by feedforward compensation: Experiment and Theory", *IEEE J. Lightwave Technol.*, vol. 10, pp. 1919-1925, 1992.

[9] Sang-Hyun. Park and Young-Wan. Choi, "Significant suppression of the third order intermodulation distortion in transmission system with optical feed-forward linearised tranmitter", *IEEE Photon. Technol. Lett.*, vol. 17, pp. 1280-1282, 2005.

[10] Joon-Jae Lee, Sang-Hyun Park and Young-Wan Choi, "Enhanced ACPR of W-CDMA signals in optical feedforward transmitter by optimisation", *IEEE Topical meeting on Microwave Photonics (MWP)*, 2005.

[11] A. K. Talwar, "Reduction of noise and distortion in amplifiers using adaptive cancellation", *IEEE Trans. on Microwave Theory and Techniques*, vol 42, pp. 1086-1087, 1994.

[12] G. Zhao, F. M. Ghannouchi, F. Beauregard and A. B. Kouki, "Digital implementations of adaptive feedforward amplifier linearization techniques", *IEEE MTT-S Int. Microwave Symposium (IMS)*, vol. 2, pp. 543-546, 1996.

[13] S. J. Grant, "A DSP controlled feed-forward amplifier lineariser", *Universal Personal Commun.*, vol.2, pp. 788-792, 1996.

[14] Y. Song, I. Oh, K. Seo, Y. Jeong & C. Kim, "Analog controlled adaptive feed-forward amplifier for IMT-2000 band", *Gallium Arsenide Application Symposium (GAAS)*, 2002.

[15] S. Kang, u. Park, k. Lee and S. Hong, "Adaptive feedforward amplifier using pilot signal", *International Conf. On Telecommunication (ICT)*, vol. 1, pp. 677-680, 2003.

[16] A. Megej and V. F. Fusco, "Low loss analogue phase shifter using varactor diodes", *Microwave and Optical Technology Lett.*, vol. 19, no 6. pp. 384-386 1998.

[17] W. T. Thornton and L. E. Larson, "An improved 5.7 GHz ISM band feedforward amplifier utilising vector modulators for phase and attenuation control", *Microwave Journal*, 1999.

[18] Analog Devices AD8341 RF vector modulator technical data.

[19] T. Ismail, C. P. Liu and A. J. Seeds, "Uncooled directly modulated high dynamic range source for IEEE802.11a wireless over fibre LAN applications", *Optical Fibre Communications (OFC)*, FE3, 2004.

[20] T. Ismail, C. P. Liu, J. E. Mitchell and A. J. Seeds, "Interchannel distortion suppression for broadband wireless over fibre transmission using feed-forward linearised DFB laser", *IEEE International Topical Meeting on Microwave Photonics (MWP)*, TE-2, pp. 229-232, 2004.

[21] T. Ismail, C. P. Liu, J. E. Mitchell and A. J. Seeds, "Feed-forward Linearised Uncooled DFB Laser in a Multi-Channel Broadband Wireless over Fibre Transmission at 5.8 GHz", *IEEE International Topical Meeting on Microwave Photonics (MWP)*, 2005.

Chapter 4

Wireless over Fibre Systems and Networks

The concept of wireless over fibre systems and signal transport schemes (RF, IF and Baseband over fibre) have been discussed in Chapter 1. In this chapter, potential millimetre-wave (mm-wave) wireless over fibre architectures are investigated. After an Introduction 4.1, a number of previously reported half and full duplex mm-wave over fibre systems for transport and distribution of broadband wireless signals are discussed in Section 4.2. Section 4.3 describes optical generation of the Local Oscillator (LO) signal for mm-wave frequency up/down conversion at the Base Station (BS). Network topologies such as star, star-tree, bus and ring are discussed in Section 4.4, together with their advantages and disadvantages. Detailed results are presented for signal transmission in a ring architecture including a link budget model. Key ideas are extended to investigate how wavelength division multiplexing (WDM) can be applied to reduce system complexity and cost. Link budget calculations together with simulation results are presented in Section 4.5 for the proposed mm-wave Gigabit/s system. A brief introduction to the use of Semiconductor Optical Amplifiers (SOA) in wireless over fibre systems is given in Section 4.6. Finally, Conclusions for this chapter are presented in Section 4.7.

4.1 Introduction

The demand for broadband wireless access, such as a huge data file downloading, real time video streaming and high definition TV signal transmission are increasing so that wireless transmission with 1 Gigabit/s (Gbit/s) and beyond data rate is attractive [1]. Instead of working in the congested 2-10 GHz range, interest is growing in the mm-wave frequency range (> 30 GHz) where large continuous frequency bands are available. By combining the existing high capacity of optical networks with wireless links at mm-wave frequencies higher data rates could be delivered to the end user. Due to higher propagation loss at these frequencies, large numbers of BSs are required and it is essential to design them to be as simple and cheap as possible.

Wireless over fibre is an attractive solution for the delivery of radio signals to a set of remote BSs. This offers the advantages of simple and economical remote BSs, centralised control of the radio signals, and a high level of transparency to the wireless modulation technique used [2]. To reduce the

BS equipment hardware, it is attractive to transport mm-wave signals directly over fibre in comparison to IF. However, transmitting signals at IF has the benefit that chromatic dispersion is greatly reduced and low bandwidth devices can be used. By incorporating WDM in the system it is possible to achieve full duplex operation on one fibre and allow different BSs to be fed by a common fibre. Such full duplex operation can be achieved using the ring architecture.

4.2 Review of Wireless over Fibre Transmission Experiments

A key issue in the implementation of a mm-wave over fibre system is the generation of the modulated optical carrier and many techniques have been proposed [3, 4]. Most techniques can be easily implemented in the downlink path, as the system cost and equipment can be shared among a large number of customers. In contrast, the realisation of the uplink path is more challenging since it is constrained by the cost of both the mobile unit and the BS. Requirement for high speed components in the BS such as the Mach-Zehnder Modulator (MZM) increase the complexity and the overall cost of the BS. Therefore it is essential to use a simple and low cost optical transmitter at the BS. A common architecture implemented has been distribution of the uplink signals at IF over fibre where the uplink mm-wave signals are first down-converted and then transported optically to the Central Station (CS) [5]. In this thesis IF over fibre techniques together with remote delivery of the mm-wave LO signal is investigated both for the uplink and downlink as a cost effective and simple distribution architecture [6]. For instance, low cost directly modulated uncooled Distributed Feedback (DFB) lasers can be used, whereas expensive external modulators are required when transmitting mm-wave signals. However, a high frequency photodiode is required to detect the optical LO and mm-wave mixers are required for frequency up/down conversion at the BS.

4.2.1 Millimetre-wave systems

To date, a number of techniques for the generation of mm wave modulated optical carriers for data transmission in a wireless over fibre system have been reported and demonstrated [7, 8, 9]. Many experiments have been conducted both for the uplink and downlink [10, 11, 12]. To overcome the severe limit in distance due to dispersion [13, 14] of double sideband mm-wave modulated signals Optical Single Sideband (OSSB) modulation using a single, dual electrode MZM has been proposed [15]. The modulator is biased at quadrature and the modulated mm-wave signal is applied to both electrodes with a $\pi/2$ phase shift between the two electrodes. The modulator produces only two spectral components which are tolerant to dispersion: an optical carrier and one sideband. Complete suppression of the other sideband can be theoretically achieved. A number of transmission experiments have been reported using this approach [8, 12]. Although this method requires the dual electrode MZM to be driven at mm-wave frequency, the conversion efficiency demonstrated is good. The main advantage of this OSSB technique is that the mm-wave generation and the modulation imposition are carried out in a single stage requiring a single, dual arm MZM. An OSSB signal may also be generated

by optically filtering (removing) one of the sidebands of a double sideband signal, however this is not very power efficient [16]. Smith *et al* [17] demonstrated a full duplex wireless system using electrical and optical SSB modulation for efficient broadband mm-wave signal transportation. A DFB laser provides a 1550 nm optical signal at the CS and is modulated by a dual electrode MZM operating as an optical SSB generator. The RF electrodes of the MZM are driven by a mm-wave carrier at 38 GHz with SSB BPSK modulation, which is generated using a Sub-Harmonically Pumped Image Reject Mixers (SHPIRM). All the mm-wave mixers used for frequency up/down conversions are sub-harmonically pumped with the LO at half the RF frequency, thereby reducing the cost of the drive electronics at both the CS and the customer unit. The author also suggested that frequency multipliers can be used instead of SHPIRM, however no results were presented. A data rate of 155 Mbit/s was obtained on the downlink using BSPK modulation. The use of an EDFA after the MZM improved the modulation depth at 38 GHz and increases the optical power in the single sideband. Wireless transmission was achieved over a 5 m path. Lim *et al* [8] carried out a similar experiment in which 155 Mbit/s and 622 Mbit/s data streams were delivered on the uplink (37.5 GHz) and the downlink (34.8 GHz) respectively over 20 km of single mode fibre (SMF) and a 2 m radio path. 60 GHz digital modulated radio signal transmission over 46 km standard fibre and optical distribution to remote antennas units serving a pico-radio cell has also been considered [18].

Shoji *et al* [19] demonstrated a mm-wave over fibre link for a point to point fixed multi-carrier wireless access system operating at 37 GHz. A 622 Mbits/s 64 QAM multi-carrier signal is imposed on a 1330 nm optical carrier by an external MZM and transmitted over a 10 km SMF with a BER<10^{-5}. The optical signal is photo-detected by a Uni-Travelling Carrier Photo-diode (UTC-PD). In this experiment, no air link was implemented. However, considering the free space transmission model, it was estimated that the 622 Mbit/s signal can be transmitted over a 2 km wireless path using directional antennas (36 dBi) with a 6 dB power margin. Kim *et al* [20] carried out experimental transmission of OFDM data over 25 km of SMF followed by a 2.6 m LOS wireless transmission at 60 GHz. In this experiment 155 Mbit/s 16 QAM OFDM data was generated and imposed on a 2.36 GHz carrier before being fed to a DFB laser diode. Frequency up/down conversion was performed using separate 57.2 GHz LO sources at the BS and CS. Wireless transmission of the 155 Mbit/s signals was achieved under LOS condition with a BER <10^{-6} and acceptable SNR (19-24 dB) at the receiver. System performance degrading factors (namely limited transmission distance) include intermodulation noise induced by self phase modulation and carrier amplitude suppression induced by linear dispersion. The performance of this system is mainly limited by the low 2.5 GHz modulation bandwidth of the DFB laser source. Also since the LO signal is generated by an independent electrical source at each BS this may not be feasible for a real system implementation, since the LO source need to be phase related to provide exact synchronisation amongst all BS. Kitayama *et al* [21] reported the implementation of a dual band compact BS and demonstrated error free transmission of 155 Mbit/s DPSK data at 59.60 GHz simultaneously with a 2.45 GHz tone on a 1552.52 nm optical carrier on the downlink over 2 km

of SMF followed by the equivalent of a 12m airlink. This compact BS prototype comprises a high speed photodiode, an Electro-absorption Modulator (EAM), dual-band power combiners and splitters, amplifiers, filters and separate antennas. Simultaneous transmission of baseband (2.5 Gbps), and mm-wave (155.52 Mbit/s DPSK at 59.6 GHz) signals by externally modulating a 1560 nm DFB laser with an EAM has already been experimentally demonstrated on the downlink [22]. A 60 GHz module for RF/optic conversion using an EAM has also been developed [23]. A full duplex system based on a high speed EAT [24] is proposed for transmission of broadband signals. A super-continuum multi wavelength light source has been used as a cost effective technique in a WDM system at the CS for the downlink [25].

Different methods have been proposed in order to solve the uplink problem. Many of them involve reusing the optical carrier from the downlink [26]. This wavelength reuse scheme eliminate the need for a separate light source at the BS by providing the optical carrier for uplink transmission, where the uplink optical signal is generated by recovering a portion of the optical carrier used in the downlink transmission [27]. Nevertheless the problem of high frequency signal transmission between the BS and the CS (the need for high speed components in the BS, dispersion caused fading) remain unsolved. A simple link configuration to reduce the number of high speed components at the BS was achieved by transmitting an unmodulated RF carrier from the CS to the BS where it is detected and used to down-convert the uplink data to an IF (it acts as a LO). In addition, the need for a light source at the BS is also omitted by reflecting part of the downlink optical carrier and modulating it, using the MZM, with the IF uplink data [28]. Although the reuse of optical carrier for the uplink offers the advantages of BS without any WDM sources, the power budget is affected restricting the transmission distance to less than 10 km without additional optical pre-amplification at the CS. Attygalle *et al* [29] proposed a technique to show how the transmission distance can be doubled by optimising the downlink and uplink modulation depths. The carrier extraction is accompanied by specially designed FBG with reflectivities between 95-99% that extracts majority of the power of the downlink carrier for uplink transmission.

When mm-wave frequency signals are imposed onto the optical carrier, sidebands are generated at spacing equal to the modulating mm-wave frequency away from the optical carrier. This causes the inter-channel spacing of a WDM feeder network for a mm-wave fibre radio system to rise. Wavelength interleaving was proposed to increase the spectral efficiency in the optical domain [30]. It is achieved by multiplexing the mm-wave modulated WDM signals with channel spacing smaller than the modulating mm-wave signal frequency. By applying this technique, channel separations of 50 or 25 GHz can be easily realised. A WDM optical interface has been demonstrated with the capacity of adding and dropping wavelength interleaved WDM channels spaced at 25 GHz and also enabling wavelength reuse, which eliminates the need for a light source at the BS. The WDM optical interface is realised using a multi-port optical circulator in conjunction with multi-notch Fibre Bragg Grating (FBG) filters [31].

The development of Gigabit wireless systems is also attracting a great deal of interest. In order to meet these demands, research has been carried out on faster wireless transmission links. For instance in 2004, wireless operators, Siemens [32] and NTT DoCoMo [33] independently achieved 1 Gbit/s real time wireless transmission using Multiple Input Multiple Output (MIMO) devices in combination with OFDM modulation scheme. Another way to increase the data rate is to use a free space optical link (FSO). It offers a number of potential advantages over similar radio systems, in particular the available bandwidth is much higher and also no operating license is needed. The FSO has already achieved 2.5 Gbit/s [34]; however, it has problems in terms of cost and size, since it requires a precise positioning to align the optical beam. An alternative is to use mm-wave transmission. Intensive research has been done to develop wireless links using the 60 GHz band [35, 36, 37] and 1.25 Gbit/s data transmission has been achieved [38]. A multi gigabit/s wireless links based on mm-wave photonic techniques is demonstrated in [39]. Ohno *et al* [40] applied photonic techniques to a wireless system and succeeded in 1 Gbit/s data transmission using a 40 GHz mm-wave system.

The applicability of >100 GHz mm-wave in wireless communication is investigated further in order to increase the data rate. Wireless data transmission at 2.5 Gbit/s was achieved with a high power 120 GHz photonic emitter using a UTC-PD that has a large bandwidth and high saturation level, to generate mm-wave signal with a power > 2 dBm at 120 GHz. A 10 Gbit/s data transmission over a 2.5 m wireless link was demonstrated by Hirata *et al* [41]. The link incorporates an active ML-LD and a MZM, which are rather expensive and require high power and high frequency drivers. Although data transmission achieved was very high the cost of the wireless link is of primary concern for commercial use. The same author also proposed a cost effective mm-wave photonic wireless link that uses a fabry-perot laser for mm-wave generation and demonstrated transmission of 1.25 Gbit/s [42]. A photonic transmitter that can transmit data at a rate up to 3 Gbit/s and also Gbit Ethernet signals is demonstrated [43]. Full duplex point-to-point mm-wave links in the 60 GHz and 80 GHz bands operating at 1.25 Gbit/s (Gigabit Ethernet) and up to 10 Gbit/s are now commercially available and deployed for outdoor bridging applications (Bridgewave, Gigabeam).

4.2.2 Optical frequency conversion

Although electrical frequency up/down conversion has been mainly considered so far frequency conversion can also be performed optically by exploiting the non-linearity effects of opto-electronic component, such as external modulators, EAM [44, 45, 46], MZM [47, 48, 49]. In this technique an optical source is modulated by an IF signal and harmonic up-conversion of the optical signal is realised via further modulation with an external modulator driven by an LO [48]. Photonic up-conversion approach based on using cascaded optical modulators is also studied [50].

Experiments have been carried out where optical down-conversion of 40 GHz signal to 3 GHz has been successfully demonstrated using an EAM [44]. A frequency up-converter incorporating cross absorption modulation in an EAM with its analog performance parameters such as phase noise and

SFDR were investigated [46]. Three 1 Gbit/s data streams were simultaneously up-converted to 20 GHz without serious power penalty or errors using a Lithium Niobate waveguide device [51]. An uplink system incorporating a 60 GHz photonic down-conversion technique is reported [52]. With this concept, neither a light source nor a mm-wave source is required at the BS since the mm-wave modulated pilot tone is fed from the CS. In the BS, a high speed mm-wave EAM and subsequent optical band pass filters are used for the photonic down-conversion. A comparison of different IF band modulation for electro-optical conversion is carried out together with data transmission experiments at 155 Mbit/s [53]. The electro-optical conversion techniques have the drawback of including significant conversion loss and sensitivity to the polarisation of optical signals [54]. The sensitivity to modulator bias voltage drift also needs to be considered [2]. Also, the modulator bandwidth can impose limitations on the frequency range for up/down conversion [55].

Frequency up-conversion can also be achieved using Cross Gain Modulation (XGM) in a Semiconductor Optical Amplifier (SOA). When optical IF and LO signals co-propagate through an SOA and are detected by a PD, frequency up-conversion is achieved with an SOA and square law photo-detection [56]. Optical IF signals modulate the SOA carrier density, which in turn modulates the optical LO signal. The conversion efficiency is proportional to the SOA optical gain and LO light intensity and can also vary depending on the optical IF and LO signal wavelengths because the optical gain in an SOA is wavelength dependent. Non-linear characteristics of the photonic SOA up converter under various conditions such as optical LO power and IF signal wavelengths [57] have been considered with SFDR measurements. It is found that the SFDR increases with the LO power.

Although, frequency up-conversion using XGM effect in an SOA having high conversion efficiency was demonstrated [55], it requires a high optical LO power to saturate the gain of an SOA. A method utilising the Cross Phase Modulation (XPM) effects in SOAs that requires a lower power than that using the XGM effect has been investigated [58]. This scheme shows good conversion efficiency with polarisation insensitivity [59]. Optical up-conversion using an SOA Mach-Zehnder Interferometer (MZI) has been reported [54] that provides conversion gain, immunity to polarisation and simultaneous up-conversion. Two 155 Mbit/s DPSK IF channels at 2.5 GHz were simultaneously up-converted to 22.5 GHz without serious crosstalk and errors taking advantage of the XPM effects of the SOA. The SOA-MZI is operated at the minimum transmission point for the second harmonic up-conversion. The results indicate that multi-channel WDM WoF signals can be simultaneously up-converted without serious crosstalk if the total optical IF power (or the number of WDM IF channels) is kept below the power level for the gain saturation of the SOAs.

A frequency up/down converter based on a single cascaded SOA, EAM configuration for bi-directional WoF system has been demonstrated in [60]. SOA XGM and photo-detection in EAM are used for frequency up-conversion and EAM non-linearity is used for frequency down-conversion. Both LO and IF are optically provided by the CS for the downlink for frequency conversion. The two modes

of the optical LO are cross gain modulated by optical IF signals. More recently, a 60 GHz WoF system has been demonstrated using this approach [61].

4.3 Local Oscillator Signal Generation

In the IF over fibre scheme, a LO signal is required at every BS for frequency up/down conversion. A separate electrical mm-wave LO source can be used and shared between the uplink and the downlink. For instance, a low phase noise dielectric resonator oscillator (DRO) can be used. The advantage of using a DRO is that the architecture is simplified, since there is no need to distribute the reference signal. However, the main problem is the stability of the device since variations in temperature will cause a shift in the output frequency. Also due to the high cost involved at mm-wave frequencies especially for a large number of BSs and the redundancy in equipment this is not a feasible solution.

The up/down conversion approach may initially appear to add complexity with the remote LO delivery. It may be possible to avoid this by incorporating low phase noise microwave monolithic integrated circuit (MMIC) oscillators. It is essential that the LO signal be spectrally pure (i.e. with a sufficiently low phase noise) since poor phase noise results in amplitude jitter in multi-level (e.g. QAM) modulation formats and reduces receiver performance and increases the BER [62, 63]. For example, 16 QAM modulation requires a SNR of about 20 dB for a BER of 10^{-5}. In a typical 40 MHz band, this corresponds to an average double sideband noise level lower than -99 dBc/Hz around the carrier [64]. More complex modulation formats require even purer signals. Despite the advancement in MMIC technologies for mm-wave systems, small and low cost MMIC LOs have yet to be produced with sufficiently low phase noise and therefore bulky and expensive oscillators would be required [65]. By locating a more expensive low phase noise optical LO source at the CS and remotely delivering its output to many BSs it is possible to distribute this expense amongst users.

A common LO signal can be optically generated at the CS and distributed on the downlink to all BSs to give exact frequency synchronisation for advanced modulation techniques. The remote delivery of the reference LO signal in combination with optical wavelength multiplexing techniques allow efficient sharing of the optical infrastructure with the data signals. The potential advantage of this single LO system include: simple receiver structure, system cost effectiveness, enhanced system reliability, minimised laser phase noise and drift as well as easy system expansion [66]. At the mobile station (MS), the LO is generated by means of a microwave oscillator or DRO. The spectral purity of the LO generated at the MS is less critical than that of the BS, since the MS can synchronise accurately with the BS. DROs are not suitable for generating LO at the BS as previously discussed, due to thermal drift. Depending on the frequency at which the LO needs to be transmitted to the BS several remote delivery schemes can apply.

The simplest approach is to transmit the LO signal at mm-wave frequencies over the optical link. Upon photo-detection at each BS, the LO is amplified before being split and fed to the up/down-converting mixers. However, this requires large bandwidth photo-diodes at the BS which are expensive

and show poor responsivity. An alternative is to consider transmission of the LO at IF rather than mm-wave frequency. At IF (<10 GHz), commercially available laser can be directly modulated. Upon detection, the LO signal at IF is amplified and then can be converted to mm-wave by one or several frequency multipliers before feeding to the mixers for frequency conversion [67]. This provides a cost effective solution since the need for the high bandwidth photo-diode is removed. However, generating a spectrally pure LO signal at mm-wave frequency when cascading several frequency multipliers is challenging.

Various optical mm-wave generation techniques are available and these can be categorised into systems using dual semiconductor laser sources, single laser sources and dual mode semiconductor laser sources [68, 69]. A comparative study is carried out in [70] highlighting issues such as cost and complexity for these techniques. A wide variety of optical heterodyne techniques can be used to generate a sufficiently narrow line width signal at mm-wave frequencies which is dispersion tolerant [62].

4.3.1 Optical heterodyne techniques

Heterodyne techniques have been investigated as a potential source for Wireless over System (WoF) systems by Simonis *et al* [71]. In this scheme two laser sources are operated so that their wavelengths differ by the required microwave or mm-wave frequency [72]. The resulting electrical beat term output from the photo-diode is then the mm-wave carrier frequency. An optical heterodyne LO source can be assumed to have two independent optical modes with optical angular frequency of $\omega 1$ and $\omega 2$. The electrical beat signal at the optical frequency difference $[\omega_2-\omega_1]$ of two optical modes can be produced.

This technique of heterodyning can produce high frequency (limited only by the photo-detector bandwidth) and high power microwave signals. The major drawback with this method is the complex circuitry and the requirement for the two optical signals to be phase correlated since the phase noise in the laser source directly translates into phase noise of the generated microwave signal. This requires the optical signals to be of very narrow linewidth or to be highly correlated leading to more complex solutions using Optical Injection Locking (OIL) and Optical Phase Lock Loop (OPLL) techniques.

In the OIL scheme [73], light from the master laser (ML) is injected into the slave laser (SL) to lock its frequency. OIL offer the advantage of using cheaper broad linewidth lasers to generate stable narrow linewidth signals and exhibits good phase noise suppression, but the disadvantage is that OIL has a small detuning range and hence the performance is limited [74].

In the OPLL technique [75], two optical sources are used to produce a beat signal at the desired LO frequency. If their optical phase are not synchronised or well correlated, the beat signal will have the linewidth as broad as the sum of the linewidths of two optical sources. To achieve narrow linewidth, the OPLL employs electrical feedback, where a sample of the optical power is tapped off and detected in a photodiode. The phase comparison between the photo-detected beat signal and the electrical reference oscillator is made using a microwave mixer as a phase detector [76]. The resulting

phase error signal is filtered with a loop filter and fed back to the SL to track phase fluctuations of the ML. Since the phase fluctuations of the ML are tracked by the SL, the detected beat signal exhibits good spectral purity. The OPLL technique has wide locking range and good tracking capabilities but the fundamental problem is the loop bandwidth and hence the phase noise reduction is limited by the practically achievable loop delay which can be challenging. For stable operation of the OPLL, wide loop bandwidth as well as short propagation loop delay is required. Optical feed-forward modulation technique achieves the same effect as the OPLL and overcomes the problem of loop delay minimisation but has strict requirements on delay matching. The phase noise on the generated beat signal is compensated by a feed-forward technique, which feeds the generated error signal forward to a MZM in one laser path [77].

To overcome the problems associated with OIL and OPLL, a technique which combines both to form an Optical Injection Phase Lock Loop (OIPLL) is used [79]. This method benefits from phase noise suppression from OIL and an extended locking range provided by the OPLL. Also the problem of short loop propagation delay becomes less important in OIPLL with the advantage that ordinary broad linewidth lasers can be used. The disadvantage of this technique is the level of complexity since both OIL and OPLL are combined.

In the OIPLL Figure 4.1, the ML is modulated at a sub-harmonic frequency of the desired mm-wave provided by the reference oscillator. Some of the light output from the ML is injected into the SL via an optical circulator. The optical circulator also ensures that no light is reflected back into the ML. The SL is tuned to lock onto the n^{th} harmonic sideband produced by the ML. The required mm-wave frequency is the offset between the two optical signals [80]. The optical output of the two lasers is then combined in an optical coupler and a sample is fed into the OPLL loop which is detected, amplified and then compared in a mixer. The output is filtered through a loop filter and passed to the SL. In this

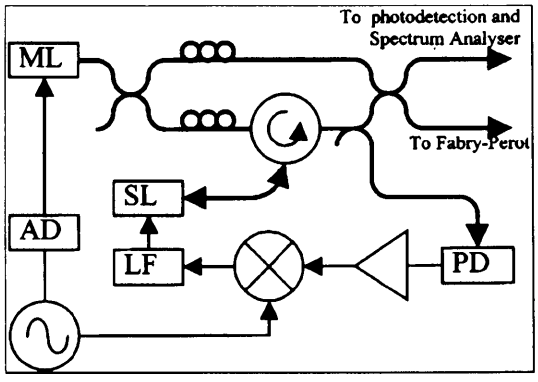

Figure 4.1 Experimental arrangement for the fiber based OIPLL system. ML: master laser, SL: slave laser, PD: photo-detector, LF: loop filter, AD: adjustable delay line. Thick line indicates the optical path [78]

way, both the OIL and OPLL are combined to produce OIPLL. Johansson *et al* demonstrated a 36 GHz 140 Mbit/s ASK modulated carrier transmitted through 65 km of fibre using an external optical modulator at the output of an OIPLL source [81, 82]. In 2002, a 36 GHz 68 Mbit/s DPSK signal

transmission over 65 km SMF without amplification and dispersion compensation with a BER of 10^{-9} was demonstrated [83]. Martinez *et al* [84] demonstrated transmission of 155 Mbit/s BPSK data at 40 GHz over a 2.2 km standard SMF using a harmonic generation technique to generate the mm-wave modulated signal. Other techniques such as double sideband suppressed carrier (DSB-SC) [85], and sideband injection locking [86] have also been reported.

Double Sideband-Suppressed Carrier (DSB-SC)

Using a MZM, two optical modes with the desired LO frequency separation can be obtained. Because the centre optical carrier is suppressed, it is called DSB-SC modulation. Since the two optical modes originate from the same source, their optical phase is correlated. Therefore, a low phase noise beat signal can be obtained after photo-detection without any feedback. This is also known as the frequency doubling technique and has the advantage that the modulator bandwidth is halved. However, an additional optical amplifier is required to increase the output power since the modulator should be biased at $V\pi$ for carrier suppression. A fourth harmonic generation technique using two MZ modulators connected in series has been investigated and a 42 GHz signal was generated from 10.5 GHz modulating input signal [87]. Generation of 76 GHz signal was demonstrated using MZ $LiNbO_3$ modulator equivalent to a fourth harmonic at the input frequency f_m, with a 19 GHz signal input [88].

Sideband Injection Locking

The sideband injection locking can also be used for optically generating mm-wave signals with low phase noise and experimental demonstrations have been reported [68]. In this scheme, the ML modulation frequency is a sub-harmonic of the desired beat frequency and this can significantly reduce the required bandwidth of the ML and the operating frequency for the RF source. Braun *et al.* have successfully generated mm-wave signals in the 60 GHz range [86]. The two SLs are injection locked to the 10^{th} modulation sidebands of a ML giving a frequency spacing of the desired mm-wave frequency. The operating principle of the sideband injection locking is that when a DFB laser acting as ML is directly RF modulated it produces multiple sidebands that have the frequency separation of the RF modulation frequency. Two of these sidebands having the required frequency separation are used to injection lock two separate DFB lasers acting as SL. The two injection locked SL are synchronised to each other since they are both locked to the same ML. When the output from the two SL beat in the PD, the desired mm-wave signal is generated with low phase noise. The drawback of this approach is that the SL should be carefully controlled with laser injection current and temperature in order to be locked to the desired sideband due to the narrow locking range. When the SLs are injection locked to a certain sideband, the presence of adjacent sidebands that are not involved in injection locking can influence the spectral characteristics of the resulting beat signals and the overall system performance.

In this thesis a 40 GHz LO source is optically generated at the CS by injection locking two slave DFB lasers to two sidebands of an externally modulated master tunable laser. Two optical components

are generated separated by the mm-wave frequency at the CS and then detected by the square law action of the photo-detector at the BS. Figure 1 illustrates the experimental arrangement of this 40 GHz LO source [89]. The received mm-wave LO signal at the BS is used for frequency up/down conversion of the data. The conversion loss of the mixer varies with the LO power. Therefore the received optical LO power at the BS is critical for optimum operation of the mixers and the overall system performance. Maximising the received LO power is essential for efficient operation of the mm-wave mixers.

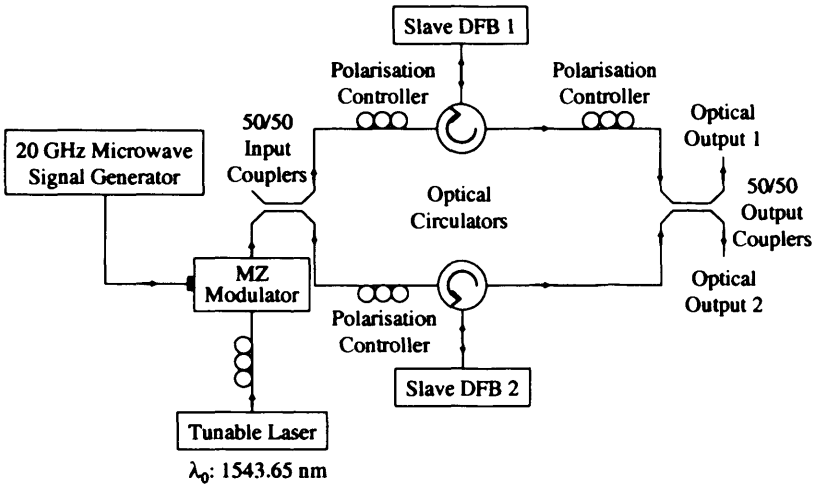

Figure 4.2 Proposed 40 GHz LO source

4.4 System Architectures

Millimetre-wave over fibre systems have been proposed for both broadcast [90] and dedicated access applications [91, 92]. In Broadcast applications such as with cable television same information is distributed to multiple users. In contrast, dedicated access applications require bi-directional information transfer for individual access. The difference between the distribution and individual broadband access type is important because different network architectures can perform well for one type, but poorly for the other. The optical generation and transportation of mm-wave signals can be categorised into several distinct techniques which determine the architecture of the wireless over fibre system. In this section a number of different architectures for distribution of broadband wireless signals are investigated.

4.4.1 Star

One of the common architectures used is the star topology shown in Figure 4.3 where the CS feeds remotely located BSs via an independent optical link [93]. Since each BS is fed individually the architecture has the advantage that it is highly reliable and easy to maintain and upgrade [94]. This is because if one link is destroyed or does not function, all the other links still operate and remain unaffected. Similarly, individual links can be upgraded as required, without affecting the operation of others. Another characteristic of the star network is that since each arm is dedicated to a specific BS, each arm can be treated as independent point to point link. However, the star architecture is the most expensive in terms of infrastructure cost since a large amount of fibre need to be installed.

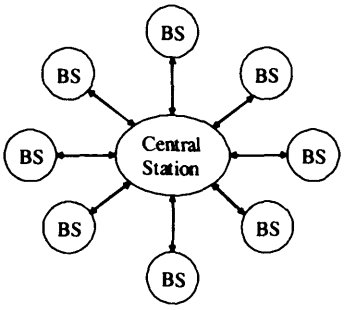

Figure 4.3 Star network architecture

The optical delivery of the LO is easier in the star network, given that no optical add and drop, filters, are required from the output of the CS to the BS. The LO is optically amplified at the CS using an optical amplifier before splitting [95]. Since no multiplexing technique is required (unless hybrid star-tree architecture is employed) excellent channel isolation (no crosstalk impairment) is obtained. Multiplexing may be used within each BS to save on the number of fibres required for the downlink carrying data signal and LO and the uplink as shown in Figure 4.4. At the BS a circulator can be used to direct the uplink and the downlink signals in conjunction with add/drop filters to separate the LO

and data signals. Another implementation is to use a Mux/Demux at the BS to separate the downlink and the uplink signals. This leads to fewer components and simplifies the BS.

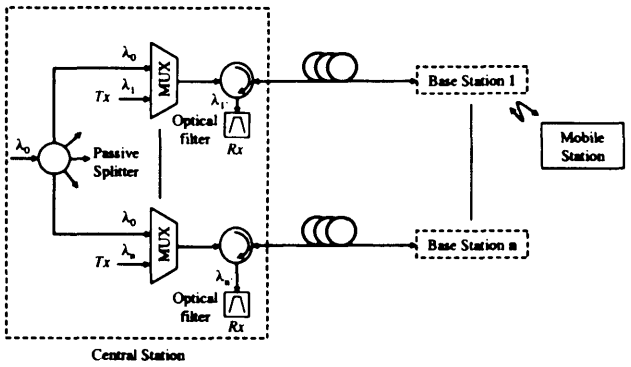

Figure 4.4 Wireless over fibre star network architecture

A number of hybrid architectures have been proposed that combine performance, ease of maintenance, and upgrade advantages of the star network with lower installation costs [96]. These architectures include double star arrangements and hybrid star-tree shown in Figure 4.5. In the double star topology, passive splitting is implemented at each remote node (RN) using a passive splitter/combiner as shown in Figure 4.5a. In this configuration, fibre is shared between the downlink and the uplink between the CS and the RN. This approach has already been reported and benefits from reduced fibre count [97]. On the downlink, signals are split and sent to all BSs. An optical amplifier is used prior to splitting of the LO signal to compensate for the loss at the coupler. On the uplink, various BSs send their signal on a separate wavelength, each of these wavelengths is then combined at the RN. Thus, on the uplink, the splitter is used as a combiner. With passive splitting the RN is greatly simplified and is less expensive in comparison to the de-multiplexing approach. While a practical implementation of a passive double star incorporating a splitter at each of the remote node has been described by Kumozaki [98] the major disadvantage highlighted for passive splitting is that added complexity is required at each BS for network synchronisation so that the CS could distinguish between the radio signals from different BSs sharing a single wavelength.

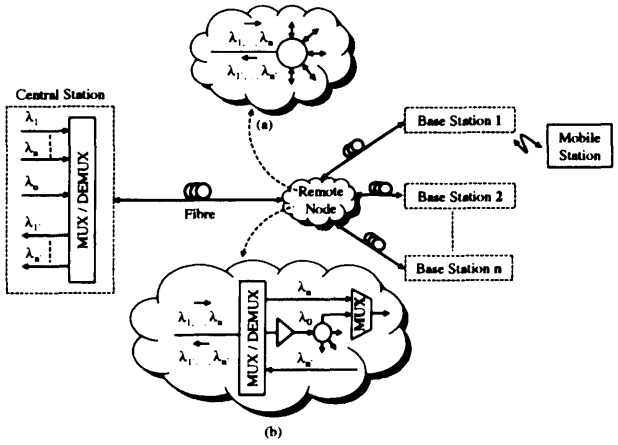

Figure 4.5 Implementation of a (a) double star architecture using passive splitting and (b) Star-Tree architecture using Mux-Demux

4.4.2 Star-Tree

A similar but alternate approach to a passive splitter at the end of the arm of the star is to de-multiplex the signals into individual wavelengths for providing broadband wireless access as shown in Figure 4.5b. The technique consists of a hybrid star-tree architecture connecting the remote BS to the CS by incorporating WDM of the optical signal and was proposed by Smith *et al* [99]. In this architecture (Figure 4.5b) each arm of the star transports multiplexed signals from the CS to a RN using a WDM link. The RN is connected to a set of BSs. The fibre link from the CS form the star part of the architecture, while the tree part is at the RNs with each branch feeding different BSs [26]. A RN de-multiplexes the input signal and distributes various wavelengths to the corresponding BSs [100]. At each RN, the LO (λ_0) along with other signal wavelengths (λ_1, λ_n) are de-multiplexed and then sent to its dedicated BS, rather than sending all wavelengths to every BS and then filtering the undesired wavelengths. When de-multiplexing at the RN on the downlink, the LO is extracted along with the other channels by a Demux and is amplified before being split into 7 equal arms for distribution to the BSs. Each of these arms is then recombined with one of the extracted channel by means of a 3 channel MUX before being sent on a separate fibre to a specific BS. On the uplink, various BS send their individual signal on a separate wavelength. Each of these wavelength is then combined at the RN and transported towards the CS where they are de-multiplexed. A different wavelength is used for uplink and downlink transmission. Optical circulators together with add/drop filters may also be considered as an alternative solution to multiplexers and de-multiplexers. However, the circulators have a limited bandwidth (typically 120 nm) which restricts the maximum number of wavelengths to be delivered to the RN. Various network layouts are discussed for the star-tree architecture in [101]. SCM can be used with optical wavelength to provide multiple radio frequencies with each radio cell.

One advantage of incorporating WDM is the possibility of sharing the downlink optical wavelength sources between different stars from the same CS, re-using the WDM optical spectrum in each separate star. These multiplexing schemes allow sharing of equipment at the CS and therefore enable simple networks to be implemented. This includes the sharing of a low phase noise mm-wave LO. In addition, WDM of the signals within the fibre can simplify the network architecture and improve deployment, since it enables full duplex operation on a single fibre and also allow different BSs to be fed by a common fibre. Also the optical links between the CS and the BSs are almost identical (unlike a ring network), providing a relatively uniform signal quality to each BS.

A full duplex star-tree network using WDM and SCM has been demonstrated at 35-40 GHz using 155 Mbit/s BPSK channels on the downlink and 58 Mbit/s BPSK channel on the uplink [99]. The proposed WDM/SCM star-tree architecture is capable of providing individual customer access to broadband services and a maximum of 7 BSs should be connected to the RN which may not be enough. However, if CWDM technology is used as a cost effective solution, then it is not possible to use more than 18 channels (assuming that each channel operate on a separate wavelength). For each

BS, two wavelengths are required for the uplink and downlink. In this scenario, a maximum of 7 BS thus correspond to 14 channels, and an additional one for the LO (which makes a total of 15 channels). It was shown in [97] that clustered star-tree architecture can provide wider coverage as compared to the simple star-tree architecture. The capacity limitations of WDM WoF system incorporating both wavelength interleaving and OSSB with carrier modulation for a star-tree architecture is analysed in [102]. The analysis shows that an amplified link is essential for transmission distance of greater then 10 km. If optical amplifiers are used then the placement of these is crucial to the overall network capacity and performance. Hence, there is a trade off between cost and network capacity. The results are summarised in Table 4.1.

Network Topology	Reach Length (km)	Span-out Length (km)	Remote Node Loss (dB)	Comments
Passive	< 9	1	< 6	Limited by optical link efficiency
Pre-amplification	< 39	5	13	Limited by EDFA saturations
Post amplification	50	5	13	Active remote node required
Pre- and post amplification	50	5	13	Needs > 2.5 dB gain at post amplifier

Table 4.1 Summary of the network dimensions achievable for the star-tree architecture with different network topologies [102]

The limitation of the network for a large scale also need to be considered and it is necessary to examine the potential crosstalk effects in this architecture. The most important characteristic is that the effects of incoherent homodyne crosstalk within optical components are not present in this architecture, since the Mux/Demux functions do not involve multiple signals at the same wavelength. This advantage has been achieved at a cost when compared to the ring architecture. This cost arises since the downlink and uplink wavelengths are constrained to be different in order to allow the downlink and uplink signals to share the same star fibre. Therefore if N wavelengths are available, the maximum number of BSs that can be serviced by a single star arm is N/2. For the ring network, if there are N wavelengths available then N BSs can theoretically be served. A technique that could minimise linear crosstalk is to modulate adjacent channels on orthogonal polarisation states as demonstrated by Kitayama [103]. In the star-tree architecture, this could produce a dramatic improvement in linear crosstalk behaviour, since most crosstalk arises from wavelengths close to the required wavelength. Such a scheme allows more wavelengths to be closely spaced in a dense WDM architecture and therefore allow more BSs to be serviced by a single fibre.

4.4.3 Bus

A bus network has been proposed as an alternative to a star network [95] and can be considered as a variant of a ring architecture in which the end of the fibre is not connected back to the CS, as shown in Figure 4.6. Two kinds of bus architectures have been considered: the single bus where a downlink fibre

links the CS to all BSs, with an Optical Add Drop Multiplexer (OADM) at each node dropping the required wavelength to a particular BS. A separate fibre is used in the uplink, with the BS adding a wavelength to the fibre linking all BSs to the CS (i.e. BSs receive signal from the top half of the bus and transmit from the bottom half). The other type is the double bus, where BS transmits and receives on both arms. A BS uses the top bus to send signals to its right and the bottom bus to send signals to its left. The double bus requires two transmitters and receivers at each station while the single bus requires only one of each per station [95]. However, the double bus can support a larger number of stations than

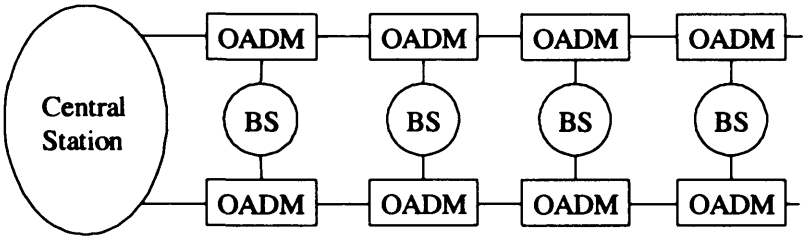

Figure 4.6 Wireless over fibre system incorporating bus architecture

the single bus because a transmission has to go through fewer taps before reaching its destination. The longest link in the single bus is from the CS to the last BS, with equal uplink/downlink distances unlike in the ring architecture. The bus architecture offers the advantage of low installation cost, compared with the star network due to reduction in the number of fibre links to the CS. However, the disadvantage is that it is difficult to achieve the same signal quality for each BS or customer. This is because the received signal is a function of the transmission distance and the number of nodes passed. The signal quality is thus dependent on the size of the network and the position of the RNs. Hence, the signal received by the BS at the far end of the bus network experiences maximum loss.

A bus network which overcomes the signal quality issues in a WoF network was proposed by Regan *et al* [104]. The author incorporated a module that detects the optical signal, and then splits the electrical signal. One portion of the RF signal from the splitter is directed to the BS, while the other portion is directed to another laser source for further transmission through the network. The major disadvantages with this technique are the complexity of the BSs and the difficulty and unnecessary expense required to extend this concept to incorporate WDM techniques. Also the requirement for linear lasers with increased channels needs to be considered. This is because the wavelengths must be individually detected and transmitted at every node.

To overcome this scaling problem, WDM techniques can be incorporated so that one fibre can transport signals for multiple BSs by feeding each BS with a unique wavelength. Kojucharow *et al* [105] proposed a WDM bus network in which FBGs are used at each node to drop wavelengths to each BS in the downlink. A separate fibre was used in the uplink to add the same wavelength back into the uplink fibre using a second FBG. Paolella *et al* [106] implemented a system demonstration of a WDM bus network using four wavelengths in both downlink and uplink directions. A single wavelength is dropped at each BS, with the same wavelength being added to the separate uplink fibre. A 30 GHz

mm-wave wireless over fibre system with DWDM channel spacing of 12.5 GHz bus architecture has been demonstrated by Zhang *et al* [107]. Examples of bus networks demonstrate the functionality of such a type of network for a WoF system but do not discuss system constraints.

4.4.4 Ring

In the ring configuration, Figure 4.7 wavelengths are multiplexed at the CS using WDM and then sent around the ring [26, 108]. The ring connects N BSs via a single unidirectional fibre path. OADMs are located around the ring to add/drop individual wavelength to the particular BS. Either the same or a different wavelength can be added back into the ring in the uplink direction. The main difference between the ring and the bus network is the fibre layout, which form a loop for a ring network, terminating at the CS. The advantage of the ring is low installation cost compared with the star network due to reduction in the number of fibre links to the CS. However, the disadvantage is that a large number of optical components are required for add/drop. Also since the CS to BS link distance is unequal, it is difficult to guarantee the same signal quality to each BS or mobile user. This is because in the ring network, the received signal quality is a function of the transmission distance and the number of nodes the signal pass through. For example, the downlink channel for the last BS of the ring will experience maximum loss and generally be worse than those channels for the first BS. The signal quality is thus dependent on the size of the network and the position of the RNs. Another important issue with the ring architecture is the complexity in upgrading the network to include new BS. To achieve this it is necessary to interrupt a number of other BS fed by the ring.

Ring networks are deployed extensively in metropolitan and longer haul networks due to their greater reliability while traditional access networks use a star architecture as this minimises the optical component cost. For short distance applications (picocells), the ring topology may not be considered effective due to high cost and increased complexity. A ring architecture can also include multiple rings from a single CS. This makes it possible to share downlink WDM sources between independent primary rings. A fibre ring connected to the CS forms a primary ring, while secondary rings can be created at RNs with multiple wavelength ADMs. Each of the BSs fed from the CS via the primary ring

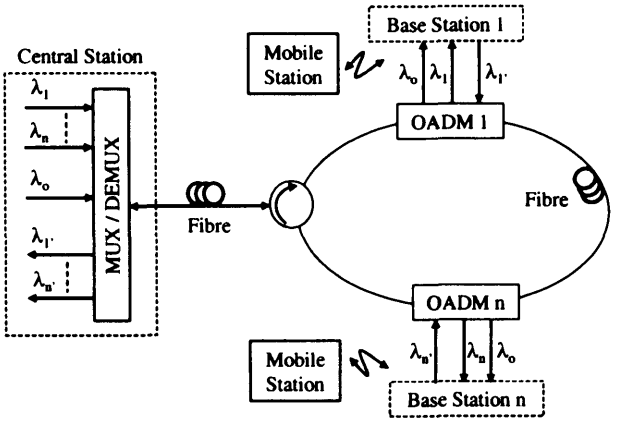

Figure 4.7. Wireless over fibre system incorporating a ring architecture

have their own unique WDM wavelength, which is used for both the downlink and uplink directions (i.e. the total number of WDM channels is equal to the number of BSs fed via a primary ring).

Haner *et al* [109] demonstrated a ring architecture with OADM used to direct the downlink and uplink information to the corresponding BSs. An alternative approach to the add/drop multiplexer is using optical filters based on Fibre Bragg Gratings (FBGs) at the receiver BS. The optical filter can be used for selecting a channel in the system [110]. A WDM ring was implemented by Heinzelmann *et al* [111]. Each OADM comprised two FBGs and two optical circulators. While each BS was allocated a single wavelength, different wavelengths were used for the downlink and the uplink. Interestingly the authors used an EAT at the BS, which detected the downlink wavelength and simultaneously modulated the unmodulated wavelength originating from the CS for the uplink [112]. This configuration simplified the BS architecture since all optical sources were at the CS, although it requires an extra FBG at each OADM. An additional benefit of using different wavelengths is that in-band crosstalk is eliminated. OADM with multiple phase shifted FBG for a mm-wave WoF system are demonstrated in [113]. Lim *et al* [102] proposed a wavelength interleaving method that increases the spectral efficiency of a mm-wave WoF network. The ring network topology is identical to that in Figure 4.7 with an OADM dropping a wavelength to each BS, with the same wavelength being added back into the ring in the uplink direction. The spectral interleaving technique requires a specially designed OADM. A single ring node demonstrated the feasibility of the technique. A power penalty of less than 0.5 dB was caused by the adjacent out of band wavelengths. A mm-wave WDM system incorporating 25 GHz channel spacing in a ring network is demonstrated [114]. The capacity limitations of a WDM ring incorporating wavelength interleaving where each BS drives a sectorised antenna interface is investigated [30]. The placements of EDFA were considered at various points along the ring [102].

The advance in WDM networks has introduced a demand for wavelength selective OADM to separate/route different wavelength channels. A WDM optical add/drop extracts one or more wavelengths from a fibre (drop function) and re-inserts these wavelengths (add function), a very important function in WDM ring as well as point-to-point links. They can be used at different points along the optical link to insert/remove or route selected channels increasing the network flexibility. This feature is particularly important in metropolitan WDM light wave services where offices or sites can be connected by different add/drop channels. There are two main types of OADM that can be used in WDM optical networks, fixed OADM that are used to drop or add data signals on dedicated WDM channels, or reconfigurable OADMs that use control electrical signals to alter the selected channel routing through the optical network. Reconfigurable devices perform add/drop on single, a group of or all wavelengths whilst the reminder pass straight through the device. The main feature of the reconfigurable OADM is to provide flexibility in re-routing optical data, bypassing faulty connections, allowing minimal service disruption and the ability to adapt or upgrade the network.

Bidirectional wavelength add-drop multiplexers using multi-port optical circulators and FBG have been proposed and experimentally demonstrated [115]. A bi-directional node for a WDM ring network is demonstrated [116, 117] and the performance of these add/drop multiplexers is not degraded by backscattering light. Ring networks with bi-directional WDM add/drop multiplexers having built in EDFAs have been analysed in [118]. All WDM channels can be added or dropped independently in each direction. The bi-directional properties of the ring minimises the number of pass through nodes before reaching the destination, thus improving the network efficiency. However, such bi-directional networks rely on the realisation of bi-directional add/drop multiplexers and bi-directional optical amplifiers.

Two desired features of OADM are low insertion loss and low crosstalk between adjacent channels [119]. The two main parameters related to the isolation of channels in an add-drop multiplexers are the through port isolation of a dropped channel and the drop port isolation of through channels. These two parameters represent the sources of the inter-channel crosstalk for the devices.

It is also important to consider the reliability, survivability and the complexity of upgrading the network. In particular, where part of a ring network requires maintenance or a node fails, then this can affect the complete network [120]. A key feature of the ring networks in general is their ability to provide increased reliability if a second fibre is used, allowing a loop protection scheme to be used in case of link or node failure. A number of dual fibre architectures have been proposed to provide protection in such circumstances [121]. In the dual fibre ring network, N nodes are interconnected with two counter directional fibre rings [122]. A broad band DWDM/SCM fibre wireless access network based on two level bi-directional path protected ring architecture is experimentally demonstrated [120]. In this architecture, the CS connects many RN via a dual fibre ring. Each RN cascades many wireless access points and can serve many customer units wirelessly. The CS is equipped with two sets of devices: one for normal operation and the other for standby. A RN includes a protection unit (i.e. 95/5 coupler and controller), bidirectional wavelength add/drop multiplexers. Experimental results demonstrated fault restoration in the ring and the architecture can perform self healing function under link failure. The network can automatically recover the fibre failure by monitoring the received optical signals. The CS can restore a set of standby devices and then reconfigure the ring network into two separate rings.

To estimate the scalability of the ring network, it is important to calculate the maximum size of the ring limited by the insertion loss of cascaded OADM. The addition of an extra OADM introduces insertion loss in the ring network. The key for successful operation of a ring network is to employ OADMs with low insertion loss and high crosstalk rejection. While these additional loss terms can be compensated for via the use of EDFAs, the different distances between the CS and the various OADMs result in different signal quality at each BS due to unequal CS to BS fibre length. It is possible to have a transmitter scheme where the power levels at the CS and uplink BS sources vary for each channel so

that the signal quality at each BS is at a constant optimum level. However, this also affects the dynamic range limitations for the link.

4.4.5 WDM and Crosstalk in wireless over fibre networks

The need to transmit greater amount of information, coupled with the need for low cost has led to the increasing importance of WDM systems [123]. This involves multiplexing multiple wavelengths and transporting them on a single fibre. In WoF networks, each BS can be assigned a single wavelength. This means that each BS can have access to the full bandwidth available on each wavelength, allowing wireless users to have access to more bandwidth. WDM offers many benefits and allows sharing of the optical infrastructure between multiple wavelengths (optical amplifiers, fibre) reducing the overall cost of the network. In addition, WDM allows a single CS to serve (simultaneously) a number of BSs, which simplifies the network architecture. Equipment can be shared at the CS, which enables better utilisation of network resources and reduces the complexity of network management [124]. Future demands can be met by designing the network for more wavelengths and adding the appropriate equipment as demand increases. There has been extensive investigation into the use of WDM for access networks [125]. In particular, incorporation of WDM technologies into star, double star, ring and bus architectures has been examined [126, 127]. Dense WDM (DWDM) systems include guard bands between optical carriers to allow for laser frequency drift. The ITU has set a 100 GHz (0.8 nm) as the standard channel separation, but this has been reduced to 50 GHz (0.4 nm) and further to 25 GHz (0.2 nm) [114] and 12.5 GHz (0.1 nm) [107]. Making the channel spacing narrower is an alternative to higher per-channel data rate.

Compared to DWDM, Coarse WDM (CWDM) allows cost savings by using uncooled laser diodes [128]. With the temperature control free approach the peltier cooler is eliminated leading to a compact and cost effective solution. The ITU has defined 18 wavelength channels for CWDM currently specified with nominal wavelengths ranging from 1270 nm to 1610 nm (in accordance with the ITU-T.694.2 CWDM grid) with 20 nm standard for channel spacing. Although the number of channels that can be used with CDWM is smaller than with DWDM, CDWM does not require narrow optical filters, cooled optical sources, or control techniques due to the wider channel spacing. CWDM filters and add/drop modules are also cheaper than DWDM ones. Therefore, CDWM is preferred for cost effectiveness.

A WDM network requires wavelength selective optical components that can multiplex or demultiplex channels or OADMs that can drop or add channels [129]. Such components are imperfect and usually do not have perfect isolation between wavelength channels and can not fully remove unwanted channels. Although optical components can reject adjacent wavelength channels by 30 dB or more, some residual signals will still be present. An important consideration that arises is the potential impact of optical crosstalk due to these imperfect optical components. Crosstalk is the action of power transfer between channels i.e. leakage from other optical signals on a detected signal. Optical crosstalk

in WDM optical networks can degrade the received signal quality, increasing the BER and affecting the signal quality and network performance. This must be taken into account when designing a network, so that the levels and power penalties are acceptable. The additional power required at the receiver to counteract the effects of crosstalk, such that the BER is kept constant, is known as the power penalty. Optical crosstalk is one of several sources of degradations in the link. Other sources of signal degradation include amplified spontaneous emission (ASE) noise due to optical amplifiers, fibre chromatic dispersion, fibre non-linearities etc. The impact of optical crosstalk in a WoF system incorporating WDM has been investigated [130, 131].

The impact of optical crosstalk depends on the modulation scheme used to transmit data. The data can either be sent at baseband or at an intermediate or radio frequency via sub-carrier modulation. The nature of the optical modulation scheme has implications for the design of the CS and the BS and potentially for optical crosstalk. A comparison of crosstalk penalty in WDM networks for externally and directly modulated lasers has been carried out [132]. In order to characterise the crosstalk effects in digital baseband transmission systems (physically), BER measurements have been performed [133]. The effect of optical crosstalk arising in mm-wave WoF network was investigated by Moura *et al* [134]. Mitchell *et al* [135] investigated the case of an optical carrier modulated with a quadrature amplitude modulated (QAM) sub-carrier. BER curves are presented and QAM is shown to suffer more crosstalk compared to standard modulation. The authors identify the fact that crosstalk affects both the amplitude and the phase of the QAM signal. Crosstalk in a metro scale ring network with passive optical add/drop has been reported by Feuer *et al* [136] and reduction in crosstalk is achieved by the isolated 2 stage add/drop multiplexers.

The optical crosstalk can be divided into two broad categories depending on whether the crosstalk channel is at different wavelength to the signal or at the same wavelength (out of band and in band crosstalk, respectively). First, the crosstalk terms that are carried on wavelengths different from the wanted signal wavelength are defined as linear crosstalk. This type of crosstalk does not severely impair network performance as it is at a different wavelength as the desired signal. These crosstalk terms can be removed by careful selection of optical filters [137] and therefore the crosstalk level do not necessarily accumulate over multiple nodes. The second type of crosstalk term is that which induces unwanted terms within the frequency band of the required signal (i.e. when the crosstalk signal is at the same wavelength as the desired signal). This is referred to as in band crosstalk or as interferometric noise or homodyne crosstalk [138]. With such crosstalk, it is not possible to remove the unwanted signals and the crosstalk level therefore accumulates over multiple nodes. It is much more detrimental to the signal as optical mixing of the optical fields upon photo-detection creates mixing terms that further degrade the signal compared to the out of band case [139]. Furthermore, since it is at the same wavelength as the signal it cannot be filtered. Typically this type of crosstalk arises from any point in the network where two signals at the same nominal wavelength are present for example, at MUX and DEMUX combinations [140]. Unwanted optical reflections induced at splices and

connectors can also give rise to interferometric noise and the effects of these reflections have been examined in [141].

4.5 Gigabit System Performance

In this section a specific architecture is analysed: the proposed low cost mm-wave Gigabit system (Figure 4.8). Link budget calculation is carried out for verification of the system performance together with simulation using Optsim. In brief the operation of the system is as follows. The LO and the IF signals are generated at the CS in the downlink and transmitted over fibre to the BS where frequency up-conversion takes place of the IF before the signals are radiated to the customer units. In the uplink mm-wave signals are radiated from the customer unit to the BS where it is down-converted to IF to modulate (directly) an uncooled DFB laser, the output of which is transported to the CS. The selection of the modulation scheme determines system bandwidth, sensitivity and complexity. Differential Phase Shift Keying (DPSK) is used, so that the receiver does not require a carrier synchronisation circuit and is easy to implement. A detailed system description is given in Chapter 5.

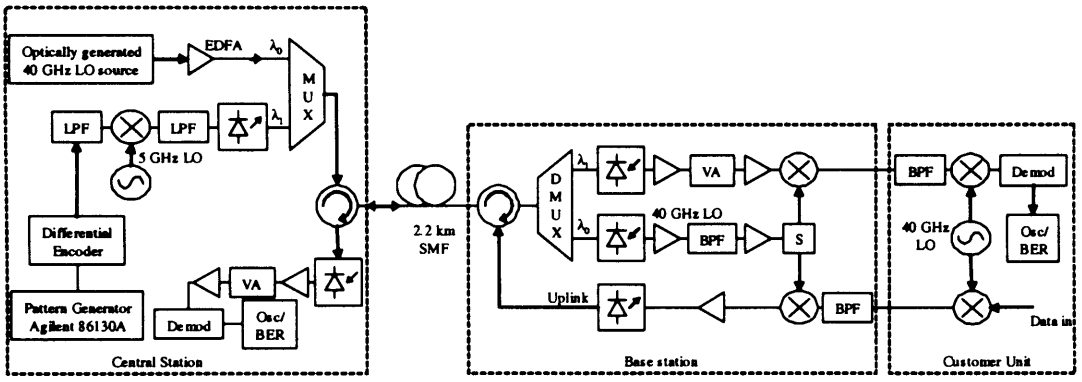

Figure 4.8. Full diagram for the mm-wave Gigabit wireless over fibre system (S=Splitter for LO)

Remote delivery of LO

The LO power at the input of each mixer used experimentally (Miteq TB0440LW1) at the BS should range between 10-15 dBm. A schematic for the LO delivered to the BS is shown in Figure 4.9. If the electrical LO power for the mixers is fixed to 12 dBm, then the minimum optical LO power required at

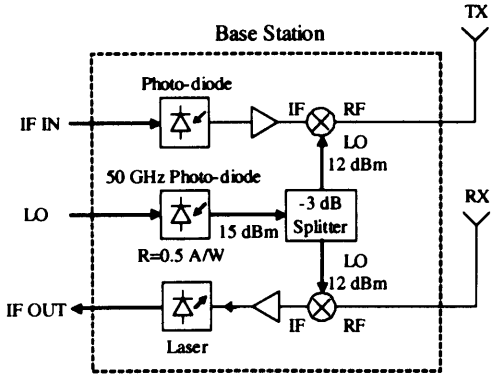

Figure 4.9 LO delivery at the BS for frequency up/down conversion

the photo-detector input can be determined. The 50 GHz photodiode (u^2t) has a responsivity of approximately 0.5 A/W. Assuming that the photo-detected current is delivered to a 50 Ohm resistor (R_L), then the received optical power at the photo-diode (Loss due to connectors are neglected) can be calculated as:

$$P_{opt} = \frac{1}{\Re}\sqrt{\frac{P_L}{R_L}} \tag{4.1}$$

P_L Electrical power delivered to the load resistor

R_L Load resistance (50 Ohm)

$\Re$ Photodiode responsivity (0.5 A/W)

Thus, the optical power required at the input of the photodiode is P_{opt} = 0.050 W (17 dBm). This power is too high to be transmitted and fibre non-linearity effects cannot be ignored. As a result, amplification is required either electrically or optically. An RF amplifier is required following the photodiode for boosting the LO signal prior to splitting. Using a 35 dB electrical gain the power required at the output of the photodiode is -20 dBm. The optical power at the input of the photodiode is therefore P_{opt} = 0.89 mW (-0.50 dBm). The output power of the SpaceK amplifier (SLKa-35-4 35) is 15 dBm, which is 2 dB below the gain compression output power of 17 dBm (maximum gain is 35 dB with a noise figure of 4 dB from manufacturer's specification). The advantage of this approach is that it is less expensive than using an optical amplifier. An alternative is to use an optical amplifier to boost the LO signal before detection. However, it is more expensive since an optical filter is required to limit the noise detected at the photodiode. Although using an electrical or optical amplifier will satisfy the LO requirement for one BS, sufficiently large gain is desired to allow sharing of the LO amongst many users using both electrical and optical amplifiers.

Ring Network

The ring network discussed in Section 4.4.4 is experimentally demonstrated in Chapter 5. The OADM employed in the ring architecture shown in Figure 4.7 is constructed using low cost coarse wavelength division multiplexing (CWDM) filters having a bandwidth of 13 nm from the centre wavelength. Each

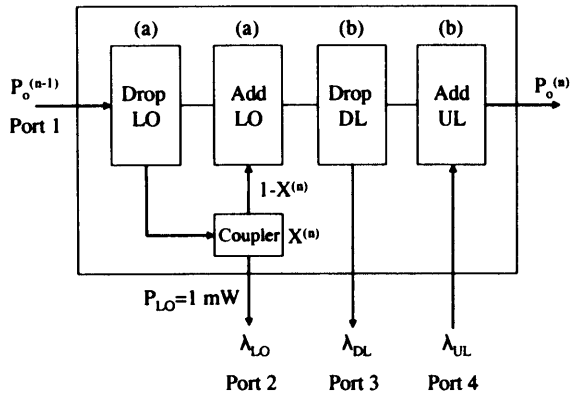

Figure 4.10. Schematic diagram of an OADM used in the ring architecture

OADM consists of an LO drop filter, an optical coupler to couple the desired amount of LO signal for the particular BS, an add filter to route the LO signal back into the ring network, a drop filter for the downlink IF signals and an add filter for the uplink IF signals. The schematic for the OADM is presented in Figure 4.10. It should be noted that the last BS in the ring will only have a drop LO filter.
Each OADM can be considered as a 4 port module
Port 1 input - all wavelengths to the device
Port 2 output - drop LO signal wavelength
Port 3 output - drop signal wavelength (downlink)
Port 4 input - add signal wavelength (uplink)
Assuming that the add/drop filters each have an insertion loss of 0.5 dB and considering the maximum optical LO power that can be transmitted down the fibre then the number of BSs that can be supported by the LO are calculated. The LO filters in the OADM are labelled as (a) and IF filters as (b). λ_1 is the downlink signal and λ_1' is the uplink signal for BS1.

LO Distribution

P_{LO} is the optical LO power required at the output port of each BS (1 mW or 0 dBm)
$P_o^{(n-1)}$ is the optical LO power at the input to the BS or the optical power from the previous BS
$X^{(n)}$ is the coupling ratio of the coupler i.e. the % LO power coupled to the BS
$1-X^{(n)}$ is the remaining LO power fed back into the ring network
n is the n^{th} BS number
$P_o^{(n)}$ is the LO output power at the n^{th} BS
N is the total number of BS
a is the insertion loss of LO add/drop modules (-0.5 dB)
b is the insertion loss of IF wavelength add/drop modules (-0.5 dB)

The coupling ratio for the LO coupler for each BS can be calculated as:

$$P_{LO} = P_o^{(n-1)} 10^{\frac{a}{10}} X^{(n)} = 1mW \tag{4.2}$$

$$X^{(n)} = \frac{P_{LO}}{P_0^{(n-1)} 10^{\frac{a}{10}}} \tag{4.3}$$

Equation (4.3) represents the coupling ratio for the LO coupler for each BS in the ring. The LO power at a particular BS can be determined as follows:

$$P_o^{(n)} = P_o^{(n-1)} \times 10^{\left(\frac{2a+2b}{10}\right)} \times \left(1 - X^{(n)}\right) \tag{4.4}$$

$$P_o^{(n)} = P_o^{(n-1)} \times 10^{\left(\frac{2a+2b}{10}\right)} \times \left(1 - \frac{P_{LO}}{P_O^{(n-1)} \times 10^{\frac{a}{10}}}\right) \tag{4.5}$$

$$P_o^{(n)} = P_o^{(n-1)} \times 10^{\left(\frac{2a+2b}{10}\right)} - 10^{\left(\frac{a+2b}{10}\right)} P_{LO} \tag{4.6}$$

The LO power dropped at the n^{th} BS can be expressed in term of that of the previous one and can be calculated by:

$$P_o^{(n)} = \alpha P_o^{(n-1)} + \beta \tag{4.7}$$

Where $\alpha = 10^{\left(\frac{a+b}{5}\right)}$ and $\beta = -P_{LO} 10^{\left(\frac{a+2b}{10}\right)}$

From this a more generalised formula can be derived:

$P_o^{(1)} = \alpha P_o + \beta$

$P_o^{(2)} = \alpha P_o^1 + \beta$

$P_o^{(3)} = \alpha P_o^2 + \beta$

$P_o^{(4)} = \alpha P_o^3 + \beta$

which can also be related to the total input LO power by

$$P_o^{(n)} = \alpha^n P_o + \sum_{\kappa=0}^{n-1} \alpha^\kappa \beta \tag{4.8}$$

The LO power at each BS output can be calculated with the following parameters.

Parameters
A= -0.5 dB and B=-0.5 dB

P_{LO}=1 mW (0 dBm)

P_0= 16.98 mW (12.3 dBm) input power to the ring

LO output power at a particular BS
BS1=10.0 mW (10 dBm)

BS2=5.64 mW (7.5 dBm)

BS3=2.85 mW (4.5 dBm)

BS4=1.09 mW (0.37 dBm)

BS5= 0 mW

The LO power fed to the ring at the circulator i.e. at the input to the first BS (12.3 dBm) is beyond the limit fixed at 10 dBm. Furthermore, the insertion loss of the circulator and the attenuation due to propagation through fibre (although this would be small due to short fibre length) between each BS has not been taken into account. With input LO power of 12.3 dBm 5 BSs can be supported without optical amplification in the ring. With lower insertion loss of the add/drop filters or using an optical amplifier in the ring then the number of BSs supported by the ring can be further increased.

IF signal distribution in the ring

Considering first the downlink. At a given base station (BS_n):

Channel n (λ_n) is dropped from the ring at BS_n (downlink) with optical power P_n

Total number of base stations is N

On the downlink, the highest attenuation occurs on λ_N which must reach the last BS on the ring (BS_N) within an acceptable power level.

λ_1 will experience attenuation of (2a+b) i.e. due to LO add/drop filter and the IF drop filter at BS1

λ_2 will experience attenuation of (2a+2b) and (2a+b) i.e. due to BS1 and BS2

λ_n will experience attenuation of (2a+2b) + (2a+2b) + (2a+2b) upto (n-1) + (2a+b)

where n=N no of BS in the ring

The last BS in the ring does not have a optical LO add filter and is (a+b), but a more general term of (2a+b) can be used to derive the expression for the no of BSs that can be supported. For all values,

$$N = \left(10^{\frac{2a+2b}{10}}\right)^{(n-1)} + \left(10^{\frac{2a+b}{10}}\right) \tag{4.9}$$

The amount of attenuation experienced in the downlink is

$$P_n = P_n^{(0)}\left[\left(10^{\frac{2a+2b}{10}}\right)^{(n-1)} \times \left(10^{\frac{2a+b}{10}}\right)\right] \tag{4.10}$$

where P_n is the power at a particular BS and $P_n^{(0)}$ is the optical input power to the ring.

$$P_n = P_n^{(0)}\left[\left(10^{\frac{a}{5}} \times 10^{\frac{b}{5}}\right)^{(n-1)} \times 10^{\frac{2a}{10}} \times 10^{\frac{b}{10}}\right] \tag{4.11}$$

If $A = 10^{\frac{a}{10}}$ and $B = 10^{\frac{b}{10}}$ then

$$P_n = P_n^{(0)}\left[\left(A^2B^2\right)^{(n-1)} \times A^2B\right] \tag{4.12}$$

when n=N then the IF optical power after N BS is:

$$P_N = P_N^{(0)}\left[\left(A^2B^2\right)^{(N-1)} \times A^2B\right] \tag{4.13}$$

The number of BSs supported for IF is

$$N = \left(\frac{\ln\left(\frac{P_N}{P_N^{(0)}A^2B}\right)}{\ln\left(A^2B^2\right)}\right) + 1 \tag{4.14}$$

Considering P_N (receiver sensitivity)=10μW (–20 dBm) and $P_N^{(0)} = 1.26 \times 10^{-3} W$ (1 dBm) then N<10.75 i.e. maximum number of BSs along the ring is 10 limited by downlink IF signal. If the receiver sensitivity is lower i.e. –30 dBm then more BSs can be fed. If the output power of the DFB laser is increased or optical amplifiers are used in the network, then the maximum number of BSs can

be significantly increased. Willner *et al* [142] observed that an optically amplified WDM ring can accommodate 25 nodes when incorporating an EDFA and a channel dropping filter in each node.

Uplink

On the uplink, the highest attenuation occurs on λ_1' which is added at BS1, and must travel through all BSs before reaching the CS with sufficient optical power. Channel n' (λ_n') is added to the ring at BS_n (uplink) with optical power P_n'

$$P_{CS}\lambda_1' = P\lambda_1'\left(10^{\frac{b}{10}} \times \left(10^{\frac{2a+2b}{10}}\right)^{(n-1)}\right) \tag{4.15}$$

assuming that the last BS in the ring is the same but in reality the last BS would have only 1 LO drop filter and also when the signal is added at the last BS then it does not experience much loss.

$$P_n' = P_n^{(0)}\left[B \times \left(A^2B^2\right)^{(n-1)}\right] \tag{4.16}$$

for n=N

$$P_N' = P_N^{(0)}\left[B \times \left(A^2B^2\right)^{(N-1)}\right] \tag{4.17}$$

$$N = \frac{\ln\left(\frac{P_N'}{P_N^{(0)}B}\right)}{\ln\left(A^2B^2\right)} + 1 \tag{4.18}$$

Considering that P_N=10 μW (-20 dBm) and $P_N^{(0)} = 1.26 \times 10^{-3} W$ (1 dBm) then N<11.25 i.e. the maximum number of BSs along the ring is 11 limited by uplink IF signal.

In the ring configuration CWDM directly modulated uncooled DFB lasers are suitable for low cost implementation. IF CWDM technology is considered for a cost effective solution, then no more than 18 wavelength channels can be used (assuming that each channel operates on a separate wavelength, 20nm spaced, between 1270-1610nm).

4.5.1 Link analysis

Figure 4.11 show the link configuration under investigation along with the corresponding devices and their parameters. Most of the devices used are commercially available. An Excel spreadsheet was created for link budget calculations for the downlink and the uplink.

Link gain

The gain of the optical link is first calculated. The available gain G is defined as the ratio between the RF power generated in the load resistance (P_{out}) and the RF power available at the source for delivery to the laser (P_{in}) [143]. The gain in a directly modulated optical link (G) is:

$$G = \frac{P_{out}}{P_{in}} \tag{4.19}$$

Assuming the source and load impedance is 50 ohms ($Z_{in}=Z_{out}$) then the gain is:

$$G = \left(\frac{\eta_L \Re}{L_{opt}}\right)^2$$
$$G(dB) = 20Log(\eta_L \Re) - 2 \times L_{opt} \tag{4.20}$$

η_L is the laser modulation sensitivity, $\Re$ is the photodiode responsivity and L_{opt} is the loss in the fibre. The total optical loss in the fibre (due to Mux-Demux, 2.2 km fibre and optical circulator) is L_{opt} = 3.8 dB for downlink and 2 dB for uplink (since the loss of Mux-Demux is excluded). With an average optical power of 2 dBm from the laser, and accounting for these losses, the link gain, noise figure and

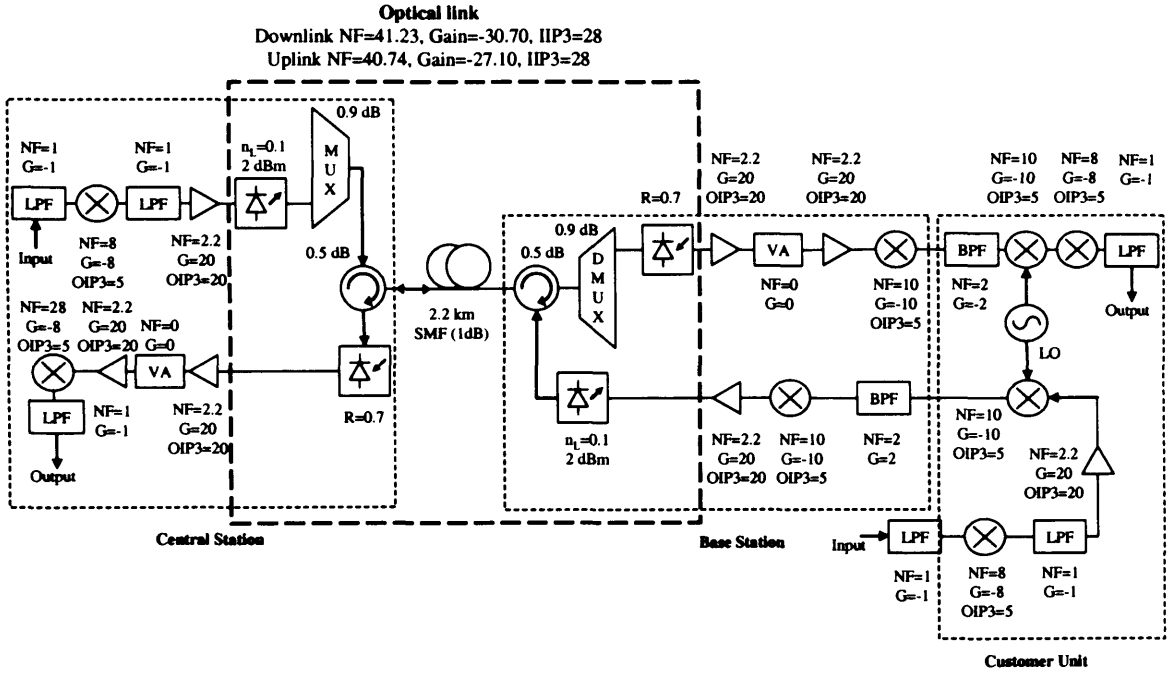

Figure 4.11. Gigabit system downlink & uplink with component specifications (Gain and noise figures are in dB)

SFDR can be calculated. The noise power spectral densities at the link output due to thermal noise (n_{th}), shot noise (n_{sh}) and laser relative intensity noise (n_{RIN}) are given by:

$$n_{th} = kT = \left(1.38 \times 10^{-23}\right)290 = 4 \times 10^{-21}(W/Hz) = -174(dBm/Hz)$$
$$n_{sh} = 2qI_{PD}R_L = 2\left(1.6 \times 10^{-19}\right)50 \times I_{PD} = \left(1.6 \times 10^{-17}\right)I_{PD} \tag{4.21}$$
$$n_{RIN} = RIN \times R_L \times I_{PD}^2 = \left(3.16 \times 10^{-15}\right)50 \times I_{PD}^2$$

k=Boltzman's constant, T=Temperature, q=electronic charge, I_{PD}=PD current, R_L=Load resistance

Downlink Optical Path

Laser slope efficiency	0.1	W/A		
Laser RIN	-145	dB/Hz		
Mean laser output power	2	dBm (opt)		
Laser input IP3	28	dBm (elec)		
PIN responsivity	0.7	A/W		
Total fibre loss	3.8	dB (opt)		
Mean received optical power	**-1.8**	dBm (opt)		
Mean photocurrent	**4.6E-04**	A		
Output thermal noise	**4E-21**	W/Hz	**-174**	dBm/Hz
Output shot noise	**7.4E-21**	W/Hz	**-171.3**	dBm/Hz
Output RIN noise	**3.4E-20**	W/Hz	**-164.7**	dBm/Hz
Total output noise	**4.5E-20**	W/Hz	**-163.4**	dBm/Hz
RF gain	**-30.7**	dB (elec)		
RF noise figure	**41.2**	dB (elec)		
SFDR	**107.2**	dB (elec)		

Uplink Optical Path

Laser slope efficiency	0.1	W/A		
Laser RIN	-145	dB/Hz		
Mean laser output power	2	dBm (opt)		
Laser input IP3	28	dBm (elec)		
PIN responsivity	0.7	A/W		
Total fibre loss	2	dB (opt)		
Mean received optical power	**0**	dBm (opt)		
Mean photocurrent	**7.0E-04**	A		
Output thermal noise	**4E-21**	W/Hz	**-174**	dBm/Hz
Output shot noise	**1.1E-20**	W/Hz	**-169.5**	dBm/Hz
Output RIN noise	**7.8E-20**	W/Hz	**-161.1**	dBm/Hz
Total output noise	**9.3E-20**	W/Hz	**-160.3**	dBm/Hz
RF gain	**-27.1**	dB (elec)		
RF noise figure	**40.7**	dB (elec)		
SFDR	**107.5**	dB (elec)		

It can be noted that the laser RIN usually dominates over shot and thermal noises.

Noise Figure (NF) and Equivalent Input Noise (EIN)

The NF in decibel [144] is a measure of the reduction in SNR between the input and the output of the link and can be expressed as [145]:

$$NF = 10\log\left(\frac{N_{out}}{kTG}\right) \tag{4.22}$$

Adding all the noise contributions and using equation (4.22) a NF of 41.2 dB (downlink) and 40.7 dB (uplink) is obtained. The output noise power can be related to the input of the link where it is referred to as the equivalent input noise (EIN), defined as:

$$EIN = \frac{N_{out}}{G} \tag{4.23}$$

The EIN then becomes -132.8 dBm/Hz (downlink) and -133.2 dBm/Hz (uplink).

Spurious Free Dynamic Range (SFDR)

After the link gain and NF have been obtained, the SFDR can be calculated. The relationship of the SFDR ($dB.Hz^{2/3}$) is given by:

$$SFDR = \frac{2}{3}[IIP3 - NF + kT] \tag{4.24}$$

where the input third order intercept (IIP3) is in dBm, NF is the noise figure in dB and kT=-174 dBm/Hz. IIP3 is the point where the fundamental and third order intermodulation (IMD) intersect. The SFDR can be improved by improving the NF or the IIP3. Linearisation results in improvement in IMD, and hence IIIP3. SFDR will ideally improve one third as fast as the IMD products, i.e. a 3 dB improvement in IMD results in a 1 dB improvement in SFDR [146]. Using equation (4.24) the SFDR is calculated to be 107.2 $dB.Hz^{2/3}$ (downlink) and 107.5 $dB.Hz^{2/3}$ (uplink).

Overall Calculation of Noise Factor and IIP3

Using the gain value, IIP3 and the noise factor for the optical link then the overall system performance can be evaluated. The total noise factor (F_{Total}) for a complete system can be determined by:

$$F_{Total} = F_1 + \frac{F_2 - 1}{G_1} + \frac{F_3 - 1}{G_1 G_2} + \frac{F_4 - 1}{G_1 G_2 G_3} \cdots \tag{4.25}$$

It can be seen that the first stage is fundamental and has a large impact on the overall system noise factor. The overall IIP3 and OIP3 of a system can be calculated as:

$$IIP3_{Total} = -10\log\left(\log^{-1}\left(\frac{-IP3_1}{10}\right) + \log^{-1}\left(\frac{G_1 - IP3_2}{10}\right) + \log^{-1}\left(\frac{G_1 + G_2 - IP3_3}{10}\right) + \cdots\right) \tag{4.26}$$

$$\frac{1}{OIP3_{Total}} = \frac{1}{OIP3_3 G_2 G_3} + \frac{1}{OIP3_2 G_3} + \frac{1}{OIP3_3} \tag{4.27}$$

The relationship between the IIP3 and the OIP3 is given by:

$$IIP3 = OIP3 - Gain \tag{4.28}$$

Using these equations calculation can be performed for various parameters for the complete system. The results for the overall system are calculated with AppCad (application designed by Agilent) and are given in Figure 4.12 for downlink with SNR of 19.29 dB and in Figure 4.13 for uplink with a SNR of 18.01 dB.

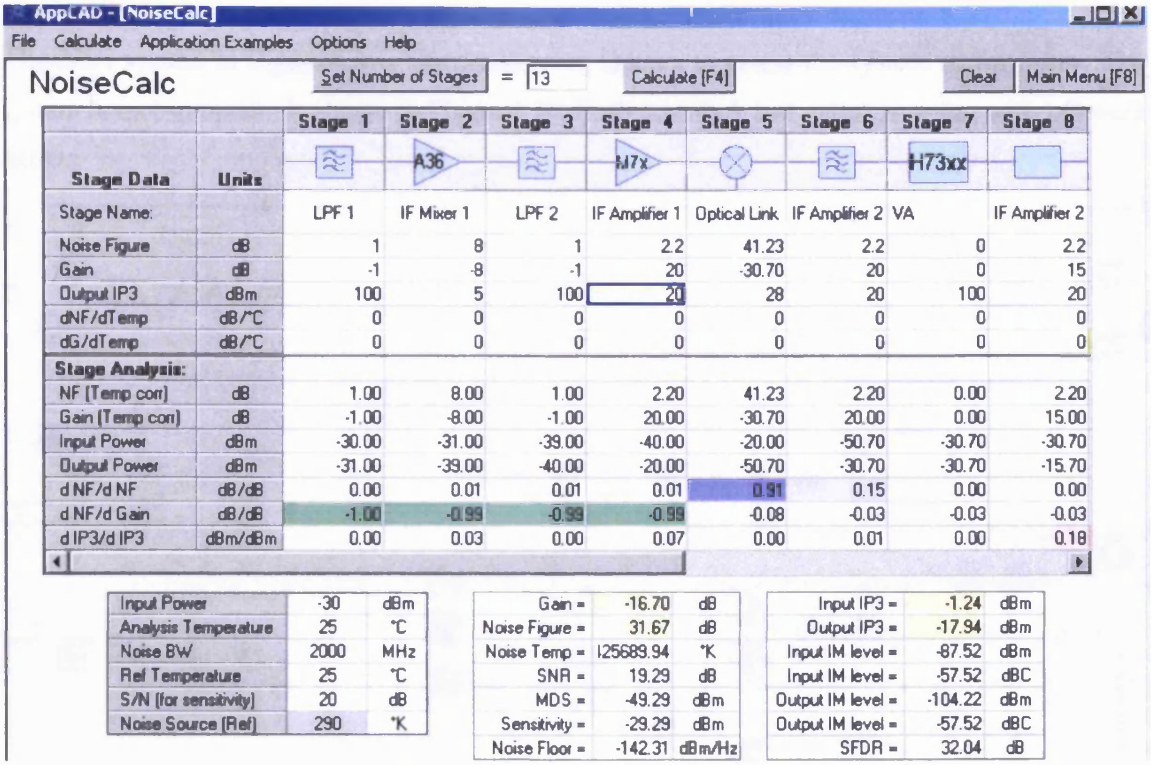

Stage Data	Units	Stage 1	Stage 2	Stage 3	Stage 4	Stage 5	Stage 6	Stage 7	Stage 8
			A36		M7x			H73xx	
Stage Name:		LPF 1	IF Mixer 1	LPF 2	IF Amplifier 1	Optical Link	IF Amplifier 2	VA	IF Amplifier 2
Noise Figure	dB	1	8	1	2.2	41.23	2.2	0	2.2
Gain	dB	-1	-8	-1	20	-30.70	20	0	15
Output IP3	dBm	100	5	100	20	28	20	100	20
dNF/dTemp	dB/°C	0	0	0	0	0	0	0	0
dG/dTemp	dB/°C	0	0	0	0	0	0	0	0
Stage Analysis:									
NF (Temp corr)	dB	1.00	8.00	1.00	2.20	41.23	2.20	0.00	2.20
Gain (Temp corr)	dB	-1.00	-8.00	-1.00	20.00	-30.70	20.00	0.00	15.00
Input Power	dBm	-30.00	-31.00	-39.00	-40.00	-20.00	-50.70	-30.70	-30.70
Output Power	dBm	-31.00	-39.00	-40.00	-20.00	-50.70	-30.70	-30.70	-15.70
d NF/d NF	dB/dB	0.00	0.01	0.01	0.01	0.91	0.15	0.00	0.00
d NF/d Gain	dB/dB	-1.00	-0.99	-0.99	-0.99	-0.08	-0.03	-0.03	-0.03
d IP3/d IP3	dBm/dBm	0.00	0.03	0.00	0.07	0.00	0.01	0.00	0.18

Input Power	-30	dBm
Analysis Temperature	25	°C
Noise BW	2000	MHz
Ref Temperature	25	°C
S/N (for sensitivity)	20	dB
Noise Source (Ref)	290	°K

Gain =	-16.70	dB
Noise Figure =	31.67	dB
Noise Temp =	25689.94	°K
SNR =	19.29	dB
MDS =	-49.29	dBm
Sensitivity =	-29.29	dBm
Noise Floor =	-142.31	dBm/Hz

Input IP3 =	-1.24	dBm
Output IP3 =	-17.94	dBm
Input IM level =	-87.52	dBm
Input IM level =	-57.52	dBC
Output IM level =	-104.22	dBm
Output IM level =	-57.52	dBC
SFDR =	32.04	dB

Figure 4.12. Overall system calculation for the mm-wave Gbit/s downlink showing link parameters and results

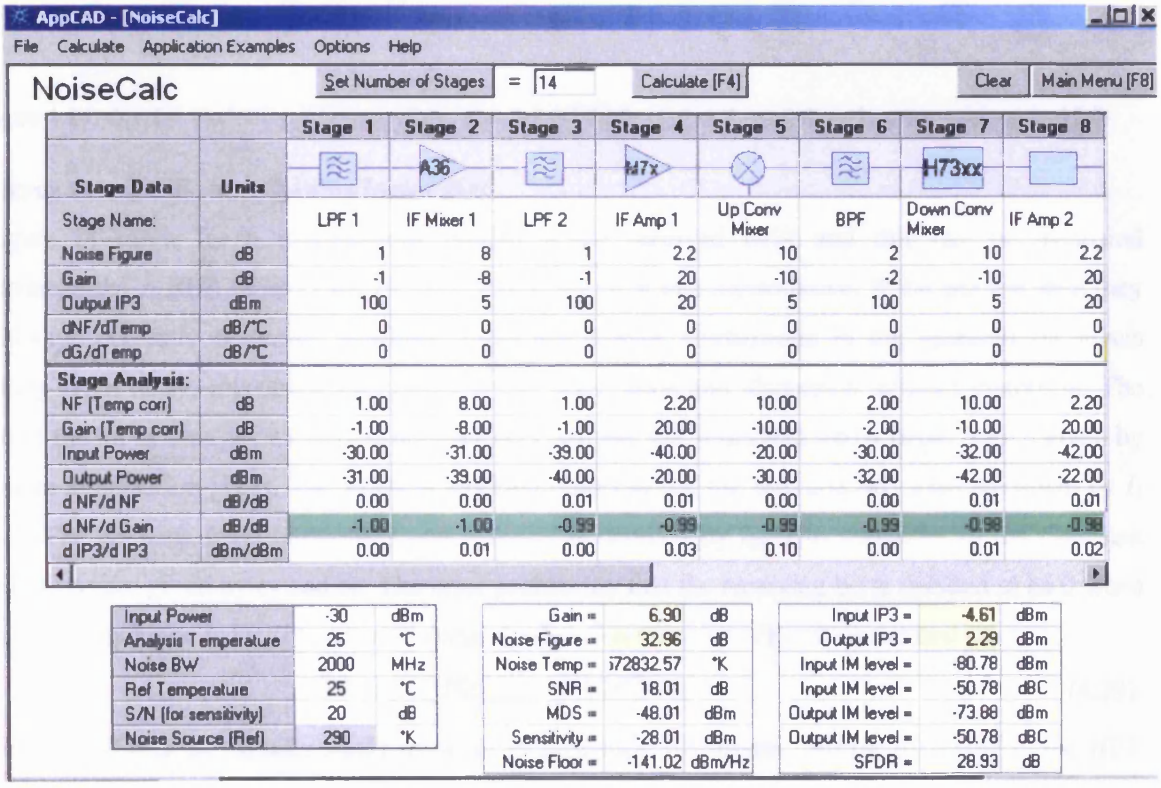

Stage Data	Units	Stage 1	Stage 2	Stage 3	Stage 4	Stage 5	Stage 6	Stage 7	Stage 8
			A36		M7x			H73xx	
Stage Name:		LPF 1	IF Mixer 1	LPF 2	IF Amp 1	Up Conv Mixer	BPF	Down Conv Mixer	IF Amp 2
Noise Figure	dB	1	8	1	2.2	10	2	10	2.2
Gain	dB	-1	-8	-1	20	-10	-2	-10	20
Output IP3	dBm	100	5	100	20	5	100	5	20
dNF/dTemp	dB/°C	0	0	0	0	0	0	0	0
dG/dTemp	dB/°C	0	0	0	0	0	0	0	0
Stage Analysis:									
NF (Temp corr)	dB	1.00	8.00	1.00	2.20	10.00	2.00	10.00	2.20
Gain (Temp corr)	dB	-1.00	-8.00	-1.00	20.00	-10.00	-2.00	-10.00	20.00
Input Power	dBm	-30.00	-31.00	-39.00	-40.00	-20.00	-30.00	-32.00	-42.00
Output Power	dBm	-31.00	-39.00	-40.00	-20.00	-30.00	-32.00	-42.00	-22.00
d NF/d NF	dB/dB	0.00	0.00	0.01	0.01	0.00	0.00	0.01	0.01
d NF/d Gain	dB/dB	-1.00	-1.00	-0.99	-0.99	-0.99	-0.99	-0.98	-0.98
d IP3/d IP3	dBm/dBm	0.00	0.01	0.00	0.03	0.10	0.00	0.01	0.02

Input Power	-30	dBm
Analysis Temperature	25	°C
Noise BW	2000	MHz
Ref Temperature	25	°C
S/N (for sensitivity)	20	dB
Noise Source (Ref)	290	°K

Gain =	6.90	dB
Noise Figure =	32.96	dB
Noise Temp =	572832.57	°K
SNR =	18.01	dB
MDS =	-48.01	dBm
Sensitivity =	-28.01	dBm
Noise Floor =	-141.02	dBm/Hz

Input IP3 =	-4.61	dBm
Output IP3 =	2.29	dBm
Input IM level =	-80.78	dBm
Input IM level =	-50.78	dBC
Output IM level =	-73.88	dBm
Output IM level =	-50.78	dBC
SFDR =	28.93	dB

Figure 4.13. Overall system calculation for the mm-wave Gbit/s uplink showing link parameters and results

4.5.2 Simulation

The Gigabit/s system in Figure 4.8 is simulated using Optsim to assess the system performance. The full system layout in optsim is shown in Figure 4.14. Both downlink and uplink together with LO were simulated.

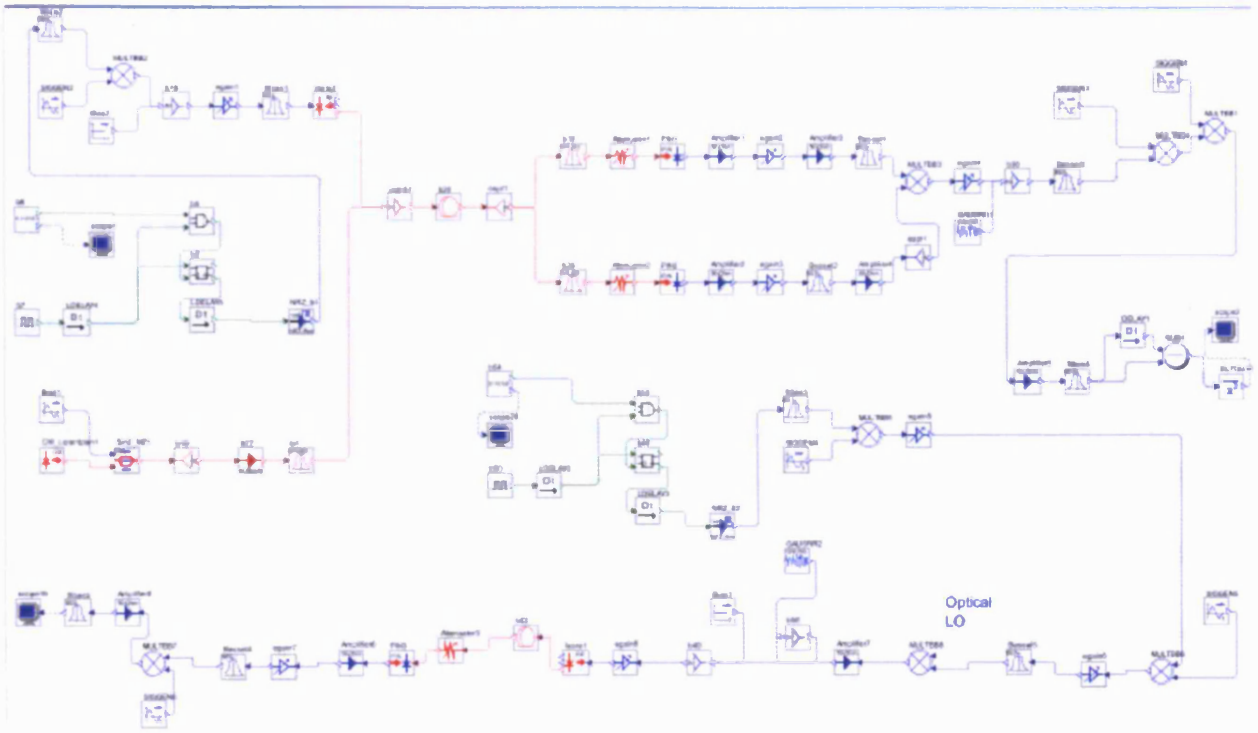

Figure 4.14. Optsim modelling diagram of the mm-wave Gbit/s system downlink and uplink with optical LO

Bit error rate (BER) and Quality factor (Q)

A figure of merit for a transmission system is the received BER and this can be measured experimentally. A BER of less than 10^{-9} is required for error free transmission. If the bits are ideal they are always correctly detected. However, there are always fluctuations in the received bit levels resulting from noise, relaxation oscillation of the laser diode and dispersion induced distortion. The value of the bit at zero or one state is not precisely defined, but is divided into a larger region given by Gaussian distribution [147]. The average received photocurrent for zero and one state are given by I_1 and I_0. The decision level between 1 and 0 levels is denoted by I_D. The variances of the Gaussian distributions are given by σ_1 and σ_0. The error probability that the receiving bit is decided to be 0 when 1 is actually received is P(0/1) and, vice versa, 1 when 0 is received is P(1/0) is defined as:

$$BER = p(1)P(0/1) + p(0)P(1/0) \tag{4.29}$$

Since 1 and 0 bits are equally likely to occur in a realistic bit stream, $p(1) = p(0) = 1/2$, the BER becomes

$$BER = \frac{1}{2}[P(0/1) + P(1/0)] \tag{4.30}$$

The expressions for these probabilities can be given by an integration of the Gaussian probability [148].

$$P(0/1)=\frac{1}{\sigma_1\sqrt{2\pi}}\int_{-\infty}^{I_D}\exp\left(-\left[\frac{I-I_1}{\sigma_1\sqrt{2}}\right]^2\right)dI \tag{4.31}$$

$$P(1/0)=\frac{1}{\sigma_0\sqrt{2\pi}}\int_{I_D}^{\infty}\exp\left(-\left[\frac{I-I_0}{\sigma_0\sqrt{2}}\right]^2\right)dI \tag{4.32}$$

Since computer models for simulation of a system typically run slower than real time, BER calculations are quite difficult. On the other hand, Q factor (defined as the difference in mean/sum of standard deviations) analysis is comparatively easy to evaluate and is used to determine the BER. The Q factor provides a qualitative description of the receiver performance because it is a function of the minimum SNR required to obtain a specific BER for a given signal. The Q factor predicts the probability of bit errors by measuring received signal strength and noise levels rather than by counting actual errors. If the total noise is assumed to follow Gaussian statistics then Q can be defined as [149]:

$$Q=\frac{I_1-I_0}{\sigma_0+\sigma_1} \tag{4.33}$$

where I_1 and I_0 are the value of 1 and 0 bit current respectively and σ_1 and σ_0 are the standard deviation of the 1 and 0 bit, respectively. The relationship of the Q factor to BER is given by the expression:

$$BER=\frac{1}{2}erfc\left(\frac{Q}{\sqrt{2}}\right)\approx\frac{1}{Q\sqrt{2\pi}}e^{\left(\frac{-Q^2}{2}\right)} \tag{4.34}$$

A BER of 10^{-9} means a Q factor of approximately 6. IF BER $<10^{-12}$ is required, Q>7 is needed. This approach is limited in that it assumes the signal to be degraded only by Gaussian noise. However, Gaussian approximation can lead to close BER estimates. The square of the Q factor may be interpreted as the equivalent SNR of the receiver and can be quoted in decibels using the conversion $10\log(Q^2)$, and a BER of 10^{-9} corresponds to a Q factor of 6 or 15.6 dB.

The eye diagram is a convenient method to assess the system performance and is generated using an oscilloscope connected to the demodulated filtered symbol stream. The simulated eye diagrams for the downlink and uplink are shown in Figure 4.15 and Figure 4.16, respectively together with the measured experimental results of the eye diagram.

The most important aspect of a modulation technique is the SNR necessary for a receiver to achieve a specified level of BER. The performance depends on how large the SNR is for a system. The probability of bit error P_e for the signal at the detector output describes the quality of the recovered data. The P_e is a function of the ratio of the energy per bit to the noise PSD (E_b/N_o) as measured at the detector input. E_b/N_o is a measure of the required energy per bit relative to the noise power. The exact relationship between P_e and E_b/N_o depends on the type of signal used. The BER for a DPSK receiver

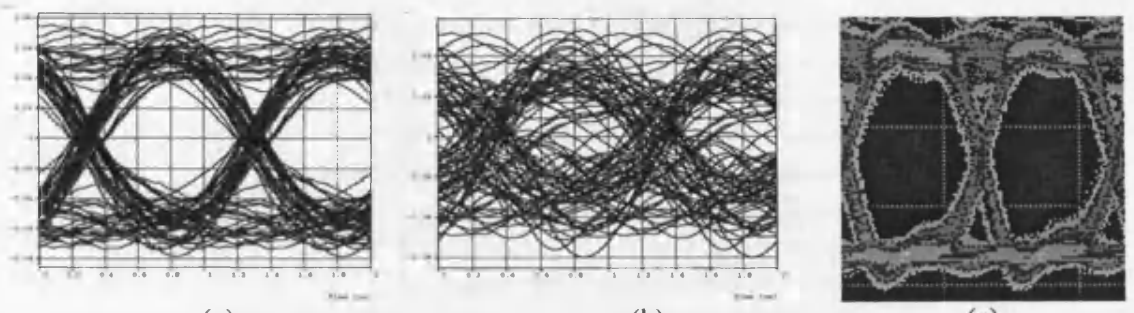

(a) (b) (c)

Figure 4.15. Simulated downlink eye diagram for the mm-wave Gbit/s system with Q factor of (a) 15.2 dB (b) 7.2 dB and (c) the measured eye diagram

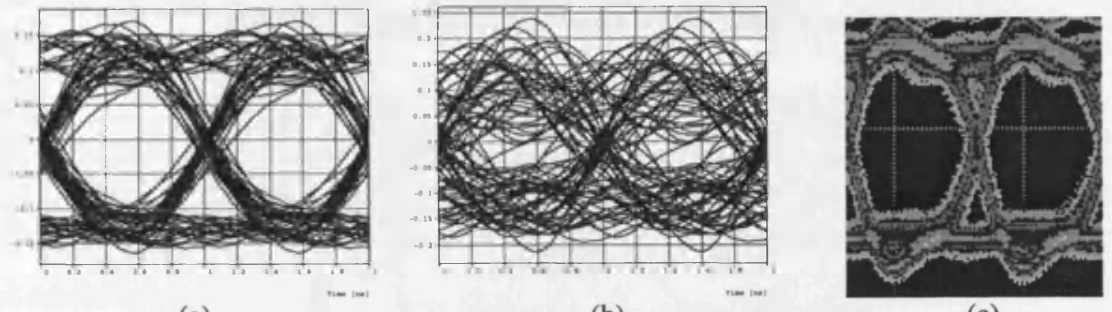

(a) (b) (c)

Figure 4.16. Simulated uplink eye diagram for the mm-wave Gbit/s system with Q factor of (a) 16.2 dB (b) 7.6 dB and (c) the measured eye diagram

can be derived under the assumption that the additive input noise is Gaussian. The BER for optimum demodulation of DPSK is:

$$P_e = 0.5e^{-(E_b/N_o)} \tag{4.35}$$

The simulated BER for the downlink and uplink are shown in Figure 4.17 and Figure 4.18, respectively. The measured BER for the system experiment are given in Chapter 5 and error free transmission is achieved for downlink and uplink when the received RF power was -16 and -17 dBm respectively. The required (E_b/N_o) for a BER of 10^{-9} is 20.03 (13.02 dB). A graph of E_b/N_o against BER is shown in Figure 4.19 for the case of optimum demodulation of DPSK. In comparing the error performance of BPSK and DPSK, it can be seen that for the same P_e, DPSK signal requires at most 1 dB more E_b/N_o than BPSK provided that $P_e=10^{-4}$ or less.

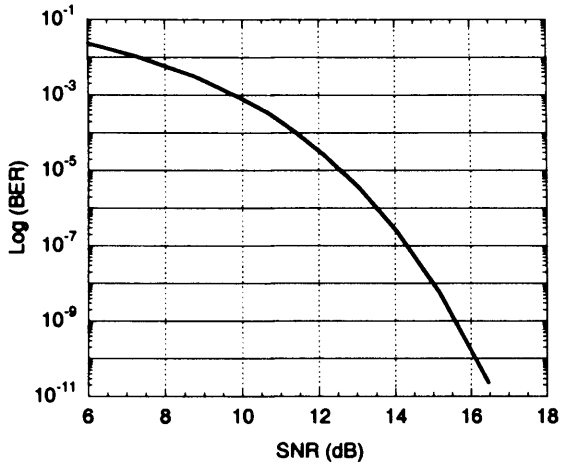

Figure 4.17. Simulated BER for the mm-wave GBit/s downlink

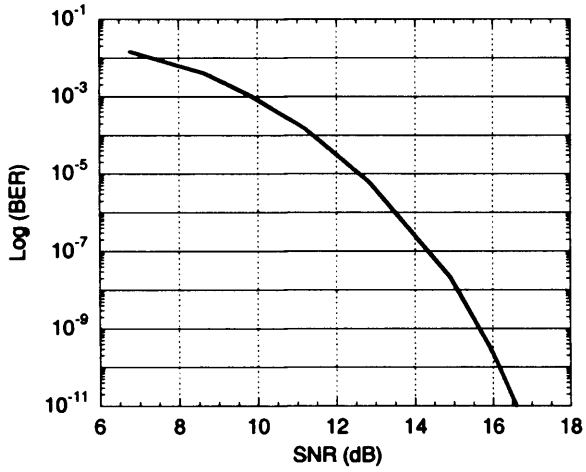

Figure 4.18. Simulated BER for the mm-wave GBit/s uplink

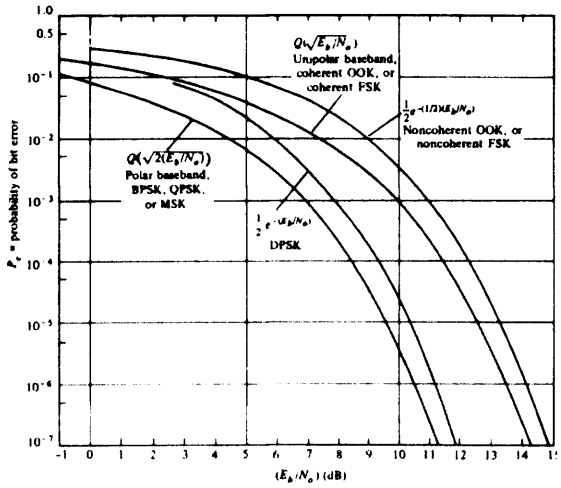

Figure 4.19. Comparison of the probability of bit error for common modulation schemes [150]

4.6 Semiconductor Optical Amplifier

An important consideration in a wireless over fibre system is the signal distribution to multiples sites. The power budget required due to fibre loss or splitting loss in such networks can be compensated by incorporating optical amplifiers such as EDFA or SOA [151]. An optical amplifier may be thought of as a laser without an optical cavity, or one in which feedback from the cavity is suppressed. Stimulated emission in the amplifier gain medium causes amplification of the incoming light. SOAs are being widely used in optical systems such as photonic frequency converters [56], wavelength converters [152] and switching elements [153]. They offer advantages such as compactness, low power consumption, monolithic integration (can be integrated with lasers, modulators) and mass production. Although, SOA do not currently give as much amplification as EDFAs at the common 1550 nm region they can be designed to amplify around the 1300 nm range [154]. They can also be used in external modulation systems that require data rates up to and beyond 10 Gbit/s, resulting in the need to boost the signal prior to transmission. Since the SOA is capable of amplifying data rates ranging from Mbit/s up to and beyond 10 Gbit/s it is a future proof technology. In addition to boosting the signal, SOAs have the ability to perform a limited amount of channel power equalisation on each wavelength in a WDM system [155]. In order to provide some level of channel equalisation, the gain of the SOA can be controlled by changing the bias current applied. However, if the bias current is lowered to lower the gain, the saturation output power and hence the linear region also reduces which in turn limits the dynamic range. Hence, the bias current of the SOA has an important influence on the link performance.

A SOA sometimes referred to as a semiconductor laser amplifier (SLA) works in a similar way to a basic laser but with an optical signal being amplified by means of stimulated emission. The structure is much the same, with two semiconductor materials on top of each other, with another material in between them forming the active region [156]. A schematic diagram of the SOA is shown in Figure 4.20. Anti-reflection coating elements are used at the end faces to avoid internal feedback and this effectively prevents the amplifier from acting as a laser. Unlike EDFAs which are optically pumped,

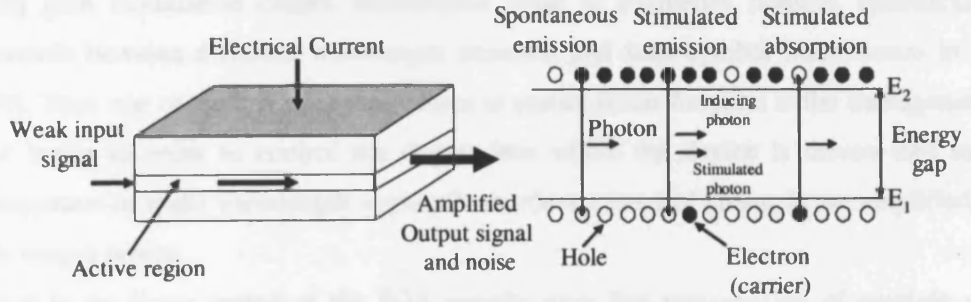

Figure 4.20. Schematic diagram of an SOA and spontaneous and stimulated processes in a two level system

SOAs are electrically pumped by injected current. An electrical current is set running through the device in order to excite electrons which are stimulated by incoming light from optical signals to move

down to their ground states. The photon given out by an electron losing energy from its excited state exactly matches the photons that caused the emission in the first place. Therefore, there are now two photons representing one particular section of a signal where previously there was one, hence, the signal has been amplified. These two photons can now cause more stimulated emission as they travel down the device, until they all exit together as a successfully amplified signal.

The gain of an SOA is influenced by the input signal power and internal noise generated by the amplification process. The output signal is accompanied by amplified spontaneous emission (ASE) produced by the amplification process. As the input signal power increases the gain decreases. If the signal power is too high then gain saturation will occur. This would not be a serious problem if the amplifier gain dynamics were a slow process. However, in SOAs the gain dynamics are determined by the carrier recombination lifetime and are in the region of hundreds of picoseconds to nanoseconds. This means that the amplifier gain will react relatively quickly to changes in input signal power. This gain saturation can cause significant distortion and this effect is even more important in multi-channel systems where the dynamic gain leads to inter-channel crosstalk. It can also limit the gain achievable when SOAs are used as multi-channel amplifiers in WDM systems. This is in contrast to the EDFA which have recombination lifetime of the order of millisecond region which means that they operate in the regime of mean power saturation leading to negligible distortion.

In previous literature, investigations have shown that SOA is a good candidate for achieving high gain microwave photonic links [157, 158]. High SNR can be obtained by increasing the average optical power. In an analogue system [159], the linearity of the link is usually determined by that of the light source. Since the gain behaviour of the SOA is not linear this will also contribute to the non-linearity and can cause problems such as generation of intermodulation products and thus affect the link performance. The optical gain varies with the input optical power and low input powers will be amplified by high gain, whereas high input powers will experience low gain. A linear region is the preferred operating regime since an exact, amplified replica of the input is required. Operating an SOA outside this region causes distortion since at high output powers, the gain saturates and compresses. The resulting gain modulation causes interference noise in frequency domain, specifically inter-channel crosstalk between different wavelength channels and inter-symbol interference in the time domain [160]. Thus one of the key operating issues to ensure linear function is the management of the input power levels in order to control the degree into which the device is driven into saturation, especially important in multi-wavelength applications where a band of channels are amplified, sharing the available output power.

Operation in the linear region of the SOA permits error free transmission of multiple channels. This operating space is defined by the input power levels, the gain and the output saturation power of the device. For example for a +10 dBm output saturation (average) power (at the -3 dB gain compression point) for a gain of 15 dB, the maximum (total) input power would be -5 dBm. The number of channels, the output power per channel and the available output saturation power level will

then define the gain required from the SOA. Non-linear distortion generated by an SOA in analog optical systems is considered [161] and expressions for the second and third harmonic distortion generated by the SOA operating under slight saturation conditions are derived. The results show that the optical power launched into the SOA should be carefully adjusted to obtain both good linearity and high dynamic range required by analog optical systems.

In the same way as for EDFAs, noise is generated by the ASE occurring along the SOA [157]. The amplification is accompanied by spontaneous emission, where photons of random phase and polarisation are added to the signal [162]. After direct detection, beat noise due to ASE of the SOA will add to the receiver noise and increase the noise floor. The laser Relative Intensity Noise (RIN) and the noise of optical amplifiers and receiver noise are the main noise sources in the optical link. The noise performance of an optical amplifier is characterised by the noise factor (F), defined as the amount of degradation in the SNR caused by the amplification process. The noise factor is a critical parameter and should be as low as possible since it determines the achievable sensitivity. The optical noise factor is a parameter used for quantifying the noise penalty added to a signal due to the insertion of an optical amplifier. That is, before light enters an amplifier the signal to noise ratio is $SNR_{(in)}$, after amplification it is $SNR_{(out)}$. Thus, optical noise factor can be defined as $NF_{opt}=SNR_{(in)}/SNR_{(out)}$ where both SNRs refer to the electrical power when an optical signal is converted to electric current using a photo-detector. The use of an optical amplifier prior to a receiver to boost the signal power enables error free operation to be obtained for considerably reduced signal powers at the input to the optical amplifier. The performance of the receiver, most often described by the BER is governed by the signal to noise ratio (SNR). The SNR depends on the signal power and is defined as SNR=Signal/Noise. To improve the SNR either the signal level should be increased or the noise level reduced or both. The sources of the noise include the receiver thermal noise, shot noise of the detector, signal ASE (Amplified Spontaneous Emission) beat noise and ASE-ASE beat noise.

The noise performance of the SOA is one of the key parameters affecting their use in microwave photonic links. The optical output signal from an SOA is composed of ASE. After detection of input optical power at the detector stage, interference is generated between ASE and ASE, which is known as spontaneous-spontaneous beat noise (sp-sp beat noise), and ASE and signal known as signal-spontaneous beat noise (s-sp beat noise). Without narrow band filter (approx 1 nm) after the optical amplifier and prior to the photodiode, significant levels of spontaneous emission are delivered directly onto the receiver. Significant improvement can be achieved by introducing a narrow band optical filter before the receiver [158]: The amplified spontaneous emission (ASE) noise power at the output of an amplifier is [163]

$$P_{sp} = N_{sp}(G-1)h\nu B_o \tag{4.36}$$

where G is the internal gain, $h\upsilon$ the photon energy ($1.3.10^{-19}$) (h is the Planck constant and v the optical frequency), B_o the optical bandwidth and N_{sp} the spontaneous emission factor between 1.4 and 4 in

semiconductor optical amplifiers and equal to 1 in an ideal amplifier. The photocurrent equivalent of the ASE noise power is

$$i_{sp} = P_{sp}\frac{e}{h\nu} = N_{sp}(G-1)eB_o \tag{4.37}$$

where e is the electronic charge. After square law detection in the receiver, the received signal power is given by:

$$S = (GI_s\eta_{in}\eta_{out}A)^2 \tag{4.38}$$

where η_{in} is the amplifier input coupling efficiency, η_{out} the amplifier output coupling efficiency, A the optical loss between the amplifier and the receiver and I_s the photo-current equivalent of the amplifier input power.

SOAs in CWDM systems

To extend the capacity and distance of CWDM systems (>100 km) requires a low cost optical amplifier operating across the entire optical bandwidth [164]. The SOA can operate in single and multi-channel environments and is the only viable technology that can be deployed to meet these expanding applications. Wide bandwidth SOAs exhibit approximately 80 nm optical gain bandwidth at the -3 dB drop from the peak gain. Access to wider bandwidth is possible if the gain required is lower [165]. In DWDM applications, the SOA provides the required bandwidth easily. Amplification of bands of wavelengths simultaneously reduces the effective cost of amplification. The characteristics of the SOA permits access to an extended gain bandwidth, to provide gain between 1260 nm and 1620 nm. EDFAs operate in the C band (1530 nm-1562 nm) and L band (1570 nm-1610 nm) and therefore only cover, at most, two CWDM channels at a time. Furthermore, EDFAs cannot amplify channels in the lower, 1300 nm region.

SOAs suffer from high noise figure (6 dB to 10 dB) and spurious effects such as those arising from Cross Gain Modulation (XGM). Also, ASE beat noise at low input levels play an important role in CWDM systems because of the relatively large bandwidth of MUX and DEMUX which is about 15 nm. XGM effect results from fast gain dynamics of the SOA. The carrier density changes in the amplifier will affect all of the input signals, so it is possible for a strong signal at one wavelength to affect the gain of a weak signal at another wavelength [162]. Gain saturation caused by one channel modifies the response of the other channels, including crosstalk between channels. WDM applications thus require a device with high output saturation power.

So far in WoF systems two separate uni-directional EDFA have been used for the up and down link [8]. A WoF system employing an SOA has been demonstrated [166]. Cascaded SOA in WoF link are employed to extend the transmission link to 150 km with directly modulated lasers [167]. While there have been previous reported demonstrations of bi-directional amplifiers they have been designed with a double switch arrangement to direct the uplink and downlink signals through conceptually

different amplifiers. A bi-directional amplifier was demonstrated using circulators, fibre grating and two EDFAs [168]. Chawki *et al* reported a new design of a WDM bi-directional amplifier using two 4 port optical circulators, fibre grating and only one EDFA [169]. A Bi-directional SOA that can provide gain in both directions could significantly reduce the complexity and cost of the system.

4.7 Conclusion

This chapter considered wireless over fibre system architectures for the transport and distribution of broadband mm-wave signals. Typical components that can be shared include the expensive low phase noise mm-wave LO. In addition WDM of the signals within the fibre simplify the network architecture and improve the deployment of BSs, since it enables full duplex operation on a single fibre and also allows different BSs to be fed by a common fibre. A number of schemes that were proposed and demonstrated showing significant simplification of optical links by incorporating dual modulation/detection capability of EAMs have been discussed. Various system architectures have also been considered. The benefit of the star architecture includes having similar paths from CS to BSs, ensuring a uniform quality of service for each BS. Star-tree provides almost identical paths between the CS and each BS both on the downlink and uplink, which therefore allows a uniform quality of service to each BS. For the downlink the wavelengths are multiplexed at the CS and de-multiplexed at the RN, while in the uplink case the wavelengths are multiplexed at the RN and de-multiplexed at the CS. A WDM uni-directional ring incorporating OADM to feed downlink and uplink wavelength channels to/from appropriate BSs is discussed in greater depth. Also described are the limits on the number of OADMs that can be cascaded, which determine the maximum number of BSs that can be serviced by a single ring. The advantages of the ring architecture such as equipment sharing and fault protection and disadvantages such as non-uniform signal quality and network upgrade complexity were discussed. Power budget calculations and simulations have been carried out for the proposed Gbit/s system using low cost components such as uncooled directly modulated lasers and CWDM passive components. The use of SOAs in analogue links is discussed with important considerations regarding non-linearity. In the next chapter, full duplex RF and mm-wave over fibre links are described experimentally to demonstrate their usefulness in a bi-directional system.

References

[1] K. Ohata, K. Maruhashi, M. Ito, S. Kishimoto, K. Ikuina, T. Hashiguchi, K. Ikeda and N. Takahashi, "1.25 Gbps wireless gigabit Ethernet link at 60 GHz band", *IEEE MTT-S Int. Microwave Symposium (IMS)*, TU4D-6, pp. 373-376, 2003.

[2] D. Novak, A. Nirmalathas, C. Lim, C. Marra and R. B. Waterhouse, "Fibre radio challenges and possible solutions", *IEEE Int. Topical Meeting Microwave Photonics (MWP)*, 2003.

[3] L. Noel, D. Wake, D. G. Moodie, D. D. Marcenac, L. D. Westbrook and D. Nesset, "Novel techniques for high capacity 60 GHz fiber radio transmission systems", *IEEE Trans. Microwave Theory & Tech.*, vol. 45, pp. 1416–1423, 1997.

[4] T. Kuri, K. Ikeda, H. Toda, K. Kitayama, and Y. Takahashi, "A compact remote antenna base station for microwave/millimetre-wave dual-band radio-on-fibre systems", *IEEE Laser & Electro-Optics Society (LEOS)*, vol.1, pp. 59-60, 2004.

[5] J. J. O'Reilly, P. M. Lane, M. H. Capstick, H. M. Salagado, R. Heidemann, R. Hofstetter and H. Schmuck, "RACE R2005: microwave optical duplex antenna link", *IEE Proceedings-J.* vol. 140, no. 6, pp.385-391, 1993.

[6] T. Ismail, C. P. Liu, J. E. Mitchell, A. J. Seeds, X. Qian, A. Wonfor, R. V. Penty and I. H. White, "Full-duplex wireless-over-fibre transmission incorporating a CWDM ring architecture with remote millimetre-wave LO delivery using a bi-directional SOA", *Optical Fibre Communications (OFC)*, OThG7, 2005.

[7] C. Lim, D. Novak and G. H. Smith, "Implementation of an upstream path in a millimetre wave fibre wireless system", *Optical Fibre Communications (OFC)*, TUC3, pp. 16-17, 1998.

[8] C. Lim, A. Nirmalathas, D. Novak, R. Waterhouse and G. Yoffe, "Millimetre-wave broad-band fibre-wireless system incorporating baseband data transmission over fibre and remote LO delivery", *IEEE J. Lightwave Technol.*, vol. 18, pp. 1355-1363, 2000.

[9] A. Kaszubowska, L. P. Barry and P. Anandarajah, "Multifunctional operation of a fibre bragg grating in a WDM/SCM radio over fibre distribution system", *IEEE Laser & Electro-Optics Society (LEOS)*, pp. 861-862, 2003.

[10] C. Lim, A. Nirmalathas, D. Novak, R. Waterhouse, and K. Ghorbani, "Full-duplex broadband fibre-wireless system incorporating baseband data transmission and a novel dispersion tolerant modulation scheme", *IEEE MTT-S Int. Microwave Symposium (IMS)*, vol. 3, pp. 1201-1204, 1999.

[11] Z. Ahmed, D. Novak, R. B. Waterhouse and H-F. Liu, "37 GHz fibre wireless system for distribution of broad-band signals", *IEEE Trans. Microwave Theory & Tech.*, vol. 45, no. 8. pp. 1431-1435, 1997.

[12] C. Lim, A. Nirmalathas, D. Novak, R. Waterhouse and G. Yoffe, "A WDM architecture for millimeter-wave fibre radio systems incorporating baseband transmission", *IEEE Int. Topical Meeting Microwave Photonics (MWP)*, T-7.4, pp. 127-130, 1999.

[13] H. Schmuck, "Comparison of optical millimetre-wave system concepts with regard to chromatic dispersion", *Electron. Lett.*, vol. 31, pp. 1848-1849, 1995.

[14] R. Hofstetter, H. Schmuck and R. Heidemann, "Dispersion effects in optical millimetre-wave systems using self-heterodyne method for transport and generation", *IEEE Trans. Microwave Theory & Tech.*, vol. 43, pp. 2263-2276, 1995.

[15] G. H. Smith and D. Novak, "Broadband millimeter-wave (38 GHz) fibre-wireless transmission system using electrical and optical SSB modulation to overcome dispersion effects", *IEEE Photon. Technol. Lett.*, vol. 10, no. 1, pp. 141-143, 1998.

[16] J. Park, W. V. Sorin and K. Y. Lau, "Elimination of fibre chromatic dispersion penalty on 1550 nm millimetre wave optical transmission", *Electron. Lett.*, vol. 33, no. 6, 1997.

[17] G. H. Smith and D. Novak, "Full duplex wireless system using electrical and optical SSB modulation for efficient broadband millimetre wave transport", *IEEE Int. Topical Meeting Microwave Photonics (MWP)*, FR2-2, pp. 223-227, 1997.

[18] H. Schmuck and R. Heidemann, "Hybrid fibre radio field experiment at 60 GHz", *European Conference on Optical Communication (ECOC)*, ThC1.2, pp. 4.59-4.62, 1996.

[19] Y. Shoji and H. Ogawa, "Experimental demonstration of 622 Mbit/s millimetre wave over fibre link for broadband fixed wireless access system", *IEICE Trans. Electron.*, vol. E86-C, pp. 1129-1137, 2003.

[20] A. Kim, Young Hun. Joo, Y. Kim, "60 GHz wireless communication systems with radio over fibre links for indoor wireless LANs", *IEEE Trans. Consumer Electronics*, vol. 50, issue 2, pp. 517-520, 2004.

[21] K. I. Kitayama, T. Kuri, R. Heinzelmann, A. Stohr. D. Jager and Y. Takahashi, "A Good prospect for broadband millimetre wave fibre radio access system-an approach to single optical component at antenna base station," *IEEE MTT-S Int. Microwave Symposium (IMS)*, vol. 3, pp. 1745-1748, 2000.

[22] J. F. Cidiou, F. Devaux, J. F. Veillard, B. L. Marty, J. Guena, E. Penard & P. Legaud, "Electro-absorption modulator for radio over fibre at 38 GHz", *Electron. Lett.*, vol. 31, pp. 1273-1274, 1996.

[23] J. Kim, Young-Shik. Kang, Yong-Duck. Chung and Kwang-Seong. Choi, "Development and RF characteristics of analog 60 GHz electro-absorption modulator module for RF/Optic conversion", *IEEE Trans. Microwave Theory & Tech.*, vol. 54, no. 2, pp. 780-787, 2006.

[24] A. Stohr, R. Heinzelmann and D. Jager, "Millimetre wave bandwidth electro-absorption modulators and transceivers," *IEEE Int. Topical Meeting Microwave Photonics (MWP)*, pp. 128-128, 2000.

[25] T. Kuri, T. Nakasyotani, H. Toda and K. Kitayama, "Characterisations of super continuum light source for WDM millimetre wave band radio on fibre systems", *IEEE Photon. Technol. Lett.*, vol. 17, pp. 1274-1276, 2005.

[26] A. Nirmalathas, C. Lim, D. Novak and R. Waterhouse, "Optical interfaces without light sources for base station designs in fibre wireless system incorporating WDM", *IEEE Int. Topical Meeting Microwave Photonics (MWP)*, T-7.2, pp. 199-123, 1999.

[27] A. Nirmalathas, D. Novak, C. Lim and R. B. Waterhouse, "Wavelength reuse in the WDM optical interface of a millimetre wave fibre wireless antenna base station", *IEEE Trans. Microwave Theory & Tech.*, vol. 49, no. 10, pp. 2006-2012, 2001.

[28] A. Kaszubowska, L. Hu and L. P. Barry, "Remote down conversion with wavelength reuse for the radio/fibre uplink connection", *IEEE Photon. Technol. Lett.*, vol. 18, no. 4, pp. 562-564, 2006.

[29] M. Attygalle, C. Lim, M. Bakaul and A. Nirmalathas, "Extending transmission distance in wavelength reused fibre radio links with FBG filters", *Optical Fibre Communications (OFC)*, OThB3, 2006.

[30] C. Lim, A. Nirmalathas, D. Novak and R. Waterhouse, "Capacity analysis and the merging of a WDM ring fibre radio backbone incorporating wavelength interleaving with a sectorised antenna interface", *IEICE Trans. Electron.*, vol. E86-C, no. 7, pp. 1184-1190, 2003.

[31] M. Bakaul, A. Nirmalathas and C. Lim, "Multifunctional WDM optical interface for millimetre wave fibre radio antenna base station", *IEEE J. Lightwave Technol.*, vol. 23, no. 3, pp. 1210-1218, 2005.

[32] http://www.siemens.com

[33] http://www.nttdocomo.com

[34] G. Nykolak, P. F. Szajowski, G. Tourgee and H. Presby, "2.5 Gbit/s free space optical link over 4.4 km", *Electron. Lett.*, vol. 35, pp. 578-579, 1999.

[35] H. Schmuck and R. Heidemann, "Hybrid fibre radio field experiment at 60 GHz", *European Conference on Optical Communication (ECOC)*, vol. 4, ThC.1.2, pp. 59-62, 1996.

[36] K. Hamaguchi, Y. Shoji, H. Ogawa. H. Sato, K. Totuda, Y. Hirachi, T. Iwasaki, A. Akeyama, K. Ueki and T. Kizawa, "A wireless video home link using 60 GHz band: Concept and performance of developed system", *European Microwave Conf.*, pp. 294-297, 2000.

[37] K. Ogusu, K. Inagaki and Y. Mizuguchi, "400 Mbit/s BPSK data transmission at 60 GHz band mm-wave using a two mode injection locked fabry perot slave laser", *IEEE Int. Topical Meeting Microwave Photonics (MWP)*, pp. 31-34, 2000.

[38] K. Ohata, K. Maruhashi. M. Ito, S. Kishimoto, K. Ikuina, T. Hashiguchi, N. Takahashi and S. Iwanaga, "Wireless 1.25 Gb/s transceiver module at 60 GHz band", *Tech. Dig. ISSCC*, pp. 298-300, 2002.

[39] A. Hirata, M. Harada and T. Nagatsuma, "Multi-Gigabit/s wireless links using millimetre wave photonic techniques", *IEEE Int. Topical Meeting Microwave Photonics (MWP)*, Tu-2.8, pp. 77-80, 2001.

[40] T. Ohno, S. Fukushima, Y. Doi, Y. Muramoto and Y. Matsouka, "Application of uni-travelling carrier waveguide photodiodes in base stations of millimetre wave fibre radio systems", *IEEE Int. Topical Meeting Microwave Photonics (MWP)*, pp. 253-256, 1999.

[41] A. Hirata, T. Minotani and T. Nagatsuma, "Millimetre-wave photonics for 10 Gbit/s wireless links", *IEEE Laser & Electro-Optics Society (LEOS)*, WN4, pp. 477-478, 2002.

[42] A. Hirata, M. Harada, K. Sato and T. Nagatsuma, "Low cost millimetre wave photonic techniques for Gigabit/s wireless link", *IEICE Tran. Electron.*, vol. E86-C, no. 7, pp. 1123-1128, 2003.

[43] A. Hirata M. Harada and T. Nagatsuma, "120 GHz wireless link using photonic techniques for generation, modulation, and emission of millimetre wave signals", *IEEE J. Lightwave Technol.*, vol. 21, no. 10, pp. 2145-2153, 2003.

[44] K. Kitayana and R.A. Griffin, "Optical down conversion from millimeter-wave to IF band over 50 km-long optical fibre link using an electro-absorption modulator," *IEEE Photon. Technol. Lett.*, vol. 11, pp. 287-289, 1999.

[45] Jun-Hyuk. Seo, Chang-Soon. Choi, Woo-Young. Choi, Young-Shik. Kang, Young-Duck. Chung and J. Kim, "Remote optoelectronic frequency down conversion using 60 GHz optical heterodyne signals and an electro-absorption modulator", *IEEE Photon. Technol. Lett.*, vol. 17, no. 5, pp. 1073-1075, 2005.

[46] Chul Soo. Park, Cheung Keun Oh, Chung Ghiu Lee, Dong-Hwan Kim and Chang-Soo Park, "A photonic up converter for a WDM radio over fibre system using cross-absorption modulation in an EAM", *IEEE Photon. Technol. Lett.*, vol. 17, no. 9, pp. 1950-1952, 2005.

[47] T. Young, J. Conardi and W. R. Tinga, "BER characteristics of $\pi/4$ DQPSK microwave sub-carrier signals on optical fibre using Mach-Zehnder modulator nonlinear up conversion", *IEEE Photon. Technol. Lett.*, vol. 8, no. 11, pp. 1552-1554, 1996.

[48] K. Kojucharow, M. Sauer, H. Kauzni, D. Sommer, F. Poegel, W. Nowak, A. Finger and D. Ferling, "Simultaneous electro-optical up conversion remote oscillator generation, and air transmission of multiple optical WDM channels for a 60 GHz high capacity indoor system", *IEEE Trans. Microwave Theory & Tech.*, vol. 47, no. 12, pp. 2249- 2256, 1999.

[49] G. Zhou, X. Zhang, J. Yao, K. Wu and R. Kashyap, "A novel photonic frequency down-shifting technique for millimetre wave band radio on fibre systems", *IEEE Photon. Technol. Lett.*, vol. 17, no. 8, pp. 1728-1730, 2005.

[50] Keang-Po Ho, Shien-Kuei Liaw and Chinlon Lin, "Frequency doubling photonic mixer with low conversion loss", *Optical Fibre Communications (OFC)*, FD2, pp. 356-357, 1997.

[51] N. Shimizu, T. Nagatsuma, O. Tadanaga, H. Miyazawa and M. Asobe, "All optical multi-channel simultaneous upconversion for microwave fibre optic links", *Optical Fibre Communications (OFC)*, FE4, 2003.

[52] T. Kuri, Ken-ichi. Kitayama and Y. Ogawa, "Fibre optic millimetre wave uplink system incorporating remotely fed 60 GHz band optical pilot tone", *IEEE Trans. Microwave Theory & Tech.*, vol. 47, no. 7, pp. 1332-1337, 1999.

[53] M. Sauer, K. Kojucharow, H. Kaluzni, M. Otto band C. Schaffer, "Comparison of different IF band modulation techniques for electro-optical conversion and fibre transmission at 60 GHz", *IEEE Int. Topical Meeting Microwave Photonics (MWP)*, T-8.3, pp. 145-148, 1999.

[54] Ho-Jin Song, Jeong Seon. Lee and Jong-In. Song, "Error free simultaneous all optical up conversion of WDM radio over fibre signals", *IEEE Photon. Technol. Lett.*, vol. 17, no. 8, pp. 1731-1733, 2005.

[55] Y. K. Seo, C. S. Choi and W. Y. Choi, "All optical signal up conversion for radio on fibre applications using cross gain modulation in semiconductor optical amplifier", *IEEE Photon. Technol. Lett.*, vol. 14, no 10, pp. 1448-1450, 2002.

[56] Y. K. Seo, J. H.. Seo and W. Y. Choi, "Photonic frequency up conversion efficiencies in semiconductor optical amplifier", *IEEE Photon. Technol. Lett.*, vol. 15, no. 5, pp. 751-753, 2003.

[57] Jun-Hyuk Seo, Young-Kwang Seo and Woo-Young Choi, "Spurious free dynamic range characteristics of the photonic up converter based on a semiconductor optical amplifier", *IEEE Photon. Technol. Lett.*, vol. 15, no. 11, pp. 1591-1593, 2003.

[58] H-J. Song, J. S. Lee and J. I. Song, "All optical frequency up conversion of radio over fibre signal with optical heterodyne detection", *Electron. Letts.*, vol. 40, no. 5, 2004.

[59] H-J. Song, J. S. Lee and J. I. Song, "Signal up conversion by using a cross phase modulation in all optical SOA-NZI wavelength converter", *IEEE Photon. Technol. Lett.*, vol. 16, no. 2, pp. 593-595, 2004.

[60] Jun-Hyuk. Seo, Chang-Soon. Choi, Woo-Young. Choi, Young-Shik. Kang, Yong-Duck. Chung and Jeha. Kim, "Frequency conversion with cascaded SOA-EAM for Bi-directional radio on fibre systems", *IEEE Int. Topical Meeting Microwave Photonics (MWP)*, MC-6, pp. 56-59, 2004.

[61] Jun-Hyuk. Seo, Chang-Soon. Choi, Young-Shik. Kang, Yong-Duck. Chung, Jeha. Kim and Woo-Young. Choi, "SOA-EAM frequency up/down converters for 60 GHz Bi-directional radio on fibre systems", *IEEE Trans. Microwave Theory & Tech.*, vol. 54, no. 2, pp. 959-966, 2006.

[62] U. Gliese, S. Norskov and T. N. Nielsen, "Chromatic dispersion in fibre optic microwave and millimetre-wave links," *IEEE Trans. Microwave Theory & Tech.*, vol. 44, pp. 1716-1724, 1996.

[63] G. H. Smith, D. Novak, "Broadband millimetre-wave fibre-radio network incorporating remote up/down conversion," *IEEE MTT-S Int. Microwave Symposium (IMS)*, vol. 3, pp. 1509-1512, 1998.

[64] L. A. Johansson, "Broadband millimetre-wave radio over fibre systems", *PhD thesis, University of London*, University College London, 2001.

[65] X. Wang, N. J. Gomes, L. G. Rojas, P. A. Davies and D. Wake, "Indirect optically injection locked oscillator for millimetre wave communication system", *IEEE Trans. Microwave Theory & Tech.*, vol. 48, no. 12, pp. 2596-2603, 2000.

[66] M-S. Kao and J. Wu, "Coherent subcarrier multiplexed star distribution system using single local oscillator", *Electron. Letts.*, 1990.

[67] H. Izadpanah, "A millimetre wave broadband wireless access technology wireless access technology demonstrator for the next generation internet network reach extension", *IEEE Commun. Mag.*, pp. 140-145, 2001.

[68] R.-P. Braun, G. Grosskopf, H. Heidrich, C. von Helmolt, R. Kaiser, K. Kruger, U. Kruger, D. Rohde, F. Schmidt, R. Stenzel and D. Trommer, "Optical microwave generation and transmission experiments in the 12- and 60-GHz region for wireless communications", *IEEE Trans. Microwave Theory & Tech.*, vol. 46, pp. 320–330, 1998.

[69] D. Wake, C. R. Lima and P. A. Davies, "Optical generation of millimetre wave signals for fibre radio systems using a dual mode DFB semiconductor laser", *IEEE Trans. Microwave Theory & Tech.*, vol. 43, pp. 2270-2276, 1995.

[70] K. E. Razavi and P. A. Davies, "Semiconductor laser sources for the generation of millimetre wave signals", *IEE. Proc. Optoelectron.* vol. 145, no. 3, pp. 159-163, 1998.

[71] G. J. Simonis and K. G. Purchase, "Optical generation, distribution and control of microwaves using laser heterodyne", *IEEE Trans. Microwave Theory & Tech.*, vol. 38, pp. 667-669, 1990.

[72] U. Gliese, T. Norskov, S. Norskov and K.E. Stubkjaer, "Multifunctional fibre-optic microwave links based on remote heterodyne detection", *IEEE Trans. Microwave Theory & Tech.*, vol. 46, pp. 458-468, 1998.

[73] L. Noel, D. Marcenac and D.Wake, "120 Mbit/s QPSK radio-fibre transmission over 100 km of standard fibre at 60 GHz using a master/slave injection-locked DFB laser source", *Electron. Letts.*, vol. 32, pp. 1895-1897, 1996.

[74] L. A. Johansson, D. Wake and A. J. Seeds, "Millimetre wave over fibre transmission using a BPSK reference modulated optical injection phase lock loop," *Optical Fibre Communications (OFC)*, vol. 3, WV3-1, 2001.

[75] U. Gliese, T. N. Nielsen, M. Brauun, E. L. Christensen, K. E. Stubkjaer, S. Lindgren and B. Broberg, "A wideband heterodyne optical phase locked loop for generation of 3-18 GHz microwave carriers", *IEEE Photon. Technol. Lett.*, vol. 4, no. 8, pp. 936-938, 1992.

[76] M. Hyodo and M. Watanabe, "A novel technique for optical generation of millimetre wave signals using multiple phase locked loop", *IEICE Trans. Electron.*, vol. E86-C, no. 7, pp. 1236-1244, 2003.

[77] R. A. Griffin and K. Kitayama, "Optical millimetre wave generation with high spectral purity using feed-forward optical field modulation", *Electron. Letts.*, vol. 34, no. 8, 1998.

[78] L. A. Johansson and A. J. Seeds, "Millimetre wave modulated optical signal generation with high spectral purity and wide locking bandwidth using a fibre integrated optical injection phase lock loop," *IEEE Photon. Technol. Lett.*, vol. 12, no. 6, pp. 690-692, 2000.

[79] C. Walton, A. C. Bordonalli and A. J. Seeds, "High performance heterodyne optical injection phase lock loop using wide linewidth semiconductor lasers," *IEEE Photon. Technol. Lett.*, vol. 10, no. 3, pp. 427-429, 1998.

[80] L. A. Johansson and A. J. Seeds, "Generation and transmission of millimetre wave data modulated optical signals using an optical injection phase lock loop," *IEEE J. Lightwave Technol.*, vol. 21, no. 2, pp. 511-520, 2003.

[81] L. A. Johansson, and A. J. Seeds, "Millimeter-wave radio-over-fibre transmission using an optical injection phase lock loop source," *IEEE Int. Topical Meeting Microwave Photonics (MWP)*, pp. 129-132, 2000.

[82] L. A. Johansson and A. J. Seeds, "36 GHz 140 Mbit/s radio over fibre transmission using an optical injection phase lock loop source", *IEEE Photon. Technol. Lett.*, vol. 13, no. 8. pp. 893-895, 2001.

[83] L. A. Johansson, C. P. Liu and A. J. Seeds, "A 65 km span unamplified transmission of 36 GHz radio over fibre signals using an optical injection phase lock loop", *IEEE Photon. Technol. Lett.*, vol. 14, no. 11, pp. 1596-1598, 2002.

[84] A. Martinez, V. Polo, J. L. Corral and J. Marti, "Experimental demonstration of dispersion tolerant 155 Mbit/s BPSK data transmission at 40 GHz using an optical coherent harmonic generation technique", *IEEE Photon. Technol. Lett.*, vol. 15, no. 6, 2003.

[85] D. Novak, G. H. Smith, A. J. Lowery, H. F. Liu and R. B. Waterhouse, "Millimetre wave fibre wireless transmission systems with reduced effects of fibre chromatic dispersion", *IEEE J. Optical and Quantum Electron.*, vol. 30, pp. 1021-1031, 1998.

[86] R. P. Braun, G. Grosskopf, D. Rhode and F. Schmidt, "Low phase noise millimetre wave generation at 64 GHz and data transmission using optical single sideband injection locking", *IEEE Photon. Technol. Lett.*, vol. 10, no. 5, pp. 728-730, 1998.

[87] T. Kawanishi, H. Kiuchi, M. Yamada, T. Sakamoto, M. Tsuchiya, J. Amagai and M. Izutsu, "Quadruple frequency double sideband carrier suppressed modulation using high extinction ratio optical modulators for photonic local oscillators", *IEEE Int. Topical Meeting Microwave Photonics (MWP)*, pp. 9-12, 2005.

[88] J. Kondo, K. Aoki, Y. Iwata, A. Hamajima, T. Ejiri, O. Mitomi and M. Minakata, "76 GHz millimetre wave generation using MZ LiNbO3 modulator width a drive voltage of 7 Vp-p and 19 GHz signal input", *IEEE Int. Topical Meeting Microwave Photonics (MWP)*, PDP-01, pp. 1-4, 2005.

[89] T. Ismail, C. P. Liu, J. E. Mitchell, A. J. Seeds, X. Qian, A. Wonfor, R. V. Penty and I. H. White, "QPSK wireless data over 12.8 km fibre transmission with remote millimetre-wave LO delivery using a bi-directional SOA in a full-duplex system incorporating a 2.2 km CWDM fibre ring architecture", *IEEE Photon. Technol. Lett.*, vol. 17, pp. 1989-1991, 2005.

[90] H. Schmuck, R. Heidemann and R. Hofstetter, "Distribution of 60 GHz signals to more than 1000 base stations", *Electron Letts.*, vol. 30, pp. 59-60, 1994.

[91] K. Morita and H. Ohtsuka, "The new generation of wireless communication based on fibre radio technologies", *IEICE Trans. Commun.*, vol. E76B, pp. 1061-1068, 1993.

[92] D. Novak, G. H. Smith, C. Lim, H. F. Liu and R. B. Waterhouse, "Optically fed millimetre wave fibre wireless communications", *Optical Fibre Communications (OFC)*, pp. 14-16 1998.

[93] S. Komaki, K. Tsukamoto, M. Okada and T. Ishida, "Trends of optically fed wireless communication systems", *IEE J. Optical and Quantum Electron.*, vol. 30, pp. 1079-1088, 1998.

[94] H. Yanikomeroglu and E. S. Sousa, "Antenna interconnection strategies for personal communication systems", *IEEE J. Selected Areas in Commun.*, 15, pp. 1327-1336, 1997.

[95] R. Ramaswami and K. Liu, "Analysis of effective power budget in optical bus and star networks using erbium doped fibre amplifiers", *IEEE J. Lightwave Technol.*, vol. 11, no. 11, pp. 1863-1871, 1993.

[96] P. P. Lannone, K. C. Reichmann and N. J. Figo, "WDM access networks", *European Conference on Optical Communication (ECOC)*, vol. 4, pp. 1-2, 2002.

[97] A. Nkansah & N. J. Gomes, "A WDM/SCM star/Tree fibre-feed architecture for pico-cellular broadband systems", *IEEE Int. Topical Meeting Microwave Photonics (MWP)*, pp. 27-274, 2003.

[98] K. Kumozaki, "A fibre optic passive double star network for microcellular radio communication systems applications", *IEICE Trans. Commun.*, vol. E76-B, pp. 1122-1127, 1993.

[99] G. H. Smith, D. Novak and C. Lim, "A millimeter-wave full-duplex fibre radio star-tree architecture incorporating WDM and SCM", *IEEE Photon. Technol. Letts.*, vol. 10, no. 11, pp. 1650-1652, 1998.

[100] Jie Lin and Fow-Sen Choa, "Demonstration of a broadband wireless backbone using ultra dense WDM technology", *CLEO*, CTuS2, pp. 276-277, 2002.

[101] C. Lim, A. Nirmalathas, D. Novak and R. Waterhouse, "Capacity analysis for a WDM fibre radio backbone incorporating wavelength interleaving", *Optical Fibre Communications*, pp. 255-357, 2002.

[102] C. Lim, A. Nirmalathas, D. Novak and R. Waterhouse, "Capacity analysis for WDM fibre radio backbones with star-tree and ring architecture incorporating wavelength interleaving," *IEEE J. Lightwave Technol.*, vol. 21, no. 12, pp. 3308-3315, 2003.

[103] K. Kitayama, "Highly spectrum efficient OFDM/PDM wireless networks by using optical SSB modulation", *IEEE J. Lightwave Technol.*, vol. 16, pp. 969-976, 1998.

[104] R. Regan, W. Rideout and D. Tang, "Antenna remoting over optical fibre using a bus architecture", *IEEE Trans. Microwave Theory & Tech.*, pp. 77-78, 1995.

[105] K. Kojucharow, H. Kaluzni, M. Sauer and W. Nowak, "A wireless LAN at 60 GHz-novel system design and transmission experiments", *IEEE MTT-S Int. Microwave Symposium (IMS)*, pp. 1513-1516, 1998.

[106] A. Paolella, K. Lafond, J. Borlando, M. Aviles and C. Simpkins, "Photonic transport for broadband wireless access and personal communication services", *IEEE Int. Topical Meeting Microwave Photonics (MWP)*, pp. 49-52, 2001.

[107] X. Zhang, B. Liu, J. Yao, Ke Wu, and R. Kashyap, "A novel millimetre wave band radio over fibre system with dense wavelength division multiplexing bus architecture", *IEEE Trans. Microwave Theory & Tech.*, vol. 54, no. 2, pp. 929- 937, 2006.

[108] M. I. Irshid and M. Kavehrad, "A fully transparent fibre optic ring architecture for WDM networks", *IEEE J. Lightwave Technol.*, vol. 10, no. 1, pp. 101- 108, 1992.

[109] M. Haner, T. N. Neilsen, J. Nykolak. H. Z. Chen, T. Tanbun-Ek, A. Vengsarkar, K. L. Walker and K. Wecht, "Broadband fibre loops with wireless access", *European Conference on Optical Communication (ECOC)*, pp. 227-230, 1995.

[110] A. Kaszubowska, L. P. Barry and P. Anandarajah, "Multifunctional operation of a fibre bragg grating in a WDM/SCM radio over fibre distribution system," *IEEE Laser & Electro-Optics Society (LEOS)*, pp.861-862, 2003.

[111] R. Heinzelmann, T. Kuri, K. Kitayama, A. Stohr and D. Jager, "Optical add drop multiplying of 60 GHz millimetre wave signals in a WDM radio on fibre ring", *Optical Fibre Communications (OFC)*, pp. 137-139, FH4-1, 2000.

[112] A. Stohr, K. Kitayama and D. Jager, "Full duplex fibre optic rf subcarrier transmission using a dual function modulator/photodetector", *IEEE Trans. Microwave Theory & Tech.*, vol. 47, pp. 1338-1341, 1999.

[113] C. Marra, A. Nirmalathas, C. Lim, D. Novak, "OADM with a multiple phase shifted FBG for a wavelength interleaved millimetre wave fibre radio system", *Optical Fibre Communications*, 2003.

[114] C. Lim, A. Nirmalathas, M. Attygalle, D. Novak and R. Waterhouse, "On the merging of millimetre-wave fibre radio backbone with 25 GHz WDM ring networks," *IEEE J. Lightwave Technol.*, vol. 21, pp. 2203-2210, 2003.

[115] J. Kim and B. Lee, "Bidirectional wavelength add-drop multiplexer using multiport optical circulators and fibre bragg gratings", *IEEE Photon. Technol. Letts.*, vol. 12, no. 5, pp. 561-563, 2000.

[116] K. C. Reichmann, N. J. Frigo, P. P. Lannone and L. H. Spiekman, "A simple Bi-directional node for WDM virtual ring networks", *IEEE Laser & Electro-Optics Society (LEOS)*, ThB2, pp. 690-691, 2000.

[117] Hyun Deok Kim, Jeong-Hun Shin, Chang-Gyu Lim, Sang-Mook Lee, Yunhee Cho and Chang-Hee Lee, "Demonstration of bi-directional WDM network", *Optical Fibre Communications*, pp. 353-355, 2002.

[118] Keang-Po Ho, Shien-Kuei Liw and F. F-K. Tong, "Bidirectional single fibre wavelength ring networks", *IEICE Trans. Commun.*, vol. E83-B, no. 10, pp. 2245- 2252, 2000.

[119] T. Ohira, H. Souda, H. Yamamoto and K. Utsumi, "CWDM transmitter/receiver modules for radio over fibre systems", *European Conference on Optical Communication*, We4.P.71, pp. 698-699, 2003.

[120] Wen-Piao. Lin, Ming-Seng. Kao and S. Chi, "A reliable architecture for broadband fibre wireless access networks", *IEEE Photon. Technol. Letts.*, vol. 15, no. 2, pp. 344-346, 2003.

[121] B. S. Johansson, C. R. Batchellor and L. Egnell, "Flexible bus: a self restoring optical ADM ring architecture", *Electron. Lett.*, vol. 32, pp. 2338-2339, 1996.

[122] Hyo-Sik Yang, M. Herzog, M. Maier and M. Reisslein, "Metro WDM networks: Performance comparison of slotted ring and AWG star network", *IEEE J. Commun.*, vol. 22, pp. 1460- 1473, 2004.

[123] G. E. Keiser, "A review of WDM technology and applications", *Optical Fibre Technology*, vol. 5, pp. 3-39, 1999.

[124] V. W. S. Chan, K. Hall, E. Modiano and K. A. Rauschenbach, "Architectures and technologies for high speed optical data networks", *IEEE J. Lightwave Technol.*, vol. 16, pp. 2146-2168, 1998.

[125] S. F. Su and R. Olshansky, "Performance of multiple access WDM networks with subcarrier multiplexed control channels", *IEEE J. Lightwave Technol.*, vol. 11, pp. 1028-1033, 1993.

[126] J. M. Senior, M. R. Handley, and M. S. Leeson, "Developments in wavelength division multiple access networking", *IEEE Commun Mag.*, vol. 26, pp. 28-36, 1998.

[127] V. Tholey, M. J. Chawki, L. Bethou, I. Legac, E. Gay and A. Poudoulec, "Demonstration of WDM survivable unidirectional ring network using tunable channel dropping receivers", *Electron. Lett.*, vol. 30, pp.1323-1324, 1994.

[128] H. Thiele, L. Nelson, J. Thomas, B. Eichenbaum, L. Spikeman and G. Van de Hoven, "Linear optical amplifier for extended reach in CWDM transmission systems", *Optical Fibre Communications (OFC)*, MF21, pp. 23-24, 2003.

[129] A. V. Tran, W. D. Zhong, R. S. Tucker and R. Lauder, "Optical add drop multiplexers with low crosstalk", *IEEE Photon. Technol. Letts.*, vol. 13, pp. 582-584, 2001.

[130] D. Castleford, A. Nirmalathas and D. Novak, "Impact of optical crosstalk in fibre radio systems incorporating WDM", *IEEE Int. Topical Meeting Microwave Photonics (MWP)*, TU1.6, pp. 51-54, 2000.

[131] D. Castleford, A. Nirmalathas, D. Novak and R. S. Tucker, "Optical crosstalk in fibre radio WDM networks", *IEEE Trans. Microwave Theory & Tech.*, vol. 49, no. 10, pp. 2030-2035, 2001.

[132] Y. Jin, Q. Zeng and W. Hu, "Comparison of intraband crosstalk penalty in WDM networks for externally and directly modulated lasers", *Electron. Lett.*, vol. 35, pp. 220-221, 1999.

[133] P. J. legg, D. K. Hunter, I. Andonovic and P. E. Barnsley, "Interchannel crosstalk phenomena in optical time division multiplexed switching networks", *IEEE Photon. Technol. Letts.*, vol. 6, pp. 661-663, 1994.

[134] L. Moura, M. Darby. P. M. Lane and J. J. O'Reilly, "Impact of interferometric noise on the remote delivery of optically generated millimetre wave signals", *IEEE Trans. Microwave Theory & Tech.*, vol. 45, pp. 1398-1402, 1997.

[135] J. E. Mitchell, P. M. Lane and J. J. O'Reilly, "Performance of radio over fibre broadband access in the presence of interferometric noise", *IEEE Laser & Electro-Optics Society (LEOS)*, pp. 29-30, 2000.

[136] M. D. Feuer, C. F. Lam, L. M. Lunardi and S. L. Woodward, "Crosstalk in a metro scale ring with passive optical add/drop", *IEEE Laser & Electro-Optics Society*, vol. 2, ThB4, pp. 694-695, 2000.

[137] J. Zhou, M. J. Omahony and S. D. Walker, "Analysis of optical crosstalk effects in multi-wavelength switched networks", *IEEE Photon. Technol. Letts.*, vol. 6, pp. 302-305, 1994.

[138] E. L. Goldstein and L. Eskildsen, "Scaling limitations in transparent optical networks due to low level crosstalk", *IEEE Photon. Technol. Letts.*, vol. 7, pp. 93-94, 1995.

[139] S. D. Dods and R. S. Tucker, "A comparison of the homodyne crosstalk characteristics of optical add drop multiplexers", *IEEE J. Lightwave Technol.*, vol. 19, pp. 1829-1838, 2001.

[140] K-P. Ho, C. K. Chan, F. K. Tong and L. K. Chen, "Exact analysis of homodyne crosstalk induced penalty in optical networks", *IEEE Photon. Technol. Letts.*, vol. 10, pp. 457-458, 1998.

[141] M. Shibutani, W. Domon and K. Emura, "Reflection induced degradations in optical fibre feeder for microcellular mobile radio systems", *IEICE Trans. Electron.*, vol. E76-C, pp. 287-292, 1993.

[142] A. E. Willner and S-M. Hwang, "Transmission of many WDM channels through a cascade of EDFA's in long distance links and ring networks", *IEEE J. Lightwave Technol.*, vol. 13, pp. 802- 816, 1995.

[143] J. Namiki, M. Shibutani, W. Domon, T. Kanai and K. Emura, "Optical feeder basic system design for microcellular mobile radio", *IEICE Trans. Commun.*, vol. E76-B, no. 9, pp. 1069-1077, 1993.

[144] T. Kurniawan, A. Nirmalathas, C. Lim, D. Novak and R. Waterhouse, "Performance analysis of optimised millimetre wave fibre radio links", *IEEE Trans. Microwave Theory & Tech.*, vol. 54. no. 2, pp. 921-928, 2006.

[145] C. Carlsson, A. Larsson and A. Alping, "RF transmission over multimode fibers using VCSELs-comparing standard and high bandwidth multimode fibers", *IEEE J. Lightwave Technol.*, vol. 22, no. 7, pp. 1694-1700, 2004.

[146] J. A. MacDonald, M. V. Kubak and A. Katz, "Wideband dynamic range improvement of microwave photonic links", *IEEE Avionics Fiber Optics & Photonics*, TuA1, pp. 67-68, 2005.

[147] D. Marcuse "Calculation of bit error probability for a lightwave system with optical amplifiers and post detection Gaussian noise", *IEEE J. Lightwave Technol.*, vol. 9, no. 4, pp. 505-513, 1991.

[148] G. P. Agrawal, "Application of nonlinear fiber optics", Optics and Photonics, academic press.

[149] N. S. Bergano, F. W. Kerfoot and C. R. Davidson, "Margin measurement in optical amplifier systems", *IEEE Photon. Technol. Letts.*, vol. 5, no. 3, pp. 304-306, 19938.

[150] L. W. Couch, Digital and analog communication systems, Fourth edition, Macmillan Publishing Company.

[151] Y. N. Singh, V. K. Jain and H. M. Gupta, "Semiconductor optical amplifiers in WDM star networks", *IEE Proc. Opto-electron.* vol. 143, no. 2, pp. 144-152, 1996.

[152] T. Durhuus, C. Joergensen, B. Mikkelsen, R. J. S. Pedersen and K. E. Stubkjaer, "All optical wavelength conversion by SOA's in a Mach-Zehnder configuration", *IEEE Photon. Technol. Letts.*, vol. 6, no. 1, pp. 53-55, 1994.

[153] X. Qian, T. Lin, R. V. Penty and I. H. White, Novel SOA based switch for multiple radio over fibre service applications", *Optical Fibre Communications (OFC)*, JThB24, 2006.

[154] A. E. Kelly, C. Tombling, C. Michie and I. Andonovic, "High performance semiconductor optical amplifier", *Optical Fibre Communications (OFC)*, THS1, vol. 2, 2004.

[155] Kamelian Application notes No 0001 Semiconductor optical amplifiers as power boosters

[156] N. K. Dutta and Q. Wang, Semiconductor optical amplifiers, World Scientific Publishing Company.

[157] R. B. Picard, M. Alouini, J. Lopez, N. Vodjdani and Jeac-Claude Simon, "Impact of the gain saturation dynamics in semiconductor optical amplifiers on the characteristics of an anlaog optical link", *IEEE J. Lightwave Technol.*, vol. 23, no. 8, pp. 2420- 2426, 2005.

[158] R. B-Picard, M-B. Bibey and N. Vodjani, "Semiconductor optical amplifiers for microwave photonic links", *IEEE Int. Topical Meeting Microwave Photonics (MWP)*, Tu-4.11, pp. 137-140, 2001.

[159] E. Udvary, T. Berceli, T. Marozsak and A. Hilt, "Semiconductor optical amplifiers in analog optical links", *ICTON*, Th.C.3, pp. 201-206, 2003.

[160] A. A. M. Saleh and I. M. I. Habbab, "Effects of semiconductor optical amplifier nonlinearity on the performance of high speed intensity modulation light wave systems", *IEEE J. Lightwave Technol.*, vol. 38, no. 6, pp. 839-846, 1990.

[161] J. Herrera, F. Ramos and J. Marti, "Nonlinear distortion generated by semiconductor optical amplifier boosters in analog optical systems", *Optics Letts.*, vol. 28, no. 13, pp. 1102-1104, 2003.

[162] E. Udvary, M. Csornyei, G. Maury and Y. Guennec, "SOAs in subcarrier multiplexed optical networks," *MIKON*, pp. 874- 877, 2002.

[163] N. A. Olsson, "Lightwave systems with optical amplifiers", *IEEE J. Lightwave Technol.*, vol. 7, no. 7, pp. 1071-1082, 1989.

[164] S. Park, R. Leavitt, R. Enck, V. Luciani, Y. Hu, P. J. S. Heim, D. Bowler and M. Dagenais, "Semiconductor optical amplifier for CWDM operating over 1540-1620 nm", *IEEE Photon. Technol. Letts.*, vol. 17, no. 5, pp. 980-982, 2005.

[165] P. P. Lannone, K. C. Reichmann and L. H. Spiekman, "Amplified CWDM systems", *IEEE Laser & Electro-Optics Society (LEOS)*, vol. 2, WY1, pp. 678-679, 2003.

[166] Hai-Han. Lu, Ying-Cong. Lin, Yuan-Hong. Su and Heng-Sheng. Su, "A radio on fibre intelligence transport system base on electroabsorption modulator and semiconductor optical amplifier", *IEEE Photon. Technol. Letts.*, vol. 16, no. 1, pp. 251-253, 2004.

[167] X. Qian, P. Hartmann, A. Wonfor, J. D. Ingham, R. V. Penty and I. H. White, "Microwave signal transmission over a directly modulated radio over fibre link using cascaded semiconductor optical amplifiers", *Optical Fibre Communications (OFC)*, vol. 4, OThB2, 2005.

[168] J. M. P. Delavaux et al, "Repeatered bi-directional 10 Gbit/s 240 km fibre transmission experiment", *Optical Fibre Communications (OFC)*, pp. 18-19, 1996.

[169] M. J. Chawki, E. Delevaque and L. Berthou, "WDM bi-directional optical power limiting amplifier including circulators EDFA and fibre grating reflectors", *European Conference on Optical Communication (ECOC)*, TuP.17, pp. 2.285-2.288, 1996.

Chapter 5

Wireless over Fibre Transmission: Experimental Results

In this chapter experimental measurements are reported for wireless over fibre systems. The Introduction 5.1, give a brief overview and states the objectives of the demonstrations presented in this chapter. Section 5.2 describes a complete wireless over fibre transmission system employing feed-forward linearisation at the base station (BS) to improve performance in a multi-channel system. In the next Section 5.3 Coarse Wavelength Division Multiplexing (CWDM) ring architecture for millimetre-wave (mm-wave) signal distribution using a bi-directional Semiconductor Optical Amplifier (SOA) together with 40 GHz Local Oscillator (LO) source is demonstrated. A high data rate mm-wave Gigabit/s (Gbit/s) over fibre transmission system using Differential Phase Shift Keying (DPSK) is experimentally investigated in Section 5.4 using low cost optical sources for IF signals and CWDM devices. Finally, the last Section 5.5 Conclusion draws some of the important results from this chapter.

5.1 Introduction

Wireless over fibre is an attractive technology for the realisation of high capacity future broadband wireless access networks. For a simple and cost efficient solution direct modulation of uncooled lasers is preferred. Signals are generated at the central station (CS) and distributed using (CWDM) filters. These filters are used as optical add/drop multiplexers (OADM) and are employed for routing different wavelengths to their intended remote BS. The CWDM filters are inherently less expensive than dense WDM filters due to fewer numbers of layers in the filter design and relaxed performance specifications. The wavelength spacing for the channels is based on a 20 nm grid to allow margin for drift from the nominal wavelength due to manufacturing tolerances, temperature range and bias current. In the following experiments CWDM devices such as uncooled laser diodes and passive WDM components are used to demonstrate how low cost full duplex systems can be constructed.

5.2 Full Duplex RF System

The performance of an optical transmission system depends greatly on the non-linearity of the laser diode source. Since the BS can receive simultaneously high and low power signals, depending on how

far the users are from the BS, any non-linearity in the optical link, such as non-linear distortion introduced by a directly modulated laser, can cause spectral re-growth from a strong input signal, interfering with a weak neighbouring channel and thus limiting the system performance. Previous demonstrations of feed-forward have mainly been over a single fibre link. The complete system configuration for a full duplex wireless over fibre system is demonstrated in Figure 5.2 together with measured optical spectra at various points. Full duplex transmission takes place between the CS and the BSs. In this system feed-forward linearisation shown in Figure 5.1 is employed at BS 1 to linearise the output of laser 2A. The aim of the experiment was to measure the effectiveness of feed-forward linearisation at the BS, hence transmission only occurred for the uplink, from the BS to CS. The remote BSs are connected via OADM to a 2.2 km single mode fibre (SMF) ring.

5.2.1 Transmission experiment

Figure 5.1 show the implementation of the feed-forward circuit, employed at BS 1 to linearise the optical intensity output of laser L_{2A} that is directly modulated with two channels. The detailed working principle of the feed-forward linearisation has been reported in [1]. For maximum cancellation of the distortion products amplitude and phase matching is critical both for the carrier cancellation loop and the distortion cancellation loop. This is facilitated with the use of variable gain amplifiers and microwave phase shifters.

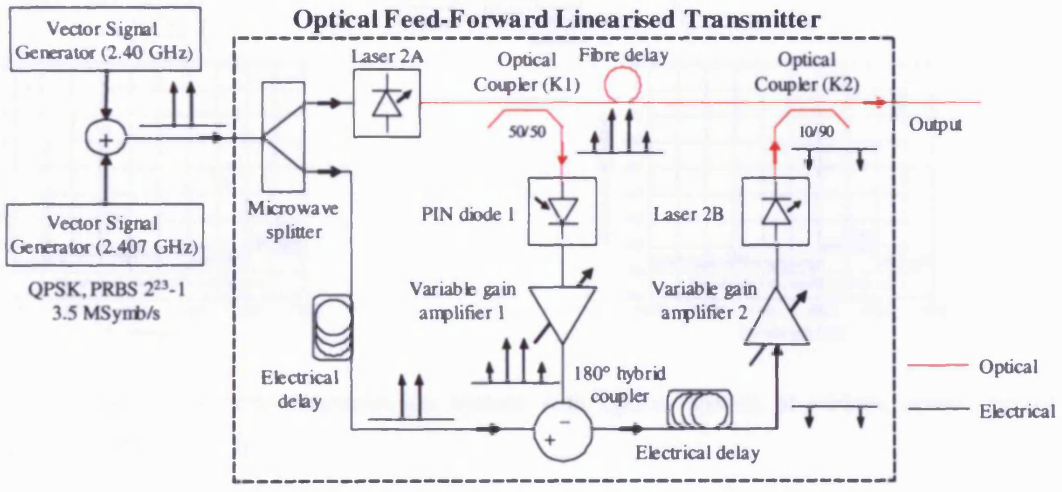

Figure 5.1 Feed-forward linearisation arrangement

For the system experiment in Figure 5.2, in the downlink direction, laser L_1, operating around 1510 nm wavelength (λ_1), and laser L_3, operating around 1570 nm wavelength (λ_3) at the CS are multiplexed and then transported to the 2.2 km fibre ring [2]. At OADM 1, λ_1 is dropped and λ_3 continues in the fibre ring and is dropped at its intended BS 2 via OADM 2. In the uplink direction, laser L_{2A} of wavelength 1532.7 nm (λ_2) at BS 1 is directly modulated by the combined output of two Rhode and Schwarz SMU200A vector signal generators providing 3.5 MSymb/s Quadrature Phase Shift Keying (QPSK) data channel at 2.4 GHz and 2.407 GHz. To compensate laser non-linear

distortion feed-forward linearisation is used. The feed-forward arrangement uses a secondary laser L_{2B} at a wavelength of 1529 nm and this can be observed in the optical spectra after the signals are added from BS 1 to the fibre ring using a CWDM filter. λ_2 now carrying the QPSK modulated data and λ_4 from BS 2 are transported back to the CS after transmission through the ring network. At the CS the wavelengths are separated using a de-multiplexer consisting of filters. The linearised modulated signal on λ_2 is detected using a 12 GHz photodiode, amplified with 50 dB gain RF amplifiers and finally demodulated using a Rhode & Schwarz FSQ8 vector signal analyser (VSA).

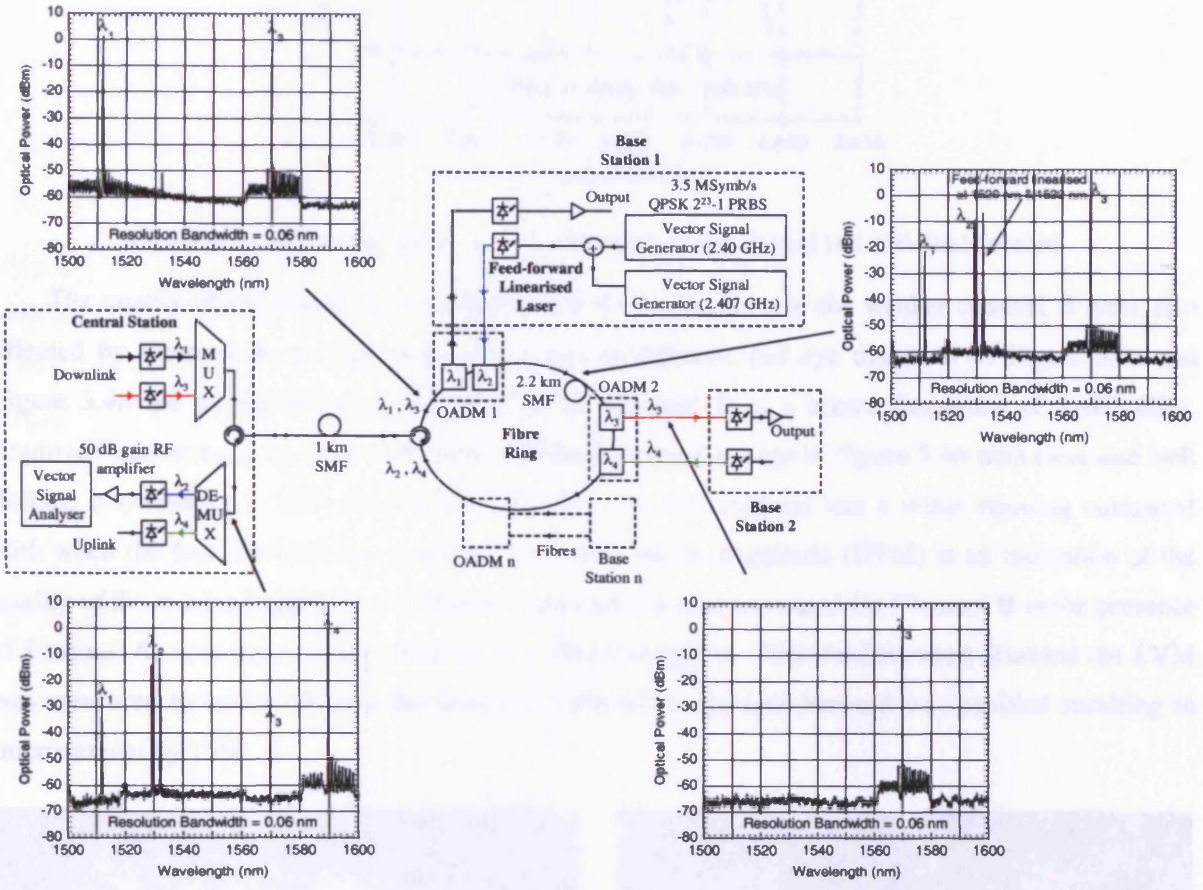

Figure 5.2 Wireless over fibre transmission system with optical spectra at various points. Feed-forward linearisation is employed at BS 1

5.2.2 Results

To illustrate the effectiveness of feed-forward linearisation in suppressing spectral re-growth two channels are applied. Channel A is fixed with +12 dBm RF power and Channel B with –20 dBm. The RF spectra of the two transmitted channels were measured at the receiver with feed-forward disabled and enabled as shown in Figure 5.3. When feed-forward was disabled, the non-linearity generated from laser L_{2A} caused spectral re-growth from Channel A to interfere with the frequency band of the neighbouring Channel B. With feed-forward enabled the non-linearity was compensated and the spectral re-growth was suppressed by 8 dB allowing the spectrum of Channel B to be clearly seen.

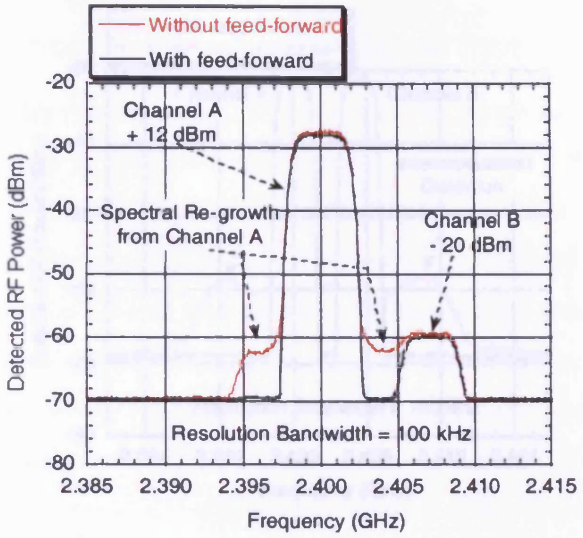

Figure 5.3 Detected RF spectra at 2.4 GHz without feed-forward and with feed-forward

The quality of the measured constellations and eye diagrams of the weaker channel B were also affected by Channel A spectral re-growth. The constellation and eye diagrams in Figure 5.4a and Figure 5.4b are measured using the VSA set to Channel B at a centre frequency of 2.407 GHz. Improved transmission has been achieved with feed-forward as seen in Figure 5.4b with clear and well defined constellations. With feed-forward enabled, the eye diagram had a wider opening compared with when the feed-forward was disabled. The error vector magnitude (EVM) is an indication of the quality of the received digitally modulated signal and was also measured for Channel B in the presence of Channel A, with input power fixed at +12 dBm throughout. With feed-forward disabled the EVM was measured to be 24.6% and decreased to 9.4% when the feed-forward was enabled resulting in improvement by 15%.

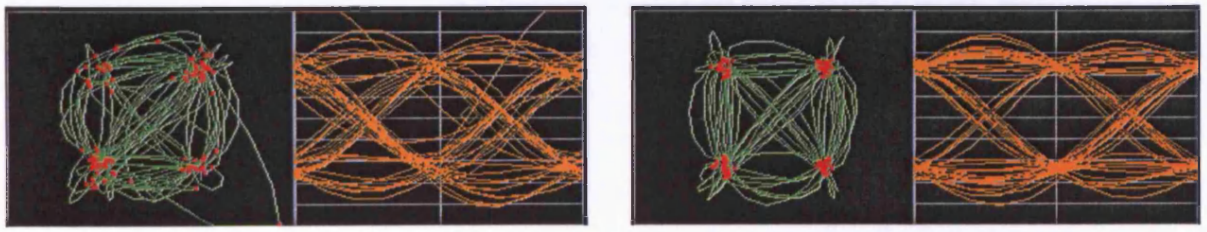

(a) (b)

Figure 5.4 Detected -23 dBm Channel B constellation and eye diagram with Channel A at +12 dBm (a) without feed-forward (b) with feed-forward

Finally the input powers of both Channel A and Channel B were set equal at +12 dBm and the measured RF spectra are shown in Figure 5.5. It can be seen that with feed-forward disabled, there was strong intermodulation distortion caused by the two high power input signals modulating laser L_{2A} and any low power signals in the adjacent channel frequency bands would have been severely degraded. With feed-forward enabled, the intermodulation distortion was suppressed by more than 10 dB.

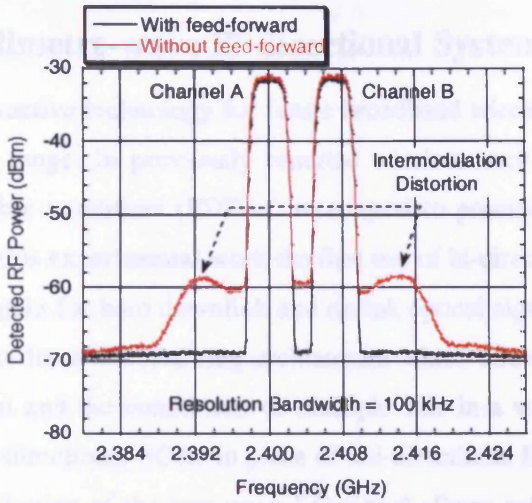

Figure 5.5 Detected RF spectra with feed-forward enabled and disabled, channels A and B are set at +12 dBm

Although the system is demonstrated at 2.4 GHz laser non-linearity gets worse at higher frequency such as 5 GHz required for the IEEE802.11a wireless LAN standard. Direct modulation of the laser at 5 GHz generates significantly high distortion and feed-forward is a successful technique that can be employed to compensate these distortion products leading to improved overall system performance.

5.3 Full Duplex Millimetre-wave Bi-directional System

Wireless over fibre is an attractive technology for future broadband wireless access systems operating in the mm-wave frequency range. In previously reported wireless over fibre systems separate uni-directional erbium doped fibre amplifiers (EDFAs) were used to provide the necessary gain for the downlink and uplink [3]. In this experimental work the first use of bi-directional semiconductor optical amplifier (SOA) to provide gain for both downlink and uplink optical signals simultaneously, together with the experimental results for a CWDM ring architecture which allows distribution of a centrally generated 40 GHz LO signal and the connection of multiple BSs in a wireless over fibre network is demonstrated. The use of bi-directional SOAs in place of uni-directional EDFAs, together with the use of CWDM and optical distribution of the mm-wave LO signal allows substantial reduction in overall systems complexity and cost, as will be necessary for the widespread adoption of mm-wave wireless access systems. It also increases utilisation of the deployed fibre, an economic advantage where leased fibre has to be used [4].

The system comprises a 12.8 km SMF backbone link with a 2.2 km fibre ring for signal distribution to a group of remotely located BSs. Optically modulated 3.5 MSymb/s wireless data signals to and from the BSs are distributed at intermediate frequencies (IF) in the 2.40 GHz to 2.50 GHz band to overcome fibre dispersion using directly modulated uncooled distributed feedback (DFB) lasers. At intermediate frequencies the signals can be transmitted over longer distances since the effect of fibre chromatic dispersion on the distribution of lower frequency IF signal is less severe than for mm-wave signals [5]. The laser emission wavelengths are selected on a 20 nm pitch CWDM grid to route signals to and from the required BS. The common 40 GHz LO source is optically generated by injection locking two slave DFB lasers to two sidebands of an externally modulated master tunable laser and distributed to multiple remotely located BSs for frequency up and down conversion to mm-wave. The delivery of the LO signal is tolerant to fibre dispersion since it is generated in a single sideband form.

5.3.1 Optically generated 40 GHz LO source

The 40 GHz LO signal is provided by heterodyning the output of two DFB lasers that are injection locked to two modulation sidebands of a Mach-Zehnder modulator (MZM) driven at 20 GHz and biased at null to give suppressed centre wavelength. This is a development of the technique reported by Braun *et al* [6] in which generation of a 64 GHz signal by optical injection locking two slave DFB lasers to the −10th and +10th modulation sidebands of a master DFB laser which was directly and heavily modulated at 3.2 GHz with +23.4 dBm input was reported. Figure 5.6 illustrates the experimental arrangement of the 40 GHz LO source used in this experiment. In Figure 5.6 the MZM externally modulates the output of the CW tuneable master laser source whose centre wavelength was set at 1543.6 nm (λ_0) with 8.1 dBm output power. When the MZM is driven by a 20 GHz microwave

signal generator with +10 dBm RF power, its optical output contains mainly two modulation sidebands located at ± 20 GHz offset from the suppressed 1543.6 nm line. Because the MZM is biased at null at 7.3V (V_π), the unmodulated optical transmission is minimum. The two main sidebands are therefore 40 GHz apart and effectively the MZ is functioning as a frequency doubler. Slave laser DFB 1 is injection locked by one sideband and slave laser DFB 2 by the other. The injection locked output of the two slave lasers are then combined in a 50% coupler forming a 40 GHz spaced reference signal. The polarisations of the two injection locked slave lasers are aligned before their outputs are combined in a 50% coupler forming the 40 GHz heterodyne beat signal. Since the two injection locked, closely spaced optical carriers travel along the same fibre polarisation can be maintained throughout.

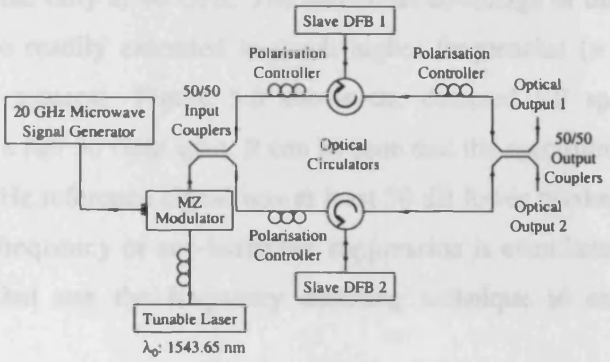

Figure 5.6 Optically generated 40 GHz LO source using heterodyning and injection locking

Figure 5.7 shows the optical spectrum at the output of the MZM and that at the output of the injection locked heterodyne LO source. It can be seen at the MZM output that the suppressed centre optical carrier at 1543.65 nm is 26 dB below the two 40 GHz spaced optical sidebands while it is at least 34 dB below at the output of the injection locked heterodyne LO source. Exact measurement of the suppressed centre optical carrier is limited by the finite resolution bandwidth of the optical spectrum analyser. The advantages of heterodyning the two injection locked slave DFB lasers instead of simply taking the frequency doubled output directly from the MZ modulator are the 15 dB increase

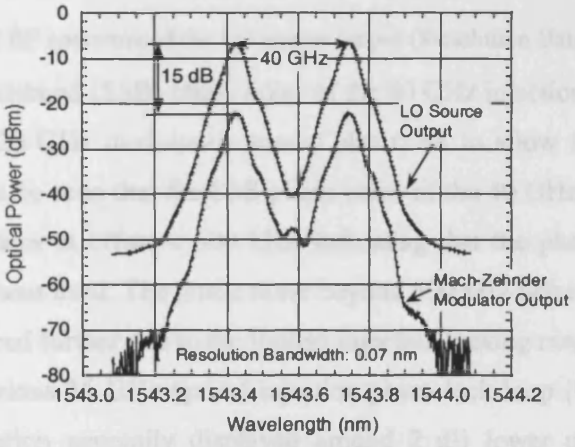

Figure 5.7 Optical spectra at the MZM output and at the injection locked heterodyne LO source output

in the optical output power level and further suppression of the tuneable laser source centre wavelength at 1543.6 nm. If high power lasers are used then the optical output power can be further increased. Since the two modulation sidebands are each offset by 20 GHz from 1543.6 nm, insufficient suppression of this centre wavelength would result in the generation of an unwanted 20 GHz signal in the detected RF spectrum of the LO source output. Although the 20 GHz beat signal can be filtered, optical filters of this high resolution would require temperature control and active tracking, greatly increasing system cost. Post detection electrical filtering would imply waste of SOA power capability in amplifying the spurious signals. This method of generating and delivering the LO over fibre is dispersion tolerant, since the dual mode signal arising from the two optical sidebands injected from the MZM result in a beat signal only at 40 GHz. The additional advantage of this generation technique is that this approach can be readily extended to much higher frequencies (> 100 GHz) increasing its attractiveness for future systems. Figure 5.8 shows the detected RF spectrum of this 40 GHz heterodyne LO source in a full 50 GHz span. It can be seen that the spectrum contained a very pure 40 GHz signal and the 20 GHz reference signal was at least 50 dB lower masked by the equipment noise floor. This level of half frequency or sub-harmonic suppression is even better than some commercial mm-wave synthesisers that use the frequency doubling technique to extend their upper output frequency limit.

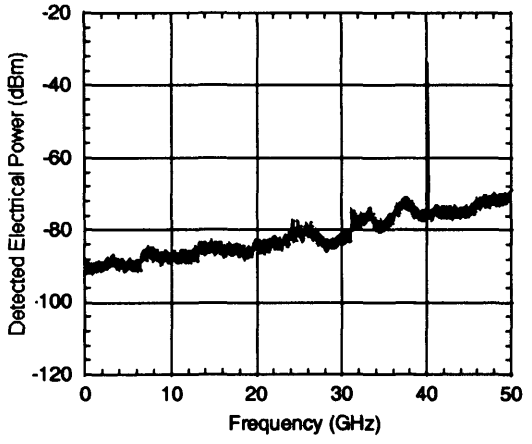

Figure 5.8 Detected RF spectrum of the LO source output (Resolution Bandwidth = 300 kHz)

The detected single sideband (SSB) phase noise of the 40 GHz injection locked heterodyne source and that of the reference 20 GHz modulation source plus 6 dB to allow for frequency doubling are shown in Figure 5.9. It can be seen that the SSB phase noise of the 40 GHz LO source follows that of the reference signal generator at offset < 500 kHz, indicating that the phase noise performance was limited only by the equipment used. The phase noise beyond 500 kHz offset remains around -110 dBc (1 Hz) and cannot be reduced further due to the limited injection locking range.

Compared to the previous 36 GHz optical injection phase lock loop (OIPLL) heterodyne source [7], the present configuration generally displayed around 2 dB lower phase noise which can be attributed to the injection level being increased using an external tunable master laser source and

absence of high power spurious optical signals injected into the two slave lasers. The latter reason can be further clarified by noting that if a slave is required to be injection locked to one of the two or more low level sidebands of a directly modulated master laser, the injection locking process can be severely affected and made unstable due to the presence of the high power optical line at the master laser centre wavelength which has to be injected into the slave laser along with other low level modulation sidebands. The present configuration does not have this problem because of the use of an external MZ modulator for generating those injection sidebands with the tunable master optical power at the centre wavelength suppressed.

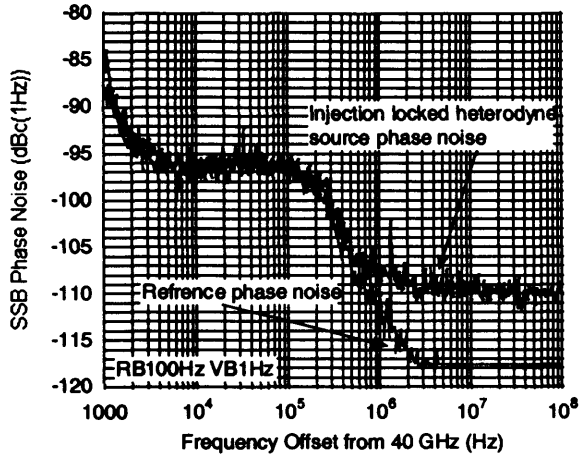

Figure 5.9 Detected single sideband (SSB) phase noise spectra of the 40 GHz injection locked heterodyne LO source and the 20 GHz reference signal generator source

5.3.2 Transmission experiment

Figure 5.10 shows the complete experimental arrangement of the wireless over fibre transmission system. Full duplex transmission occurs between the CS and BS 1. BS 1 is connected via OADM 1 to a 2.2 km SMF ring. The fibre ring in turn is connected to the CS via a bi-directional SOA and a 12.8 km backbone SMF. The OADMs used are constructed using low cost CWDM filters and are employed for routeing different wavelengths to their intended remote BSs. Measured optical and detected electrical spectra at various points in the transmission experimental arrangement are also shown in Figure 5.10.

In the downlink direction, laser L_1, operating at 1512.3 nm wavelength (λ_1), at the CS is directly modulated with 3.5 MSymb/s QPSK data at 2.40 GHz carrier frequency (Channel 1) provided by a vector signal generator. Laser 1 is a CWDM uncooled directly modulated laser with bias current set to 40 mA. The modulated output of laser L_1 (λ_1) is multiplexed with the output of the optically generated 40 GHz LO source whose two sidebands are centred around wavelength λ_0. Both λ_0 and λ_1 are then transported to the fibre ring via the 12.8 km SMF and the bi-directional SOA. The SOA used is a Kamelian OPA22-N-C-FA device having a 3dB bandwidth of 59 nm at a centre wavelength of 1500 nm with a bias current of 160 mA and provides simultaneous gain for downlink and uplink. From the

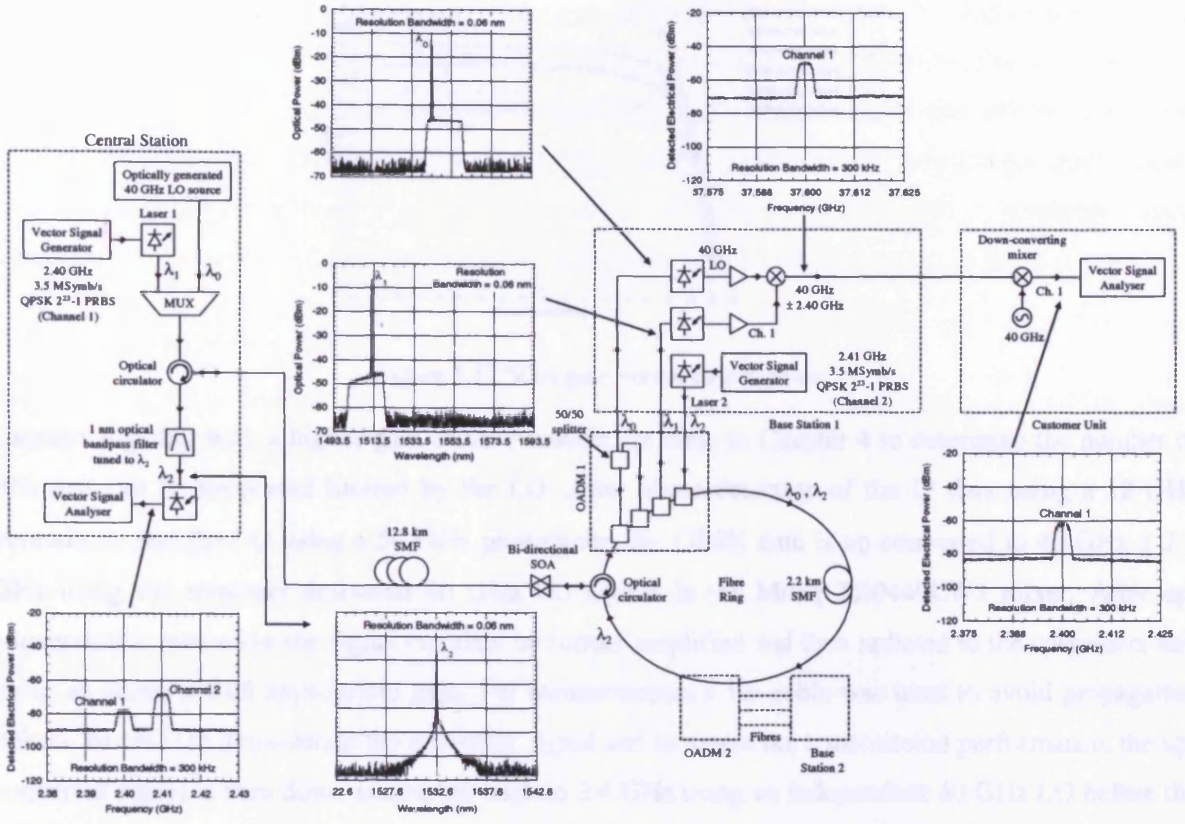

Figure 5.10 Full duplex wireless over fibre transmission experimental arrangement with electrical and optical spectra at various points

manufacturers data sheet the SOA gain is in the region of 20 dB (Figure 5.11) with a saturation output power of approximately 9 dBm (Figure 5.12) and a noise figure of 8.6 dB (Figure 5.13).

At OADM 1, the λ_1 signal, carrying the QPSK data, is dropped using a CWDM filter and delivered to BS 1. Around 50% of the λ_0 power carrying the LO is also dropped and delivered to BS 1 by OADM 1 whilst the remaining 50% is allowed to proceed to OADM 2 and to be used for further frequency conversions at another BS. The CWDM filters centred at 1550 nm have a ± 6.5 nm tolerance resulting in 13 nm bandwidth and the LO wavelength at 1543.65 nm falls within the filter bandwidth. The LO signal can potentially be distributed to more BSs using different coupling ratios for the optical

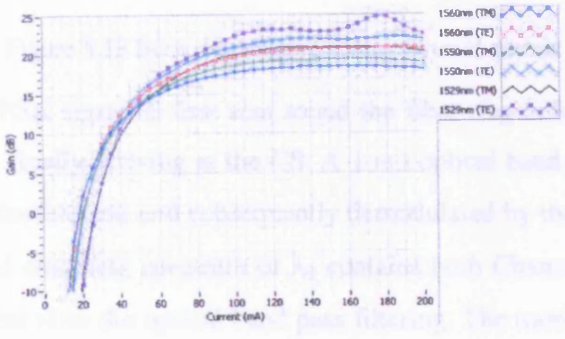

Figure 5.11 SOA gain versus forward current

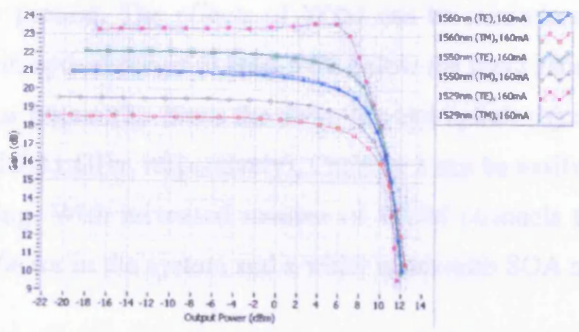

Figure 5.12 SOA gain versus output power

couplers together with a higher gain SOA. Analysis are done in Chapter 4 to determine the number of BSs that can be supported limited by the LO. After photo-detection of the IF data using a 12 GHz photodiode and the LO using a 50 GHz photodiode, the QPSK data is up-converted to 40 GHz ± 2.4 GHz using the remotely delivered 40 GHz LO source in the Miteq TB0440LW1 mixer. After up-conversion to mm-wave the signal can then be further amplified and then radiated to the customers unit using an antenna with appropriate gain. For measurements a 1m cable was used to avoid propagation effects. In order to demodulate the downlink signal and to assess the transmission performance, the up-converted signal is then down-converted back to 2.4 GHz using an independent 40 GHz LO before the QPSK data is detected using a VSA.

In the uplink direction, Laser 2 of 1532.7 nm wavelength (λ_2) at BS 1 is directly modulated with 3.5 MSymb/s QPSK data at 2.41 GHz (Channel 2) provided by another VSG. The 2.2 km fibre ring allows more base stations to be remotely connected in order to provide sufficient wireless coverage. λ_2

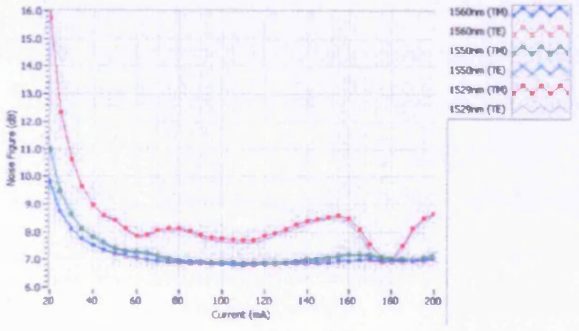

Figure 5.13 SOA noise figure versus forward current

now carrying the uplink QPSK signal is first sent round the fibre ring before going through the SOA and the 12.8 km SMF, and finally arriving at the CS. A 1 nm optical band pass filter (BPF) is used to select λ_2 which is then photo-detected and subsequently demodulated by the VSA. As can be observed in Figure 5.10, the detected electrical spectrum of λ_2 contains both Channel 1 and Channel 2 signals even though λ_1 is not present after the optical band pass filtering. The transfer of the Channel 1 signal onto λ_2 can be attributed to the cross gain modulation (XGM) characteristic of the SOA where both λ_1

and λ_2 are simultaneously present. The effects of XGM can be minimised if a higher output power SOA is used with total input optical power at least 5 dB below the input saturation power or if the SOA is operated within the linear region [8]. Since the downlink and uplink signals use different sub-carrier frequencies (2.40 GHz and 2.41 GHz, respectively), Channel 2 can be easily selected for demodulation by simple electrical filtering. With increased number of WDM channels the SOA bandwidth would become the main limiting factor in the system and a wider bandwidth SOA needs to be used.

5.3.3 Experimental results

Figure 5.14a show the constellation and eye diagram for the downlink Channel 1 QPSK signal measured and demodulated by the VSA while Figure 5.14b show the corresponding results for the uplink Channel 2 signal. Successful full duplex transmission has been achieved as evident from the clear and well defined constellations and widely open eye diagrams as well as low 10.5% and 7.8 % EVM values for the downlink and uplink directions, respectively.

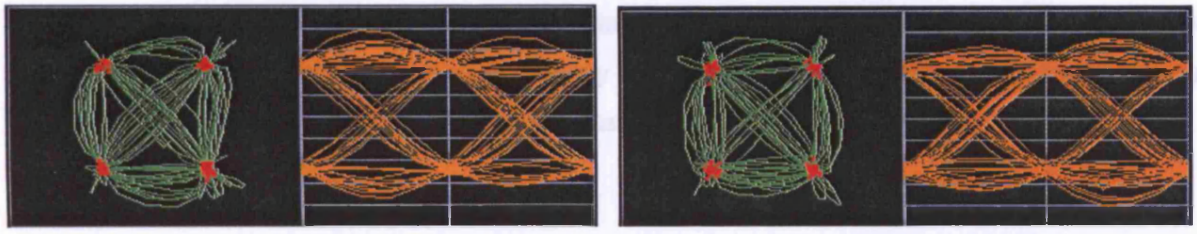

(a) Downlink (b) Uplink

Figure 5.14 Demodulated 3.5 MSymb/s QPSK data for the downlink and the uplink. The two quadrants show the constellation diagram and eye diagram

5.4 Millimetre-wave Gigabit Transmission

Millimetre-wave frequencies are being considered for future broadband wireless access systems to support the increased data rate. In this experiment differential phase shift keying (DPSK) modulation is used, because of its simplicity in implementation, to construct a 1 Gigabit/s wireless over fibre system. Previous experiments [9] using this modulation have been reported at 68 Mbit/s data transmission using a 36 GHz modulated optical carrier [10] and multiple quantum well asymmetric fabry perot modulator/photodetector for passive picocells [11, 12]. Differential encoding of symbols onto PSK significantly reduces the complexity in the demodulator [13]. Whenever a bit or sequences of bits change state, the change is encoded as a phase change in the modulated carrier. If the bit sequence does not change, the phase remains the same. Because the information is encoded in the phase change between symbol points, there is no requirement for the carrier recovery or the use of synchronised frequency reference sources, as with BPSK modulation. Demodulation of DPSK requires knowledge of current and previous symbol points to accurately measure the change in phase. This allows the performance of the system to be assessed relatively easily [7]. The objectives of this demonstration are to investigate the feasibility of a Gigabit/s system using low cost CWDM devices.

5.4.1 Transmission experiment

The complete experimental setup for the DPSK Gigabit/s transmission is shown in Figure 5.15. In the downlink signal path the modulated output of the laser carrying 1 Gigabit/s DPSK data at 5 GHz IF together with 40 GHz optical LO signal are multiplexed at the CS using a CWDM add filter and then transported over 2.2 km SMF. The laser diode for the IF signals is a 1570 nm, commercially available fibre pigtailed uncooled directly modulated DFB device with a mean optical output power of 3 dBm at a bias current of 40 mA. At the BS the LO and the IF are de-multiplexed using a drop filter and individually photo-detected. The LO signal is photo-detected using a U^2t XPDV2120R 50 GHz bandwidth PIN photo-detector and amplified using a Miteq JS4-26004000-30-5A (26 GHz to 40 GHz) low noise amplifier. A 40 GHz BPF with a bandwidth of 200 kHz and insertion loss of 1.8 dB was used at the output of the amplifier for the LO signal to limit the noise bandwidth. The LO signal is further amplified using a high power SpaceK Lab SGKa-17-20 amplifier to increase the power to a suitable level to drive the mixers (+12 dBm). A -3 dB 40 GHz splitter was used to divide the LO power to allow up/down conversion at the BS. The IF signal at 5 GHz is detected using a Discovery DSC30S-39 22 GHz photodiode. The photo-detected IF signal is amplified in a Miteq AMF-2D-005080-25-13P amplifier with a gain of 25 dB. Since a mm-wave attenuator was not available to add loss to the up-converted signal a variable step attenuator was used in the IF path to allow the IF power to be adjusted. After further amplification using a Miteq AFS5-00101200-22-S-5 amplifier, the IF signal is up converted to 35 GHz (lower side band) using the 40 GHz optical LO source in a Miteq TB0440LW1 mixer. The up-converted signal is passed through a 1 metre RF cable and then down-converted to 5

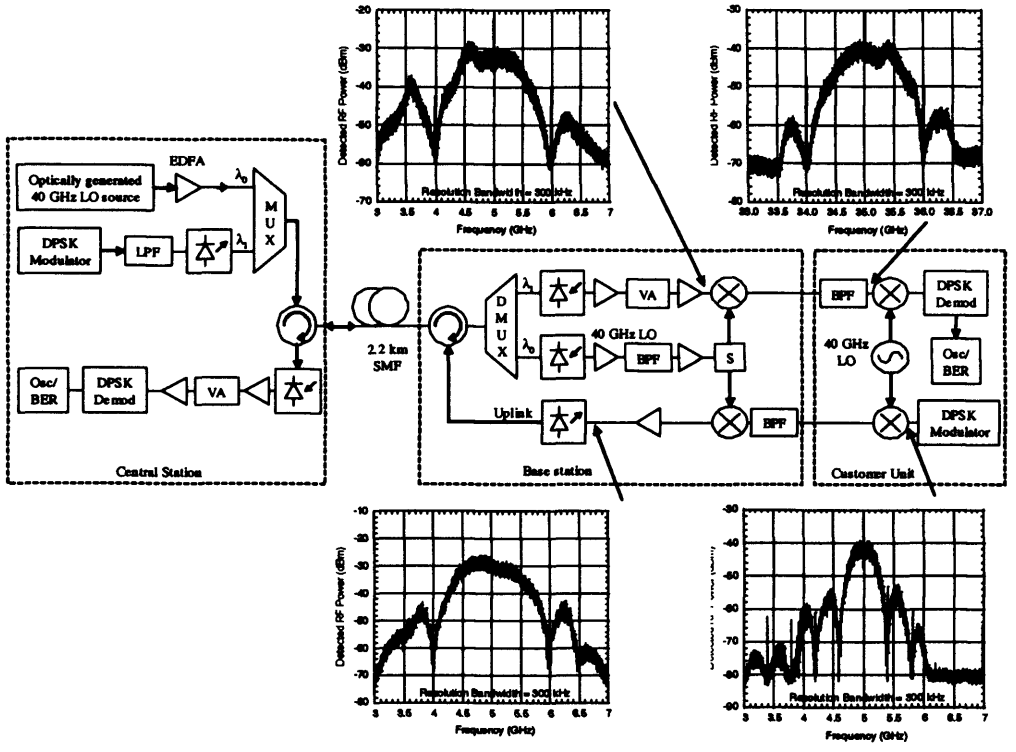

Figure 5.15 Full duplex gigabit wireless over system (VA-variable attenuator)

GHz IF using an independent 40 GHz LO signal to allow demodulation. A BPF at a centre frequency of 35 GHz with a bandwidth of 2 GHz and an insertion loss of 1.5 dB was used to limit the noise bandwidth. The frequency response of the mm-wave filter centred on 35 GHz is shown in Figure 5.16. A modular HP7000 series spectrum analyser was used to detect the modulated optical signals. In the uplink direction DPSK baseband data is first modulated at 5 GHz IF and then up-converted to 35 GHz which is then transmitted over 1 m RF cable and then received at the BS. The received data at 35 GHz is down-converted to 5 GHz using the optical LO and then directly modulate the uplink laser. The optically modulated IF signals are transported over 2.2 km fibre, is received at the CS, photo-detected, amplified and then demodulated to assess the performance.

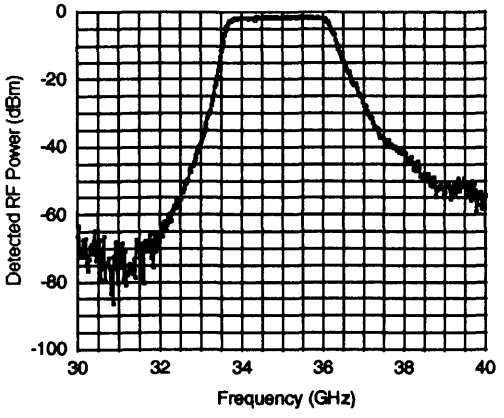

Figure 5.16 Frequency response of the mm-wave filter centred around 35 GHz

5.4.2 40 GHz LO source

The LO signal generated at the CS is remotely delivered and can be shared amongst BSs in a WDM system to reduce overall cost and to give exact frequency synchronisation for advanced modulation techniques. The 40 GHz LO signal is optically generated as shown in Figure 5.17 by driving the Mach-Zehnder (MZ) biased at $V\pi$ for double sideband suppressed carrier modulation (DSB-SC). The MZ is

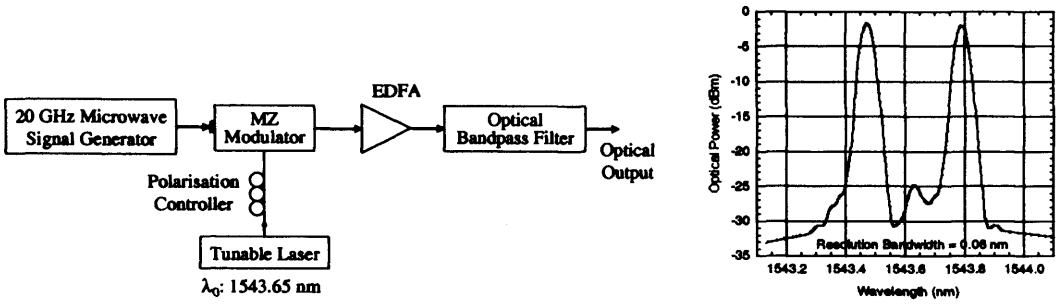

Figure 5.17 Optically generated 40 GHz LO source and the optical spectrum at the output

driven by a $f_{LO/2}$ microwave signal generator with +10 dBm RF power and its optical output contains mainly two modulation sidebands offset from the suppressed carrier. The suppression of the centre wavelength around 1543 nm is about 23 dB as demonstrated in Figure 5.17, which show the optical spectrum of the 40 GHz LO signal after the erbium doped fibre amplifier (EDFA) and the optical band pass filter at the CS. Since the LO output from the MZ is weak an EDFA was used to increase the level with a 1 nm optical band pass filter to reduce the amplified spontaneous noise (ASE). After photo-detection at the BS a 40 GHz mm-wave LO filter with a bandwidth of 200 kHz and insertion loss of 3.5 dB is used to limit the noise bandwidth. The frequency response of this filter is shown in Figure 5.18. Figure 5.19 show the phase noise of the 20 GHz reference signal plus 6 dB due to frequency doubling and of 40 GHz LO optical signal with and without the electrical filter. The phase noise response with the electrical filter is < -120 dBc/Hz at 10 MHz offset.

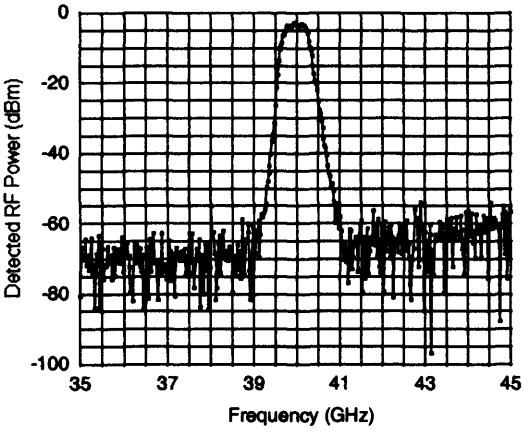

Figure 5.18 Frequency response of the LO filter centred around 40 GHz

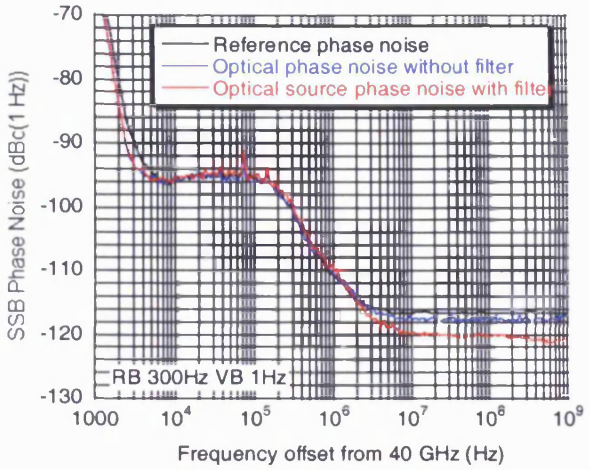

Figure 5.19 Detected single sideband (SSB) phase noise spectra of the 40 GHz LO source and the 20 GHz reference signal generator source

5.4.3 DPSK modulator and transmitter

Phase shift keying is a digital modulation scheme that conveys data by changing, or modulating the phase of a reference signal i.e. the carrier wave. For modulation schemes such as DPSK differential encoding of data is required. In this modulation technique the phase of the carrier for the current signal element is dependent on the state of the previous signal element. Let $D_{IN(k)}$ be a sequence of binary bits that are the input to a differential encoder and let $D_{OUT(k)}$ be the output of the differential encoder. Then $D_{OUT(k)}= D_{IN(k)} \oplus D_{OUT(k-1)}$ ($\oplus$ is modulo 2 addition). Table 5.1 provides the truth table. A bit transition from 0 to 1 or 1 to 0 is encoded as a binary 1, whereas no change in bit is encoded as a binary 0.

$D_{IN(k)}$	$D_{OUT(k-1)}$	$D_{OUT(k)}$
0	0	0
0	1	1
1	0	1
1	1	0

Table 5.1 Implementing a high speed differential encoder-Truth table

One circuit that can be used to implement the above equation for a differential encoder is to use an exclusive-OR (XOR) gate with a one bit period delay in the feedback path as shown in Figure 5.20. The XOR gate, compares the input with the previously differentially encoded output bit, by means of a bit delay. Two D-type flip flops can be used for synchronising the two input signals into the XOR gate triggered by the clock signal from the pattern generator. However, implementing a 1 bit period delay (1 bit period = 1 ns at 1 Gbit) in the feedback path can be difficult when working with discrete components. A circuit without such critical delays is more practical. One such implementation that does not involve delay in the feedback path is shown in Figure 5.21. Here, a divide by 2 counter has a

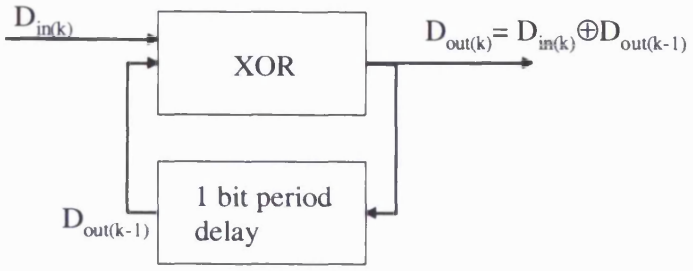

Figure 5.20 Implementation of the differential encoder using an XOR gate output

clock gated with the data. When the data is high, the counter changes state, which is equivalent to adding a 1 modulo 2. When the data is low, the counter state remains the same, which is equivalent to adding a 0 modulo 2.

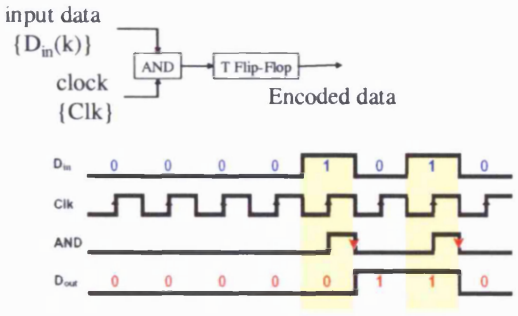

Figure 5.21 Illustration of a differential encoder with a divide by 2 counter

Differential encoding can be implemented using the high speed logic parts from the 13751DE Inphi encoder [14]. The 13751DE differential encoder can support data rates upto 13 Gbit/s and performs modulo two addition of the input data bit with the previous output bit. Figure 5.22 show the DPSK modulator and transmitter used [9]. A 1 Gbit/s 2^{23}-1 PRBS data was first differentially encoded using the Inphi encoder. The resulting baseband DPSK signal was then used to modulate the phase of a 5 GHz LO signal in a double balanced mixer. A mini-circuits 2.25 GHz low pass filter was used to limit the occupied spectrum. The DPSK signal is then used to directly modulate a 6 GHz bandwidth DFB laser with a 1570 nm centre wavelength emission.

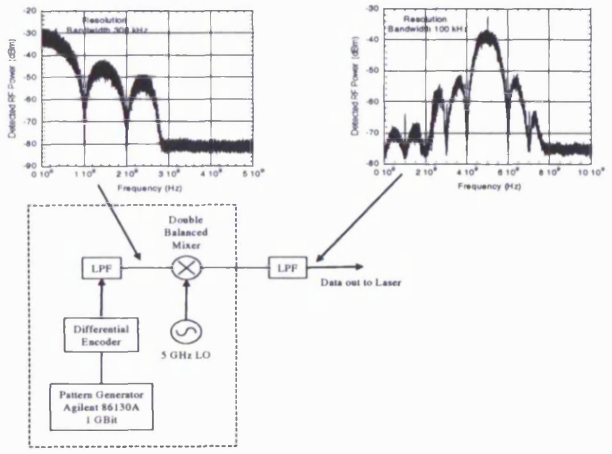

Figure 5.22 DPSK modulator and transmitter

5.4.4 DPSK demodulator and receiver

In order to differentially decode data, each current bit must X-OR with the previous one. The DPSK demodulator only needs to determine changes in the incoming signal phase and is implemented as shown in Figure 5.23 consisting of a splitter, a phase shifter and a double balanced mixer. A semi-rigid cable was used to connect the various components. The demodulation of the DPSK signal was performed directly on the switched 5 GHz carrier using a delay line and a double balanced mixer. The -3 dB splitter (Mini-circuits ZFSC-2-10G) equally divides the power of the incoming encoded signal into two paths. One of the paths was delayed by one bit period τ which is equal to $(1\ \text{Gbit/s})^{-1}$ or 1 ns in reference to the other. A phase shifter (ARRA model 9428) was used in the delay to allow tuning the differential delay between two paths. Time delays were measured using the HP 8753D network analyser (30 kHz-6 GHz). The two paths were then recombined in a double balanced mixer (WJ M86C) to recover the data. The mixer functions as a phase comparator that compares the phase of its two input signals on the RF and LO ports. Given that these have a delay of 1 ns, the mixer actually compares the phase of the current bit with that of the previous bit. The recovered data pass through a 2^{nd} order low pass filter with -3 dB bandwidth of 2250 MHz to limit the noise bandwidth of the signal before being fed to the digital oscilloscope for eye diagram monitoring.

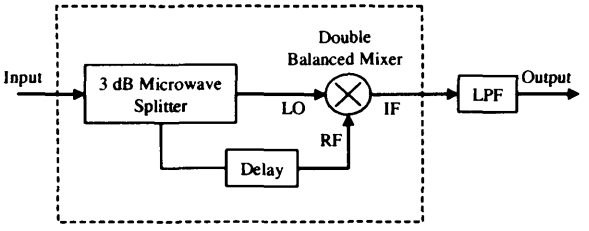

Figure 5.23 Implementation of the DPSK demodulator

5.4.5 Experimental results

To measure the performance of the complete system eye diagrams and bit error rate (BER) measurements were produced. Figure 5.24 and Figure 5.26 show the eye diagrams of the recovered 1 Gbit/s 2^{23}-1 PRBS data for the downlink and uplink respectively, measured using 0 dB, 10 dB and 20 dB RF attenuation applied to the IF signal before up-conversion. It can be seen that with 0 dB attenuation the eye diagram was wide open for both downlink and the uplink. With 10 dB attenuation applied to the IF signal the eye diagram was reasonably good and can still be clearly seen. However, with 20 dB attenuation the amplitude of the eye is very much reduced and is beyond the detectable range. The detected pattern sequence are observed in the time domain using the Agilent Infinium 1.5 GHz oscilloscope and are shown in Figure 5.25 and Figure 5.27 for the downlink and the uplink respectively.

By setting the pattern generator to an 8 bit sequence the data rate can be easily measured on the oscilloscope. As shown in Figure 5.25 the duration of one bit is 1 ns, which corresponds to a data rate

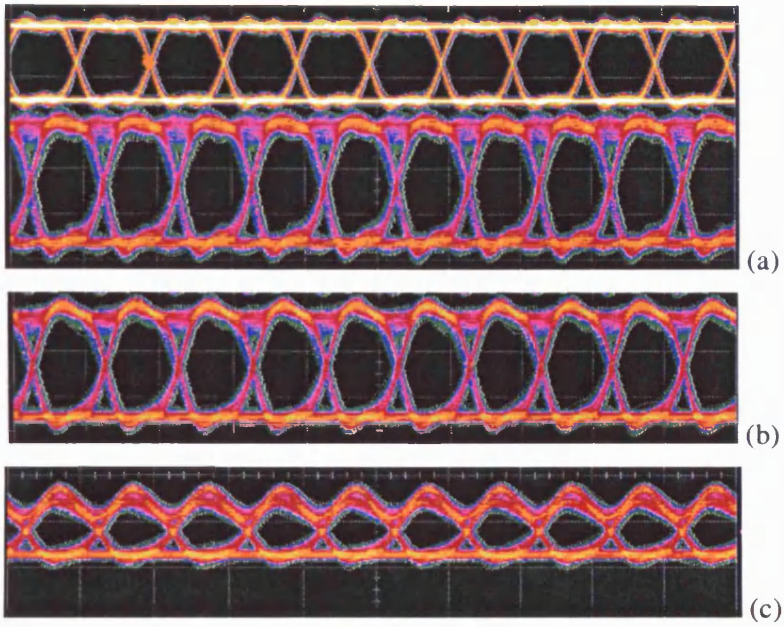

Figure 5.24 Detected downlink eye diagrams at 1 Gbit/s (a) upper trace reference transmit input, lower trace receiver demodulated with 0 dB attenuation (b) 10 dB attenuation (c) 20 dB attenuation

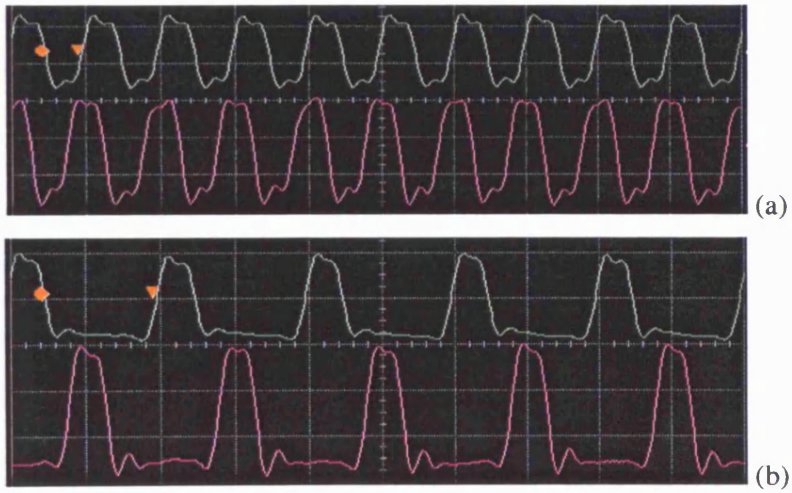

Figure 5.25 Detected downlink pattern sequence (a) upper trace reference path, lower trace system output, sequence is 10101010, (b) upper trace reference path, lower trace system output, sequence is 10001000

of 1 Gbit/s. The output sequence is clearly detected at 1 Gbit/s with the reference input sequence shown for comparison. Figure 5.28 shows the measured bit error rate (BER) as a function of the 5 GHz RF source power and it can be seen that error free transmission (BER < 10^{-9}) was achieved for downlink and uplink when the received RF power was -16 and -17 dBm respectively. With a lower received RF power the BER increases.

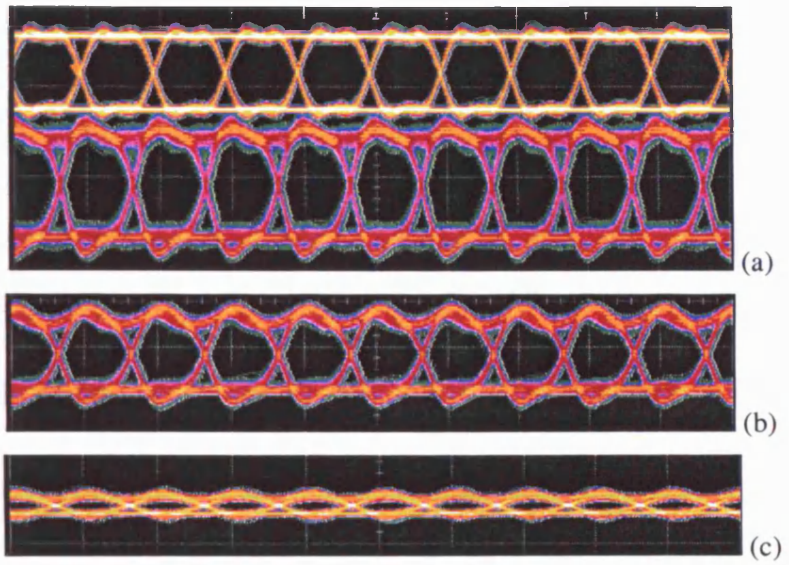

Figure 5.26 Detected uplink eye diagrams at 1 Gbit/s (a) upper trace reference transmit input, lower trace receiver demodulated with 0 dB attenuation (b) 10 dB attenuation (c) 20 dB attenuation

Figure 5.27 Detected uplink pattern sequence (a) upper trace reference path, lower trace system output, pattern sequence is 10101010, (b) upper trace reference path, lower trace system output, pattern sequence is 11101110

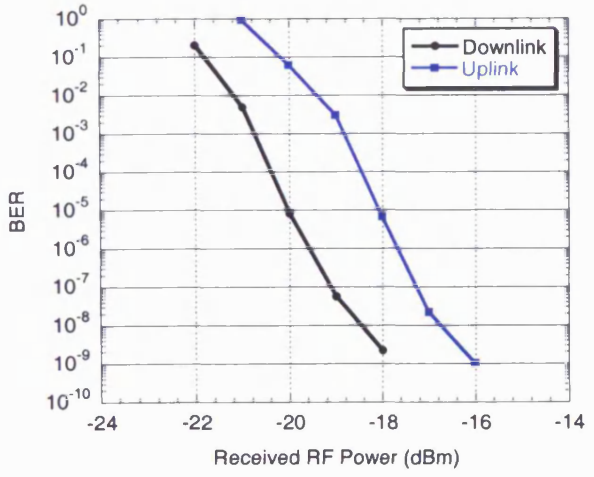

Figure 5.28 Detected overall system BER for the downlink and uplink

5.5 Conclusion

In this chapter feed-forward linearisation is demonstrated to compensate for laser non-linear distortion in a multi-channel wireless over fibre system. Overcoming laser non-linearity improves the system performance. In the experiment, two channels each with 3.5 M/Symbs of QPSK data have seen 8 dB reductions in the spectral re-growth caused by a strong input channel. Successful transmission was achieved with feed-forward evident from clear constellations with improvement in EVM from 25% to less than 10%. Laser non-linearity becomes more severe with two strong input channels leading to interchannel distortion that can completely mask a third adjacent channel. A reduction of 10 dB in intermodulation distortion was achieved with feed-forward compensation. It is also shown that the CWDM architecture allows efficient distribution of signals from the CS to the BS and vice versa. The results suggest that feed-forward linearisation allows successful transmission of multiple channels in a wireless over fibre system.

A full-duplex millimetre wave 3.5 MSymb/s QPSK wireless data over 12.8 km fibre transmission system with a bi-directional SOA; incorporating 2.2 km CWDM fibre ring architecture has been experimentally demonstrated. Low cost CWDM components such as uncooled lasers and filters are used to construct the network. Successful transmission has been achieved as evident in the clear and well defined constellations and eye diagrams as well as low 10.5% and 7.8 % EVM values for the downlink and uplink respectively. The cost savings obtained from the use of CWDM and bi-directional SOA technology; together with the improved fibre utilisation resulting will make such solutions more attractive for future mm-wave access systems.

A 1 GBit/s DPSK modulated wireless signals at 5 GHz IF together with remote delivery of LO signals at 40 GHz from the CS to the BS was demonstrated. IF signals are transmitted using low cost uncooled CWDM lasers without optical amplification. An EDFA employed at the CS was used to amplify the LO signal.

References

[1] T. Ismail, C. P. Liu and A. J. Seeds, "Uncooled directly modulated high dynamic range source for IEEE802.11a wireless over fibre LAN applications," *Optical Fibre Communication (OFC)*, FE3, 2004.

[2] T. Ismail, J. E. Mitchell and A. J. Seeds, "Linearity enhancement of a directly modulated uncooled DFB laser in a Multi-Channel wireless-over-fibre system", *IEEE MTT-S Int. Microwave Symposium (IMS)*, TU1A-2, 2005.

[3] G. H. Smith and D. Novak, "Broadband millimetre wave fibre radio network incorporating remote up/down conversion", *IEEE MTT-S Int. Microwave Symposium (IMS)*, vol. 3, pp. 1509-1512, 1998.

[4] T. Ismail, C. P. Liu, J. E. Mitchell, A. J. Seeds, X. Qian, A. Wonfor, R. V. Penty and I. H. White, "Full-duplex wireless-over-fibre transmission incorporating a CWDM ring architecture with remote millimetre-wave LO delivery using a bi-directional SOA", *Optical Fibre Communications (OFC)*, OThG7, 2005.

[5] C. Lim, A. Nirmalathas, M. Attygalle, D. Novak and R. Waterhouse, "On the merging of millimetre-wave fibre radio backbone with 25 GHz WDM ring network", *IEEE J. Lightwave Technol.*, vol. 21, no. 10, pp. 2203-2210, 2003.

[6] R. P. Braun, G. Grosskopf, D. Rhode and F. Schmidt, "Low phase noise millimetre wave generation at 64 GHz and data transmission using optical single sideband injection locking", *IEEE Photon. Technol. Lett.*, vol. 10, no. 5, pp. 728-730, 1998.

[7] L. A. Johansson, "Broadband millimetre-wave radio over fibre systems", *PhD thesis, University of London,* University College London, 2001.

[8] T. Ismail, C. P. Liu, J. E. Mitchell, A. J. Seeds, X. Qian, A. Wonfor, R. V. Penty and I. H. White, "QPSK wireless data over 12.8 km fibre transmission with remote millimetre-wave LO delivery using a bi-directional SOA in a full-duplex system incorporating a 2.2 km CWDM fibre ring architecture", *IEEE Photon. Technol. Lett.*, vol. 17, pp. 1989-1991, 2005.

[9] S. Levy, R. Nagarajan, A. Mar, P. Humphrey and J. E. Bowers, "Fibre-optic PSK subcarrier transmission at 35 GHz using a resonantly enhanced semiconductor laser", *Electron. Lett.*, vol. 28, pp. 2103-2104, 1992.

[10] L. A. Johansson, C. P. Liu and A. J. Seeds, "A 65 km span unamplified transmission of 36 GHz radio over fibre signals using an optical injection phase lock loop", *IEEE Photon. Technol. Lett.*, vol. 14, no. 11, pp. 1596-1598, 2002.

[11] C. P. Liu , A. J. Seeds, J. Chadha, P. Stavrinou, G. Parry, M. Whitehead, A. Krysa and J. Roberts, "Bi-directional transmission of broadband 5.2 GHZ wireless signals over fibre using a multiple quantum well asymmetric fabry perot modulator/photodetector", *Optical Fiber Communication (OFC)*, FM8, pp. 738-740, 2003.

[12] C. P. Liu , A. J. Seeds, J. Chadha, P. Stavrinou, G. Parry, M. Whitehead, A. Krysa and J. Roberts, "Design, fabrication and characterisation of normal incidence 1.56 μm multiple quantum well asymmetric fabry perot modulators for passive picocells", *IEICE Trans. Electron*, vol. E86-C, pp. 1281-1289, 2003.

[13] Y. Doi, S. Fukushima, T. Ohno, Y. matsuoka and H. Takeuchi, "Phase shift keying using optical delay modulation for millimetre-wave fibre-optic radio links", *IEEE J. Lightwave Technol.*, vol. 18, pp. 301-307, 2000.

[14] http://www.inphi-corp.com/products/13751de.html

Chapter 6

Conclusion

This thesis has presented original work on feed-forward linearisation for a directly modulated Distributed Feedback (DFB) laser for application in Wireless over Fibre (WoF) systems. The main achievement of the work is a simultaneous reduction of noise and distortion in semiconductor lasers at microwave frequencies leading to enhanced Spurious Free Dynamic Range (SFDR). With the rapid growth of wireless technologies, millimetre-wave (mm-wave) over fibre emerges as one of the potential candidates for future broadband wireless services and the performance of such systems has also been investigated in this thesis. This final chapter summarises the main conclusions of the work and presents recommendations for future work.

6.1 Summary of the Thesis

Summary of Chapter 1

The first chapter gave background to the thesis and presented fixed wireless mm-wave systems and wireless LAN technologies. An introduction to WoF and various signal transport schemes are considered which highlight the advantages of centrally controlled hardware leading to simple and low cost remote Base Station (BSs). The relative merit of direct and external modulation is outlined and issues like noise and distortion properties are investigated for WoF links. The distortion level of most lasers and modulators is generally not low enough to meet the stringent requirement for multi-channel transmission in WoF systems. The optical transmitter limits the system channel capacity and signal quality, hence distortion compensation becomes necessary. While the optical modulation depth (OMD) per channel that can be applied to a laser is limited by laser non-linear distortion, a linearised transmitter enables the OMD per channel to be increased, providing an increased system power budget and performance. The chapter concludes with a statement of the objectives of this thesis, a summary of the results of the research and an outline of the structure for the remaining chapters.

Summary of Chapter 2

Chapter 2 gives an overview of linearity and distortion and reviews the operating principle of different linearisation techniques proposed in the literature for directly modulated semiconductor lasers and external modulators. Techniques include pre-distortion, dual parallel, cascade coupling, polarisation

mixing, optical injection locking (OIL), electro-optical feedback, quasi-feedforward and feed-forward linearisation. A background to the generation of non-linear distortion in semiconductor lasers is also given.

The disadvantage of electro-optical feedback is that its operating bandwidth is limited because of potential instability of the feedback loop at high frequency. Quasi-feedforward requires two lasers of very similar distortion properties and is therefore difficult to implement. In general, pre-distortion can achieve substantial reduction of distortion in modulators only. For semiconductor lasers, pre-distortion is not a very effective technique. Furthermore, the operational bandwidth of pre-distortion is restricted to < 2 GHz and it is therefore not suitable for higher microwave frequencies. The feed-forward technique is more effective since it not only suppresses third order intermodulation distortion (IMD) and higher order products, but also reduces laser relative intensity noise (RIN). Since noise limits the dynamic range in a system, reducing non-linear distortion together with laser RIN provides a significant improvement in SFDR. Unlike pre-distortion, feed-forward can also eliminate both second and third order distortion and thus this technique can be applied to both lasers and modulators. The main conclusion of the chapter was that feed-forward is more suitable for linearising lasers and modulators for microwave applications beyond 2 GHz. Feed-forward linearisation has not previously been demonstrated at modulation frequencies above 3 GHz or with low cost uncooled lasers at 1550 nm, as required for IEEE802.11a wireless systems operating at 5.2 GHz.

Summary of Chapter 3

In this chapter theoretical and experimental work on feed-forward was carried out. Although this work concentrated on directly modulated lasers the technique can also be applied to externally modulated transmitters. An analysis of the distortion reduction performance of feed-forward was performed. Through this study an understanding is gained for the choice of major design variables and how they affect the performance of the system. Theoretical noise reduction in feed-forward is also investigated and the limitations are identified. Adaptive techniques have been discussed for a robust feed-forward system to overcome laser drift and environmental changes.

In the experimental section a feed-forward system has been built and experimentally investigated. Two DFB lasers used in feed-forward have been characterised by measuring their modulation response. The feed-forward system can be viewed as being made up of two loops: the carrier cancellation loop and the distortion cancellation loop. The method for testing and tuning feed-forward are described in detail and the performance of individual loop is studied. After fine-tuning, the two loop are put together to form the complete system. Feed-forward linearisation has been demonstrated at the highest frequencies 5.2 GHz required for wireless applications using a low cost uncooled laser under direct modulation, achieving simultaneous 26 dB third order IMD suppression (i.e. from -45 dBc to -71 dBc) and 7 dB RIN reduction. As a result the SFDR was enhanced by 15 dB to 107 dB (1 Hz). The measurement of RIN has confirmed that feed-forward can reduce RIN of the laser. These results

indicate that feed-forward linearisation is an effective technique for obtaining the required system dynamic range. The operational bandwidth of feed-forward was measured to be 500 MHz at 5.2 GHz with at least 24 dB distortion suppression and is the widest reported to date. The limiting factors in the performance are due to frequency dependent loss in the microwave cable and the degree of amplitude flatness and phase non-linearity of the components in the system resulting in amplitude and phase mismatch. Further improvements involve employing optical components with shorter fibre pigtails, allowing reduced length of microwave cables required and to alleviate the effect of the microwave frequency dependent loss, thus extending the bandwidth.

Transmission of multi-channel broadband QPSK signals using feed-forward is demonstrated. The first transmission of triple (two high power and one low power) 11 Msymb/s QPSK modulated channels centred around 2.4 GHz over 2.2 km single-mode fibre (SMF) using a feed-forward linearised laser is reported. An 11dB interchannel distortion suppression and 10.5 dB power advantage compared to the non-linearised case is achieved allowing the weaker channel to be detected successfully. Feed-forward linearisation is also demonstrated at 5.8 GHz. An improvement in EVM of 15% for 16 QAM and 14% for 64 QAM has been observed with feed-forward. Intermodulation distortion is reduced by 13 dB when two input channels are at +10 dBm input level.

In conclusion, these results suggest that feed-forward compensation is a promising technique for improving the dynamic range of wireless over fibre systems operating well into the microwave frequency range. This allows successful multi-channel transmission in a wireless over fibre system for wireless LAN applications and fixed wireless access systems such as WiMAX.

Summary of Chapter 4

This chapter examined network architectures for distribution of broadband wireless signals. A survey of available technologies was carried out, identifying their main advantages and/or disadvantages. Heterodyne techniques such as Optical Injection Locking (OIL), Optical Phase Lock Loop (OPLL), Optical Injection Phase Lock Loop (OIPLL) and sideband injection locking are considered for the generation of a mm-wave Local Oscillator (LO) signal. Network architectures such as star, double star, star-tree, bus and ring were investigated and important limitations for these systems were discussed. A deeper analysis of the ring architecture was presented. Reliability and scalability of the ring network was identified as an important factor.

In the star network all BSs are connected to the central station (CS) using a separate fibre link. One of the advantages of a star network is that any faulty node does not affect the rest of the network, and it is easy to add and remove nodes allowing upgrade ability. However, the main disadvantage of star networks is that it requires more fibre than a bus or ring network. A double star and star-tree network is a combination of two or more star networks connected together. In the Bus topology all BSs are connected along the main fibre called the bus or backbone. In the ring architecture all BSs are connected to one another in a closed loop. The advantages of the ring architecture such as equipment

sharing and fault protection and disadvantages such as non-uniform signal quality and network upgrade complexity were discussed. Power budget calculations and simulations have been carried out for the proposed Gigabit/s (Gbit/s) system using low cost components such as uncooled directly modulated lasers and Coarse Wavelength Division Multiplexing (CWDM) passive components. The use of Semiconductor Optical Amplifiers (SOAs) in WoF links is discussed with important considerations regarding non-linearity.

Summary of Chapter 5

In this chapter RF and mm-wave over fibre links are described experimentally to demonstrate their usefulness in a full duplex bi-directional system. Experimental demonstration is carried out for two 3.5 MSymb/s QPSK modulated wireless channels centred around 2.4 GHz transmitted over fibre with feed-forward linearisation at the BS to improve the dynamic range of a directly modulated uncooled DFB laser. Signals are generated at the CS and distributed using a CWDM 2.2 km fibre ring architecture. A reduction of 10 dB is observed in the spectral re-growth caused due to strong input from the adjacent channel together with reduction from 25% to < 10% in EVM at an input level of -25 dBm of the weaker channel. Intermodulation distortion is reduced by 10 dB when two strong channels are present at +12 dBm input level.

The use of a bi-directional SOA to provide gain for both downlink and uplink optical signals simultaneously, with experimental results for a CWDM ring architecture which allows distribution of a centrally generated 40 GHz LO signal and the connection of multiple BSs in a WoF network is demonstrated for the first time. Successful transmission is achieved with 10.5% and 7.8% EVM values for the downlink and the uplink, respectively, together with clear and well defined constellations and eye diagrams. The use of bi-directional amplifier, together with CWDM and optical distribution of the mm-wave LO signal allow substantial reduction in overall system complexity and cost.

A full experimental demonstration of a mm-wave Gbit/s system using uncooled CWDM components is described. Successful transmission of 1 Gbit/s DPSK signals over 2.2 km of single fibre with frequency up/down conversion for wireless transmission in the 40 GHz band has been demonstrated with a BER < 10^{-9}. The experimental results and BER are compared to theoretical predictions. This chapter successfully verified the feasibility of wireless over fibre systems for distribution of broadband mm-wave signals using low cost uncooled laser sources and CWDM passive components.

6.2 Objectives Realised

A number of objectives for this work were stated in the introduction and these are discussed below.

The two main objectives were to improve SFDR of semiconductor lasers and investigate low cost mm-wave system architectures. The first objective has been demonstrated, with experiments showing a

successfully implemented feed-forward system at 5.2 GHz for the first time using directly modulated DFB lasers and enhanced the SFDR to (107 dB.$Hz^{2/3}$) a level suitable for fibre transmission of multi-channel wireless signals at frequencies > 5 GHz, considerably above that previously achieved. Also demonstrated is the use of uncooled commercially available DFB lasers in such systems for the first time, offering reduced system cost. The feed-forward system presented in this work can improve the performance of WoF systems and increase capacity as demonstrated by multi-channel data transmission experiments at 2.4 GHz and 5.8 GHz. The research results achieved suggest that it is possible to construct a WoF link using low cost uncooled directly modulated DFB laser with sufficient dynamic range for multi-channel or multi-operator broadband wireless signal transmission. To compensate for laser output drift and environment changes adaptive techniques can be implemented and these are discussed in greater depth in Chapter 3.

The second main objective has been demonstrated by two transmission experiments, in the mm-wave range. To enable distribution of the signals to a number of BSs with economical use of optical fibre, an architecture has been developed based on a CWDM fibre ring. The MUX, DEMUX and optical add-drop modules (OADMs) are all commercially available CWDM components. Using an optical coupler and an OADM, a fraction of the common LO signal power can be tapped off and directed to a BS and the remaining LO power is then routed back to the ring and directed to subsequent BSs. A successful generation of high spectral purity 40 GHz mm-wave LO signal is demonstrated for frequency up and down conversions at the BS. As with the previous 36 GHz mm-wave source [1], all the parts used were simple low cost, low frequency off the shelf components. The 40 GHz mm-wave signal is constructed using two slave lasers injection locked by a master tunable laser which was externally modulated at 20 GHz. This new configuration in comparison to the previous 36 GHz signals using Optical Injection Phase Lock Loop (OIPLL) [1] has resulted in better single sideband phase noise as well as significant suppression of spurious modulation signals such as the half frequency at 20 GHz at the optical output of this LO source. With this LO source the frequency of operation can easily be extended to the upper mm-wave region.

The use of a bi-directional SOA to provide gain for both downlink and uplink optical signals simultaneously, with experimental results for a CWDM ring architecture which allows distribution of a centrally generated 40 GHz LO signal and the connection of multiple BSs in a wireless over fibre network was demonstrated. The use of bi-directional amplifier, together with CWDM and optical distribution of the mm-wave LO signal allows substantial reduction in overall system complexity and cost and permits efficient use of the optical fibre infrastructure.

To meet future needs for increased data rates 1 Gbit/s wireless access, requiring mm-wave carrier frequencies, techniques for mm-wave modulated optical signal generation and distribution for low cost signal multiplexing using CWDM techniques is experimentally demonstrated. The work demonstrates for the first time that uncooled DFB laser sources together with passive CWDM devices can be used in a mm-wave Gbit/s systems.

All the experiments reported were performed with low cost uncooled DFB lasers except for LO generation. The use of uncooled lasers is attractive, as no peltier cooler will be needed. As the expected lifetime of an uncooled DFB laser generally is longer than a peltier cooler, this will not only result in a less complex arrangement, a large reduction in power consumption and small size, but the expected lifetime of the system will also increase leading to higher reliability [2]. This is an important step towards a practical and potentially very low cost mm-wave systems.

6.3 Novel Results Achieved

The novel results of this work are:

The first implementation of feed-forward linearisation at 5.2 GHz to reduce non-linear distortion using uncooled directly modulated laser sources with potential applications in WoF systems. In previous work Fock *et al* [3] have demonstrated feed-forward at lower frequencies for CATV applications. Suppression of third order IMD is reported at cellular frequencies in [4] with enhanced ACPR of W-CDMA signals [5]. In this experiment no observations were made for laser RIN reduction. Feed-forward linearisation has not previously been demonstrated at modulation frequencies above 3 GHz or with low cost uncooled lasers at 1550 nm, as required for IEEE802.11a wireless systems operating at 5.2 GHz. In this work feed-forward is demonstrated at the highest reported frequency of 5.2 GHz with 500 MHz linearisation bandwidth having at least 24 dB distortion suppression. The main results are simultaneous reduction of 26 dB IMD3 distortion and 7 dB in laser RIN reduction resulting in enhanced SFDR by 15 dB to 107 $dB.Hz^{2/3}$ [6]. The performance can be further improved using short fibre pigtailed optical components and linear RF components. The first multi-channel transmission experiments using feed-forward at 2.4 GHz with QPSK and 5.8 GHz using QAM modulation have been carried out. The performance of feed-forward was assessed with two strong channels and a third weak channel.

In WoF systems the BS needs to be low cost and of minimised complexity. In this work an IF over fibre scheme is implemented to avoid using mm-wave modulated optical signal source at the BS. The received uplink radio signals are down-converted to lower IF to directly modulate uncooled low cost optical sources and transmitted through optical fibre with low dispersion penalty. Up-conversion from/to mm-wave frequencies takes place in the BS using a centrally generated LO signal and distributed to BSs on a separate wavelength. With this architecture, the difficulties of generating a mm-wave modulated optical signal at the BS for the uplink is removed. Furthermore the LO can be used to deliver a mm-wave carrier to a number of BS, allowing cost sharing amongst BSs. Previous demonstrations of mm-wave over fibre systems have been reported using separate uni-directional erbium doped fibre amplifiers (EDFAs) to provide the necessary gain for the downlink and uplink [7, 8]. SOA have also been used in WoF systems to extend fibre distance [9, 10]. However, no previous demonstrations have been reported using a bi-directional SOA. In this work [11] the use of bi-directional SOAs in place of uni-directional EDFAs or uni-directional SOAs, together with the use of

CWDM and optical distribution of the mm-wave LO signal, allows substantial reduction in overall systems complexity and cost, as will be necessary for the widespread adoption of mm-wave wireless access systems. It also increases utilisation of the deployed fibres, an economic advantage where leased fibres have to be used.

A mm-wave WoF transmission is also demonstrated, supporting broadband wireless data transmission rate at 1 Gbit/s. The use of uncooled components in Gbit/s wireless systems has not been investigated before. In the present work, successful transmission is achieved for 1 Gbit/s data. Previous WoF transmission experiments at Gbit/s rates have used expensive photonic components such as the UTC-PD [12]. Although data transmission achieved was very high the cost of the wireless link is of primary concern for commercial use. Here, a low cost Gbit/s solution is presented.

6.4 Suggestions for Further Work

In carrying out this work several important areas for further investigation have been identified. The performance of feed-forward can be improved in several ways. Future work would therefore be directed towards improvement of the devices and could involve replacing some of the components in the system with those that satisfy the criteria for maximum distortion reduction for broadband frequencies. These components should also have a linear phase response over the bandwidth in which the system is tested for accurate amplitude and phase matching. Also the use of optical components with shorter fibre pigtails would alleviate the frequency dependent loss in the delay matching path. This would enable wider bandwidth suppression and allow simultaneous 2.4 GHz and 5 GHz multi-channel transmission. The feed-forward then can be tested with real wireless LAN and WiMAX signals. Another improvement includes investigating adaptive techniques to be implemented in feed-forward circuitry to compensate changes such as component aging (laser output variation) or temperature drift. The penalty, however, is extra complexity. Details on various adaptive techniques are given in Chapter 3.

Although full duplex mm-wave systems have been demonstrated, the downlink and the uplink transmission were carried out separately due to limited equipment available at the time. Future experiments could involve simultaneous transmission of uplink and downlink transmission. The experiments also need to be validated for a higher number of wireless channels with simultaneous transmission. In the implementation of the mm-wave Gigabit/s system using direct modulation of the uncooled DFB laser (Chapter 5) the transmission of DPSK data was demonstrated. Larger data rates could be achieved for the downlink and uplink using higher order complex modulation such as QAM which are more spectrally efficient. An investigation of using such modulation schemes should be conducted to check the system performance. Finally, the use of SOA in a Gbit/s system should be investigated as a potential low cost mm-wave over fibre Gbit/s solution for a large number of BSs.

References

[1] L. A. Johansson, and A. J. Seeds, "Millimeter-wave radio-over-fibre transmission using an optical injection phase lock loop source," *IEEE Int. Topical Meeting on Microwave Photonics (MWP)*, pp. 129-132, 2000.

[2] L. A. Johansson, "Broadband millimetre-wave radio over fibre systems", *PhD thesis, University of London,* University College London, 2001.

[3] L. S. Fock & R.S. Tucker, "Simultaneous reduction of intensity noise and distortion in semiconductor lasers by feedforward compensation," *Electron. Lett.*, vol. 27, pp. 1297-1299, 1991.

[4] Sang-Hyun. Park and Young-Wan. Choi, "Significant suppression of the third order intermodulation distortion in transmission system with optical feed-forward linearised transmitter," *IEEE Photon. Technol. Lett.*, vol. 17, pp. 1280-1282, 2005.

[5] Joon-Jae Lee, Sang-Hyun Park and Young-Wan Choi, "Enhanced ACPR of W-CDMA signals in optical feedforward transmitter by optimisation," *International Topical meeting on Microwave Photonics (MWP)*, pp. 59-62, 2005.

[6] T. Ismail, C. P. Liu and A. J. Seeds, "Uncooled directly modulated high dynamic range source for IEEE802.11a wireless over fibre LAN applications," *Optical Fibre Communications (OFC),* FE3, 2004.

[7] C. Lim, A. Nirmalathas, D. Novak, R. Waterhouse and G. Yoffe, "Millimetre-wave broad-band fibre-wireless system incorporating baseband data transmission over fibre and remote LO delivery", *IEEE J. Lightwave Technol.*, vol. 18, pp. 1355-1363, 2000.

[8] C. Lim, A. Nirmalathas, M. Attygalle, D. Novak and R. Waterhouse, "On the merging of millimetre wave fibre radio backbone with 25 GHz WDM ring networks", *IEEE J. Lightwave Technol.*, vol. 21, no. 10, pp. 2203-2210, 2003.

[9] Hai-Han. Lu, Ying-Cong. Lin, Yuan-Hong. Su and Heng-Sheng. Su, "A radio on fibre intelligence transport system base on electroabsorption modulator and semiconductor optical amplifier", *IEEE Photon. Technol. Letts.*, vol. 16, no. 1, pp. 251-253, 2004.

[10] X. Qian, P. Hartmann, A. Wonfor, J. D. Ingham, R. V. Penty and I. H. White, "Microwave signal transmission over a directly modulated radio over fibre link using cascaded semiconductor optical amplifiers", *Optical Fibre Communications (OFC),* vol. 4, OThB2, 2005.

[11] T. Ismail, C. P. Liu, J. E. Mitchell, A. J. Seeds, X. Qian, A. Wonfor, R. V. Penty and I. H. White, "QPSK wireless data over 12.8 km fibre transmission with remote millimetre-wave LO delivery using a bi-directional SOA in a full-duplex system incorporating a 2.2 km CWDM fibre ring architecture", *IEEE Photon. Technol. Lett.*, vol. 17, pp. 1989-1991, 2005.

[12] A. Hirata, M. Harada K. Sato and T. Nagatsuma, "Low cost millimetre wave photonic techniques for Gigabit/s wireless link", *IEICE Trans. Electron.*, vol. E86-C, no. 7, pp. 1123-1128, 2003.

UNIVERSITY OF LONDON

SENATE HOUSE. MALET STREET, LONDON, WCIE 7HU

REPRODUCTION OF THESES

A thesis which is accepted by the University for the award of a Research Degree is placed in the Library of the College and in the University of London Library. The copyright of the thesis is retained by the author.

As you are about to submit a thesis for a Research Degree, you are required to sign the declaration below. This declaration is separate from any which may be made under arrangements with the College at which you have *pursued* your course (for internal candidates only). The declaration will be destroyed if your thesis is not approved by the examiners, being either rejected or referred for revision.

Restriction of access to thesis for 2 years from date of award, per UCL 11/5/06.

Academic Registrar

To be completed by the candidate

NAME IN FULL (please type surname in BLOCK CAPITALS)

Tabassam ISMAIL

THESIS TITLE Feed-forward Linearisation of a Directly Modulated Semiconductor Laser and Broadband Millimetre-Wave Wireless over Fibre Systems

DEGREE FOR WHICH THESIS IS PRESENTED Doctor of Philosophy (Ph.D.)

DATE OF AWARD OF DEGREE *(To be completed by the University)*: 28 FEB 2007

DECLARATION

1. I authorise that the thesis presented by me in *[2006] for examination for the MPhil/PhD Degree of the University of London shall, if a degree is awarded, be deposited in the library of the appropriate College and in the University of London Library and that, subject to the conditions set out below, my thesis be made available for public reference, inter-library loan and copying.

2. I authorise the College or University authorities as appropriate to supply a copy of the abstract of my thesis for inclusion in any published list of theses offered for higher degrees in British universities or in any supplement thereto, or for consultation in any central file of abstracts of such theses.

3. I authorise the College and the University of London Libraries, or their designated agents, to make a microform or digital copy of my thesis for the purposes of inter-library loan and the supply of copies.

4. I understand that before my thesis is made available for public reference, inter-library loan and copying, the following statement will have been included at the beginning of my thesis: The copyright of this thesis rests with the author and no quotation from it or information derived from it may be published without the prior written consent of the author.

5. I authorise the College and/or the University of London to make a microform or digital copy of my thesis in due course as the archival copy for permanent retention in substitution for the original copy.

6. I warrant that this authorisation does not, to the best of my belief, infringe the rights of any third party.

7. I understand that in the event of my thesis being not approved by the examiners, this declaration would become void.

***Please state year by hand, using a pen.**

DATE 20-03-2006 SIGNATURE

Note: The University's Ordinances make provision for restriction of access to an MPhil/PhD thesis and/or the abstract but only in certain specified circumstances and for a maxiumum period of two years. If you wish to apply for such restriction, please enquire at your College about the conditions and procedures. External Students should enquire at the Research Degree Examinations Office, Room 261, Senate House.

THIS DECLARATION MUST BE COMPLETED AND RETURNED WITH THE EXAMINATION ENTRY FORM